VALIDATION PAGE

Doctoral Candidate: **FILIPPOS ALOGDIANAKIS**

Doctoral Thesis Title: **Statistical Assessment and Probabilistic Prediction of Bridge Deterioration using Structural Condition Recordings**

The present Doctoral Dissertation was submitted in partial fulfillment of the requirements for the Degree of Doctor of Philosophy at the ***Department of Civil and Environmental Engineering*** *and was approved on the 17 of December, 2018. by the members of the* ***Examination Committee****.*

Examination Committee:

Research Supervisor:	Dr. Dimos Charmpis Associate Professor, Univ. of Cyprus	(Name, position and signature)
Committee Member:	Dr. Michael F. Petrou Professor, Univ. of Cyprus	(Name, position and signature)
Committee Member:	Dr. Loukas Dimitriou Assistant Professor, Univ. of Cyprus	(Name, position and signature)
Committee Member:	Dr. Ioannis Xenidis Associate Professor, Aristotle University of Thessaloniki	(Name, position and signature)
Committee Member:	Dr. Boulent Imam Senior Lecturer, University of Surrey	(Name, position and signature)

DECLARATION OF DOCTORAL CANDIDATE

The present doctoral dissertation was submitted in partial fulfillment of the requirements for the degree of Doctor of Philosophy of the University of Cyprus. It is a product of original work of my own, unless otherwise mentioned through references, notes, or any other statements.

…….…….. [Full Name of Doctoral Candidate]

…….... [Signature]

Περίληψη

Τις τελευταίες δεκαετίες έχουν δαπανηθεί τεράστια ποσά για τη συντήρηση των γηρασκουσών γεφυρών ανά τον κόσμο. Η αξιόπιστη εκτίμηση του ρυθμού φθοράς και της διάρκειας ζωής των γεφυρών αποτελούν ουσιώδη στοιχεία για τον καθορισμό βέλτιστων προγραμμάτων συντήρησης, αποκατάστασης/ενίσχυσης ή ανακατασκευής. Στην παρούσα διατριβή χρησιμοποιήθηκαν δημοσιευμένα δεδομένα από επιθεωρήσεις υφιστάμενων γεφυρών από την Ομοσπονδιακή Διοίκηση Αυτοκινητοδρόμων των ΗΠΑ. Κύριος σκοπός της διατριβής ήταν η ανάπτυξη μιας νέας μεθόδου για την πρόβλεψη του ρυθμού φθοράς των γεφυρών υπό διάφορες συνθήκες, αξιοποιώντας δεδομένα μόνο ενός έτους επιθεωρήσεων. Για την επίτευξη αυτού του σκοπού αναπτύχθηκε μια γενική μεθοδολογία καθοδηγούμενη από δεδομένα, για να μοντελοποιηθεί μακροσκοπικά και να διερευνηθεί η φθορά γεφυρών και να αναδειχθούν οι σημαντικότεροι παράγοντες που επηρεάζουν τη δομικής κατάσταση γηρασμένων γεφυρών.

Αρχικά, η υπάρχουσα βάση δεδομένων εμπλουτίστηκε με επιπρόσθετες πληροφορίες για τη συμπερίληψη υποψήφιων παραγόντων σχετικών με το κλίμα και τη σεισμική επικινδυνότητα, που θα μπορούσαν να επηρεάσουν τη δομική κατάσταση των γεφυρών. Ακολουθήθηκε διαδικασία ανάλυσης δεδομένων, αξιοποιώντας στατιστικές μεθόδους, για τον προσδιορισμό των κρίσιμων παραγόντων φθοράς. Παράγοντες που βρέθηκαν να έχουν τη μεγαλύτερη επίδραση στη δομική κατάσταση ήταν η ηλικία της γέφυρας, τα δομικά υλικά της, ο σεισμικός κίνδυνος της τοποθεσίας, διαβρωτικές συνθήκες που οφείλονται στην ύπαρξη νερού κάτω από τη γέφυρα και στη χρήση αλάτων κατά του παγετού. Εστιασμένη έρευνα διεξήχθη σε ολόκληρη την παράκτια περιοχή των ΗΠΑ που ανέδειξε ως κρίσιμη απόσταση τα 2-3 χιλιόμετρα από την ακτογραμμή προς στην ενδοχώρα, μέχρι την οποία διαβρωτικοί παράγοντες από τη θάλασσα δύνανται να επηρεάσουν τη φθορά γεφυρών. Αξιοποιώντας τα παραπάνω αποτελέσματα, πραγματοποιήθηκε διεξοδική μελέτη για την εξέλιξη της δομικής φθοράς στο χρόνο. Εστιασμένα δείγματα γεφυρών τμηματοποιήθηκαν βάσει των χρησιμοποιούμενων δομικών υλικών και των περιβαλλοντικών συνθηκών έκθεσης και αναλύθηκαν με γνώμονα την ηλικία και τη φθορά χρησιμοποιώντας πιθανότητες μη-ικανοποιητικής-δομικής-κατάστασης. Τα αποτελέσματα έδειξαν ότι ο συνδυασμός αλάτων κατά του παγετού, ύπαρξης νερού κάτω από τη γέφυρα, καθώς και ύπαρξης κατασκευαστικών αρμών σε μη συνεχή καταστρώματα, έχουν διαφορετική επιρροή στα υλικά των διαφορετικών τμημάτων μιας κατασκευής.

Τα ευρήματα της ανάλυσης έτυχαν επεξεργασίας και συγκρίθηκαν με αντίστοιχα αποτελέσματα που αναφέρονται στη βιβλιογραφία σχετική με τη διάβρωση προς αναζήτηση

πιθανών αιτίων και προελεύσεων, αλλά και προς επικύρωση της διαδικασίας ανάλυσης και των αποτελεσμάτων της.

Η αυξητική τάση των πιθανοτήτων μη-ικανοποιητικής δομικής κατάστασης με την αύξηση της ηλικίας μελετήθηκε και αξιοποιήθηκε για την ανάπτυξη μιας μακροσκοπικής μεθόδου πρόβλεψης της μελλοντικής φθοράς γεφυρών. Η μέθοδος μετατοπίζει (αντιγράφει) πιθανότητες και προσαρμόζει κατάλληλα την κλίμακα του χρόνου λαμβάνοντας υπόψη στατιστικές ιδιότητες των μετατοπισμένων δεδομένων. Η τελική κατανομή προκύπτει από την παλινδρόμηση κατάλληλης συνάρτησης αθροιστικής κατανομής στα μετατοπισμένα και προσαρμοσμένα δεδομένα. Στην εργασία παρέχονται οι ιδιότητες, οι εξαρτήσεις της μεθόδου και τα αποτελέσματα της επικύρωσης των προβλέψεών της για όλα τα διαθέσιμα δείγματα. Τέλος, παρουσιάζεται μια εφαρμογή της μεθόδου στο πλαίσιο διαχείρισης κύκλου ζωής γεφυρών, όπου πραγματοποιείται συγκριτική αξιολόγηση διαφορετικών προγραμμάτων αποκατάστασης με βάση το αναμενόμενο κόστος.

Παρόλο που η παρούσα έρευνα αναφέρεται σε γέφυρες, το αναπτυγμένο πλαίσιο μπορεί να επεκταθεί και σε άλλα γηράσκοντα συστήματα και έργα υποδομής που επηρεάζονται από φθορά, υπό την προϋπόθεση ύπαρξης αντίστοιχων διαθέσιμων δεδομένων.

Abstract

In the last decades, vast budgets have been spent to maintain the aging bridges all over the world. Reliably estimating the deterioration rates and the lifetime of bridges are essential aspects in determining optimal programs regarding maintenance, rehabilitation or reconstruction. Published bridge inspection data from the US Federal Highway Administration were utilized to quantitatively treat the high uncertainties governing structural deterioration. The main purpose was to derive a novel method for forecasting the bridge deterioration rate under various circumstances, utilizing inspection results of only one year of published data. To achieve this, a data-driven framework was developed to investigate bridge deterioration and result in predominant factors that would allow its modelling.

Initially, the existing database was enriched with information from other reliable databases, to include candidate deterioration factors regarding climate and earthquakes. A data analysis process, including various statistical methods, was performed and critical factors of deterioration were identified. Specifically, the age of a bridge, its structural materials, the earthquake hazard at its region, aggressive conditions due to water underneath the bridge and use of deicing salts, were found to be the factors affecting structural deterioration the most. A closer investigation was performed to the whole coastline region of the US. Critical distances from the coast were identified, indicating that corrosive agents from the sea can affect deterioration at distances up to 2-3 km inland. Utilizing the above results, a thorough study was performed on the progress of structural deterioration with time. Focused samples were segmented based on structural materials used and various exposures, and were analyzed with respect to age and deterioration using probabilities of non-satisfactory bridge condition. The results showed that combinations of the factors (deicing salts, water under a bridge and the existence of construction joints on non-continuous decks) have different effect on the materials of the bridge parts of deck, superstructure and substructure. The findings of this work were discussed and compared to corresponding results reported in literature on corrosion, in an effort to determine possible justifications and origins and provide validation and credibility for the analysis procedure and its outcomes.

The dependency of non-satisfactory condition probabilities to age was studied and utilized to develop a macroscopic method to predict future deterioration. The Shifting Scaling Data Regression (SSDR) method was developed, according to which the initially calculated probabilities are shifted (copied) and then scaled using a consistent factor that

accounts for the statistical properties of the shifted data. The final distribution is derived by fitting the shifted and scaled data points with an appropriate Cumulative Distribution Function. The SSDR's properties and dependencies were displayed and the predictions of the method were validated utilizing all available samples. Furthermore, an application of the SSDR was demonstrated in the framework of life cycle management of a bridge, where various rehabilitation schedules were comparatively assessed with respect to expected costs.

Although the research conducted herein refers to bridges, the developed framework can be extended to other infrastructure systems and facilities affected by structural deterioration, provided that respective data are available.

TABLE OF CONTENTS

TABLE OF APPENDICES

LIST OF FIGURES

LIST OF TABLES

LIST OF ANNOTATIONS

AASHTO:	American Association of State Highway and Transportation Officials
ADT:	Average Daily Traffic
AIC:	Akaike Information Criterion
ANOVA:	Analysis of Variance
ANSS:	National Seismic System
CCP:	Cumulative Condition Probability
CDF:	Cumulative Distribution Function
CFR:	Code of Federal Regulations
CP:	Condition Probability
DOT:	Department of Transportation
EDA:	Exploratory Data Analysis
FHWA:	Federal Highway Administration
FO:	Functionally obsolete
GAO:	Government Accountability Office
GIS:	Geographic Information System
IDW:	inverse distance weighted
MAP-21:	Moving Ahead to the 21st Century
NBI:	National Bridge Inventory
NBIS:	National Bridge Inspection Standards
NDEVC:	Non-Destructive Validation Center
NEIC:	National Earthquake Information Center
NOAA:	National Oceanic and Atmospheric Administration
PCA:	Principal Components Analysis
PDF:	Probability Density Function
PGA:	Peak Ground Acceleration
PR:	Probability of Rehabilitation
PV:	Present Value
RH:	Relative Humidity
SD:	Structurally Deficient
SSDR:	Shifting Scaling Data Regression
USGS:	United States Geological Survey

1 Introduction

1.1 General

From the dawn of human civilization, man has developed and incorporated various infrastructure facilities to promote population, economic growth and evolve technologically to today's civilization. Infrastructure has been recently redefined as *'the physical components of interrelated systems providing commodities and services essential to enable, sustain, or enhance societal living conditions'* by (Fulmer, 2009). Apart, though, from building new infrastructure facilities, maintaining the already existing ones in functional condition is a challenge all modern societies have to face.

Bridges constitute one of the oldest infrastructure facilities. They are structures built to span physical obstacles (water, valley, road), providing passage over them without interrupting the way underneath. Bridges have been used for thousands of years and built by different materials and designs, which evolved throughout human history. From prehistoric time, man would have used the naturally fallen tree logs to surpass an obstacle in a safer and less time-consuming way. Although many bridges must have been built in ancient times, not many have survived due to their temporal nature and/or the nondurable construction materials. This changed during the Roman period (200 BCE- 305 CE), when a vast road network (120,000 km) was built to connect the provinces, providing access to the armies to preserve and expand the Empire's territory (Labate , 2016). The introduction of durable mortars, as well as the introduction of the arch, revolutionized bridge construction, which continued to be used up to the 18^{th} century. In the early industrial revolution, the first cast iron bridge was built in England in 1779 (Billington , et al., 2017). During the second industrial revolution, in the19^{th} century, the concrete and steel materials were introduced in the form of reinforced concrete, structural steel and prestressed concrete, which would ever since revolutionize bridge design and construction (Billington , et al., 2017).

During the past century, a large number of bridges was built throughout the world to meet the increased transportation demands of the globalized society, whose ability to function efficiently relies on the utilization of multiple infrastructure networks. Among them, surface transportations still constitute its backbone and, at the same time, bridges compose weak links throughout the road network (Kutz, 2004). Interruptions to a bridge's functionality can cause multiple delays, increased detour lengths accompanied by increases in user costs, impacting a nation's economy. Such interruptions can also be caused from repair works or rehabilitations performed to preserve a bridge's functionality, as well as

promote passenger safety, both of which could be compromised from excessive deterioration of a bridge's structural condition. Structural deterioration can reduce dramatically the bridge's useful lifespan, demanding at the same time vast budgets to be annually allocated for necessary interventions to be performed.

The magnitude of the problem can be understood by considering the case of the US (Fig. 1.1), whose bridge stock consists of more than 600,000 bridges, of which 40% are older than 50 years (ASCE, 2017). Nine percent of the bridges are considered 'structurally deficient', a term corresponding to significant defects that require reduced weights or speed limits (Golson, 2015). Although not all mentioned bridges comprise a threat to public safety, there have been cases where bridge collapses occurred and resulted in human casualties (Penn, 2018). The Association of Civil Engineers (ASCE) 2017 report card on infrastructure revealed the high number of structurally deficient bridges (Fig. 1.1(b)) and estimated a $123 billion cost for their rehabilitation (ASCE, 2017). Despite the poor condition ratings of infrastructures received from ASCE, the US are placed 11th in the world regarding infrastructure within the Global Competitiveness Report of 2016-2017 (World Economic Forum, 2016), revealing that even larger problems exist in other countries.

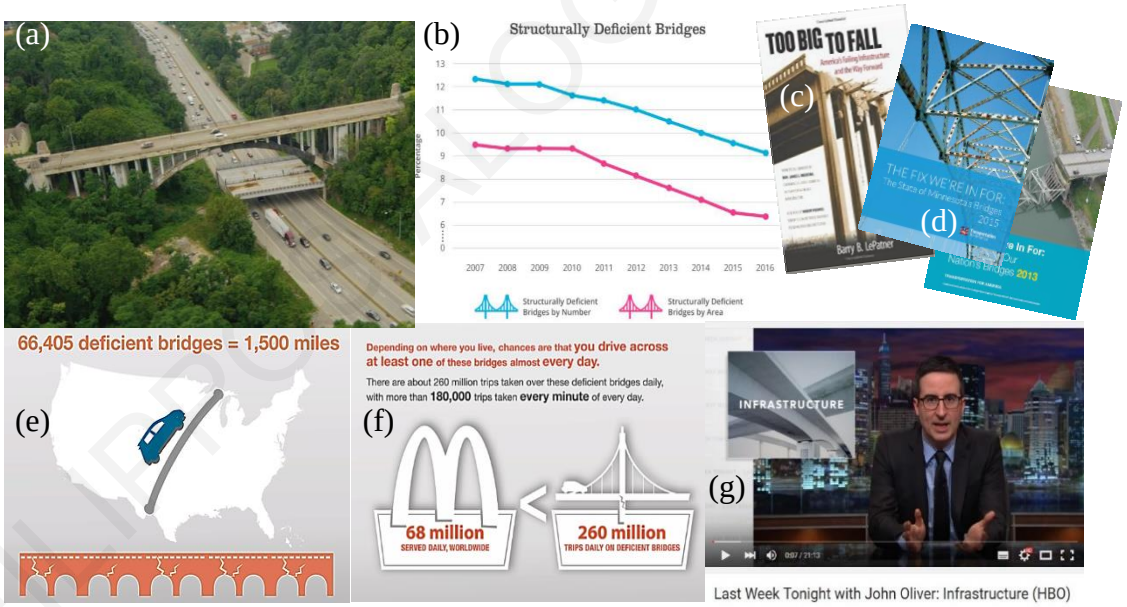

Figure 1.1: Magnitude of the problem in the US (a) Bridge built over highway ,under a highway bridge, to protect vehicles from falling debris, image taken from (Kroft, 2012). (b) Structurally deficient bridges from ASCE infrastructure report card (ASCE, 2017). (c) Book concerned with US failing infrastructure and ways to tackle it (LePatner, 2010). (d) Yearly reports at State and national level regarding bridge condition (Transportation for America, 2013). (e) Picture showing the equivalent distance of deficient bridge miles on the US map (Transportation for America, 2013). (f) Picture revealing the amount of passengers affected by deficient bridges daily (Transportation for America, 2013). (g) HBO channel's late-night talk and news satire television program hosted by comedian John Oliver on infrastructure.

A key element to effectively managing existing stocks is the reliable estimation of the deterioration rate and the lifetime of bridges, which are essential aspects in determining optimal maintenance and/or rehabilitation schedules. However, the structural performance of bridges in time is governed by high uncertainties, which need to be quantitatively treated, in order to be able to make rational decisions regarding maintenance and rehabilitation.

An important step toward the effective handling of such uncertainties is the gathering and exploitation of respective data. Typically, the data collected refer to current bridge conditions and are used in conjunction with Bridge Management Systems (BMS) to decide on the necessity and degree of priority of any potential intervention and to allocate corresponding funds. Frequent inspections ensure that the BMS is up-to-date regarding the structural condition of the bridge stock. However, in order to estimate future needs and optimally allocate available budgets, models to predict the future stock condition are essential.

Various deterioration models exist, varying from linear regression to much more involved Markov-chain models. The basic purpose of all models is to link the recorded condition of the infrastructure to influential measurable factors. Existing methods utilize bridge condition records, including inspection results, for a number of years. Unfortunately, this leaves subjectivity of the inspectors and revisions in inspection standards to influence the prediction outcomes. Furthermore, most available models are not sufficiently validated to provide reliable bridge service life predictions and changes in evaluating the 'as is' condition of a bridge can render past evaluations obsolete.

1.2 Thesis objectives

The present thesis utilizes existing bridge data from the US to study macroscopically the structural deterioration of bridge materials in different environments and estimate the time-to-rehabilitation. The US database was chosen in this study due to its plurality and consistency, as well as the lack of available, organized, local or other bridge data elsewhere. In general, countries in Europe do not allow access to their relevant data, while there are no such data maintained in Cyprus (although there are currently efforts to initialize a Cypriot bridge inventory). Additionally, the variety of factors affecting deterioration together with the uniformity of structural design and inspection standards within the US territory provides the advantage of generalizing the results and conclusions regarding the studied deterioration. Even if other inventories were available e.g. across Europe, such generalization would not be possible due to the variety of the countries' standards. However, similar exposure factors

to the ones in a specific region can be found in the US, so the US experience, as incorporated in its bridge inventory data, can be transferred elsewhere.

Bridge condition data were used in this regard to evaluate bridge deterioration rates, while other data concerning types of construction, environmental exposure etc. were also employed to capture factors responsible for alarming deterioration. This work's objectives were set and tackled based on the knowledge acquired via a data-driven approach. The chapters are also organized in a similar way; starting from the description of the database to the development of a novel method for time-to-rehabilitation predictions, to end with a demonstration of applying it to a lifecycle example. Furthermore, as different topics are investigated, the literature review for each topic is provided within each chapter's introduction.

The Thesis objectives are:

- identify factors, which affect bridge deterioration;
- utilize those factors to study the aging process for various materials and environmental exposures;
- develop a method that can reliably predict deterioration rates for bridges made of various materials and are exposed to various environments;
- show how method predictions can be utilized by other researchers and practitioners.

The approaches used and developed in this work can be adjusted to be applied also to infrastructure facilities other than bridges, which are under deterioration of any form, provided that condition data are available. Furthermore, this study actually demonstrates the benefits gained for a nation's problem by allowing free access to its databases that are relevant to the problem.

1.3 Thesis outline

In **Chapter 2**, a literature review of the various methodologies followed to model structural deterioration is presented and the research needs addressed in the thesis are identified.

In **Chapter 3**, information is provided for the National Bridge Inventory (NBI), its history, legislative procedures, inspections and standards, oversight of the process and its reliability.

In **Chapter 4**, the NBI of the year 2016 is read, filtered and processed to track errors. Evaluations of structural condition reveal the deterioration of different structural bridge

parts. To describe various environmental exposures, data from United States Geological Survey (USGS) and the National Oceanic Atmospheric Administration (NOAA) are employed. To estimate local environmental exposures for each bridge, spatial interpolation methods are utilized. The combined database is then analyzed using data analysis procedures, to determine which variables affect the structural condition of a bridge.

In **Chapter 5**, the coastline effect on bridge structural parts is studied for the conterminous US coast. To perform this task, factors affecting structural condition found in Chapter 3 are utilized, along with bridge distances from the coast, as well as additional factors from literature. The US coastline is divided based on these factors to delimit the critical coastline distance affecting bridges.

In **Chapter 6**, the information of Chapters 3 and 4 are used to perform meaningful segmentations of the stock of bridges, to determine deterioration with age under different environmental exposures. Cumulative condition probability is then introduced to reveal the probability of a bridge, of a particular age, to be in a deteriorated condition. Structural deterioration and aging are studied using bivariate plots for various bridge parts, environmental exposures and materials. The results allow for comparisons among various environments and construction materials.

In **Chapter 7**, a novel method to probabilistically estimate the time-to-rehabilitation of a bridge is presented. The method uses cumulative condition probabilities taken from segmented samples of chapter 5 to perform its predictions. Established rules in materials accelerated testing are adopted to predict the time-to-rehabilitation, due to similar tendencies observed between condition probabilities and factors recorded in such tests. Thus, the so-called Shifting Scaling Data Regression (SSDR) method was developed, in which recorded probabilities are shifted (copied) and then time-scaled, to predict future stock conditions and hence time to bridge rehabilitations. The method is compared to other methodologies and validated using appropriate bridge samples.

In **Chapter 8**, the new method is applied on a hypothetical concrete bridge, to demonstrate the method's utilization for bridge life-cycle costing reduction. Various rehabilitation schedules are comparatively assessed with respect to the expected total rehabilitation cost, as well as the expected cost due to the possible need for bridge replacement, to conclude on optimal bridge interventions in terms of cost.

Finally, in **Chapter 9**, an extended summary is presented along with the major conclusions of this study. In the same chapter, recommendations for future research are also included.

2 Literature review - identification of research needs

In this chapter the uncertainties that govern bridge deterioration are presented along with the inherent complexity of the overall phenomenon that limits the applicability of mechanistic models. The state-of-the-art deterioration models utilizing inspections are reviewed followed by their restrictions. Corresponding research needs are identified, which justify the contributions made in this thesis.

2.1 Introduction

During the past century a huge number of infrastructure facilities was constructed to meet societal needs. Despite the incorporation of new materials and the evolution of engineering practices in design and construction, structural deterioration threatens the functionality of bridges and the safety of users. The huge number of bridges constructed has formed stocks, which are aging and deteriorating at various rates due to environmental, accidental and man-made factors (Frangopol, et al., 2017).

Structural deterioration, though, is governed by high uncertainties, as it is affected by uncertainties and risks linked to various phases of a structure's life cycle: design, construction, exposure to threats and usage (Adric & Lu, 2016). Bridge structures are composite, incorporating different materials. Among them, the most widely applied are reinforced concrete, prestressed concrete and steel. As these materials can be used for the construction of different structural parts, they can be exposed to different loads and different environments. Mechanisms that decrease the load capacity of a structure are fatigue and corrosion (Melchers & Beck, 2018). Wet-dry cycles, freeze-thaw cycles, the splash zone, high temperatures and humidity may alter the corrosion rates of steel, especially in presence of aggressive agents, such as chlorides (Neville, 1995). Additional effects, such as fatigue creep and construction errors, can increase the modelling uncertainties (Melchers & Beck, 2018).

In the following sections, the common approaches of modeling and predicting deterioration are reviewed. First, mechanistic deterioration models that are used in structural reliability methods are presented. Then, a general description of inspections performed to evaluate bridges is given, followed by the statistical deterioration methods that utilize them. Furthermore, issues of the reviewed statistical models are discussed and specific research gaps are identified.

2.2 Mechanistic models

To model corrosion, the reduction of material volume due to rust formation is described through a time function, which depends on environmental conditions and steel type. Similar procedures have been followed to assess the durability of paint systems under different environmental exposures (Kallias, et al., 2017). Contrary to structural steel corrosion, where rust formation can be noticed and treated at early stages, corrosion of reinforcement or tendon steel are linked to cover cracking and cross-section loss, which can even lead to failure. Chlorides from aggressive environments are known to affect reinforcement and tendon corrosion (Neville, 1995; Balafas & Burgoyne, 2010). Thus, research has been focused on the modelling of chloride ingress (Tuuti, 1982; Neville, 1995; Stewart & Rosowsky, 1998; Balafas & Burgoyne, 2010; Bertolini, et al., 2013; Liu & Weyers,1998) and the definition of a threshold signifying corrosion initiation before cover cracking appears. Unfortunately, the predictive capabilities of corrosion initiation models are limited due to their sensitivity to the chloride threshold and its large variability (Angst, 2018). More information regarding corrosion can be found in Chapter 6.

In addition to corrosion, other deterioration factors may coexist. Efforts to model fatigue have been reported (Curtis & Irvine, 2015), however the coupled effect of corrosion and fatigue has not been dealt with. Other factors such as creep, temperature, as well as atmospheric pollution and environment change (Kumar & Imam, 2013), are also significant and can make the task of modelling even more complicated.

Mechanistic models are widely used for design purposes, but their applicability in deterioration modelling is linked with certain disadvantages. Specifically, they can be applied only to specific simple scenarios, the available inspection data cannot yet be utilized to validate their predictions, while experimental and field data are generally insufficient for producing the required model inputs (Nickless & Atadero, 2018).

2.3 Inspections of bridge condition

To keep infrastructure facilities in functioning and at the same time safe state, inspections are performed to evaluate their structural condition. Inspections are carried out by specialized personnel following specific standards, which provide rules and processes, to assist in performing their task safely and consistently. During an inspection, condition ratings are attributed to structural elements or macro-elements (i.e. deck, superstructure, substructure, etc.) based on pre-specified rating scales, used to report the extent of structural deterioration observed. The inspections are organized in records for each bridge, where,

besides condition ratings, additional information such as age, characteristics of the bridge, average daily traffic, etc., is provided.

Inspection results are utilized to estimate infrastructure needs and allocate funds for maintenance, rehabilitation or reconstruction purposes. The use of inspection standards assists in achieving uniformity among inspection reports and aims at reducing the subjectivity of inspectors, as most inspections performed are visual. Thus, the changes in inspection standards over years are unavoidable. For the case of the US, changes in inspection standards are presented in Chapter 3.

2.4 Statistical models

Statistical models account for the different factors affecting structural deterioration by utilizing inspection records of built infrastructure. In this way, although the distinguished effect of each deterioration factor is not clear, the joint contribution of all coexisting factors and uncertainties is actually given in a quantified form in the structural evaluation results. Statistical models can be categorized to deterministic, stochastic process and artificial intelligence ones based on the way predictions are performed. For modelling structural deterioration the most apparent influencing factor to be utilized is age.

2.4.1 Deterministic models

Linear regression models have been initially used to forecast future structural condition of bridges in the States of New York (Fitzpatrick et. al, 1981) and Wisconsin (Hyman & Hughes, 1983). The models utilized previous inspection years and the only factor considered was bridge age. Regression analysis with a third degree polynomial function was performed for the bridges of the State of Illinois to derive deterioration models of various bridge parts (Bolukbasi et al. 2004). For the State of Indiana, different years of inspections from the NBI were utilized along with factors of traffic volume, highway system, bridge type and age, which were included in the analysis (Jiang & Sinha, 1988). Among these factors, only highway system, bridge type and age were found statistically significant (Jiang & Sinha, 1988). The analysis resulted in polynomial functions of age for the condition of substructures supporting concrete and steel superstructures of non-interstate bridges.

Deterministic models have been found inferior to stochastic models for predicting future condition ratings (Jiang & Sinha, 1988). This can be attributed to the fact that deterioration is a stochastic process and regression analysis provides values corresponding to the mean condition in a deterministic way (Jiang & Sinha, 1988).

2.4.2 Stochastic process models

Markov Chains comprise the most common stochastic process utilized for modelling deterioration of infrastructure facilities (Madanat et al. 1997;Jiang & Sinha, 1989; Zambon, et al., 2017). Markov chain is a case of the Markov process that has a series of discrete random states. For the case of bridges, condition ratings represent the different states of deterioration and, for each state, the probabilities of transitioning from one state to another are estimated. These probabilities are organized in a matrix comprising the transition probability matrix. The present state of bridge conditions is represented by a vector and, by multiplying it by the transition probability matrix, the future condition can be predicted.

According to Mauch and Madannat (2001), Markov chain discrete-time models can be furtherly categorised to state-based and time-based. State-based models predict probability of the condition state that a facility will be at a given time, whereas time-based models predict the probability of the time taken by the infrastructure facility to change condition state (Mauch & Madannat, 2001). Further, categorization can be made based on the inclusion of time dependency: in *homogenous* Markov chains, transition probabilities are time-independent (stationary); in *inhomogeneous* Markov chains, the transition probabilities are functions of time (Zambon, et al., 2017). The most frequently used type is the homogenous Markov chain models, in which research evolution has been mainly in the estimation of the transition probabilities, in order to limit expert judgment by using increased inspection data (Thompson & Johnson, 2005).

In a homogenous state-based model, the transition probabilities of one state to another are simply estimated by calculating the frequency of transitions between two inspection records (Zambon, et al., 2017). The time step between inspection records used varies depending on the condition ratings utilized and the interval inspections are performed. Such models do not incorporate the effects of different factors on transition probabilities. Other homogenous Markov chains use regression approaches on inspection data to model the effect of various factors (e.g. age, average daily traffic, etc.) and the expected value output by the model is used to calibrate the transition matrices incorporating the factors' effects (Jiang & Sinha, 1988). Linear regression has been utilized incorporating the effect of average daily traffic and age by (Jiang & Sinha, 1988). Poisson and negative binomial regression (Madanat & Ibahim, 1995) and probit regression (Madanat et al., 1997) were used on the Indiana NBI data set to model effects of age, average daily traffic, climatic regions and materials of bridge decks to condition ratings.

Disadvantages of utilizing the Markov chain approaches regard their memoryless assumption, meaning that a bridge's future condition is dependent only on the current condition. Furthermore, no actual validation of their long-term predictions is available, only a kind of partial validation.

2.4.3 Artificial Intelligence models

Artificial Intelligence models are methodologies, such as Artificial Neural Networks (ANN), Case Base Reasoning (CBR) and Bayesian Belief Networks (BBN), which can learn from input data and utilize the learnings in making predictions.

2.4.3.1 Artificial Neural Networks

ANN are computational models with a 'neural' term used to represent the brain-inspired properties they tend to mimic. The neurons are simple units working in parallel forming different layers with no central control. Information is placed in the neurons and connections are formed during the learning process, where weights are calculated and attributed to each connection, in order to produce the end result. (Russel, 1995). Various types of Neural Networks have been utilized to predict structural deterioration utilizing past inspection records.

Five individual ANN were utilized by Li & Burgueno (2010) to develop bridge damage models based on Michigan NBI data. Specifically, to predict abutment rating, the variables of annual temperature difference, average daily truck traffic, approach type and structural type were chosen (Li & Burgueno, 2010). Inspection and maintenance records of Wisconsin's bridges were analyzed to model the deterioration of bridge decks (Huang, 2010). The Backward Prediction Model (BPM) was developed by Lee, et al. (2008) based on ANN for generating condition ratings when limited inspection records are available. The model utilizes the limited bridge records along with additional datasets such as traffic volume, population and climate to predict structural condition. The methodology was extended by incorporating Elman Neural Networks, time-based and state-based models, for the long term prediction of substructure condition (Bu, et al., 2015). Validation of the short-term predictions indicate that the method has similar performane with that of Markov chains, but differ a lot in their long term prediction results (Bu, et al., 2015).

Dissadvantages of ANN regard the deterministic nature of their results, thus they share the same dissadvantage with regression models (Morcous, et al., 2002). Another limitation regards the large number of data needed for reliable training. The most important issue,

though, regards the complicated procedures taking place attributing weights that best fit the training, rendering the output weights questionable, as it is difficult to understand the way they are produced.

2.4.3.2 Case Base Reasoning

Computational methods based on CBR are inspired by human reasoning, whose function is to solve new problems based on past solutions to similar problems. The methodology selects specific previous situation data and reuses results and experience to fit a new solution (Avramenko, et al., 2002). Thus, when a new problem is introduced, a cyclic process is followed, where the problem is matched with the most similar ones and the stored solutions are retrieved. Then, CBR proposes a candidate solution, if it doesn't meet the necessary requirements it adapts it by attributing a new solution, forming a new solution case (Avramenko, et al., 2002).

CBR has been utilized for modelling of bridge elements deterioration utilizing the data from Ministry of Transportation in Quebec (Morcous, et al., 2002). Parameters used in the model concerned materials, geometry, structure types, etc. and the results were compared to a multinomial regression developed for the same data, showing that CBR performs better (Morcous, et al., 2002).

A major disadvantage of CBR are that it may not be able to function when limited data exist. Attributing weights requires engineering judgement, thus subjective and domain specific knowledge for case adaptation, which makes it a task that is not simple (Morcous, et al., 2002).

2.4.3.3 Bayesian Belief Networks

BBN constitute probabilistic graphical models utilized to represent variables and the dependencies among them. The graphs consist of nodes and arcs representing variables and their relationships, respectively. The corresponding variable distribution is assigned to each node, while conditional probabilities are attributed to each arc. BBN are utilized when uncertain information is available for variables or relationships among them. This information is used as a prior to update and form the posterior distribution based on Bayes theorem. When variable distributions and relationships are time-variant, as is the case in structural deterioration, then the term 'dynamic' is introduced to signify this change. Rafiq, et al. (2015) developed a BBN model to represent deterioration of UK's railway masonry bridges. The model was combined with Markov chains to perform predictions, while, when new inspections would be available, the transition probabilities would be updated.

2.5 Issues of reviewed methods

The methods reviewed in this chapter share certain common disadvantages, which are presented in this section. These regard the reliability of the data utilized and the validation of the models' prediction results, as well as the factors taken to consideration and the interpretation of their effect.

2.5.1 Dependency on the reliability of older inspections

The statistical deterioration methodologies share a common disadvantage, which is linked to their dependency on multiple past inspections. In all reviewed work, a basic step before proceeding to probability calculations is the filtering of the inspection data for different years for each bridge. In many cases data have been excluded due to errors in coding or due to inappropriate evaluations for deterioration modelling. These errors can be attributed to human factor, errors performed during inspection procedure or minor rehabilitation work that has been performed. Furthermore, a 2001 survey conducted to assess the reliability of visual inspections of the NBI revealed that 95% of the examined sample was found to vary plus or minus 2 condition ratings (based on the 10-scale evaluation), 68% of which were found to vary plus or minus 1 condition rating (Phares et.al, 2004). Such observations render information of older inspections dubious and, therefore, filtering of untrusted inspections may result in selection biases, which are not traceable afterwards.

2.5.2 Lack of validation of long-term predictions

The way inspection data are utilized, validation of the different methodologies is only limited to verifying that the model fits the data. This is due to the way the different inventory years are utilized: either change in condition (state-based models) or duration in certain condition (time-based models) is attained by tracking individual bridges in time. As there are limited years of inspections that can be utilized, only few condition changes or condition durations can be tracked, which are utilized based on the bridge age to model deterioration of a single bridge. The validation of the attained model is performed by comparison of its output regarding condition or duration with a portion of the initial number of brides, which were intentionally not taken to consideration by the model (test sample).

Validating long-term predictions would require utilizing bridges up to a specific age limit, deriving a model and utilizing older bridges to validate the long-term results. Such

validation is usually not performed, as the Markov models normally require several bridges of all ages at each condition. Leaving out older bridges would reduce the number of bridges in bad conditions thus, more optimistic models would be derived. Therefore, only short-term validation is performed by utilizing models that have used all relevant data to predict the condition of a specific bridge and compare predictions with new inspection results.

2.5.3 Selection of deterioration factors

All reviewed statistical models make an initial selection of limited candidate factors linked to deterioration based on design principles. Factors explicitly taken to consideration during design may have a different statistical effect on the condition of the built structure compared to other factors arising during the structure's lifetime, as the structure was specifically designed to withstand the former factors. Although hypothesis testing with statistical significance is a useful tool, it can be misleading if the number of candidate variables is limited. Thus, such approaches may lead to inadequate models due to bias in variable selection. As the effect of uncertainties is incorporated in structural condition ratings, the selection among candidate factors from more complete lists is necessary. Furthermore, filtering of candidate factors should be performed by utilizing data analysis processes, such as the ones presented in the study of (Chang, et al., 2017), where initially a covariance matrix filters 30 NBI and 3 added candidate factors to eliminate similar effects and penalised linear regression is utilized to select among the remaining ones.

2.5.4 Lack of validation between models and literature

Although factors affecting deterioration are utilized to statistically model it and, in many cases, comparisons are made between the derived models, no further effort is made to link model results to actual deterioration mechanisms involved, such as corrosion or fatigue. Thus, models are statistically validated to reliably represent data, but the models' output cannot be generalized, as the deterioration mechanisms lack validation based on existing knowledge and literature. As mentioned above, there is also a necessity for calibrating existing mechanistic models or deriving new mechanistic models to describe the process of deterioration better. Statistical models can be utilized to assist in this task, as they can reveal both the qualitative and quantitative effects of the factors involved.

Such effort can lead to more suitable statistical models by incorporating additional factors and at the same time point out areas where future experimental research can be

conducted. The derived results can be utilized to enrich the knowledge of the mechanisms taking place and develop new or enhance existing mechanistic models.

2.6 Research needs

Based on the review of previous approaches presented in this chapter and their identified issues and disadvantages, the following research needs can be stated:

- Factors of bridge deterioration should be formally identified by studying a much broader selection of candidate factors.
- Validation of the quantitative and qualitative effects of the deterioration factors should be performed and linked to the relevant available literature.
- A method is required that can perform long-term predictions utilizing only limited data on past bridge conditions, preferably using just one year of inspection records. A way to validate such predictions is desirable.

This thesis attempts to contribute toward meeting these research needs by utilizing inspection records for just one year. It should be mentioned that, although the NBI database of the US containing such records is used, the methodologies applied and developed herein can be applied also to other inventories/countries and certain research results could be generalized.

3 The National Bridge Inventory

Before 'delving' into an analysis of the data of the National Bridge Inventory, details about the history of the database, the use of its information, as well as its reliability should be presented. In this chapter, such information has been gathered to reveal the reliability, but also the shortcomings of this large database.

3.1 What is the National Bridge Inventory?

The US Federal Highway Administration (FHWA) is responsible, by law, for the maintenance of an organized annual inventory - the National Bridge Inventory (NBI) - that includes more than 600,000 highway infrastructures (mostly bridges, culverts and a few tunnels) with spans longer than 6.1m located in the US. It is utilized to promote public safety by first evaluating the infrastructure needs and then allocating the appropriate funds. To accomplish this, each State is obliged to perform a variety of periodical inspections according to the National Bridge Inspection Standards (NBIS), to attain certain information for the structural and functional condition of each bridge. The collected information is then coded and sent to the FHWA, where the budgets for each State are agreed.

3.2 Brief historical note

The importance of road safety and the need for an organization to manage arising issues was well understood since 1893, when the Office of Road Inquiry was established. The inclusion of bridges in Federal Aid programs dates back to 1916, when the name of the organization was altered to Bureau of Public Roads. After many predecessors, the FHWA was created within the Department of Transportation as an agency in 1966 and began its action in 1967 (FHWA, 2012). In the same year, the collapse of Silver Bridge in Ohio River caused 46 deaths, despite having been inspected (Fig. 3.1). Long forensic investigations revealed that the bridge was not thoroughly examined to identify the flaw of the critical member (Bullard, et al., 2012; Lichtenstein, 1994). This raised the need for the implementation of certain inspection standards and the first National Bridge Inspection program was initiated in 1968 (FHWA & DOT, 2014). In 1971, the first NBIS were created by the FHWA and the American Association of State Highway and Transportation Officials (AASHTO). The following year, the first NBI was composed from the inspections performed nationwide in accordance with the NBIS. From 1972 up to present, yearly data have been collected for more than 600,000 bridges located in the US, constituting NBI the

richest bridge inventory at least nationwide (50 States, District of Columbia and Puerto Rico).

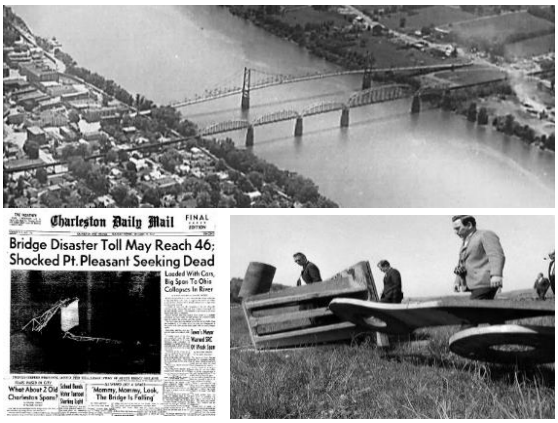

Figure 3.1: The silver bridge collapse at Point Pleasant and the structural part responsible for the failure.

3.3 Oversight responsibilities and legislation

The inspections and Federal aid programs have different levels of oversight. The principal statutes establishing the Federal-Aid Highway Program are found in Title 23 of the United States Code (23 U.S.C.), while regulatory requirements are generally found in Title 23, Highways, of the Code of Federal Regulations (CFR), section 650. The Federal-Aid funds are authorized by the Congress for Highway bridges. Each State, in accordance with 106.23.USC, defines the responsibilities of the FHWA and level of cooperation for the administration of the program. In order to receive Federal aid funds, each State must perform the necessary bridge inspections according to the NBIS for all owners except for the Federal. Their compliance is assessed by FHWA in accordance with 23 CFR 650 C, along with the composition of the NBI, which is published each year. Biannual reports regarding the condition of bridges for the Congress are also prepared by FHWA, as well as reports published by FHWA in the Federal Register used to improve the NBIS by permanent administrative laws. The funds apportioned to each State are available for a period of three years to be used for maintaining, rehabilitating or rebuilding the bridges. The overall procedure is oversighted by the Government Accountability Office (GAO), which conducts periodical investigations to monitor the procedures, each entity's level of compliance, as well as the overall efficiency of the whole program. The GAO reports problems to the responsible agencies and recommends changes to be performed and additional investigations to be carried out to track the progress.

3.4 Inspection Procedure

The NBI includes structures made of various materials, lengths and owners that comply with the NBIS. Each State is responsible to carry out inspections, to update the structural and functional condition of the bridges under its jurisdiction. The most common inspections are the 'routine' inspections. Those are usually visual inspections performed at least once every two years, during which in-depth inspections may be scheduled or recommended by the inspectors. All specifications to qualify the inspection teams and procedures are included in the NBIS. The information gathered for each bridge is in specific coded form displayed in the FHWA coding guide (FHWA, 1995). This guide also includes instructions for the required information, while allowed methods of determining, measuring or evaluating different aspects of a bridge can be found along with their appropriate coding. All coded reports are sent to the FHWA, where checks for errors and inconsistencies are performed.

3.4.1 Condition ratings

Different types of inspections exist among the structures included in the NBI, depending on the structure type (bridge, culvert or tunnel). Inspectors evaluate each bridge following a scale ranging from failed (0) to perfect (9), which must be representative of the whole structural component evaluated (Table 3.1). Each condition rating represents specific types and extents of failures that can be detected during an inspection. The coding guide provides general indications, but a more detailed version for each material type is used to attribute a rating.

Table 3.1: General condition ratings for evaluation of the main bridge components (FHWA, 1995).

RATING	CONDITION	Explanation
9	EXCELLENT	
8	VERY GOOD	No problems noted.
7	GOOD	Some minor problems.
6	SATISFACTORY	Structural elements show some minor deterioration.
5	FAIR	All primary structural elements are sound but may have minor section loss, cracking, spalling or scour.
4	POOR	Advanced section loss, deterioration, spalling or scour.
3	SERIOUS	Loss of section, deterioration, spalling or scour have seriously affected primary structural components. Local failures are possible. Fatigue cracks in steel or shear cracks in concrete may be present.
2	CRITICAL	Advanced deterioration of primary structural elements. Fatigue cracks in steel or shear cracks in concrete may be present or scour may have removed substructure support. Unless closely monitored it may be necessary to close the bridge until corrective action is taken.
1	"IMMINENT" FAILURE	major deterioration or section loss present in critical structural components or obvious vertical or horizontal movement affecting structure stability. Bridge is closed to traffic but corrective action may put back in light service.
0	FAILED	out of service - beyond corrective action.

3.4.2 Evaluated bridge components

For each bridge, three condition ratings are recorded for its macro-components –deck, superstructure and substructure– each of which is evaluated and given a rating corresponding to the overall condition of the respective elements. Additional inspections of the foundations are performed to evaluate scour for bridges located over waterways. The deck is the structural part that carries traffic directly on it, superstructure supports the deck and connects the substructure elements together and the substructure is responsible for supporting the superstructure and transfers the applied loads to the bridge foundation. The FHWA uses the mentioned ratings along with other measurements to attribute a sufficiency rating on a 100 scale used for prioritization of rehabilitation/reconstruction and, therefore, budget allocation.

3.4.3 Inspection types and frequency

Five different types of inspections are performed according to AASHTO notation (Inventory, Routine, Damage, In-Depth and Interim) that vary in depth and frequency.

When a newly built bridge is delivered to traffic, an 'Inventory' inspection needs to be performed within 90 days for State or 180 days for local jurisdiction. Its main purpose is to fully document the structure's details for the NBI and to determine analytically the loading capacity of each bridge. Apart from the data required from FHWA and NBIS during this inspection along with prior review of the plans, the baseline structural conditions are determined and the critical members of each structure are identified. A similar inspection is also performed when rehabilitation action has been taken and a bridge has undergone changes in structural or/and geometrical configuration. For the last case, additional inspections should be included.

The 'Routine' Inspection is regularly scheduled at least once in 24 months. Observations and necessary measurements are performed to determine the physical and functional condition of the bridge, to identify the progression or development of structural problems compared to prior inspections. These inspections are performed from deck, ground or water level or by using adequate means to access the evaluated areas of the structure. The inspection results are accompanied by the appropriate site photographs and reports regarding maintenance/repair recommendations or by a requirement for a further, more in-depth inspection.

Another type of inspection is the 'Damage' inspection, whose main purpose is to assess structural damage resulting from environmental factors or human actions. The duration of this inspection may vary depending on the extent of the damage that has to be evaluated and

it may be followed by more thorough inspections. These are also the so-called 'in-Depth' inspections, which are time consuming and demand specialized personnel (e.g. divers for under water inspections) to be performed, whereby deficiencies of structural members that cannot be seen by other inspections are evaluated. Nondestructive tests and other techniques are used, in order to fully evaluate the bridge. The last type of inspections are the 'Interim' inspections performed to monitor documented deficiencies.

3.5 Public disclosure and form of the NBI

Each year an NBI data file is uploaded to the FHWA website containing all information gathered by the States. The information collated regards 116 different parameters named as items that are strictly coded according to the guide (FHWA, 1995). The files are downloaded in .txt format; every line represents a listed structure and each character/number of the coded file has a certain length (columns) based on the item described. The total information could be categorized into eight groups (Radovic, et al., 2016): general description, functional or operational capacity, design, geometric information, waterway and approach data, work recommendations and project costs and bridge loading and structural ratings.

The information of the NBI is publicly accessible. Although this database has been in electronic form since 1972, some items have been periodically disclosed to the public (Lwin, 2007). An example for public disclosure policy was due to the events of 11 September 2001, when the FHWA removed the whole NBI file from its website. After a specific study regarding government Agency data, FHWA decided that all information would be available to interested users, as the information provided could not be used for harm (FHWA, 2012).

3.6 Reliability of the NBI

Since 1972, many inspection records have been collected and several revisions have been performed due to the mechanisms mentioned above. Over the years both the GAO and FHWA revealed flaws that created errors or undermined the level of data accuracy. Their importance lies on the fact that Federal Aid funds are apportioned based on the total deficient deck area of each State. Thus, the FHWA's policy is to minimize errors that could affect the overall program and jeopardize public safety.

Since 1988, the GAO has found important inconsistencies regarding items decisive for the apportionment of funds. There have been cases, such as in the State of Georgia in 1986, where the substructures of wooden structures were arbitrarily given lower ratings (GAO, 1988). This could be linked to the specific policy of apportioning funds, which has been criticized as a counter-incentive for reliable evaluation (House of Representatives, 2010).

Hence, FHWA was able to detect such inconsistencies, but was not able to prevent inconsistencies of similar nature from happening in the future (GAO, 1988). There were also errors of mathematical nature noticed by the same report that led to under-estimation of the actual needs of California (GAO, 1988).

Another source of important errors was the quality of the performed inspections. The most common inspections are visual (routine). Despite some State effort to perform such investigation on a local scale, the first national scale investigation was firstly conducted by FHWA (Moore, et al., 2001). The specific investigation was performed by the Non-Destructive Validation Center (NDEVC) of FHWA, which tested the reliability of visual inspections. Specifically, 10 field inspections were used to evaluate a sample of 49 inspectors from 25 States; the investigation included both NBI ratings and element level ratings (Phares, et al., 2004). The results revealed significant variations for both types of inspections; for NBI ratings specifically, 95% varied within two rating points, while 68% varied within one (Phares, et al., 2004). The reasons for these deviations were attributed to the general form of the condition ratings from the coding guide, as well as the inspection teams, their training and the procedures followed.

The ability of FHWA to implement and upgrade its level of effectiveness can be measured by the overall number of bridges in poor condition, which is shown to have decreased from 2002 to 2013. This implies that the bridges should be safe for the public to travel with preventive maintenance or corrective work performed based on the actual condition. From an investigation of the DOT's database of New York's bridges, the U.S. projected average bridge failure rate is between 87 and 222 bridges annually, with an expected value of 128.55 (Wesley , et al., 2014). Most of these bridge failures are linked to hydraulic failures and accidental factors, but few (5%) deal with deterioration and fatigue (Wesley , et al., 2014), which can be either avoided or safely planned to be repaired. In 2007 the collapse of the I-35 steel bridge in Minneapolis triggered a series of investigations from GAO and FHWA, but also the implementation of new policies. Specifically, FHWA investigation revealed extensive errors for more than one third of bridges of the same type as I-35 (FHWA, 2009). In the same report, it is pointed out that, despite tracking these errors, there is no time limit for the States to correct them.

In 2012, the law 'Moving Ahead to the 21st Century (MAP-21) Act' was signed (Federal register,2014). Its importance lies to the fact that the States would be evaluated annually from FHWA for their compliance, while financial penalties for the non-compliant States would be imposed. Specifically, FHWA will use 23 inspection criteria, called Metrics, to perform the annual compliance review. These metrics directly affect the NBI data

reliability, as a random sample of bridges is reevaluated from inspection personnel and the new evaluations are compared to those published in NBI (FHWA, 2013). Additionally, there is a time frame of 12 months for the non-compliant States, within which they need to provide a plan of corrective actions, in order for the financial penalties for corrections not to be imposed. Furthermore, since 2014, apart from the three main structural evaluation groups (deck, superstructure and substructure), a complementary element-level inspection and evaluation is also required (FHWA, 2012). The whole procedure led to a 97% reduction in errors from 2008 to 2013 (Fig. 3.2).

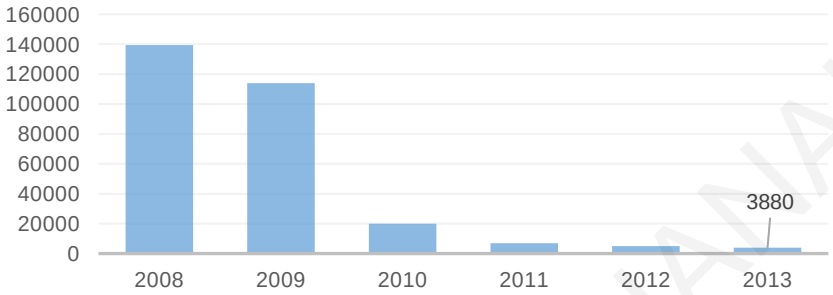

Figure 3.2: Errors found from the edit-update program of FHWA for different NBI records.

3.7 Exploitation of NBI for research (literature review)

Besides the initial purpose of the NBI to monitor the overall program, the inventory has been used for research purposes around the world. Reasons for selecting the NBI is the free online availability of data, its consistency and the reliability stemming from the fact that a monitored continuous process of improving the quality of both inspections and data is performed. The ongoing research using the inventory has led to the advancement of sophisticated Bridge Management Systems (Enright & Frangopol, 1998). First, in 1982, the inventory was used to present infrastructure budgeting needs for the succeeding years (National Research Council, 1984). The NBI of the State of Indiana was used to model the deterioration of bridge substructures (Jiang & Sinha, 1989). The different bridge types and performance patterns using descriptive statistics and the 1988 NBI record were presented by Dunker and Rabbat (1990). Using similar methodology, the same authors also used the inventory to present the 40 years of prestressed concrete bridges (Dunker & Rabbat, 1992) and to assess highway bridge deficiencies (Dunker & Rabbat, 1995).

In 1991, new bridge inspection strategies were proposed by Hachem et al. (1991), after statistically analyzing the NBI and using various deterioration models. Veshosky et al. in 1994 utilized the NBI to study superstructure deterioration using regression analysis, revealing age as the primary factor and ADT following. Ordered-probit models (Madanat et

al., 1995) and Poisson regression models (Madanat & Ibrahim, 1995) were also applied to multiple NBI datasets for the estimation of condition transition probabilities and to evaluate bridge deterioration. Additional work in deterioration modeling and transition probabilities has been presented by Madanat et al. (1997). Probabilistic and semiparametric hazard models were used to incorporate random effects of the earlier probit models for the estimation of transition probabilities (Mauch & Madanat, 2001; Mishalani & Madanat, 2002). The results of studies performed by researchers and DOTs that used the NBI were presented by Ramey and Wright (1997), to compare the different deterioration rates between States. Inventory data were also used to develop a method that calculates annual risks associated to scour failures of foundations, with the purpose to prioritize repair of critical bridges (Stein et al., 1999). Chase and Gaspar presented a method that linked the reduction of load-carrying capacity to bridge deterioration using regression analysis and Markov chains for both NBI and Hungary's database (Chase & Gaspar, 2000). Regression analysis was also performed for the bridges of the State of Illinois to derive deterioration models of various bridge parts (Bolukbasi et al., 2004). The NBI Florida records from 1992-2005 were utilized to study deterioration patterns using hazard functions (Sobanjo et al., 2010). The 2007 inventory of North Dakota was also analyzed, using GIS regression analysis and Pearson correlation, to identify critical sources of deterioration (Kim & Yoon, 2010). A number of distributions were used to model the reliability of Wisconsin's bridge decks using the 2005 inventory (Tabatabai et al., 2011). Artificial Neural Networks were used to develop a model that generated historical bridge condition ratings, in order to fill-in inspection records (Lee et al., 2008). The same method was used to predict the long term bridge performance utilizing NBI records (Bu et al., 2014). Various performance measures were also developed using descriptive statistics and the NBI records were analyzed to reveal deterioration trends and structural performance (Farhey, 2010; 2012; 2013; 2014; 2015, 2016). In addition, recent research using the NBI includes prediction of structural deficiency ratio of bridges (Adarkwa & Attoh-Okine, 2016), detection of concrete dek condition deterioration parameters using two step cluster analysis (Radovic et al., 2016), integration of bridge management systems and non-destructive evaluations (Hearn & Shim, 1998).

Apart from the mentioned studies that are linked to deterioration modelling, the NBI has been used for other purposes, such as: the automatic detection of logical inconsistencies (Din et al., 2016), adaptive optimization on system level management (Liu & Madanat, 2014), risk assesment of stream modifications (Jones et al. 2015), estimation of load impacts on bridges (Weissman et al., 1993), effect of truck weight regulations on US bridge network (Ghosn & Moses, 2000).

4 Data analysis

In this chapter, processes of extracting and gathering sample data and their statistical analysis are presented. The data of the NBI, as well as of additional sources, are jointly used to simulate each bridge's environment adequately. A number of statistical methods are utilized to quantify and summarize the influence of environmental factors on bridge condition. The results rank the factors based on the severity of their effect on the structural condition of the evaluated bridge components.

4.1 Introduction

Today's society relies on data collected from multiple sources, which are then combined and processed to produce information that assists decision making at various levels, ranging from everyday life to very specialized cases. All these processes can be included in the broad term of 'Data Analysis', where various tools, such as data visualization, hypothesis testing and other statistical methods, are employed to handle samples and select the most appropriate variables that should be used to model reality.

Infrastructures in general encompass various engineering aspects, which can be treated effectively when relevant data are available. In this respect, experimental data are important. Hence, materials and their application can be tested (e.g. Wan, et al., 2006, Dimitriou, et al., 2018) and then mechanistic models can be derived to simulate their properties, which are subsequently applied in structural design (Zhou, et al., 2004). In such cases, the implementation of data analysis procedures is very rare. On the other hand, data analysis is often used in the area of project costing (Dimitriou, et al., 2017) and has been utilized for managing infrastructure levels of service (Dimitriou & Stathopoulos, 2016; Pereira, et al., 2018). An additional aspect, which affects users and decision makers regards managing infrastructure needs using information gathered by monitoring/inspecting structures. Infrastructures and more specifically bridges are exposed to many factors, which could worsen their structural condition. When reliable data are available, a data analysis process can confirm or challenge building practices and design processes already applied, but also assist in modelling deterioration by identifying factors affecting it.

The NBI has been used by many researchers to investigate structural deterioration and material performance for bridges. In the various statistical methods that have been utilized for this task, the explanatory variables are usually selected by expert judgement (Mauch & Madanat, 2001; Chang, et al., 2017). Such approaches may derive erroneous models due to

the lack of other variables, which may be affecting structural deterioration more. Another common practice usually employed is the utilization of bridge data of one individual State and inclusion in the assessment of additional explanatory variables, such as weather data and other data available from GIS (Kim Yail & Yoon, 2010). In these cases, although maintenance policies and acquired data can be considered uniform, the limited variation of exposure factors can lead to modelling errors. On the other hand, when utilizing the whole US bridge sample, many exposures have to be taken to account and not including them in the analysis may also lead to misleading results due to averaging. Furthermore, questions arise regarding the effect of typical factors suggested by experts, which have already been taken to account during the design process. Thus, a process is needed to select the variables, which should be incorporated in modelling structural deterioration. Recently, data analysis procedures have been utilized to select among factors affecting deterioration. Relevant efforts have been made either by including limiting assumptions for the factors considered (Radovic, et al., 2016) or by studying an individual State and considering only NBI factors (Chang, et al., 2017).

In this chapter, NBI data for the conterminous US are utilized to study the factors affecting the structural condition of bridges. To achieve this, it is assumed that hazard driven maintenance/rehabilitation policies are predominant and that the State effect can be neglected. Additional reliable sources were used, such as Climatic data from National Oceanic and Atmospheric Administration, (NOAA, 2017) and earthquake hazard data from United States Geological Survey (USGS, 2017), and were combined with bridge data using spatial interpolation methods. Data analysis procedures (fig. 4.1) were utilized to explore and attain an appropriate model for the combined dataset, whose main purpose is to reveal the predominant factors affecting structural condition.

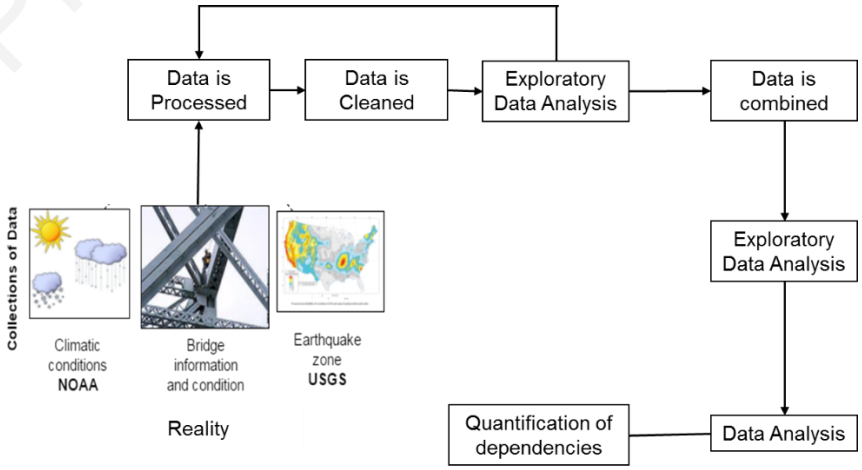

Figure 4.1: Data analysis processes utilized in this chapter.

4.2 Description of analyzed data

4.2.1 Selection of NBI information

The NBI files processed are the most recent ones, which were released in 2017 and refer to 2015-2016 inspections. The information coded in these files, which are freely downloadable in .txt format, is associated with 116 primary items for a total of 614,387 structures. One text file holds the information for all structures of each of the 52 States; each structure is represented by a line in the file of the respective State; the data for each item are given through one or more characters/digits within the overall 434 specified positions in each line, as described in the coding guide (FHWA, 1995).

Initially, 68 items were selected, for which data were extracted from the NBI files. These data items provide information about bridge identification, location, dimensions, usage, materials, structural evaluation, inspection details, rehabilitation actions and various costs Appendix (A-I.1.1). The selection of the data items was made to serve the basic purpose of studying bridge deterioration, as well as to validate data correctness. The data were processed to track inconsistent codings, as well as logical errors. Then, a first filtering of the data was performed to reduce the number of structures included based on the specific interests of this study. Further reductions were also performed at a later stage for combining all data available and facilitating their analysis.

4.2.1.1 Information extraction from NBI files and identification of inconsistencies

The required information was extracted from the NBI text files using a self-developed Matlab code implementing three main processes (Appendix A-I.1.1-A-I.1.3). In the initial process, Matlab's *scanf* function was utilized to read the data for the 68 selected items (Appendix A-I.1.2.1). For the case of character inputs, the read information was immediately 'translated' to predetermined numeric values, which are easier to handle. For the case of numeric inputs, on the other hand, the read digits were combined and the input precision (decimal point) was attributed to produce the actual data value. The second process checked the numeric data values with respect to the limitations provided in the guide (FHWA, 1995). Out-of-range codings were given certain numeric values to indicate the type of error identified (Appendix A-I.1.2.2). The third process gathered all extracted information into a single matrix, to facilitate data analysis and the search for logical inconsistencies (Appendix A-I.1.2.3).

The total number of inconsistencies (violations of the guide specifications) detected was 12,404. The whole process followed was described in a report and sent to FHWA

(Appendix, A-I.1.3). A complementary Excel file was also included to help each State authorities locate the type of error made for structures located within their territory (not contained in this Thesis). Inconsistencies included errors in coding items, the vast majority of which was performed in coordinates (items 16 and 17) and in year of future ADT estimate (item 30). Inconsistent records of coordinates were processed to include entries that didn't include all the necessary digits of precision. Thus, lower precision records were salvaged, reducing exclusions to 2035 bridges, where no value was available. Regarding the year of future ADT estimate, as this information would have no impact on the current stage of the study, the inconsistent records were kept with appropriate coding.

As mentioned in chapter 3, there are continuous efforts to limit mistakes and inconsistencies, as well as to improve the quality of inspections. To investigate the effectiveness of these efforts, older NBI databases were also examined with respect to inconsistencies following the aforementioned processes. This investigation was concentrated only in identifying wrong bridge coordinates. Figure 4.2 shows the number of mistakes found in each year's NBI database. It can be noticed that most coordinate mistakes have been corrected over the last years.

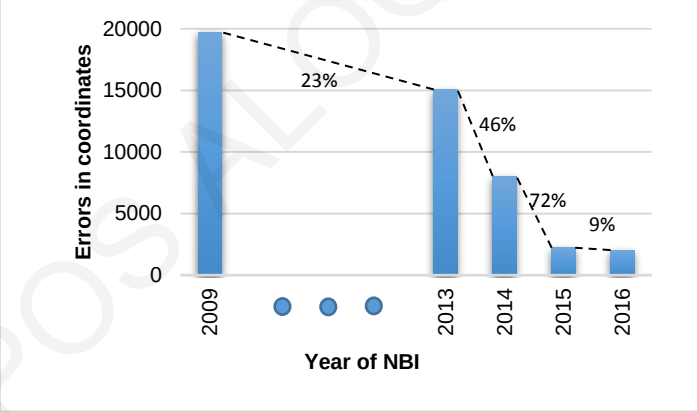

Figure 4.2: Number of bridge coordinate mistakes in the NBI databases of various years. Percentages show the relative reduction in the number of mistakes from past to recent years.

4.2.1.2 Filtering of extracted data

Not all structures included in the NBI database are of interest in this study, therefore certain criteria were used to exclude these. More specifically, the following structures were removed from the assembled matrix: 138,248 culverts, 5,277 filled arch bridges, 1803 structures built before 1900, 64 structures with logical inconsistencies in their data, 62 structures with year of reconstruction greater than 2017, 137 structures with year of inspection before 2006 corresponding to bridges of lower conditions that have not been reevaluated and 2035 structures with missing coordinate. Moreover, 23,555 bridges were

excluded, as they had superstructure materials different from concrete, steel and prestressed concrete. In total, the exclusions were 166,750 (the aforementioned exclusion criteria created some overlaps), leaving a remaining population of interest of 447,637 bridges.

4.2.2 Climatic normals

Structures are affected in the long term by local weather conditions, therefore the most appropriate respective data to take into account are the 'climatic normals' (Arguez et al. 2012). Although other data sources could be utilized for weather information, only NOAA provided the climatic data needed for this study. NOAA sustains a large collection of climatic and weather data, manages and maintains a relatively dense network of weather stations all over the US and a sparser network over the world. The US climatic normals are average values of climatological variables over a 30-year period (1981-2010) characterizing the conditions at each location (NOAA, 2017). The data are taken at about 9500 stations, forming a scattered network of measurement points. This network is reduced depending on the availability of specific measuring instruments (e.g. hourly recording stations for dew point temperature are only 420). The selection of climatological data for the present study was based on the available literature on materials corrosion, as well as on other relevant studies that used NBI or other inventories. Hence, the climatic normals utilized are:

Annual precipitation/rainfall

Rainfall could be linked to bridge deterioration due to the leakage of decks to superstructure and substructure elements (Radomski, 2002). As the amount of rainwater leaked to bridge elements can indicate the intensity of precipitation as a deterioration factor, data on the total annual rainfall (in inches) were included in the analyses of the present work.

Days of snow depth above 1 inch in a year

Snow is taken into account as a load on structures, but operational bridges are not really affected by the load associated with the total depth or maximum depth of snowfall throughout the year. However, bridges, as part of the roadway network, are subjected to the general actions taken to restore driving safety, when a certain snow depth is reached. Frost formation can take place even for limited snowfall, which affects the structure through the mechanism of freeze thaw cycles (Radomski, 2002). The most serious effect, though, is the anti-icing procedures that could damage the deck directly, as well as the deicing chemicals

that would be absorbed from the structural elements (Radomski, 2002). To investigate these effects, the snow depth of 1 inch was adopted as a threshold, as deicing is applied even on few centimeters of snow to prevent the formation of frost (White, et al., 2006). As this procedure may be repeated, the duration in days is indicative of the effect of deicing. Thus, the map of US regions where deicing is allowed was copied as an image (FHWA, 2017) and, using Google Earth, the corresponding coordinates were identified to be included in the analysis.

Minimum monthly average temperature

Corrosion is accelerated by increase of temperature, as its chemical reaction is exothermic (Bentur, et al., 1997). Hence, minimum average temperature was taken into account, actually the lowest monthly average value in the vicinity of each bridge.

Monthly diurnal temperature range

The monthly diurnal temperature range is the difference between the monthly maximum and minimum temperature. Changes in temperature from low to high on a daily basis can affect structures due to freeze and thaw cycles, changes of humidity content inside the pores of concrete structures (Bentur, et al., 1997) or changes in time of wetness of steel structures (Orchard Ltd., 2004). The diurnal temperature range provided the information needed to calculate also maximum temperature, as well as average temperature, if needed.

Hourly dew point temperature and relative humidity

The dew point temperature is a weather attribute that actually reveals the maximum concentration of water that could be present in the air. A higher dew point temperature corresponds to a greater amount of water vapor that the air can hold. Relative Humidity (RH) is the percentage of water vapor in the air relative to the amount needed for saturation at the same temperature, i.e. it is a measure of the concentration of vapor in the air. A smaller difference between the air temperature and the dew point temperature corresponds to a higher relative humidity, i.e. the atmosphere is closer to the state in which water vapor would condense. The hourly observations for dew point temperature taken from NOAA were transformed to monthly data for uniformity to other data. Further on, the RH was also estimated using the following equation (eq.4.1) linking relative humidity, dew point temperature T_d and air temperature T with satisfactory accuracy (Lawrence, 2005):

$$RH \approx 100 - 5 \cdot (T - T_d) \quad (4.1)$$

The air temperature used in this equation was the maximum temperature, which corresponded to the minimum RH. It is worth mentioning that RH calculated by the above equation is an abstract measure of the water content in the air, but normally it is also affected by the microclimate at the bridge's surrounding.

Seasonal average of temperature data

The monthly data cannot be utilized in analysis, but can provide a more appropriate seasonal average, avoiding the equating of mild and high extreme areas mentioned earlier. Thus, preliminary exploration of the data was performed to categorize monthly temperature data (minimum temperature, diurnal temperature and dew-point) in to two groups corresponding to warm and cold seasons (Fig. 4.3). Warm months were those with almost all temperatures above 0 ^{o}C, while cold months were those that lower temperatures could be noticed. For the rest of the analysis, the warm months' data were taken to consideration, as most corrosion processes are halted during prolonged low temperatures below 0 ^{o}C (Bentur, et al., 1997). Additionally, the diurnal temperatures showed greater variation and higher values for warmer periods. Between the two seasonal temperature groups, a high Pearson correlation was found revealing that lower temperatures of 'cold' months are generally related to lower temperatures in 'warm' months.

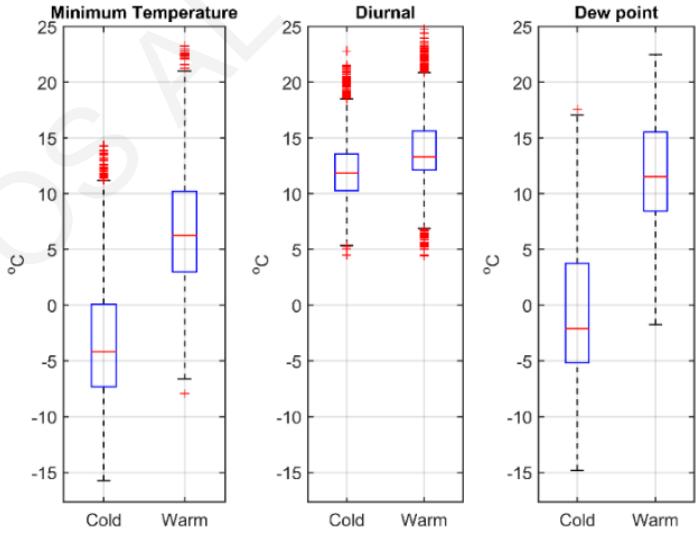

Figure 4.3: Box plots of temperature observations of the weather stations. Cold months refer to November, December, January, February and March; Warm months refer to April, May, June, July, September, October.

Weather station elevation

The elevation data of each weather station was also taken into consideration for later analyses, but not for deterioration. Errors were noticed in some elevations and were corrected using Google Earth.

4.2.3 Coastal areas

The combination of the corrosion factors mentioned earlier, as well as the existence of airborne chlorides, render the coastline as an interesting area to analyze. Thus, high precision coastline/shoreline coordinates were downloaded from NOAA (NOAA, 2017) and offset to certain distances using AutoCAD. The total distance spanned inland was 10 km with one-kilometer distance categories to be attributed to each bridge. Additional divisions for the first kilometer (at 250m and 500m inland) provided adequate categories to study the effect of airborne chlorides. This categorization of distances allowed also the determination of the critical distance, up to which the coastline affects structures. Further detail is provided in Chapter 5, where case studies are presented for different coastal regions of the US.

4.2.4 Earthquake hazard (PGA)

Earthquake resistance is a crucial attribute for a structure's service life. Damage to bridges results usually from complex effects by various contributing variables that interact together. In earthquake design, the soil consistency, the structure's fundamental period, as well as the Peak Ground Acceleration (PGA) and the earthquake duration are indicative for the hazard that needs to be taken into account for seismic design and estimating expected damage (Chen & Duan, 2017). PGA, usually measured in terms of the acceleration of gravity (g), is the main variable typically used to represent the intensity of a ground motion (Chen & Duan, 2017), but the seismic effect can be magnified by the other mentioned factors.

The US has various networks that collect real time seismic data. Specifically, the National Seismic System (ANSS), whose aim is to provide situational awareness for emergency responses for the whole US, the National Earthquake Information Center (NEIC), the National Strong Motion Project and 15 regional USGS networks. Although a vast amount of data exists for earthquake incidences within the US territory, a more general characterization would be more suitable for the purposes of the analysis to follow. Seismic hazard maps are a product of analysis that considers past faults and earthquakes, behavior of seismic waves travelling the crust and near-surface site conditions (USGS, 2017). Such maps are available from USGS, derived from analyzing data from the whole US network in cooperation and under the monitoring of ANSS. The seismic hazard with 2% probability of exceedance in 50 years, measured in PGA units (g), was chosen to be incorporated in the analysis process. Relevant data were downloaded from USGS for the conterminous US in the form of gridded data-points (every 6 km) that formed a dense network of calculated hazard points.

4.3 Combining the datasets

The aforementioned datasets provide information with different spatial distributions. As an initial step, to avoid sampling errors and to achieve an even greater level of uniformity of standards, bridges and weather stations located only in the conterminous US (spatial distribution of PGA) were selected.

Each dataset's spatial distribution serves a different purpose. Bridges are located where needed to provide continuity of transportation network, weather stations to track weather changes of certain terrain and PGA data are the products of analysis, gridded to provide accurate design parameters for the seismic design. In this section, the spatial distributions of the complementary data are used to estimate/predict the values of these attributes in the vicinity of each studied bridge. This is achieved by using spatial interpolation, which utilizes the main assumption of geography that 'everything is related to everything else, but near things are more related than distant things' (Tobler, 1970).

Numerous spatial interpolation methods and respective combinations are available in the literature and software packages. A basic step toward deciding on choosing appropriate interpolation methods suited for the particular datasets studied herein includes validating the different methods for the desired level of precision. Additionally, the type of data plays a significant role as well as the network of observation, if it is gridded or scattered and its density. The NOAA data are scattered due to weather station locations while the USGS data are densely gridded (with respect to bridge size).

The USGS proposes four different interpolation methods to be used for the earthquake hazard data depending on the smoothness of the results to be achieved. Specifically, inverse distance weighted (IDW), Kriging, natural neighbor and spline. As this study required PGA values at specific points (bridge locations) and not surfaces, smoothness of the results was not a priority. Thus, IDW was selected, which provided the simplest proposed interpolation method. The values predicted by IDW were validated using an application provided in the USGS webpage. On the other hand, the complexity of climatic data and their scatter, demanded a more sophisticated approach. Generally, for spatial interpolation of climatic data, Kriging interpolation is preferred (Sluiter, 2009) as it takes to account the spatial variation of the studied attribute with distance. Additional studies reveal the superiority of Kriging to other methods for precipitation data (Mair & Fares, 2011; Hartkamp et. al 1999).

4.3.1 Short description of methods used

As mentioned, IDW is a deterministic method, correlating only distance to the spatial distribution of the studied attribute using the formula (eq.4.2) (Longley, et al., 2005). For the case of PGA, linear interpolation was performed, using unit exponent in the formula (eq. 4.2). For the application of IDW to the earthquake data no limitations restricted the method since the network was densely gridded.

$$F(r) = \underbrace{\sum_{i=1}^{m} w_i \cdot z(r_i)}_{\text{General form of interpolation}} = \frac{\sum_{i=1}^{m} \frac{z(r_i)}{|r - r_i|^p}}{\sum_{j=1}^{m} \frac{1}{|r - r_j|^p}} \qquad (4.2)$$

where,

$F(r)$: the value of point r where no observation exists; r_i, r_j: the points of observations; $|r\text{-}r_{i \text{ or } j}|$: distance between observation i or j and point of interest; p: exponent with 0 value corresponding to the mean of all observations, 1 to linear and 2, to inverse distance squared.

For Kriging spatial correlation is assumed between locations of certain distance or/and direction to explain the variation of the studied attribute. Different kriging estimators exist, their difference lies to variations of the basic linear regression estimator $Z^*(u)$ defined in formula (eq.4.3) (Goovaerts, 1997). To decide which kriging type should be used firstly the correlation between elevation and weather attributes was confirmed to be below strong (0.75). The certain limit restricts the selections of kriging by excluding the application of multiple regression to consider elevation changes (Goovaerts P. 2000). Additionally, the assumption that a constant local mean (eq.4.3) exists instead of a constant and known mean (eq.4.3) lead to the selection of ordinary Kriging. To determine the weights, the variance of the estimator (eq.4.4) is minimized. To see if these assumptions are validated, the histograms were plotted showing the distribution of the studied attribute (e.g. temperature data in fig.4.4)

$$Z^*(u) - m(u) = \sum_{a=1}^{n(u)} \lambda_\alpha \left[Z(u_a) - m(u_a)\right] \quad (4.3)$$

$$\sigma_E^2(u) = Var\{Z^*(u) - Z(u)\} \; (4.4)$$

Where,

u: location vector for estimation point ua: location of the neighboring data points; *n(u)*: number of data points in local neighborhood used for estimation of $Z^*(u)$; *m(u)*, $m(u_a)$: expected values (means) of *Z(u)* and $Z(u_a)$; λ_α: kriging weight assigned to datum $z(u_a)$ for estimation location u; $\sigma_E^2(u)$: variance of the estimator

To incorporate spatial correlation, the variation between observations of distance groups (h) is calculated in a semivariogram using the formula (eq. 4.5) (Longley, et al., 2005). For isotropic data, the semivariogram can be simplified into a radial function dependent on h. The data are fitted appropriately using different functions (linear, spherical, exponential, Gaussian), for the temperature observations illustrations of the anisotropic variogram and isotropic variogram fit are presented in Figure 4.4, the rest fitted models can be found in Appendix (A-II.1).

$$\gamma(h) = \frac{1}{2Var[\{z(r+h) - z(r)\}]} \approx \frac{1}{2N_h \sum_{(ij)}^{N_h} [z(r_i) - z(r_j)]^2} \quad (4.5)$$

Where, γ(h): the semivariogram*;* N_h:of pairs of points which are separated by the vector h within a small tolerance Δh (size of a histogram bin), *$z(r_i)$:observations at points $r_{i,.}$*

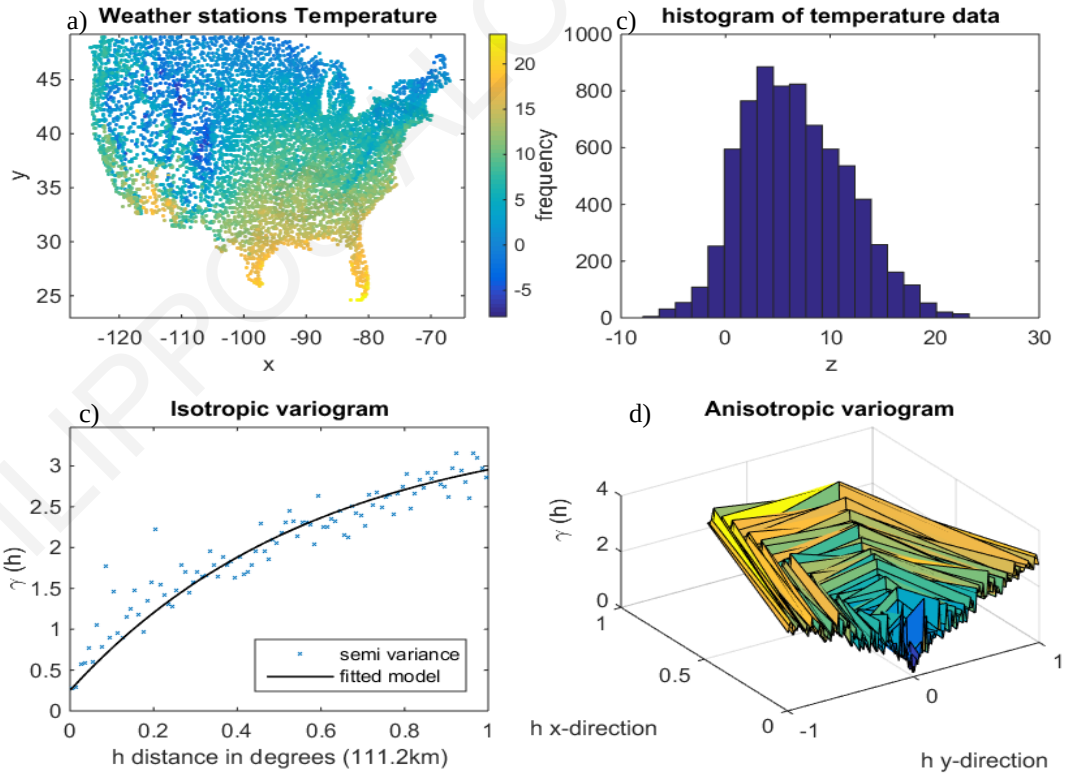

Figure 4.4: Plots using the matlab code of Wolfgang Schwanghart a) weather stations in the US, b) the histogram indicating the distribution of the phomenon studied (in this case the minimum average Temperature), c)the isotropic variogram and d)the anisotropic

To perform ordinary Kriging interpolation the gstat package in R (R-core team, 2008). Cross-validation Krigging contained in the same package was utilized to determine restrictions based on minimizing the mean square error (MSE). Specifically, the cross-validation process temporarily excluded observations and predicted the missing value. The residuals of the prediction and the actual value were calculated by the temporarily excluded observation that exist in that same location. The MSE was calculated using the residuals and was normalized (NRMSE) dividing by the range of each dataset presented in Table 4.1. The restriction imposed for ordinary Kriging were:

- Maximum Euclidean distance selected for kriging interpolation was 1^o latitude/longitude corresponding to 111.2 km
- Minimum of two observations and a maximum of 10
- Maximum of two observations per quadrant

Table 4.1: Cross validation results using Weather stations are excluded and their values are predicted.

Data	Observations	Method	Model RMSE	NRMSE	Predicted
Temperature (^{o}C)	7186	Ord. Kriging	0.901	0.0111	441519*
Diurnal Temp (^{o}C)	7186	Ord. Kriging	1.3050	0.0188	441524*
Annual Precipitation (in)	8864	Ord. Kriging	3.4216	0.0010	441298
Snow depth >1in (days)	4970	Ord. Kriging	13.70	0.0005	437027
Dew Temp (^{o}C)	412	Ord. Kriging	0.6265	0.0133	289466
Earthquake (g)	611309	IDW	-	-	443603

*Differences to the predicted number of bridges are due to singularities that occur within the R package g-stat.

4.3.2 Results

The MSE and NRMSE shown in Table 4.1 are very low and even lower errors are anticipated as stations are located strategically to capture climatic changes from the geographic terrain. Most errors occurred in dew point temperature as the hourly weather stations are less. The results of interpolation are shown briefly in Figure 4.5 while more detailed figures can be found in Appendix (A-II.2- A-II.8). Although a GIS package could have been utilized for handling, combining and visualizing the datasets, the capabilities of Matlab and R-package software's data extracting, processing and analyzing are adequate, provided that respective programming code can be written.

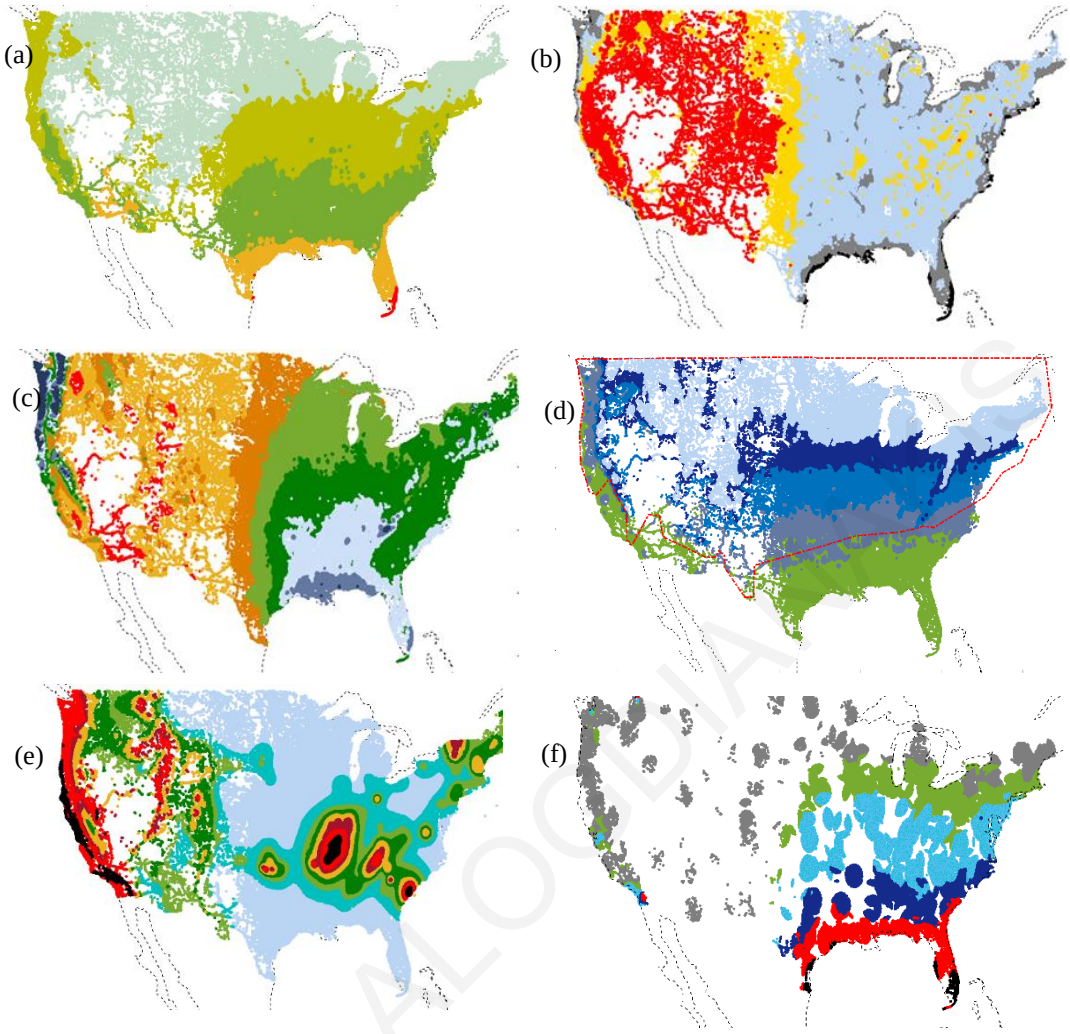

Figure 4.5: Interpolation results, the maps are not colored uniformly, each colored point represents a bridge for: a) minimum average temperature; b) diurnal temperature; c) annual precipitation in inch; d) annual snow depth in days above one inch e)peak ground acceleration in g(m/s^2) and f) dew point temperature.

4.4 Data analysis of bridge population and main assumption

The previous processes successfully read and combined the different datasets resulting to 443603 bridge records. Before moving to the data analysis process, information that assessed the validated prior processes or contained irrelevant information were excluded. The mentioned exclusions left 31 items climatic data, PGA and the inclusion or not within the deicing region.

All bridge data combined with the environmental factors are going to be studied assuming that bridge maintenance policies are more hazard driven than State-dependent. An initial step was to explore the content of the data, through Exploratory Data Analysis (EDA).

Then statistical modelling is applied using analysis of variance (ANOVA) and negative binomial regression analysis.

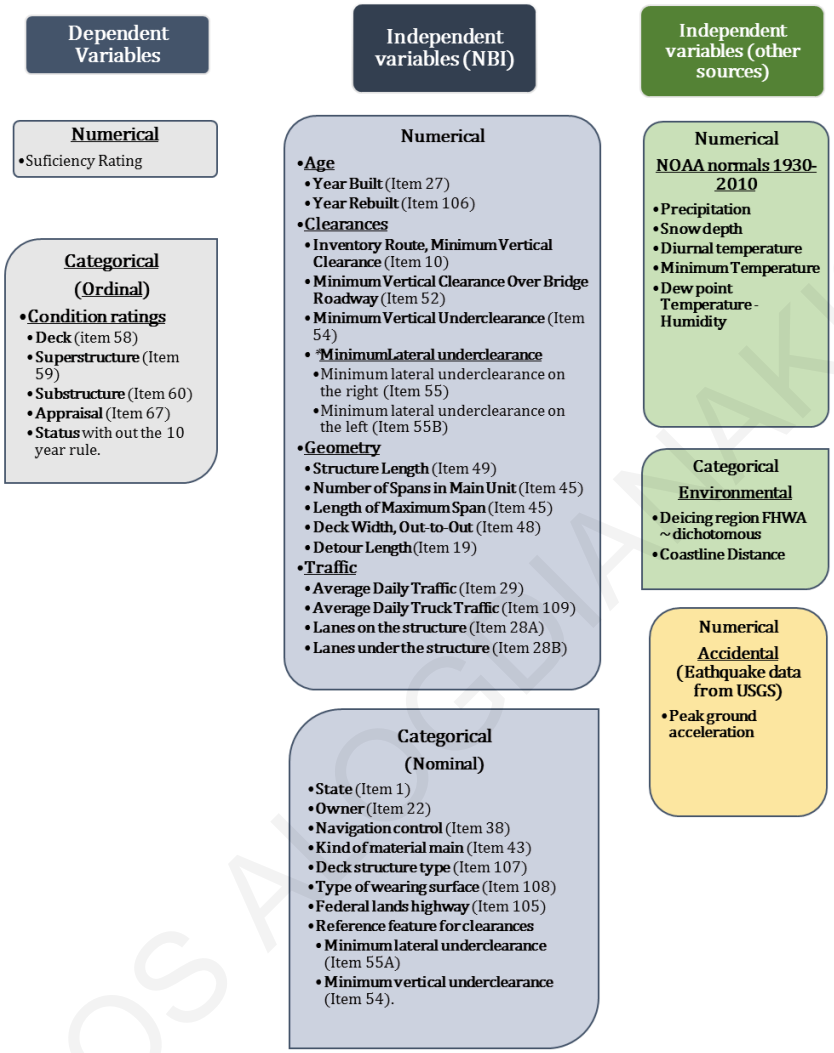

Figure 4.6: Organising the selected variables in numerical/categorical, response and potential predictor and deriving or not from the NBI.

4.4.1 Exploratory data analysis (EDA)

A basic step to start the EDA process is to categorize the data to dependent and independent variables based on whether they were the product of evaluation (structural condition ratings, etc.) or offered information for the bridge. Additional categorization was performed regarding the content of each variable to numeric or categorical (Fig. 4.6). The tools used in EDA are mainly graphical helping the analyst notice unexpected features and proceed to decide the appropriate methods that should follow (Tukey, 1977). Descriptive statistics were calculated for continuous variables while pie-charts and bar-charts are

presented in the Appendix (A-II. 9-12). Additional bar charts were also plotted to investigate the consistency in materials of each deck type (item 107) and the consistency in deck type of each type of wearing surface (item 108). Such clarifications would be of great use for the appropriate selection of items for further analysis as well as for interpretation of results. The measure of linear correlation is described by the estimated Pearson coefficients. Their values range from 0 to 1 where 0 shows no correlation, 0.65 to 0.75 reveals moderate and strong correlations above 0.75. Negative correlations also exist and are presented with negative values. The correlation plots utilized corrplot-package in (R-core team, 2008).

4.4.1.1 EDA results: dependent variables

Initially, the dependent variables were studied, to track similarities but also to test the appropriateness of each dependent variable for the following analysis. All dependent variables are numerical, sufficiency rating is continuous on 0-100 scale while the rest condition ratings and structural appraisal are categorical ordinal variables with a scale from 0-9. Also, deficiency status of a bridge is a categorical variable that states if a bridge is structurally deficient (SD)[1], functionally obsolete (FO)[2] or not (good condition). Based on the deficiency status the following can be stated from the histograms (Appendix, A-II.9):

- The deficiency status, reveals that after the 2015-2016 inspection 76% of the bridges have no deficiency with a sufficiency rating above 50, functionally obsolete represent 14% of the population and structurally deficient bridges are the rest 10%.
- An increase in condition ratings 4 can be noticed in SD histograms, but this increase does not affect the lower ratings. This provides the useful information that the critical condition of rehabilitation/reconstruction is 4.
- Replacement and rehabilitation[3] can be seen by the corresponding histograms of sufficiency rating SD and FO bridges.

Pearson correlation

- All response variables are positively correlated (blue colored circles in Figure 4.7).
- Moderate correlations exist between condition ratings of linked structural elements deck-superstructure, superstructure-substructure, while the correlation weakens to low between more distant elements (deck-substructure).

[1] Structurally deficient are rated for the three structural parts (deck, superstructure or substructure) with 4 or less or/and if the waterway adequacy are rated below or equal to 2.

[2] Functionally obsolete bridges lack geometrical features such as lanes, shoulder widths, or vertical clearances that are not adequate to meet traffic demand or under the risk of being flooded.

[3] Sufficiency ratings below or equall to 80 are eligible for rehabilitation while below or equal to 50 are eligible for replacement

- High correlations exist between appraisal structural evaluation and substructure but also superstructure. The stronger correlations show the importance of these elements to the description of the overall structural condition, whereas the deck condition has a lower link.
- High correlation exists also between sufficiency rating and that of Appraisal structural evaluation. Substructure and superstructure are moderately correlated with sufficiency rating while deck has a weak correlation.

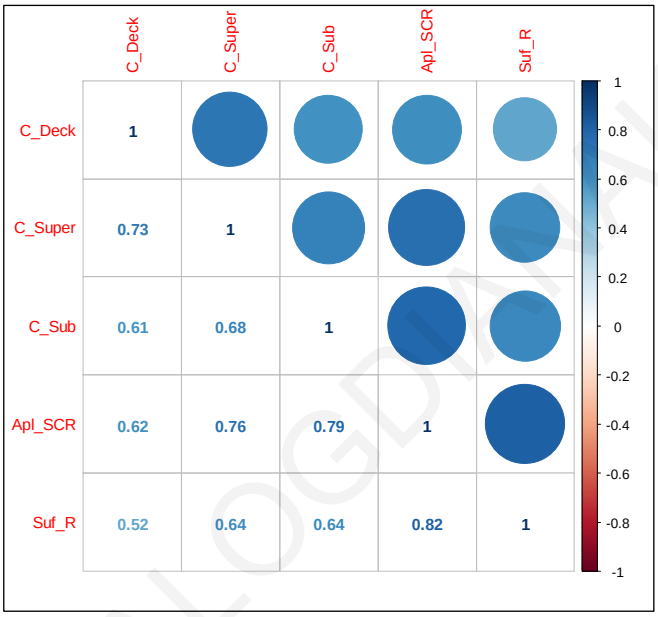

Figure 4.7: Correlogram of dependent variables (condition ratings of deck, superstructure and substructure appraisal structural condition rating and sufficiency rating), providing both graphical and numerical information.

4.4.1.2 Conclusions for dependent variables

From this analysis it is evident that each rating is important for a bridge's structural description. The ratings of appraisal structural condition and sufficiency rating combine different types of information and reveal an overall categorization of the bridge. The continuous scale of sufficiency rating and its sensitivity to structural deficiency can be used with the numeric variables to reveal correlations between candidate factors. On the opposite side, as this study aims to discover bridge deterioration and their effect in specific structural parts, Appraisal rating will not be used further on.

4.4.1.3 EDA results, independent variables NBI

The figures of the Appendix (A-II.10 - A-II.11) show the distributions of the numeric variables selected, their descriptive statistics and the categorical variables. Most bridges are above water are of shorter length than 25m have 1 span and 2 lanes to traffic. To summarize

the bridge sample the different materials along with the bridges built/rehabilitated per year are presented in Figure 4.8. The materials shown represent both continuous and simply supported spans for each category. The certain figure provides additional information regarding the samples influences:

Materials

- Concrete and steel materials are used mostly before 1950. The same year prestressed concrete is invented (Sanabra-Loewe & Capellà-Llovera, 2014). Up to 1970 all materials are used at the same frequency but after that period prestressed concrete is used more.

Rehabilitations

- The term rehabilitation is utilized for the year of reconstruction Item 106, corresponding to major repair work or rehabilitation (FHWA,1995). There is a rise of rehabilitations after 1950's, while the year 1970 corresponding to the creation of the NBIS seems to be coinciding with an increase in reconstructions. The number of rehabilitations rises reaching the number of bridges built at the same year of materials of concrete or steel. Change of materials when a bridge is reconstructed can be noticed as bridges before 1950 appear to be built from prestressed concrete. Additional information regarding rehabilitated bridges is provided in Chapter 6 (section 6.2.3).

Historical

- The introduction of the US to the World War of the US in 1942 that led to an increase in war expenses reducing construction funds which can be noticed.

Socio-technological

- There are local maxima within each 4 to 5 years up to 1975. It could be probably linked to the custom of "cutting ribbons to new structures" the parties in power to show their accomplishments while still in power as a means of advertisement. Another interesting notice is the reduction of their magnitude after 1975. The certain notice could be linked to the acceptance of televised presidential debates as the acceptable/preferable means of candidate competition. Introduced in 1960 when 27milion people watched the debate up to 1980 when that number doubled (Holz, et al., 2016).

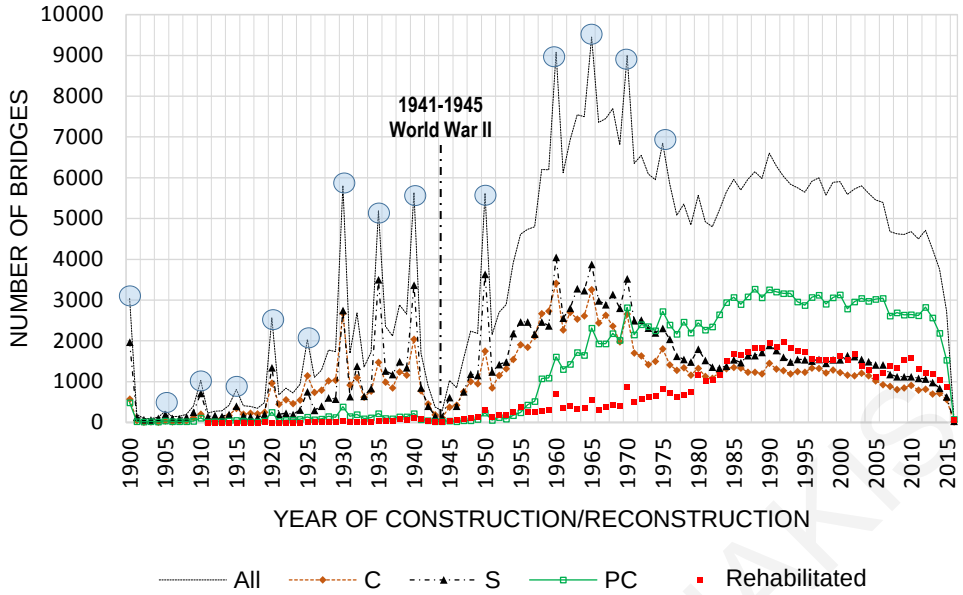

Figure 4.8: Bridges built per year based on construction materials concrete (C) steel (S) and prestressed concrete (PC); circled maxima are linked to the "ribbon cutting" custom of politicians to advertise the work performed during their service for the nearby elections.

Pearson correlation

Pearson correlation was used to analyze the independent variables of the NBI (fig. 4.9). The results showed that:

- The strongest correlation was found between minimum vertical clearance over and inventory vertical clearance. Both measure the same thing if the inventory route is a highway or a railway. Another strong correlation can be noticed between lanes on structure and deck width.
- Moderate correlations were found between deck width and average daily traffic (ADT), as well as between ADT and lanes on the structure, which could be anticipated from the previous notice.
- Weaker correlations were noticed between length and number of spans year built and year rebuilt as well as between maximum span and Length.
- Absence of correlation between sufficiency rating and all other variables apart from items referring to age of a bridge (Year Built and Year Reconstructed). It is also worth mentioning that these two variables are not taken directly to consideration for the calculation of the sufficiency rating (FHWA, 1995).

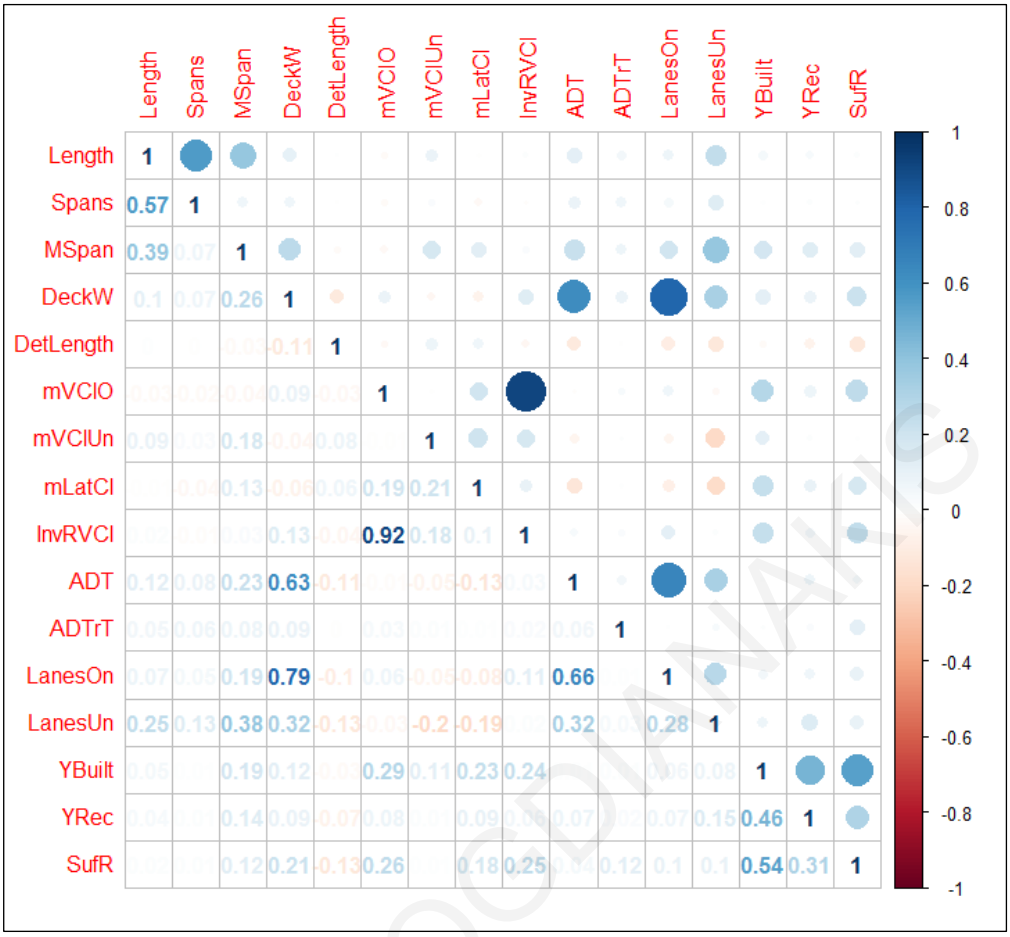

Figure 4.9: Correlogram of independent NBI variables providing both graphical and numerical information. Variables :Length, number of Spans, Deck Width, Detour Length, min. Vertical Clearance Over bridge, min. Vertical Underclearance, min. Lateral clearance, Inventory Route.

4.4.1.4 EDA results, independent variables environment

The same procedure was carried on for the environmental data descriptive statistics and histograms Appendix (A-II.11).

Pearson correlation

- Strong correlations seem to exist among the main temperatures (minimum and maximum). The same applies between dew point temperature and minimum temperature, while a moderate correlation can be noticed between dew point and maximum temperature. Another strong negative anticipated correlation can be noticed between temperature data and the days of snow depth above 1inch. This could be also noticed from the corresponding maps.
- Weak negative correlation can be seen among dew point and snow, revealing that in colder areas less humidity content can be within the air. On the contrary, the weak correlation between dew point and precipitation[4]. Also, the diurnal range temperature

[4] Dew point temperature when reached from the environmental temperature water starts to form.

has a weak and negatively linked to precipitation showing that when big difference during the day exist lower rainfall is anticipated.

- Relative humidity appears to be weakly negatively correlated with diurnal range temperature, weakly and positively with precipitation. The finding of correlation between earthquakes and humidity can be justified from location and no causal effect can be attributed.
- No correlation was found between sufficiency rating and the other variables. The same is noticed for coastal areas and other variables.

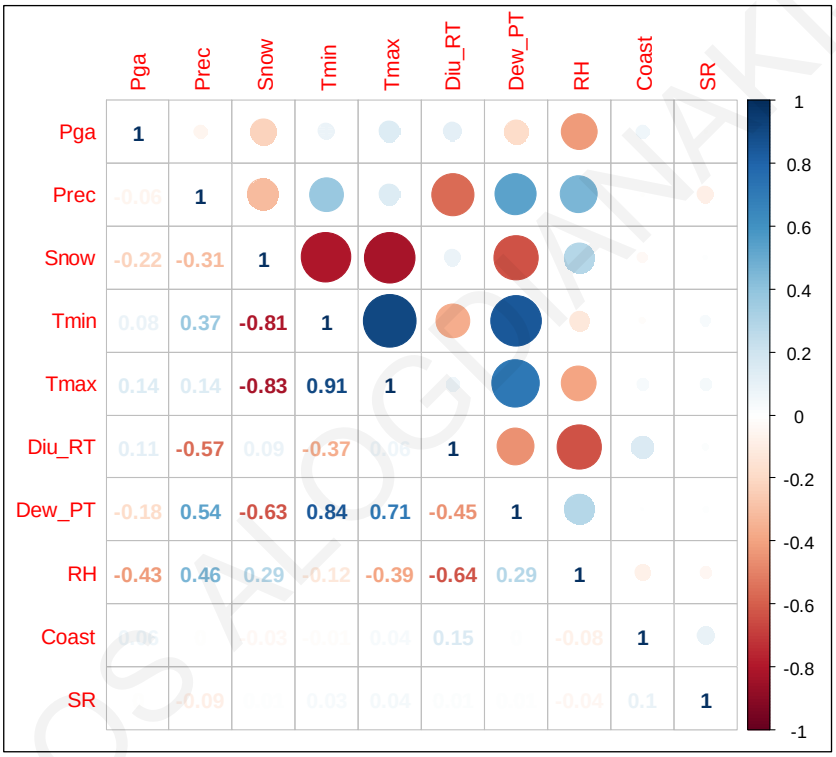

Figure 4.10: Correlogram of independent environmental variables providing both graphical and numerical information.

Conclusions for independent variables

- Low correlations with in the NBI reveal that each information is unique on its kind.
- The most predominant factor for Appraisal rating seems to be age.
- Climatic regions have moderate to high correlations between them which is anticipated as values of temperature max due to the fact that diurnal temperature which is added to temperature min has a narrower value range.
- No climatic variable appears to have correlation with sufficiency rating.
- Coastline appears to be worth investigating due to the fact that it appears to have no correlation with other values.

4.4.2 Statistical Modeling

Analysis in the previous part revealed, the distribution of each numerical variables' values, as well as the strength of linear relationships with the use of correlations. The sample used includes also categorical variables which were not included in the EDA. Thus, in this part initially EDA, is extended to incorporate categorical variables. For this to be performed Analysis of Variance (ANOVA) was utilized, where categorical data can be analyzed. To be able to identify the relationships among all variables (categorical and numerical), all numerical data was transformed to categorical using the histograms from the EDA, to form meaningful categories. After analyzing all variables with ANOVA an oversighted dimensionality reduction process was performed using Principal Components Analysis (PCA) to exclude unnecessary variables. In the end, regression analysis is utilized to attain a model which better describes the data.

4.4.2.1 ANOVA

Hypothesis testing helps to notice if differences/similarities can be generalized from the categories of the studied sample to the same categories of the population. An initial (null) hypothesis is formed for the sample that no significant difference exists among the categories being tested, which is accepted or rejected based on the results of the suitable statistical test. The results take to account the different types of errors that exist and quantify the difference among groups as well as the importance/significance of the finding (Biau, et al., 2009).

The simplest form of hypothesis test is the t-test, where two groups are compared to test if they belong to the same distribution. When more than two groups are present in a single independent variable then one-way ANOVA can be performed since the comparisons are performed in a way that the errors are not accumulated thus providing a better model (Triola, 2015). As the case of the NBI includes multiple groups in different items, ANOVA was chosen for the current analysis.

A critical step before applying any statistical methods, is ensuring that the underlying assumptions, are met or approximated (Gaito, 1980), to avoid misleading results. For the case of ANOVA the assumptions according to (Gamst, et al., 2008) are: a) the error components associated with the scores of dependent variable are independent of one another, b) the aforementioned errors are normally distributed, c) the variances across the levels or groups of the independent variable are equal.

Based on Gamst et. al. (2008), the first assumption is the most important and can be considered valid only if the observations are independent. For the case of the NBI as each bridge is an independent entity and is contained within the inventory, thus this assumption

is met. Furthermore, the normality of the distributed error terms, is met if the distribution of the independent variable (condition rating) is normally distributed. Despite the bell-shaped histogram noticed in Appendix (A-II.9) the ordinal scale of the condition rating, provides a violation to this assumption. Such violation can be considered not to affect the analysis, as decimal ratings can be interpreted as a scale of deterioration. Moreover, the analysis is robust to more extreme violations of this assumption (Schmider, et al., 2010). For the last assumption, the group categories cannot be enriched (the sample is the actual population of the US) and bridges with in a group may also vary due to many other factors, thus the violation of this assumption is treated methodologically.

4.4.2.2 ANOVA methodology

The information within the NBI is interconnected as no bridge condition can be irrelevant for example to age or material or climate. As ANOVA is used for categorical data, to incorporate also the effect of numeric variable types to condition ratings, all numeric data were transformed to categorical. Special attention was given to the grouping process so that meaningful groups would be formed with adequate sample sizes. In one case, such as the year of construction/reconstruction the two items were joined and the groups were formed with respect to Figure 4.7. In other cases, such as the case of clearances (vertical, horizontal), studies of vehicle impact (Agrawal, et al., 2011) were used to determine the lowest limits to form categories which could indicate such effect on bridges.

Each independent variable considered was analyzed for the dependent variables of condition ratings (superstructure, substructure and deck). One-way ANOVA was equipped as the multiple levels of all variables could not be performed through a factorial design. The analysis reveals the existence of a significant difference among the studied groups of one independent variable, for the considered dependent variable. In all studied cases the significance level (α=0.05), was met as the population is sufficient (above 1000) (Gamst, et al., 2008). Furthermore, as many factors are related to a bridge condition, significant differences are anticipated for each variable analyzed. To assess the importance of the differences found for each variable's groups, ANOVA results were visualized using multiple comparisons Tukey-Kramer method (Wilcox, 2009). An illustration of ANOVA analysis is performed to study the Chapters main assumption that bridge maintenance/rehabilitation policies are hazard driven.

4.4.2.3 Testing the main assumption using ANOVA

In this part ANOVA and multiple comparisons, were utilized to test the assumption that maintenance/rehabilitation policies of each State are more hazard driven than State

dependent. Two hypothesis tests were performed, one to reveal differences in State policies and the second to reveal differences within a State. Specifically, in the first hypothesis test, two States were selected to have similar environmental conditions. This analysis would reveal if these States share common hazard-driven policy or differ due to different individual State policies. The second hypothesis test was performed on a State where one environmental condition would change within the States territory.

To select among the whole US, the maps of the environmental variables (fig. 4.5), were used. Specifically, to find two States environmentally similar, earthquake hazard (fig. 4.5e) precipitation (fig. 4.5c), limited the selection of north eastern States of Figure 4.11. Then, from minimum temperature map (fig. 4.5a) the snow-depth map (fig. 4.5d) and the State boarders map (fig. 4.11), the States of Michigan and Wisconsin were chosen for between States analysis. To select the individual State, the maps of Figure 4.5 were utilized and a known factor of structural condition deterioration, deicing, was selected. Arkansas was selected as the individual State, as all considered environmental factors were similar except deicing region (red line in fig. 4.5d) and seismic hazard (fig. 4.5e) which also variated from very low levels to some of the highest noticed. Moreover, deck structural condition evaluation was selected as it constitutes the bridge part which is more exposed to deicing salts and the least affected by earthquakes (Chen & Duan, 2014).

Figure 4.11: States selected to study the State effect; with green the two States with very similar environmental conditions; with orange the individual State where all other environmental factors are similar except deicing region.

ANOVA is conducted on each null hypothesis stating that no difference exists among the groups studied. Indication of an existing difference rejects the null hypothesis if the finding is significant, stating that groups of within the considered variables are significantly different. Specifically, the F-value (Table 4.2), reveals the existence of a difference while "Prob > F", (Table 4.2) indicates a significant finding, if a value lower than the significance

level (a=0.05) is achieved. These values are calculated based on the different sum of swuares calculated for the different groups of each variable. Specifically, total sum of squares value is calculated by subtracting the value of the dependent variable (deck condition) of each observation (bridge), from the whole samples' mean and summing the squared differences found. The error term or within group sum of squares is calculated by subtracting the value of the dependent variable (deck condition) of each observation, from the corresponding groups' (State or deicing category) mean and summing the squared differences found. By subtracting the sum of squares corresponding to the error from the total sum of squares, the between groups of the selected variable, sum of squares is calculated.

The mean sum of squares of Table 4.2 is calculated by dividing each sum of squares category by the corresponding degrees of freedom. For State variable the degrees of freedom indicate the number of States reduced by one, thus as two States are analyzed value one is found. The total degrees of freedom correspond to the sample size reduced by one observation and the degrees of freedom for the error term, correspond to the total degrees of freedom, reduced by the variables' degrees of freedom.

The F-value is calculated by dividing the variables mean sum of squares with the mean sum of squares of the error. Then using the calculated F-statistic and the degrees of freedom the p-value is calculated. Although, not shown here larger F-values correspond to smaller p-values indicating significant findings (Sawyer, 2009). Additionally, to reveal the descriptive strength of each variables effect to the dependent variable studied the coefficient of determination (R^2) or eta squared η^2 (Gamst, et al., 2008) given by the formula (eq.4.6), was used.

$$R^2 = \frac{SS_A}{SS_{tot}} \quad (4.6)$$

Where: SS_A=, refers to the sum of squares of the variable; SS_{tot}: the total sum of squares of the sample;

Table 4.2: ANOVA results for the two hypothesis tests conducted,

Hypothesis test	Sum of Squares (SS)	Degrees of Freedom	Mean SS	F-statistic	Prob>F	R^2
I. Between States effect	58.4	1	58	44	3E-11	0.0002
Error	26,732.1	20168	1	-	-	-
Total	267,904.7	20169	-	-	-	-
II. Within State deicing effect	216.3	1	216	192	4E-43	0.020
Error	10,462.0	9264	1.1	-	-	-
Total	10,678.3	9265	-	-	-	-

The results in Table 4.2, both reject the null hypothesis and indicate significant differences. A direct comparison between the F-statistics indicates that the difference within an individual State where different hazards exist, is larger than differences between States where all environmental hazards are similar. Furthermore, the same is indicated by R^2 value which shows that 0.02% of the variance can be explained by the State –variable while 0.2% of the variance can be explained within a State by a change of an environmental variable. Since significant differences were found, Tukey-Kramer multiple comparison test was used to visualize the results of Table 4.2 (fig. 4.12). In the same figure, each circle represents the mean of the studied group, while the line indicates the standard error of its estimation. Additionally, the mean year of construction was estimated, as it was noticed from section 4.4.1.3 to have the highest correlation to sufficiency rating, which is also correlated with the deck's structural condition. Although both differences are significant the larger deviation of the group means Figure 4.12a and the smaller difference between the years of construction of the same groups, indicate that variation of a hazard, in this case earthquake and deicing region, within a State affect more the condition of a bridge than a change in State. Thus, the assumption that maintenance policy is hazard driven appears to be plausible.

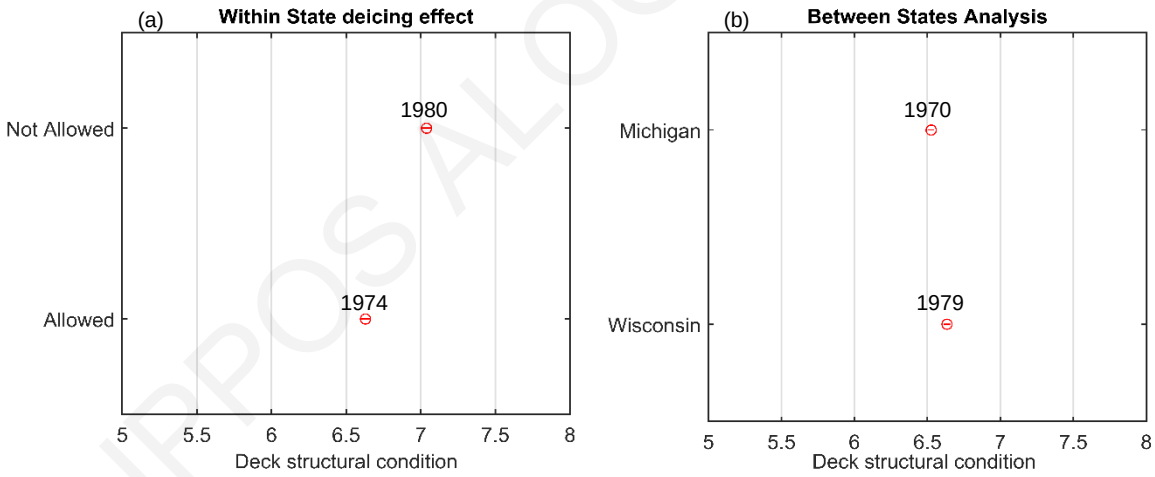

Figure 4.12: ANOVA results for a) individual State and b) for between States analysis. The numbers above each circle indicate the mean year built of each group which showed a high correlation with sufficiency rating and is anticipated to have an effect on condition.

4.4.2.4 ANOVA results

From the selected 41 variables (Figure 4.6), 38 (excluding sufficiency rating, bridge status and Appraisal condition rating) were analyzed using ANOVA. Three different response variables were used for the three different condition ratings. For each response variable related independent variables were chosen for its analysis. An additional variable was formed using the super structure material to separate among continuous or simple spans to indicate structural joints, and their effect on condition ratings of deck and substructure.

The analysis included only the effect of each independent variable to the condition rating, the summary of its' results were included in each Table (4.3, 4.4 and 4.5). For each variable analyzed multiple comparisons have been used to visualize the differences among the groups. In the last column of each table a reference to the Appendix has been included.

Table 4.3: ANOVA ranked results for variables relative to superstructure condition (Appendix A-II.13).

Variabbles	Total Sum of Squares	Degrees of Freedom	Sum of Squares	F-statistic	Prob>F	R^2	Ref.
Year (Re) constructed	578606.10	6	172338.08	28787.98	0E+00	0.2979	A
Main Material	641831.01	5	73130.62	11408.65	0E+00	0.1139	B
Deck Width	641738.55	3	44141.09	10921.13	0E+00	0.0688	C
Length of Max. Span	641393.13	4	23546.35	4223.73	0E+00	0.0367	E
Length	641831.01	5	15103.42	2138.04	0E+00	0.0235	D
Lanes On	641687.95	3	14509.44	3420.77	0E+00	0.0226	J
Min Lateral Clearance	200708.70	3	2891.42	830.80	0E+00	0.0144	M
Snow depth above 1 inch	641191.36	4	6948.30	1213.82	0E+00	0.0108	Y
Max.Temperature	638353.36	4	6754.94	1179.45	0E+00	0.0106	S
Deicing Region	641831.01	1	5637.74	3931.05	0E+00	0.0088	Z
Annual Precipitation	637614.41	7	5310.18	529.43	0E+00	0.0083	X
Peak Ground Acceleration	641808.61	7	5312.98	528.96	0E+00	0.0083	AB
Navigation Control	641831.01	2	4856.03	1690.91	0E+00	0.0076	R
Relative humidity	419404.63	5	3134.28	429.03	0E+00	0.0075	W
Min. Vertical Clearance Under	641831.01	3	4672.17	1084.28	0E+00	0.0073	K
Distance from Coast line	23031.85	11	158.54	12.10	5E-23	0.0069	AA
Min. Temperature	638793.31	4	3873.51	673.40	0E+00	0.0061	T
Inventory Route Clearance	641212.65	7	3884.07	1350.72	0E+00	0.0061	L
Dew point Temperature	641831.01	6	3875.13	449.09	0.00E+00	0.0060	V
Average Daily Traffic	641831.01	7	1832.85	181.48	1E-269	0.0029	O
Lanes Under	641831.01	4	1756.55	304.34	6E-262	0.0027	I
Diurnal Temperature Range	638888.80	4	1620.02	280.60	2E-241	0.0025	U
Reference feature for Clearances	641831.01	2	1466.23	507.85	5E-221	0.0023	N
Number of Spans	641520.63	3	1304.80	301.25	2E-195	0.0020	F
Detour Length	641831.01	6	1104.27	127.42	1E-161	0.0017	Q
Truck traffic	641831.01	4	486.43	84.11	2E-71	0.0008	P
Owner	641831.01	5	378.82	52.39	2E-54	0.0006	G
Federal Lands Highway	641829.35	7	305.22	30.15	5E-42	0.0005	H

Table 4.4: ANOVA ranked results for variables relative to deck condition (Appendix, A-II.14).

Variabbles	Total Sum of Squares	Degrees of Freedom	Sum of Squares	F-statistic	Prob>F	R^2	Ref.
Year (Re) constructed	511544.08	6	130624.14	23271.93	0E+00	0.2554	A
Wearing Surface	568997.40	10	26514.73	2168.13	0E+00	0.0466	E
Deck Width	568929.47	3	18825.95	5059.94	0E+00	0.0331	D
Deck Type	555572.95	8	13279.36	1330.65	0E+00	0.0239	C
Length of Max. Span	568572.99	4	7873.43	1556.28	0E+00	0.0138	F
Max.Temperature	565568.87	4	5002.04	984.05	0E+00	0.0088	Q
Lanes On	568857.78	3	4903.09	1285.55	0E+00	0.0086	K
Dew point Temparature	364258.85	5	3138.47	495.21	0E+00	0.0086	S
Length	568.997,40	5	904,33	710,68	6E+05	0,0079	P
Snow depth above 1 inch	568417.89	4	4377.84	859.96	0E+00	0.0077	W
Deicing Region	568997.40	1	3691.30	2896.59	0E+00	0.0065	X
Min. Temperature	566017.08	4	3309.30	649.14	0E+00	0.0058	R
Peak Ground Acceleration	568977.33	7	1870.52	209.01	3E-297	0.0033	Z
Annual Precipitation	565141.54	7	1775.29	198.66	1E-295	0.0031	V
Relative humidity	364258.85	5	789.67	123.79	2E-131	0.0022	U
Min.Vertical Clearance	568997.34	3	1197.66	311.90	3E-202	0.0021	G
Owner	568997.40	5	953.20	148.87	2E-158	0.0017	I
Navigation Control	568997.40	2	944.94	368.96	8E-161	0.0017	AA
Distance from Coast line	19704.78	11	31.10	2.76	1E-03	0.0016	Y
Detour Length	568997.40	6	698.01	90.81	2E-114	0.0012	O
Diurnal Temperature	566154.97	4	389.60	76.01	2E-64	0.0007	T
Truck traffic	568997.40	4	236.82	46.18	7E-39	0.0004	N
Lanes Under	568997.40	4	206.41	40.24	9E-34	0.0004	L
Average Daily Traffic	568997.40	7	188.43	20.99	2E-28	0.0003	M
Ref. feature Clearance	568997.40	2	175.47	68.42	2E-30	0.0003	H
Span Type	568997.40	1	172.10	134.21	5E-31	0.0003	B
Federal Lands Highway	568995.55	1	71.15	55.47	9E-14	0.0001	J

Table 4.5: ANOVA ranked results for variables relative to substructure condition (Appendix, A-II.15).

Variabbles	Total Sum Squares	Degrees of Freedom	Sum of Squares	F-statistic	Prob>F	R^2	Ref.
Year (Re) constructed	586954.69	6	171129.41	27927.01	0E+00	0.2916	A
Deck Width	650919.78	3	18374.64	13678.53	0E+00	0.0847	F
Length of Max. Span	650493.75	4	37198.76	6721.66	0E+00	0.0572	E
Length	650997,42	5	4255,05	2997,15	0E+00	0,0327	B
Min. Lateral Clearance	184242,43	3	1598,60	1518,96	0E+00	0,0260	G
Span Type	650997.42	1	9844.06	6810.34	0E+00	0.0151	C
Navigation Control	650997.42	2	7910.92	2728.24	0E+00	0.0122	I
Peak Ground Acceleration	650984.72	7	6281.13	617.33	0E+00	0.0096	W
Average Daily Traffic	650997.42	7	5755.05	565.17	0E+00	0.0088	K
Relative humidity	408112.32	5	3326.68	468.24	0E+00	0.0082	T
Distance from Coast line	20559.76	11	163.79	14.02	3E-27	0.0080	X
Snow depth above 1 inch	650369.32	4	4803.83	824.41	0E+00	0.0074	U
Annual Precipitation	647542.34	7	4300.26	421.42	0E+00	0.0066	S
Ref. feat. Clearance	650997,42	2	3204,80	1097,21	0E+00	0,0049	H
Max. Temperature	647667.49	4	2914.70	498.50	0E+00	0.0045	P
Dew Point Temperature	408112,32		354,22	248,34	1E-265	0,0043	R
Diurnal Temperature	648184.10	4	2336.57	399.30	0E+00	0.0036	Q
Owner	650997.42	5	2311.03	316.05	0E+00	0.0035	M
Deicing Region	650997.42	1	2207.12	1508.96	0E+00	0.0034	V
Detour Length	650997.42	6	2171.96	247.47	4E-317	0.0033	J
Min. Temperature	648114.78	4	1832.75	312.99	2E-269	0.0028	O
Number of Spans	650637.70	3	1636.40	372.66	9E-242	0.0025	D
Truck traffic	650997.42	4	1526.37	260.61	4E-224	0.0023	L
Federal Lands Highway	650995.51	1	625.29	426.46	1E-94	0.0010	N

4.4.2.5 Conclusions for ANOVA

ANOVA was performed to investigate the impact of each independent variable to the dependent variables (condition ratings). The analysis's limitations regard the relationship among variables which all together describe a bridge and are responsible for its current condition rating. Since, not more than one variables have been studied at once, the results of the analysis provide indications of the group means, of the single variable studied. Despite that, certain conclusions can be made regarding distinctive patterns noticed from the ranked results and their multiple comparisons:

- The year of construction and reconstruction appear to be the most affecting factor for condition ratings. They are ranked 1st in each Table of the results describing most of the variance (26-30%). Additionally, they appear to have big differences among their group means in the multiple comparisons.

- Materials appear to have the next most important effect for condition ratings of superstructure and deck, where information is provided from the NBI. Deriving from superstructure material main type, the span type appears to affect also substructure condition. In general, materials of concrete seem to have a better rating than other materials. Furthermore, continuous spans can be noticed to have better condition ratings than simple spans. Thus, among superstructure materials prestressed concrete in continuous spans has the highest condition rating. Also, steel continuous spans have a higher condition rating than concrete continuous spans and a lower condition rating than simple spans of prestressed concrete.
- The design of a bridge appears to have an effect on all condition rating, with more demanding designs having better ratings. These include increased deck width (and lanes on structure), length, maximum span and peak ground acceleration. Specifically, for peak ground acceleration a pattern is evident in the multiple comparisons for all condition ratings where increase in earthquake hazard decreases condition rating while a further increase above 0.2g is accompanied with increase in condition ratings (fig. 4.13). A possible explanation to this notice can be attributed to a seismic design demand coinciding with that specific limit. Also, from Figure 4.13, it can be noticed that peak ground acceleration affects mostly the condition ratings of superstructures and substructures, than of decks.

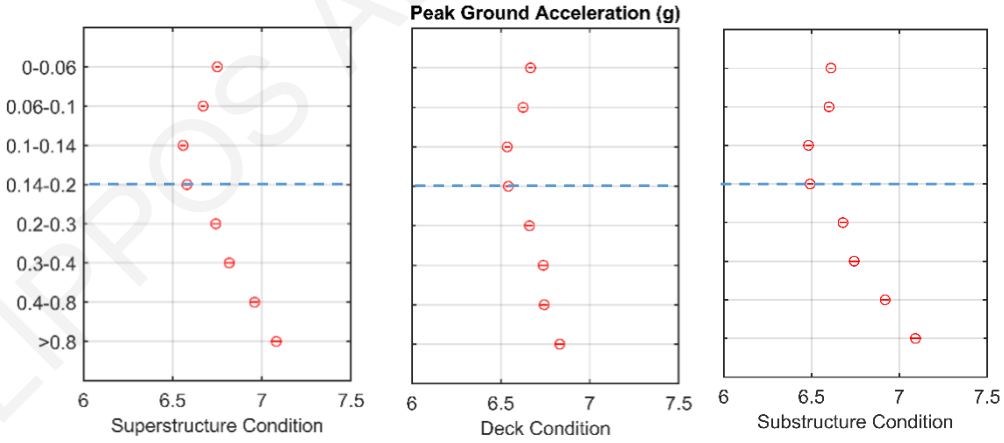

Figure 4.13: ANOVA results for groups of: Peak ground acceleration in g=9.81m/s^2 and its effect on condition rating of superstructure, deck and substructure. The blue line indicates a possible limit of application for seismic design demands.

- Average daily traffic as well as truck traffic appear to have a very limited effect among condition ratings (fig 4.14). A possible explanation could be attributed to the existence of adequate standards and their good application and/or an organized and oversighted process of bridge posting accompanying bridge inspections. Despite the mentioned notices an effect similar to peak ground acceleration but of lower intensity, appears for

super structure and substructure condition, which could also be attributed to adequate design standards both for average daily traffic (fig. 4.13a) and truck traffic (fig. 4.13b). The same cannot be observed for the condition rating of deck where all groups of either variables appear to variate within small limits.

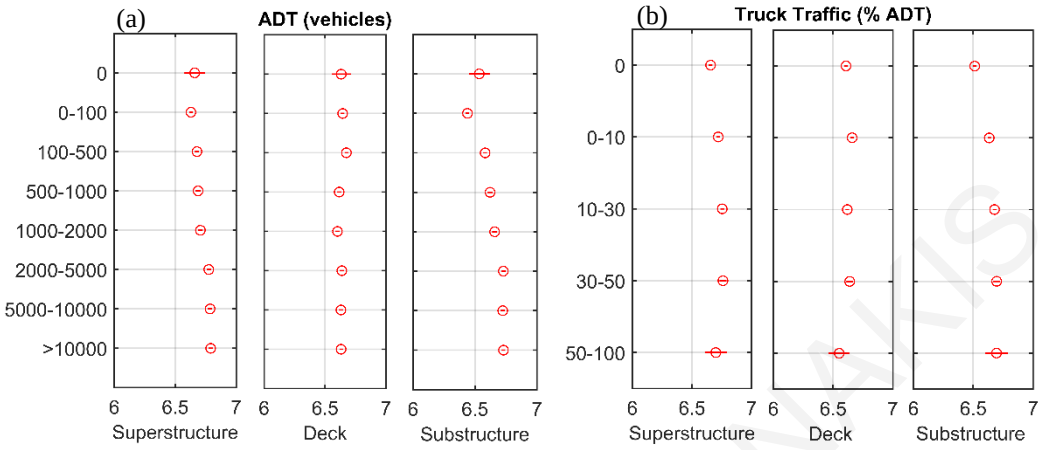

Figure 4.14: ANOVA results for groups of ADT (a) and truck traffic (b) for the condition rating of superstructure, deck and substructure.

- Owner as well as Federal Lands Highway designation appear to have a very small effect to all condition ratings.
- Minimum clearances, vertical, lateral and inventory route appear to affect more superstructure and substructure conditions only for the smallest distance group. Specifically, inventory route minimum vertical clearance (corresponds to minimum vertical clearance from the road's surface to a structure above), appears to affect the condition rating of superstructure, while substructure is affected more by minimum lateral clearance. A possible explanation could be attributed to the vehicle collisions and accidental actions. On the other hand, despite the increased difference and high rank attributed for the case of inventory route clearance, the sample size of the smallest distance group corresponds only to 0.58% of the all groups analyzed. Thus, the lower condition rating could be attributed to other confounding variables such as year of construction and/or material.
- Regarding the effect of weather and environment, maximum temperature, snow depth in days, minimum temperature and being within the deicing region appear to affect more than other environmental effects. Specifically, warmer climates have higher condition ratings for the different structural parts considered. This applies for both maximum and minimum temperature. Despite the strong correlation indicated in section 4.4.1.4, snow depth above 1 inch appears to have a slightly different pattern compared to temperatures, with the first group (corresponding to less than half a day),

being in higher condition. On the other hand, while an increase in snow days from half a day to 7.4, has a lower condition, no further reduction in condition follows the increase in snow days (fig. 4.15a). The same can be noticed from the inclusion or not within the deicing region (fig. 4.15b). It should be mentioned, that for the case of deck condition rating there is a very slight reduction noticed for increased days of snow depth above 1 inch. Thus, from these results it appears that the amount of deicing applied affects has a minor effect in structural condition ratings, in comparison to the absence of deicing.

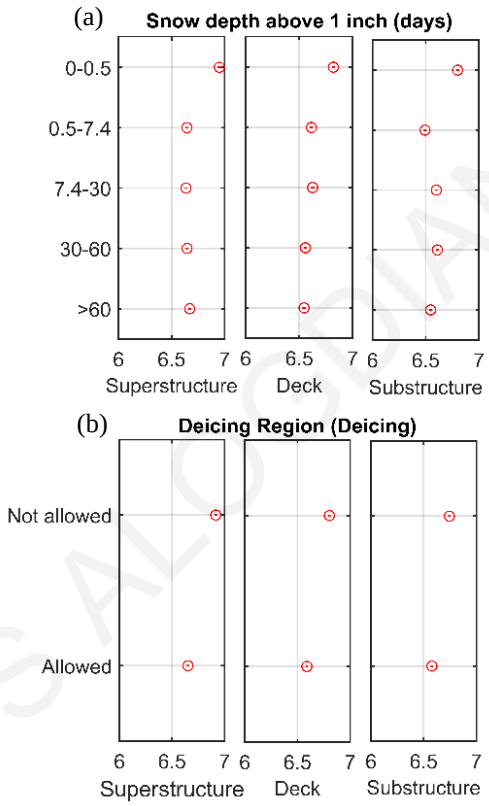

Figure 4.15: ANOVA results for groups of: a) snow depth above 1 inch in days and b) being in deicing region where deicing is allowed or not, for superstructure, deck and substructure condition.

- Among the rest of the weather variables annual precipitation appears to have an effect on structural condition ratings but there is no clear pattern indicating a reduction of condition with increase in precipitation.
- Similar patterns noticed for peak ground acceleration can be noticed for diurnal range temperature, which could be explained by the similarity among the maps of each variable (fig. 4.5 b and e). As increased thermal loads could be anticipated for increased diurnal temperature ranges thus lower condition ratings, this is not noticed. Superstructure and substructure which are less exposed to thermal loads than deck

have a similar pattern to that of peak ground acceleration. On the other hand, deck condition appears not to have a similar pattern indicating that, although peak ground acceleration increases, deck condition remains the same. An observation that cannot be made for diurnal temperature range, where all condition ratings appear to be equal except for the first category, which corresponds to coastal areas.

- Dew point temperature appears to have an effect similar to temperature on the other hand, relative humidity (where dew point has been utilized) shows a pattern where increase in relative humidity corresponds to lower condition ratings.
- From the variable navigation control it can be noticed that bridges located over water have a lower condition rating. Water underneath the bridge appears to effect substructure condition more than superstructure and deck.
- Smaller distances from the coast appear also to have an effect, more on condition ratings of substructure and superstructure and less on deck's condition.

4.4.3 Dimensionality reduction using PCA

A basic step before performing statistical modelling is reducing the dimensions (variables) of a high dimensional data set. Usually dimensionality reduction processes are applied in EDA (Martinez & Martinez, 2005), where variables for further analysis are selected and explored, as methods such as PCA reduce the dimensions based on variable variances and not their effect on dependent variables. PCA performs transformations to the data resulting to a change in coordinates (dimensions/variables). Linear combinations of the original variables are formed based on their variances, resulting to uncorrelated variable groups, principal components (Jolliffe, 2010). All principal components describe the total variability of the dataset, while only the few first describe most of the sample's variability. The number of the principal components to be incorporated can be decided by the cumulative percentage of variance explained.

In this study, the process is performed after all variables were studied for their effect on the dependent variable. Thus, an oversighted exclusion of variables would be performed. PCA results of the numeric variables were utilized to reduce their dimensions and ANOVA results to reduce categorical variables. Initially, small manipulations were performed to the dataset regarding outliers and extreme variances noticed, to avoid misleading results deriving from PCA's sensitivity to variance. Hence, ADT instead of vehicles was transformed to thousand vehicles. Additionally, as different types of numeric variables are incorporated, two PCA's were performed (fig. 4.16), one to reduce bridge related data from the NBI and the second to reduce weather, environmental data. Furthermore, variables with

increased missing values were not included either in PCA or in regression analysis. These variables were: dew point temperature and relative humidity (73% missing values), clearances (minimum vertical clearance with 77% missing values, distance from the coast with 96%, lateral clearance with 78% and lateral clearance with 83%) the last exclusion was performed to year of reconstruction where 85% of the bridges have not been reconstructed.

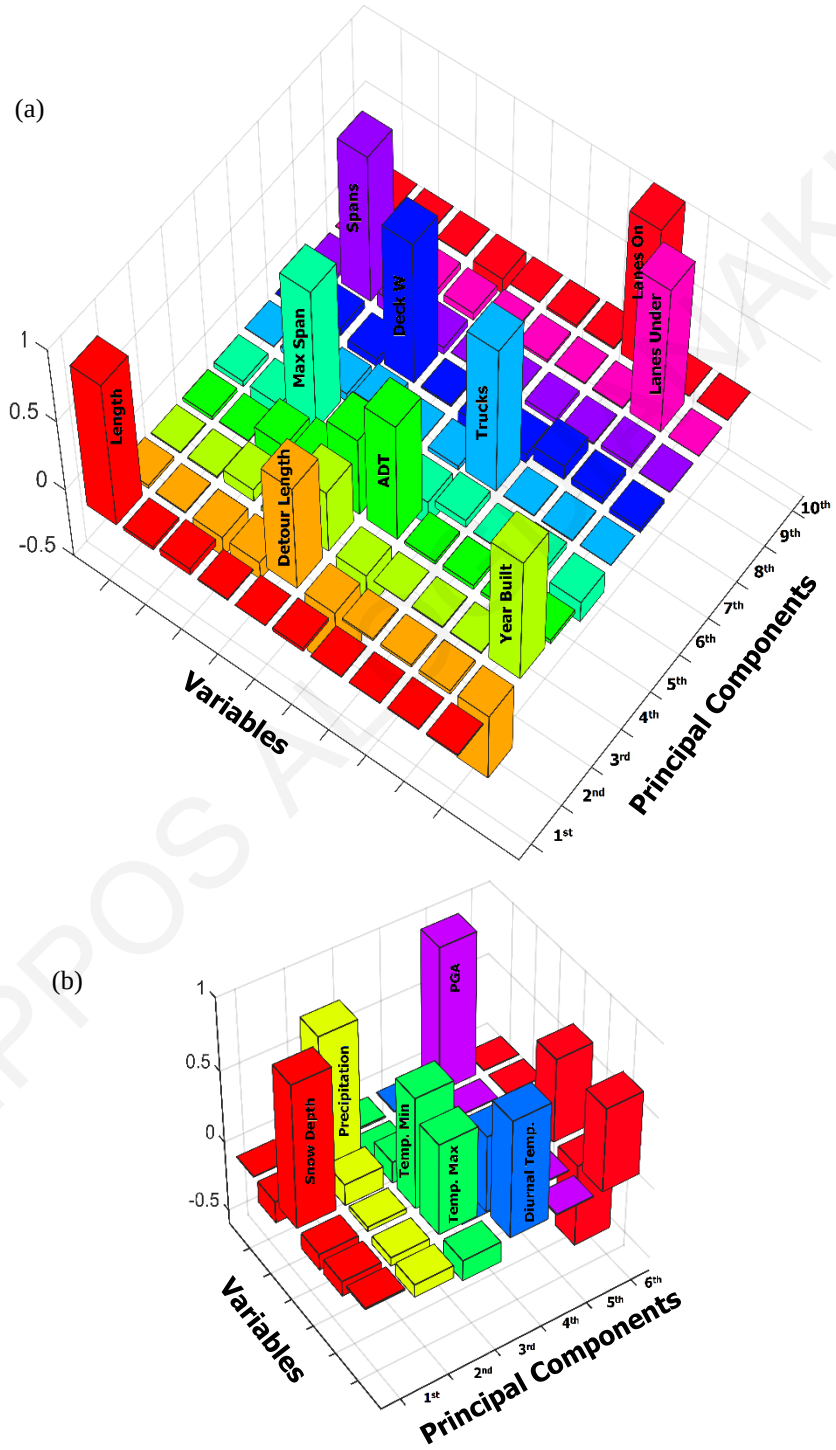

Figure 4.16: Principal components analysis of a) NBI variables and b) weather and peak ground acceleration variables.

A variability above 95% was utilized to incorporate variables of each dataset. Thus, for the NBI variables the first five principal components (fig. 4.16a) were chosen, explaining 99.54% of the data's variability. These included the variables: length; ADT; length of maximum span; deck width; detour length; year of construction and year of reconstruction. From the environment dataset first two principal components included variables of snow depth above 1 inch and annual precipitation describing 99.2% of the dataset's variability. Despite, PCA's results the variable of peak ground acceleration was also included as it was noticed to affect all condition rating in the ANOVA results also truck traffic was included as additional information for ADT. Regarding categorical variables, main material would be used for superstructure condition ratings, span type (generated from main material) for deck and substructure. Type of deck and type of wearing surface would also be included for deck condition ratings. Furthermore, navigation control and deicing region would be introduced to model all condition ratings.

4.4.4 Regression analysis

Regression analysis is a statistical process for estimating the relationship among variables. Specifically, many techniques are utilized to modelling and further analysis of a dependent variable and its relationship with one or more independent variables. It is commonly used for prediction and forecasting but it has also been utilized in achieving a better understanding of the importance of each independent variable, utilizing the attained model. The regression process leads to a function that models the change in the dependent when any of the independent variables is varied and the rest are kept fixed. As the estimates of the dependent variable comprise the conditional expectation, special attention should be given in the distribution of the dependent variable.

4.4.4.1 Negative binomial distribution

In section 4.4.2.1 the normality assumption for performing ANOVA was mentioned to be violated due to the non-continuity of condition ratings as well as the non-negative values. Structural condition ratings can be regarded as count data, as observations (bridges) can only take non-negative integer values and they are product of counting. To model such data binomial, Poisson or negative binomial distributions can be used due to the fact that condition ratings are not dichotomous (Hosmer, et al., 2013). The negative binomial distribution (eq.4.6) was selected as it provided the additional capability to model over dispersed data in contrast to the Poisson (Hilbe, 2011).

For negative binomial regression to be performed, no violations to the negative binomial distribution should exist. Specifically, according to Hilbe (2011), these violations

include: (a) no zero in data, (b) excess zeros in data, (c) data separated in to two distributions, (d) censored observations, (e) truncated data, (f) data structured as panels clustered or longitudinal data (g) some responses occur based on the value of another variable and (h) endogenous variable in the model. Violation (g) refers to cases where an event does not begin until a certain value is reached from another variable, for the case of NBI this has not been noticed. Violation (h) refers to cases of omitted variables or not incorporated in the model increasing its errors.

$$P\{X = k\} = \binom{k + r - 1}{r} p^k (1 - p)^r \quad (4.6)$$

Where,

X: discrete random variable, k: non-negative integer values representing number of successes, r: number of failures (r>0) and p: the probability of success (0<p<1).

4.4.4.2 Regression analysis methodology

To model the effect of the reduced independent variables of section 4.4.3 negative binomial regression analysis was utilized. Three different regression functions would be derived, one for each structural condition rating. For each condition rating a selection of the categorical variables was performed based on the ANOVA results to include material variables for each condition rating. Additionally, groups of categorical variables were merged to form a larger group due to limited sample size, such were the variables of type of deck and type of wearing surface.

An additive, generalized linear model fit was calculated using MASS library in R (R-core team, 2008). An initial regression was performed to fit a model using all independent variables corresponding to each dependent variable. Then each initial model was refined by omitting variables that were found to be insignificant. To achieve this, a stepwise regression process was utilized, where independent variables would be added (forward) or removed (backward) and the Akaike Information Criterion (AIC) was used to indicate if a better model was achieved. This process was performed both ways, forward regression where variables are added and backwards where variables are removed. The results of the initial regression were compared to the refined model and unnecessary variables would be omitted. Despite that, from the process of omitting variables ADT was deliberately excluded, as all bridges carry highway traffic and a better understanding of the variables effect was needed.

4.4.4.3 Regression results

The regression analysis results are displayed with the regression function of each structural condition rating while, coefficients, errors and model's details are presented in Tables. Thus, Equation 4.7 and Table 4.6 correspond to superstructure condition, Equation (4.8) and Table 4.7 to deck condition and Equation (4.9) and Table 4.8 to substructure condition. the coefficient shows the effect of each variable to the condition. In each regression function (eq.4.6, 4.7 and 4.8) the logarithm of the corresponding condition rating is equated to an intercept term and the added independent variables multiplied by each variable's coefficient. The intercept term is a grand average of the dependent variable, while the effect of the different variables is revealed from the coefficients estimated, provided in each Table. Categorical variables can be noticed to have no values for their first group and values for the other groups this is due to the 'dummy' (fake) variables generated to model them. Specifically, for each group of a categorical variable (with more than two groups) one dummy variable is generated. Dummy variables in contrast to numerical variables can take only value 1 to indicate to specialize the model for the specific group or 0 to exclude it. Thus, despite the fact that it is a coefficient estimate, it is a value that changes the model similar to the intercept.

Positive coefficients indicate increase in the logarithm of the condition rating while, negative indicate decrease. The coefficients' magnitude is related to the variation each variable includes, thus ADT may take values from 0 to 100000, while peak ground acceleration varies from 0 to 2.5. The error term, next to each estimated coefficient, reveals the standard error of the estimated coefficient. The magnitude of the error is presented as the z-value where the coefficient estimated is divided by the error term, with larger z-values indicating smaller errors. The calculated z-values are utilized to calculate the p-values which are compared to the different significant levels and each variables' significance is determined. Significance, levels are denoted by symbols, with (***) indicating high significance and no stars no significance. In the last rows of each table, the regression details are given. Null and residual deviance indicate the remaining variance of the model, before the models variables were included using only the intercept term (null deviance) and after the inclusion of the variables (residual deviance). Inclusion of the variables is also denoted by reduction of degrees of freedom. In the end two AIC values, AIC_o corresponding to the initial regression and AIC after the stepwise process to omit the unnecessary variables, lower AIC values corresponding to a better fit of the model. AIC values can only be used as a

goodness for a specific model (i.e. superstructure condition) and not for comparing two different models.

To interpret the results the significance of each variable has to be taken to account. Non-significant variables are variables which include larger errors in the estimation of their coefficient, thus their use as predictors is limited. From the significant variables, the sign of their estimated coefficient is the first indication of the effect of the predictor to the independent variable. Then the magnitude of the coefficient can be also considered although as previously mentioned it depends on the predictors' variance.

$$\ln(\text{Superstructure Condition}) = \text{Intercept} + C_1*\text{Length} + C_2*\text{Deck width} + C_3*\text{Year of construction} + C_4*\text{Detour Length} + C_5*\text{ADT} + C_6*\text{PGA} + C_7*\text{Precipitation} + C_8*\text{Snow depth} + C_9*\text{Deicing region} + C_{10}*\text{Material} + C_{11}*\text{Water underneath} \quad (4.7)$$

Table 4.6: Regression analysis results for superstructure condition rating

Variables		Coefficient Estimates	Std. Error	z-value	Pr(>|z|)	Sig.
(Intercept)		-5.3E+00	5.53E-02	-95.74	< 2E-16	***
Length (m)		-4.8E-05	4.66E-06	-10.37	< 2E-16	***
Maximum Span (m)		omitted				
Deck width (m)		7.16E-04	1.09E-04	6.55	5.7E-11	***
Year Constructed (date/Year)		3.66E-03	2.80E-05	130.78	< 2E-16	***
Detour length (km)		1.45E-04	2.54E-05	5.72	1.1E-08	***
ADT (vehicles)		2.7E-08	3.55E-08	0.75	4.5E-1	
Truck traffic (% ADT)		omitted				
Peak Ground Acceleration (g)		4.9E-02	3.31E-03	14.82	< 2E-16	***
Precipitation (inches)		-5.6E-04	5.42E-05	-10.29	< 2E-16	***
Snow depth above 1 inch (days)		1.6E-04	2.50E-05	6.21	5.17E-10	***
Deicing Region	Not allowed					
	Allowed	-2.53E-02	1.75E-03	-14	< 2E-16	***
Material	Concrete continuous					
	Concrete simple	-9.69E-03	2.49E-03	-3.90	9.8E-05	***
	Prestressed Concrete continuous	2.10E-02	3.09E-03	6.80	1.1E-11	***
	Prestresssed Concrete simple	1.82E-02	2.27E-03	8.00	1.2E-15	***
	Steel Continuous	9.75E-04	2.71E-03	0.36	7.2E-1	
	Steel Simple	-4.61E-02	2.36E-03	-19.51	< 2E-16	***
Water Underneath	No					
	Yes	-7.31E-03	1.51E-03	-4.84	1.3E-6	***

Significance codes: 0 '***' 0.001 '**' 0.01 '*' 0.05 '.' 0.1 ' ' 1

Regression information:

Null deviance: 91352 on 391443 degrees of freedom

Residual deviance: 63276 on 391428 degrees of freedom

AICo = 1529806, AIC: 1529804

$$ln(\text{Deck Condition}) = \text{Intercept} + C_1*\text{Length} + C_2*\text{Max. Span} + C_3*\text{Deck width} + C_4*\text{Year of construction} + C_5*\text{ADT} + C_6*\text{PGA} + C_7*\text{Precipitation} + C_8*\text{Snow depth} + C_9*\text{Deicing region} + C_{10}*\text{Type of wearing surface} + C_{11}*\text{Type of deck} + C_{12}*\text{Water underneath} + C_{13}*\text{Span type} \quad (4.8)$$

Table 4.7: Regression analysis results for deck condition rating

Variables		Coefficient Estimates	Std. Error	z- value	Pr(>|z|)	Sig.
(Intercept)		-4.60E+00	5.73E-02	-80.235	< 2E-16	***
Length (m)		-3.31E-05	5.09E-06	-6.505	7.75E-11	***
Maximum Span (m)		-1.47E-04	5.27E-05	-2.799	5.13E-03	**
Deck Width(m)		-2.95E-04	1.18E-04	-2.508	1.21E-02	*
Year Constructed (date/Year)		3.30E-03	2.92E-05	112.911	< 2E-16	***
Detour Length (m)			omitted			
ADT (vehicles)		1.04E-07	3.67E-08	2.827	4.70E-03	**
Truck traffic (% ADT)			omitted			
Peak Ground Acceleration (g)		2.40E-02	3.39E-03	7.075	1.50E-12	***
Precipitation (inches)		-1.41E-04	5.52E-05	-2.557	1.06E-02	*
Snow depth above 1 inch (days)		-1.23E-04	2.59E-05	-4.745	2.09E-06	***
Deicing Region	Not allowed					
	Allowed	-1.31E-02	1.78E-03	-7.333	2.25E-13	***
Type of Wearing Surface	Bituminous					
	Epoxy Overlay	-6.19E-03	5.50E-03	-1.125	2.60E-01	
	Gravel	-3.13E-02	3.80E-03	-8.245	< 2E-16	***
	Integral Concrete	6.67E-02	3.32E-03	20.076	< 2E-16	***
	Latex Concrete	-2.96E-02	3.84E-03	-7.698	1.38E-14	***
	Low Slump Concrete	-3.39E-03	4.78E-03	-0.71	4.77E-01	
	Monolithic Concrete	-7.83E-03	1.67E-03	-4.681	2.85E-06	***
	None	8.94E-03	2.18E-03	4.109	3.97E-05	***
	Other	1.82E-02	4.49E-03	4.054	5.03E-05	***
Type of deck	Concrete Cast-in-Place					
	Concrete Precast Panels	-5.36E-03	2.01E-03	-2.673	7.51E-03	**
	Open/Closed Steel Grating	-3.79E-02	3.95E-03	-9.615	< 2E-16	***
	Other	-1.55E-02	3.12E-03	-4.978	6.43E-07	***
Water underneath	No					
	Yes	3.69E-03	1.59E-03	2.317	2.05E-02	*
Span type	Continuous					
	Simple	9.06E-03	1.52E-03	5.955	2.60E-09	***

Signif. codes: 0 '***' 0.001 '**' 0.01 '*' 0.05 '.' 0.1 ' ' 1

Regression information:

Null deviance: 79666 on 382617 degrees of freedom

Residual deviance: 61553 on 382594 degrees of freedom

AIC_o: 1490967 AIC: 1490963

$$ln(Substructure\ Condition) = Intercept + C_1*Length + C_2*Deck\ width + C_3*Year\ of\ construction + C_4*Detour\ length + C_5*ADT + C_7*Truck\ traffic + C_8*PGA + C_9*Precipitation + C_{10}*Snow\ depth + C_{11}*Deicing\ region + C_{12}*Span\ type + C_{13}*Water\ underneath \quad (4.9)$$

Table 4.8: Regression analysis results for substructure condition rating

Variables		Coefficient Estimate	Std. Error	z-value	Pr(>|z|)	Sig.
(Intercept)		-6.20E+00	5.17E-02	-120.08	< 2E-16	***
Length (m)		-4.72E-05	4.63E-06	-10.21	< 2E-16	***
Maximum Span (m)				omitted		
Deck Width (m)		1.04E-03	1.08E-04	9.55	< 2E-16	***
Year Constructed (date/Year)		4.11E-03	2.61E-05	157.88	< 2E-16	***
Detour Length (km)		7.90E-05	2.56E-05	3.082	0.00206	**
ADT (vehicles)		2.67E-08	3.55E-08	0.75	0.451	
Truck traffic (% ADT)		2.68E-04	7.33E-05	3.663	0.00025	***
Peak Ground Acceleration (g)		6.72E-02	3.29E-03	20.44	< 2e-16	***
Precipitation (inches)		-3.62E-04	5.40E-05	-6.703	2.04E-11	***
Snow depth above 1 inch (days)		1.47E-04	2.52E-05	5.835	5.39E-09	***
Deicing Region	Not allowed					
	Allowed	-1.71E-02	1.73E-03	-10	< 2e-16	***
Span type	Continuous					
	Simple	-2.96E-02	1.44E-03	-20.567	< 2e-16	***
Water underneath	No					
	Yes	-1.13E-02	1.54E-03	-7.369	1.71E-13	***
Significance codes: 0 '***' 0.001 '**' 0.01 '*' 0.05 '.' 0.1 ' ' 1						
Regression information:						
Null deviance: 92938 on 391415 degrees of freedom						
Residual deviance: 64088 on 391403 degrees of freedom						
AIC_o : 1525368 AIC: 1525368 no change in AIC despite the omitted variable						

4.4.4.4 Regression analysis conclusions

- All condition ratings are affected mostly by year of construction, with increase in year of construction corresponding to increase in condition.
- Average daily traffic is not significant for superstructure and substructure condition, while it is significant for deck condition.
- For all condition ratings, increase in ADT has a positive contribution. On the other hand truck traffic is a significant predictor for substructure condition with a positive effect, while it has been omitted for the other condition ratings.
- The effects of peak ground acceleration have a significant positive effect to all condition ratings, with increased contribution for superstructure and substructure, validating ANOVA's conclusions (4.3.2.5).

- Annual precipitation, has a significant negative effect to all condition ratings which mostly seems to affect superstructures.
- Deicing reduces all condition ratings with an increased negative coefficient for superstructures, indicating that they are affected most. On the other hand, increase of days of snow depth above one inch, affects positively superstructures and substructures, and negatively deck. Thus, the conclusions of ANOVA that although deicing salts do affect superstructures and substructures, their quantity does not. On the contrary, for deck increased days of days above one inch, corresponding to more direct application of deicing and ice removal processes reduce its condition rating.
- Superstructure materials, continuous spans have increased condition ratings compared to simple spans. Thus, if materials were to be ordered from higher to lower condition ratings, this order would be: continuous spans of prestressed concrete, simple spans of prestressed concrete, continuous spans of steel or continuous spans of concrete, simple spans of concrete, simple spans of steel.
- Continuous spans also affect positively substructure condition ratings while deck condition ratings are negatively affected.
- Water underneath the structure has an increased negative contribution to the condition rating of substructures, while it affects in a much less negative way superstructures and in a positive way deck condition rating.
- Length appears to have a minor negative effect for all condition rating.
- Maximum span has a minor negative and less significant effect for deck rating while it has been omitted by the stepwise process for superstructure an substructure.
- Deck width has a positive effect for superstructure and substructure while, a negative for deck condition rating.
- Detour length has a small positive effect for condition ratings of superstructure and substructure, it is less significant for substructure and has been omitted for deck condition.
- For deck, the wearing surfaces ordered from higher to lower condition are: integral concrete, other, none, bituminous, monolithic concrete, epoxy overlay, low slump concrete, latex concrete, gravel.
- For deck, the deck types ordered from higher to lower condition ratings are: concrete cast in place, concrete precast panels, other, open/closed steel grating.

4.5 Conclusions

In this Chapter, factors affecting structural condition of bridges, were studied using data from existing bridges. To achieve this, inspection data of more than 600,000 bridges located in the US were utilized from the National Bridge Inventory (NBI). Since, the US territory contains a large variety of environmental exposures, databases such as the United States Geological Survey (USGS) and the National Oceanic Atmospheric Administration (NOAA), were used to introduce additional variables regarding climate and earthquake hazard. To estimate their values for each bridge location, spatial interpolation methods were utilized. The combined dataset was then analyzed using data analysis procedures, to determine which variables affect the structural condition of a bridge.

The exploratory data analysis showed that, the selected NBI variables had low correlations among them in contrast to weather variables which were moderately to highly correlated. ANOVA and multiple comparisons revealed useful patterns, which indicated the effect of each variable to structural condition rating. More over the analysis showed the existence of certain thresholds after which variables had a different effect to the condition ratings such were:

- Deicing region and snow depth above one inch in days, where although deicing region coincided with more than 0.5 days of snowfall above one inch, further increase in days did not affect superstructure and substructure condition and slightly reduced deck's condition rating.
- Peak ground acceleration affected most substructure and superstructure condition and less deck. A distinct similar pattern among all condition ratings reveals that, increase in peak ground acceleration more than 0.2g has a meliorating effect.

Furthermore, from the regression analysis the structural conditions of deck superstructure and substructures were confirmed to be mostly affected by:

- The year of construction, where recently built bridges corresponded to higher condition ratings for either structural parts.
- The materials of deck and superstructure, where highest ratings for deck condition corresponded to cast in place deck with wearing surfaces of integral concrete. For superstructures, higher condition rating corresponded to prestressed concrete.
- Span type affected all condition ratings, for superstructures and substructures continuous spans had higher condition ratings than simple spans, while for deck they corresponded to lower condition ratings.

- Peak ground acceleration, whose increase, increased the condition ratings all structural parts.
- Being located within the US deicing region. Superstructures and substructures were affected more by the presence of deicing than by the amount of deicing applied. On the other hand, deck showed the same dependency to other structural parts regarding deicing with the additional dependency to the amount of deicing applied.
- Precipitation with increase in precipitation corresponding to lower condition ratings.
- Water underneath the structure affected mostly substructure's condition rating and less the condition rating of the deck's.

Less important factors for the structural condition ratings were:

- Average daily traffic, truck traffic and detour length, whose increase was corresponded to small increase in condition ratings.
- Length, maximum span, and deck width also had a very small effect in the condition ratings.

5 Coastline effect on bridges

The analysis of the previous chapter revealed the most important factors affecting bridge condition ratings. Among these, the distance from coastline was found to have a significant effect and that it should be studied separately, as no correlation was noted with other environmental factors. The methodology followed in the present chapter examines the effects of coexisting factors, in order to select consistent samples, where the primary differentiator is the distance from the seacoast. The main aim is to find the critical distance, within which coastline effects are observed on bridge deterioration. The procedures followed herein test the reliability of the NBI, the sensitivity of the recorded ratings and the consistency of the gathered data and the final findings.

5.1 Introduction

Marine and coastal environments are considered to be highly corrosive to structures built from common materials, such as concrete, prestressed concrete and structural steel. Their effect can be mostly attributed to the high concentration of chloride ions contained in sodium chloride (sea-salt) in seawater (Brown, et al., 1995), which causes corrosion to various forms and types of steel (embedded or structural). Specifically, in the case of steel, chlorides attack the passive layer formed at the outer steel surfaces that protects the inner parts from further corrosion (Schweitzer, 2010); in the case of concrete, chlorides cause a drop in the concrete's pH and hence result in reduced cover protection capacity for the embedded steel (Bentur, et al., 1997). The chlorides' aggressiveness stems from the fact that the electrochemical reactions taking place do not consume the chlorides.

Chlorides can reach a structure's surface either through direct contact of seawater (marine structures) or through seawater droplets carried by wind (Cole, et al., 2003a). The latter are also known as airborne chlorides and are the predominant natural way for chlorides to reach a distant from the coast structure (Neville, 1995). Travel distances can exceed 2km or can be much less depending on terrain and wind regime, making the coastal zone's limits affected by chlorides difficult to determine (Neville, 1995). A complete study needs to consider the procedures of airborne salt production, travelling and deposition, as well as the consequent deterioration mechanisms and intensity of their effects on structures. Airborne salt results primarily from droplets produced by breaking bubbles in the whitecaps on the sea surface (Blanchard & Woodcock, 1980). Their concentration depends on the percentage area of whitecaps formed on the sea surface, the bubble sizes generated, as well as the wind

(intensity, direction, etc.). The produced particles become airborne and exhibit an attenuating concentration with height, with maximum concentration observed just above sea level (Blanchard & Woodcock, 1980). Then, the airborne salts are transported inland by wind and deposited on the structures' surfaces.

Various methods exist to measure the concentration of deposited chlorides, see e.g. (Ambler & Bain, 1955), with the wet-candle method being the most popular one. This method consists of an experimental setup placed in predetermined locations, in accordance with specific national standards. After a preset duration, the content of each setup is collected and analyzed with various methods (e.g. chromatography), in order to determine the concentration of the deposited chlorides. Other experimental methods include the Japanese salt sampler (Mishikawa & Tanaka, 1993) and the advanced Japanese salt sampler that can also measure the wash-off from precipitation (Chen, et al., 2013). In all cases, chloride deposition is assessed in combination with the specific characteristics of specimens made of materials such as metals, concrete or mortars, in order to measure surface chloride as well as ingress. In general, the experimental setup is placed at various distances or/and heights (Mustafa & Yusof, 1994), in order to measure the attenuation of deposited chlorides with distance. The deposition can be measured in monthly intervals, while the specimens are analyzed in larger intervals to measure chloride ingress.

In general, the attenuation of chloride deposition with distance can be fitted by an exponential function (Feliu, et al., 1999), but, as can be expected, the deposition rates vary significantly mostly due to seasonal or local changes. For example, an average reduction of the initial chloride deposition exceeding 90% was observed after about 200m distance from the coast in studies conducted in Brazil (Meira, et al., 2010) (Pontes, et al., 2009) and Bangladesh (Hosain, et al., 2009). In another study conducted in Taiwan (Chen, et al., 2013), the seasonal average was calculated and results showed a seasonal percentage of about 88% reduction of the initial deposition at distances exceeding 1km for autumn and winter. In the same study, the critical height of monthly precipitation above 100mm was found to reduce the adhesive airborne salt, provided the wind has direction from sea to inland. The critical speed of such winds, categorized as 'saline', was estimated to be above 3m/s using the wet-candle method in Spain (Morcillo, et al., 2000). Moreover, the effect of elevation has an important effect on the deposition rates. A 60% difference was noticed between the initial setup placed at 5m height and a second at 15m height, both located at 30m from the coast (Mustafa & Yusof, 1994). Blanchard and Woodcock (1980) also noticed an inversion layer for speeds between 3m/s and 8m/s that causes a sudden increase in sea salt concentration at

altitudes of 500m and 600m above sea level. Additional factors, such as terrain topography and obstacles or channeling effects, can alter the deposition rates significantly. Further information on these factors can be found in an Australian study regarding atmospheric corrosion (Cole, et al.; 2003a; 2003b; 2003c; 2004a ; 2004b).

The atmospheric deposition of chlorides is of major importance also because its effect on materials provides useful information on durability of steel and concrete structures. Ambler and Bain (1955) observed that the amount of corrosion in steel varies linearly with the deposition of chlorides. The effects of atmospheric deposition of chlorides on concrete are more complicated than steel. Surface chlorides reach the steel bars through water absorption and chloride diffusion (Neville, 1995). Thus, properties of concrete, such as water binder ratio and curing, affect diffusion and surface chloride content (Song et al. (2008). Mortars with high cement content, lower absorption capacity and lower porosity were found to be more resistant to sea salts (Hosain, et al., 2009). Environmental properties like temperature and humidity levels also greatly affect chloride transport through concrete. Laboratory tests performed by Alhozaimy, et al. (2012) on reinforced concrete specimen with varying temperatures and chloride content at high relative humidity (85%) showed that there is a limit to the increase in temperature (at 40^{o}C), after which corrosion is reduced.

Extrapolating results from experimental tests to real structures may be problematic. Test specimens have controlled material quality and exposure (regarding position and duration); such characteristics may vary significantly in structures due to prolonged exposure, as well as the coexistence of other factors. Thus, measurements of the deterioration in actual areas of chloride deposition could be utilized for delimiting the coastal effect due to longer exposures. Chen et al. (2013), in their study on airborne chlorides, instead of using specimens, measured the surface chloride content on real structures and found a linear correlation to the measurements of their experimental setup. Medeiros et al. (2013) studied the chloride content of a 40-year old concrete building's exposed columns; despite the lower depositions of chlorides due to the 700m distance from the coast, their accumulation was noticed to cause major differences compared to the core sample at different position as well as height. Similar conclusions were drawn for concrete bridge structures by McGee (2000) in his study on Tasmanian bridges and by Tanaka et al. (2006) for prestressed concrete bridges located in the first 500m inland from the coast of Japan.

In this work, the effect of airborne chlorides to a sample of almost 20,000 bridge structures is studied using NBI data, with the purpose of macroscopically delimiting the coastline effect on deteriorating bridges. To perform this, high accuracy coastline

coordinates were combined with bridge coordinates to form 12 distance groups up to 10km inland from the coast.

5.2 Analyzed bridge sample and coastal distance zones

The US coastline has a total length of about 95,000 km hosting more than 9,300 km of highway (Qin, et al., 2007) with several bridges. In addition to the deterioration factors addressed in Chapter 4, bridges in coastal areas are exposed to airborne chlorides from seawater, as well as to other factors that may interact to intensify or reduce the chlorides' corrosive effect. In this section, these factors are noted and the procedure followed to determine the distances of bridges from the seacoast for the dataset under study are presented. The bridges are then grouped into zones according to their coastal distances to facilitate the subsequent analysis.

In Chapter 4, the most important factors affecting bridge condition ratings were derived: (i) year of construction, (ii) year of reconstruction, (iii) structural material, (iv) location (correspondingly specifying the earthquake hazard and the potential for deicing at each region), (v) water presence underneath the bridge and (vi) yearly precipitation. Moreover, the ground elevation for each bridge was determined using ordinary Kriging interpolation between known elevations of weather stations. The wind data provided by NOAA (2017b) could not be included in the analysis for coastal bridges. This was due to the fact that wind data regarded only 56 weather stations in all US territory, which could not provide a dense network to interpolate wind. Furthermore, the wind information regarded hourly records of predominant wind magnitude and direction. Although average speed and directions were calculated from the data and verified from older studies (Klink, 1999) to observe irregularities, studying such variating factor with average speed and direction could be misleading. It is also worth mentioning that additional variables should be added to take wind data to account, such as direction of the structure and information regarding the terrain. Attaining and incorporating such information would induce a large degree of complexity of the study and change its macroscopic nature, which is based on condition ratings. It should finally be mentioned that the US coast is also exposed to the accidental effects of tsunamis (Ghobarah, et al., 2006) and hurricanes (Padgett, et al., 2008), which could cause severe damage to bridges. In fact, the East coast is vulnerable to hurricanes (ASCE, 2010), see map in Appendix A-III.1 taken from this source) and the West coast to tsunamis (USGS (2017), see map in Appendix A-III.2 taken from this source). It can be macroscopically deduced from these maps that, for the tsunami and hurricane hazards, certain geographic uniformity exists.

Figure 5.1 provides a visualization of the whole dataset of US bridges using their interpolated elevations, as well as the designation of the deicing and high earthquake hazard regions (found in Chapter 4 to affect bridge condition). A more detailed figure with additional elevation categories is given in the Appendix (A-III.3). Regarding earthquake hazard and precipitation, detailed maps are provided in the Appendix of Chapter 4 (A-II.2, A-II.6). Figure 5.1 indicates differences between the east and west coasts in ground elevation and earthquake hazard.

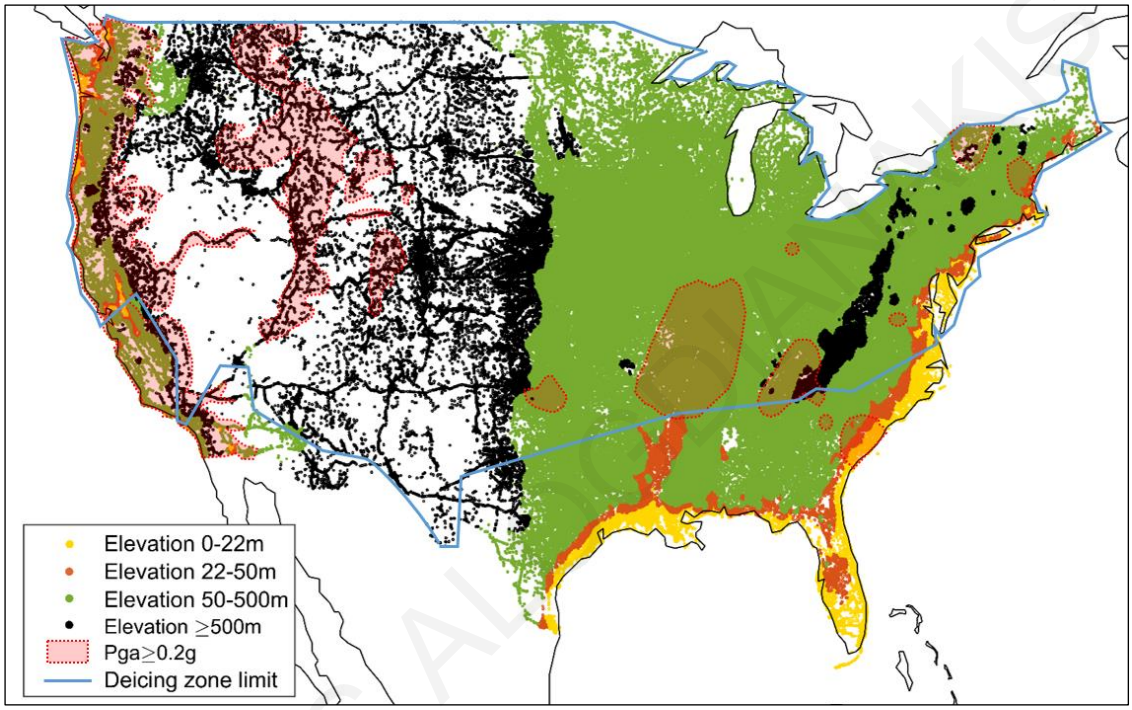

Figure 5.1: Information for elevation, deicing, and earthquake hazard (peak ground acceleration) for the bridges located in conterminous US.

The bridge distances from the coast were estimated using the bridge and coastline coordinates provided by NBI and NOAA (NOAA, 2017a), respectively. The US coastline includes various geographic details, such as cuspate forelands, tombolos, spits, bays, lagoons and barrier islands, creating a complicated pattern for distances to be calculated (Fig. 5.2). Additionally, the presence of many rivers, which flow into the sea and exhibit varying salinity levels throughout the year, create the need to define a reference coastline to study the effects of airborne chlorides. This was achieved by smoothening or eliminating certain geographical details, making this way the coastline profile simpler. Hence, the NOAA coordinates were imported into AutoCAD software and, by visualizing also the surrounding terrain form using satellite images of Google maps, the reference coastline coordinates were determined. Moreover, wide rivers directly linked to the sea, bays, lagoons and barrier islands were considered to have seacoast limits, after their periodical salinity levels were

checked from sites of local agencies. A characteristic example is the case of Florida's Caloosahatchee River, which is displayed in Fig. 5.2; salinity levels for this case were taken

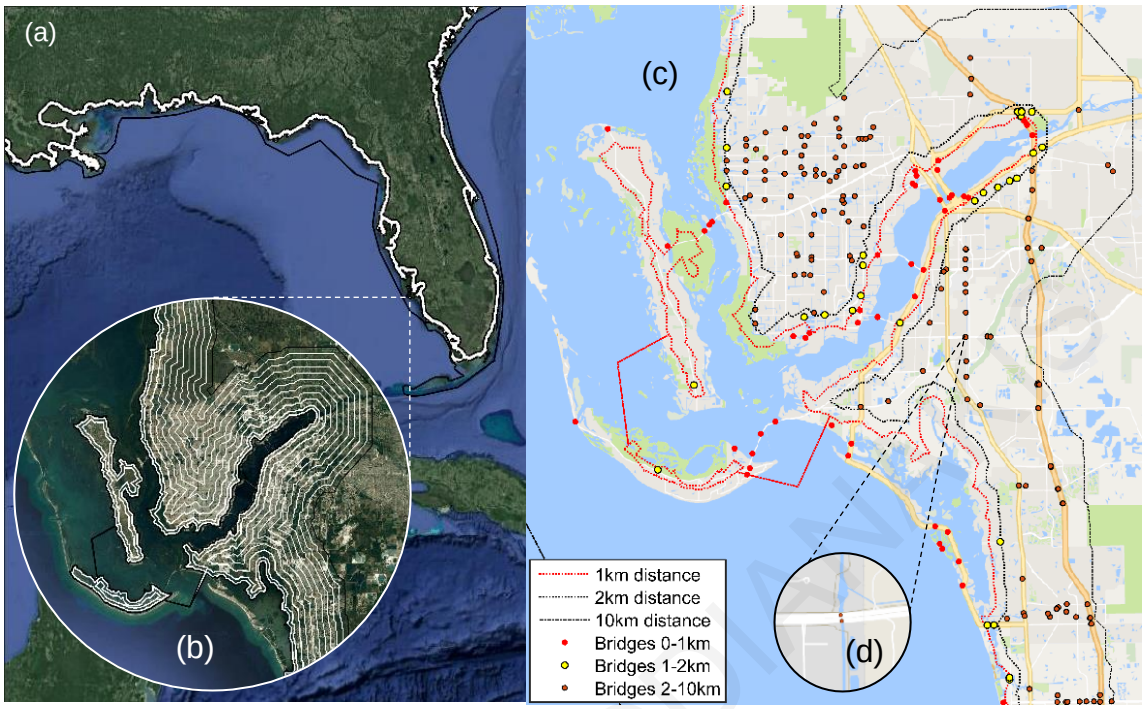

Figure 5.2: Accuracy of drawn distance zones: a) the coastline width of 10km of the state of Florida, b) a zoom in to the certain region where some of the mentioned details existed c) the roadmap and the precision of the coordinates of the NBI as well as the precision of the overall procedure and d) a zoom in, in an area where bridges are located over water parallel to the highway.

from Charlotte Harbor Wateratlas (CHNEP, 2017) web page. Other geographical details, such as small rivers and streams, which only created unnecessary complications, were ignored.

To facilitate the analysis regarding bridge distances from the seacoast, a number of distance zones were specified. Thus, using AutoCAD's 'offset' command, the reference coastline was copied inland at equal distances: a new 'parallel' line was drawn every 1km and up to 10km from the original coastline. According to the referenced literature, the overall coastal region included by the 10km border inland should be enough for changes in airborne chlorides effects to be noticeable. Additional offset lines were generated within the first kilometer at distances of 250m and 500m from the coastline, in order to be able to observe the gradual attenuation of airborne chlorides effects very near the seacoast. To make sure that all bridges over seawater (marine bridges) would be included in the analysis, a wider (extended) shape was formed for the first distance zone (from seacoast to 250m inland) surrounding the islands (Fig. 5.2). Thus, the first distance zone was defined as a polygon using the coastline (together with the extension to include islands) and its 'parallel' line at 250m inland. Similarly, the other distance zones were defined as polygons using consecutive lines at the aforementioned distances up to 10km from the coast. To make sure that bridges

on islands are properly handled, the defined mainland polygons were linked with the islands' distance zones by drawing thin connecting polygons (see red lines in Fig. 5.2(c)).

In order to assign bridges to corresponding distance zones, the coordinates of the polygon vertices were imported into Matlab software. The accuracy level achieved by the overall procedure is demonstrated in Fig. 5.2(c) and d, where satellite and roadmap images of Google maps are shown in the background. Inevitably, due to the coastline simplifications made at regions with complex landscapes, some errors in the assignment of bridges to distance zones should be expected, which are however very few to noticeably affect the results of this study.

Before presenting the main analyses of this chapter, an exploratory data analysis was performed to gain some insight into the coastline bridge sample assessed (see A-III.4, A-III.5 at the Appendix). The basic characteristics of the sample (comprising of all bridges with distance <10km from the coastline) can be summarized as follows:

- The overall population of the sample is 19,214 bridges with an average year built of 1973.
- The reconstructed bridges are about 20% of the overall population.
- Regarding the bridges' spatial distribution, most of these are located within areas where: deicing is allowed (76%), the seismic hazard corresponds to PGA<0.2g (71%), the elevation is <50m (90%) and the annual precipitation is >40in (84%).
- More than half (58%) of the sample's bridges are over water.
- The superstructure of the sample's bridges is made of either concrete (25%), prestressed concrete (36%) or steel (38%).
- Concrete is the dominant material for the decks of the sample's bridges (95%).
- As no categorization for substructure's material is provided in the NBI, concrete is assumed for all bridges.

5.3 Analysis of interactions of factors affecting bridge deterioration

In the previous chapter, lower condition ratings were noticed closer to the coast, but, to delimit the coastline effect, a closer examination should be performed. A first step to distinguish the main effects is to explore the interactions between potentially influencing factors.

5.3.1 Interaction plots

As the aim of this work is to study bridge deterioration, the dependent variable in all analysis cases considered is the condition rating of basic bridge components (deck,

superstructure, substructure), while independent variables correspond to factors potentially affecting the dependent variable value. The interactions considered in this study are two-way, meaning that two independent variables are studied simultaneously with regard to their effect on the dependent variable. Although the bridge sample size was adequate, continuous variables, such as bridge age, precipitation or elevation, could create misleading results due to their non-uniform spatial distributions. Thus, the following meaningful categorizations of independent variable values were made based on the results of the previous chapter:

- *year of construction* and *year of reconstruction* were grouped into one independent variable with values organized in 7 age-levels (4 for the year of construction and 3 for the year of reconstruction);
- *seismic hazard* was considered through a dichotomous variable indicating bridge locations with $PGA<0.2g$ or $PGA\geq0.2g$;
- the *effect of deicing* was also included through a dichotomous variable indicating bridge locations where deicing is allowed or not;
- the presence of *water underneath* the bridge was also taken into account through another dichotomous variable indicating presence or no presence;
- for *precipitation* and *elevation*, dichotomous variables were specified based on the corresponding sample means, as there were no easily evident patterns and due to their complicated spatial distributions.

A convenient way to visually present and analyze two-way interactions is by using an interaction plot for categorical data. To facilitate its explanation, a distinction can be made between the two independent variables examined at any time: the *focal* variable represents the main variable of focus and the *moderator* points to the various levels/groups of values for the other variable (Baron & Kenny, 1986). For each pair of independent variables, two plots are created by interchanging the aforementioned roles. The focal variable's levels are displayed through different lines in the plot, while the moderator's levels are displayed on the horizontal axis of the plot. The effect of each interacting pair of independent variables is studied by computing the average value for the dependent variable (Simonoff, 2003). For each level of a focal factor, the computed means are connected with lines between consecutive levels of the moderator, creating a continuous graph for each focal level. All interaction plots are organized together in an $n\times n$ table, where n corresponds to the number of considered variables. In this table, each column displays one moderator variable, while each row one focal variable. The interaction plots for superstructure condition are presented in Fig. 5.3; the interaction plots for deck and substructure conditions can be found in the

Appendix (A-III.6 and A-III.7). To index the interaction pairs in these figures, capital letters have been used for the focal variables (rows) and Latin numbers for the moderating ones (columns).

5.3.2 Interpretation of interactions

The key to interpreting interactions is the tracking of slope changes between the lines of the focal variable levels. Crossings or high slope differences of the lines of a focal variable indicate that significant interactions exist, while there are no significant interactions for small differences in slope or parallel lines. Significant interactions reveal that the two factors analyzed (focal and moderating) are not as important as their interaction. Thus, their effects on the dependent variable should be studied together. Additionally, for the case of non-significant interactions, the visualization assists in confirming the combined effect of two variables by comparing the means among the different levels of the focal variable.

In this study, more emphasis was appointed to the explanation of the main effects of distance from the coast and year of construction/reconstruction, thus they were placed in the first two columns/rows of the plots-tables. This placement assisted in showing the effect and interactions of the other variables on distance from coast as a moderator variable (column I), while column II reveals each variable's effect for the different age groups.

Using all mentioned indications for the interaction plots the following remarks can be made regarding the plots-table of Fig. 5.3. The predominant factors affecting bridge superstructures near the coastline appear to be: (a) year of construction/reconstruction, (b) seismic hazard and (c) allowing or not deicing procedures. These conclusions are based on plots B-I, C-I, D-I, A-II, A-III and A-IV. The magnitude of effects can be noticed in column I of the plots-table and can be confirmed for different years of construction/reconstruction in column II. Plots C-IV and D-III show the combined effect of seismic hazard and deicing policy, which reveals difference regarding the mean condition rating as well as similar slopes of interaction lines. Analogous effects were observed also for substructure condition in Appendix (A-III.7), while the remark that deck condition is not affected by high seismic hazard is confirmed in Appendix (A-III.6). Furthermore, from interaction plot B-I, a pattern of lower condition ratings near the coast can be noticed for different years of construction/reconstruction. This does not apply for the case of bridges reconstructed before 1960 and bridges constructed before 1940, but this inconsistency could be attributed to the small sample sizes within the first distance zones. Additionally, the interaction plot B-I displays more inclined interaction line slopes for older bridges, probably due to their prolonged exposure. Also, the similar line slopes and differences in mean values of plot A-

II reveal small but constant changes due to distance from coast. On the contrary, the large differences noticed in line slopes of C-II reveal better condition ratings for all years of construction/reconstruction for higher seismic hazard, which implies better standards, practices etc. utilized for higher PGA. Although changes in the line slopes can also be noticed in plot D-II, this effect could be attributed to the spatial distribution of seismic hazard areas (Fig. 5.1).

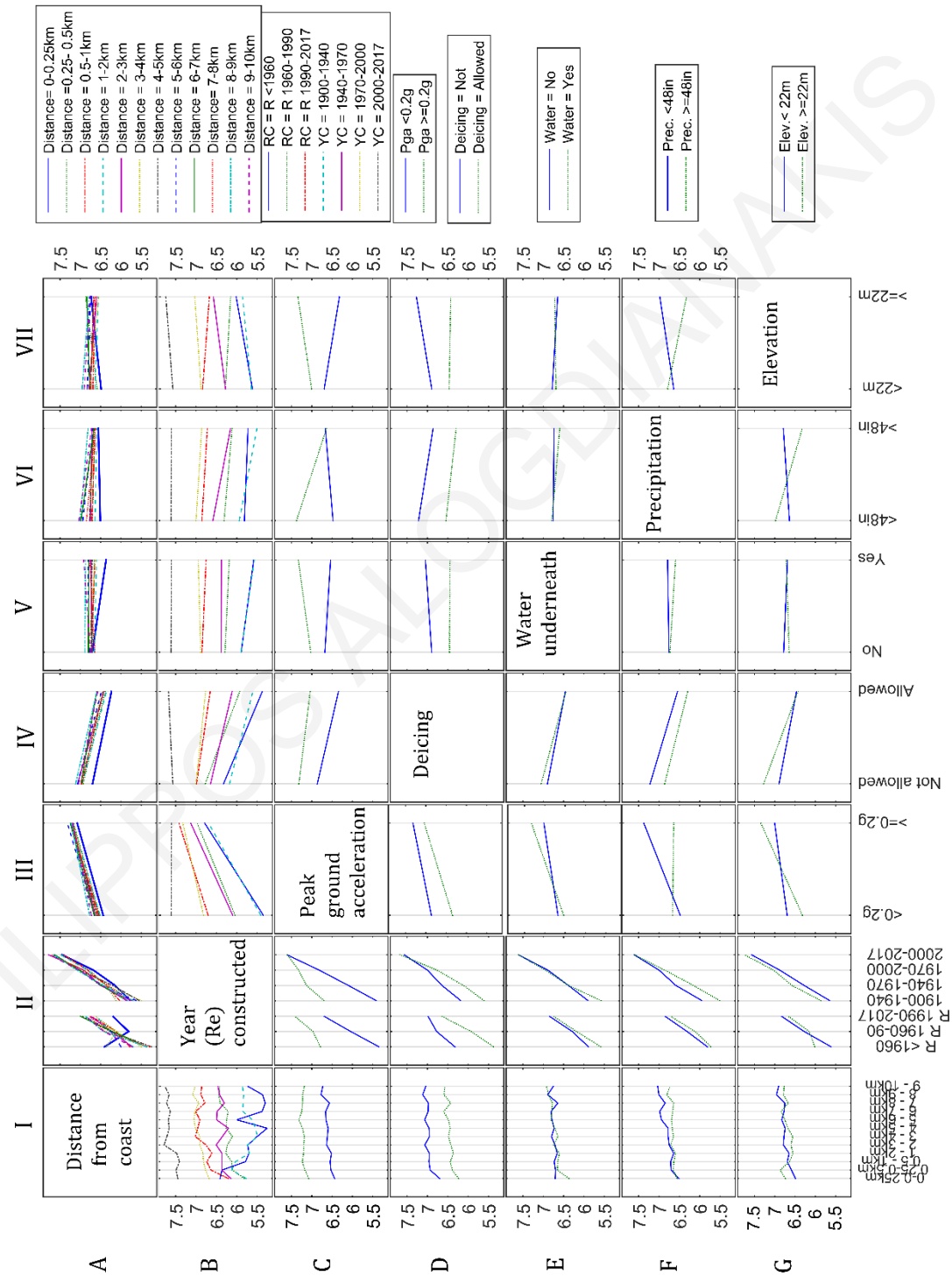

Figure 5.3: Interaction plots for the dependent variable (superstructure condition) and the considered main effects.

The presence of water underneath the bridge appears to affect condition ratings only for the first coastal distance zone (see plots E-I and A-V), probably due to the fact that there are bridges over seawater in this zone. Referring to water underneath the bridge as a focal variable (row E), only small differences can be seen for the other moderating variables. Precipitation level does not seem to have any special significant effect on coastal bridges either (see plot F-I). A difference can be noticed, however, in plot F-II for the factor of 'year of construction', but this could be attributed to a combination of effects from deicing policy and seismic hazard. For instance, plots F-III and C-VI indicate similar condition ratings for the two precipitation levels in regions with lower PGAs, while the combination of higher PGAs with higher precipitation level yields worse bridge conditions. Also, notice the similar patterns of interactions with elevation (see plot F-VII). Furthermore, interaction lines with similar slopes are shown in plots F-IV and D-VI, but there are differences in the condition means when the deicing policy and the precipitation level are varied. As regards elevation (see plot G-I), the most interesting observation is that coastal bridges at higher elevations are in a little better condition.

5.4 Main analysis

The most significant factors affecting coastal bridge condition have been identified in the previous section. The acquired information will be used to properly segment the overall bridge sample and study the coastline effect with an approach different to ANOVA, focusing on deterioration for each coastal distance zone.

5.4.1 Sample segmentation

The analysis of interactions of the previous section showed that the main effects considered alter the bridge condition ratings without interacting with each other. This finding was utilized to perform a more focused examination of the overall sample, by separating it in segments based on the factors of earthquake hazard and deicing policy. Thus, four segments of coastline bridges were created in total: the overall sample was divided in two segments corresponding to lower ($PGA<0.2g$) and higher ($PGA\geq0.2g$) earthquake hazards and then each of these two segments was subdivided in two more segments to distinguish between areas where deicing is allowed or not. The geographical locations of the 4 segments allow a simplification in the way they can be referenced: a segment is either at the West (higher seismic hazard) or the East (lower seismic hazard) and either at the North (within deicing region) or the South (deicing not allowed) of the US.

Apart from earthquake hazard and deicing policy, ground elevation was also more closely examined for the first coastal distance zone (up to 250m inland) and for the 4 sample segments defined above (see Appendix A-III.8). Although some patterns of increase in mean condition with increase in elevation were noticed, they showed some inconsistencies and therefore could not be generalized. These results do not lead to the conclusion that the effect of elevation should not be considered, but probably that it should be combined with terrain information. As such information was not taken into account, no exclusion or separation was made for the factor of elevation. It should be acknowledged that elevation, terrain topography as well as water underneath the bridge, can affect the structural condition of bridges, especially within close distance from the sea.

5.4.2 Analysis procedure

The segmented coastline provided an appropriate sample for more detailed analysis. The effect of airborne chlorides will be studied for each sample segment using the predetermined coastal distance zones. A different approach to ANOVA will be followed to highlight the effect of bridge deterioration on structural condition. Although ANOVA revealed in Chapter 4 condition differences for various distances near the coast, the calculated condition means and standard errors due to the sample's variability within each distance zone were not easy to interpret. Due to the range of condition ratings (0-9), if bridges with high ratings existed within a distance zone, increased ratings would be noticed in ANOVA, concealing the effect of those with lower ratings and also creating larger standard errors. Thus, to highlight lower ratings, an alternative analysis approach should be employed to utilize the proportion of bridges below or equal a critical rating for each distance zone. Condition rating 5 was specified as such, as it can be regarded as a threshold indicating both significant bridge deterioration (Chapter 3) and need for rehabilitation (Chapter 4). The proportions of significantly deteriorated bridges were estimated for each distance zone and structural component (deck, superstructure and substructure) and expressed as percentages. Each structural component's percentage was connected with lines between consecutive distance zones to form continuous graphs. It should be mentioned that the scale of the distance axis in all figures of this section is qualitative and the 3 first distance zones correspond to the first 1km.

The condition rating provides an indication of the deterioration state but, as previously stated, it is linked with several factors affecting it. Thus, for example, if more newly built bridges exist in a certain coastal distance zone, a lower percentage of deteriorated bridges would be anticipated. To take into account the effect of year of construction/reconstruction

and of the utilized materials to the ratings, a way to ensure that consistent samples are comparatively assessed should be provided. Therefore, the presented results include sample sizes for all distance zones, while the consistency of the zones' samples can be verified through the stacked bar plots given for year of construction/reconstruction and for utilized materials. Using such information, one can first check the homogeneity of samples with respect to year of construction/reconstruction and materials and then, if the samples are approved, interpret variations in condition ratings.

The main results are provided in two parts for East and West coasts distinguishing the two seismic hazard levels considered; for each part, the results are given separately for North and South coasts distinguishing the locations in or out of the deicing region. An additional analysis has been included for Florida state due to its low elevations and its Peninsula shape; this combination of characteristics leads to increased travelling length of airborne chlorides. Moreover, an extra analysis is given referring to an older inventory (2009) for the same coastal distance zones, in order to compare results with respect to the ones of past inspections. Such a comparison provides useful information regarding the validity of the findings of the whole procedure followed.

5.4.3 Results for low seismic hazard (East coast)

The results of the analysis for the East coast are displayed in Figs 5.4 (North) and 5.5 (South). The East coast generally comprises of lower elevations and is also prone to hurricanes, thus, the effect of airborne chlorides can be expected to be more evident than in the West coast. The North part is expected to have increased percentages of lower condition ratings due to deicing practices implemented; the South part should be more representative for the airborne chloride effects due to the warmer weather and the absence of chlorides from deicing. Certain notes can be made regarding year of construction/reconstruction as well as superstructure materials. Specifically, the North part has older bridges, it has more reconstructed bridges and in most cases the superstructure material is steel. The South is comprised of younger bridges, there is a low percentage of reconstructions, while the most common superstructure materials are concrete and prestressed concrete. In both North and South parts, the simple spans are more common than continuous spans. Also, for each separate sample (North/South), the chart of years of construction/reconstruction (Figs 5.4(b) and 5.5(b)) as well as of superstructure material (Figs 5.4(c) and 5.5(c)) presents a roughly uniform pattern across the different distance zones, facilitating the interpretation of the results in Figs 5.4(a) and 5.5(a).

Similar patterns can be observed in Figs 5.4 (a) and 5.5(a) for the percentage of bridges below or equal condition 5. In both figures, increased percentages can be noticed near the coast. Additionally, the expectation of increased percentages in the North due to deicing is confirmed. In both North and South parts, superstructure and substructure condition ratings seem to be affected more than the deck's. This observation could be attributed to the fact that decks are generally more protected by the surrounding superstructures or non-structural obstacles, on whose surfaces airborne chlorides settle. It is also interesting to note the interchanging relative position of the lines for substructure and superstructure in Figs 5.4(a) and 5.5(a), which indicates higher deterioration of substructures in warmer areas (South) and of superstructures in colder areas (North). This note could be linked to the effect of wet-dry cycles, which can be expected to be more frequent in the South due to increased evaporation and temperatures.

For the coastal part within the deicing region, increased percentages can be noticed at distances 4-8km from the coast for both superstructure and substructure (Fig. 5.4 (a)). Since small differences can be noticed in the years of construction/reconstruction in these distance zones (Fig. 5.4 (b)), only part of this increase could be attributed to the small increase in old bridges corresponding to the distances of 6-8km. The increased percentage of deteriorated superstructures and substructures at distances 4-8km could be linked to leakages from bridge joints commonly encountered in simple spans. This is justified by the increased percentages of simple span bridges in these distance zones (Fig. 5.4 (c)) combined with the fact that deicing salts are used in the North. A lower intensity of the same effect can be noticed for the deck. Thus, based on the increased percentages of deteriorated bridges observed in the distance zones closer to the coast, airborne chlorides seem to affect structures that are within the first 1km inland. For larger distances from the coast, the deicing practices implemented are mainly responsible for the still high concentration of chlorides deposited, while sea chlorides carried through the atmosphere do not have a noticeable effect.

For the South East coast, the results are more straightforward to interpret, as the graphs are noticeably smoother (Fig. 5.5). Based on the increased percentages of conditions ≤ 5 closer to the coast (Fig. 5.5 (a)), superstructures and substructures appear to be affected by airborne chlorides within the first 2-3km inland. Decks appear to be affected only within the first 250m from the coast. It is pointed out that the source of chlorides on bridges of the South coast is only the sea. Thus, the smooth attenuation of deteriorated bridge percentages within the first distance zones can be regarded as the pure effect of airborne chloride deposition. In conclusion, although differences in materials and years of

construction/reconstruction in the North and South parts of the East coast (Figs 5.4 (b,c)) and 5.5 (b,c)) do not permit direct comparisons, it can be stated that deicing exhibits a more uniform and dominant effect at the North, while airborne sea chlorides have a more significant contribution to the deterioration of bridges near the coast in the South where deicing is not implemented.

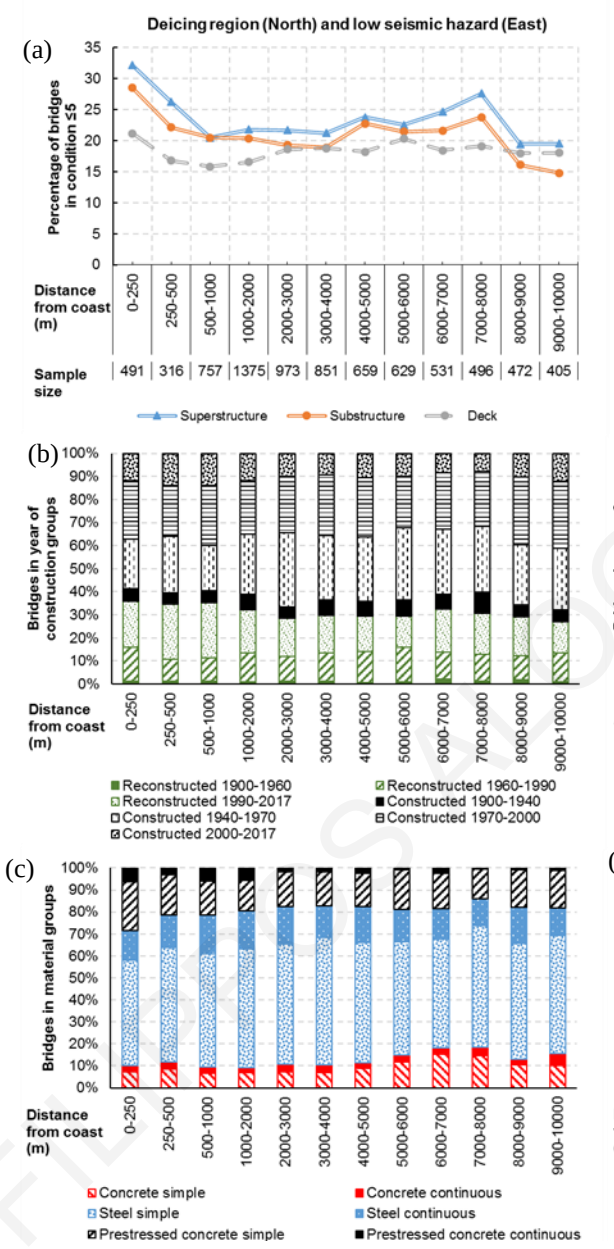

Figure 5.4: Bridges within regions of low earthquake hazard and deicing for the different distances from coast, (a) percentage of bridges below or equal condition 5, (b) stacked column chart for years of construction and (c) stacked column chart for materials of superstructure.

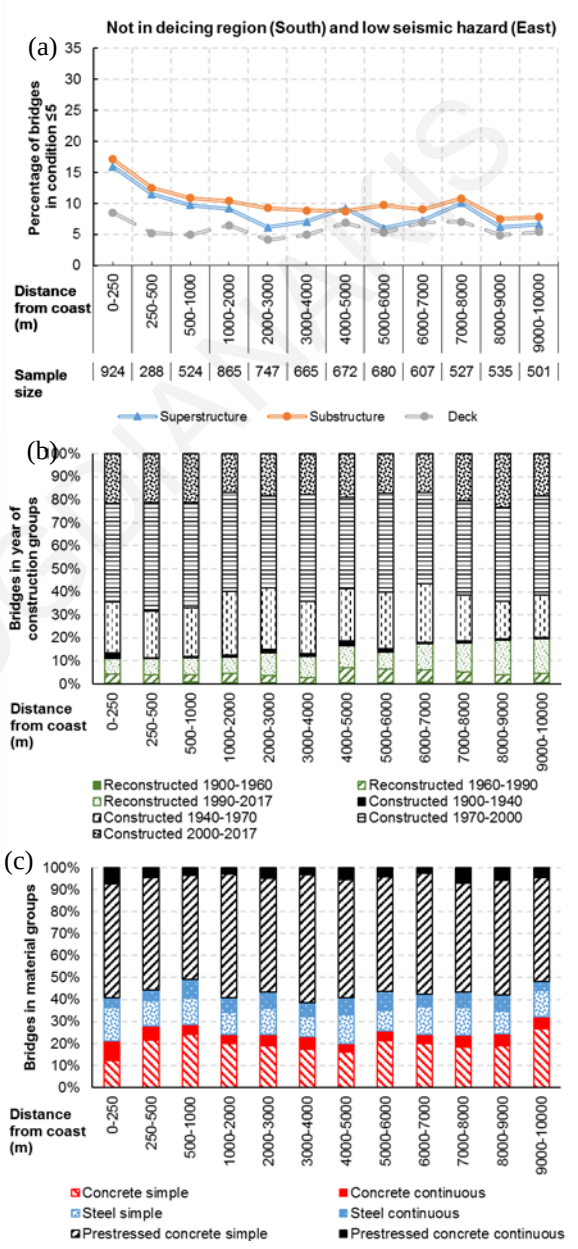

Figure 5.5: Bridges within regions of low earthquake hazard and deicing is not allowed for the different distances from coast, (a) percentage of bridges below or equal condition 5, (b) stacked column chart for years of construction and (c) stacked column chart for materials of

5.4.4 Results for high seismic hazard (West coast)

The results of the analysis for the West coast are displayed in Figs 5.6 (North) and 5.7 (South). In contrast to the East coast, the materials and years of construction/reconstruction for the West coast bridges have a clearly non-uniform pattern across the different distance zones (Figs 5.6(b,c) and 5.7(b,c)). This does not assist in interpreting results, thus only general remarks can be made. Hence, according to Figs 5.6(c) and 5.7(c), there are more continuous and less steel bridges in the West compared to the East coast. Furthermore, it is

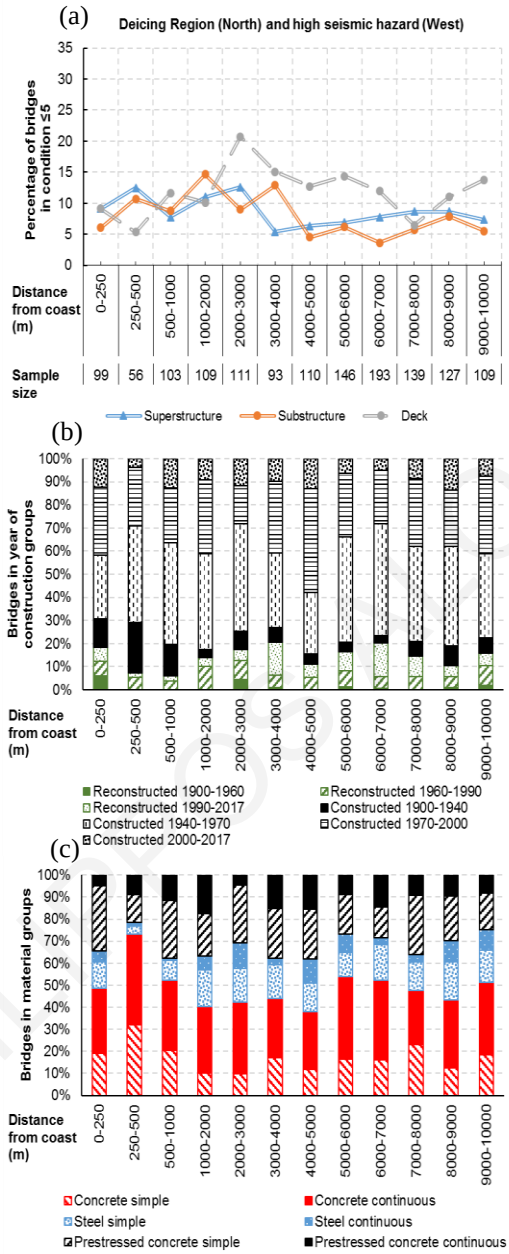

Figure 5.6: Bridges within regions of high earthquake hazard and deicing for the different distances from coast, (a) percentage of bridges below or equal condition 5, (b) stacked column chart for years of construction and (c) stacked column chart for materials of superstructure.

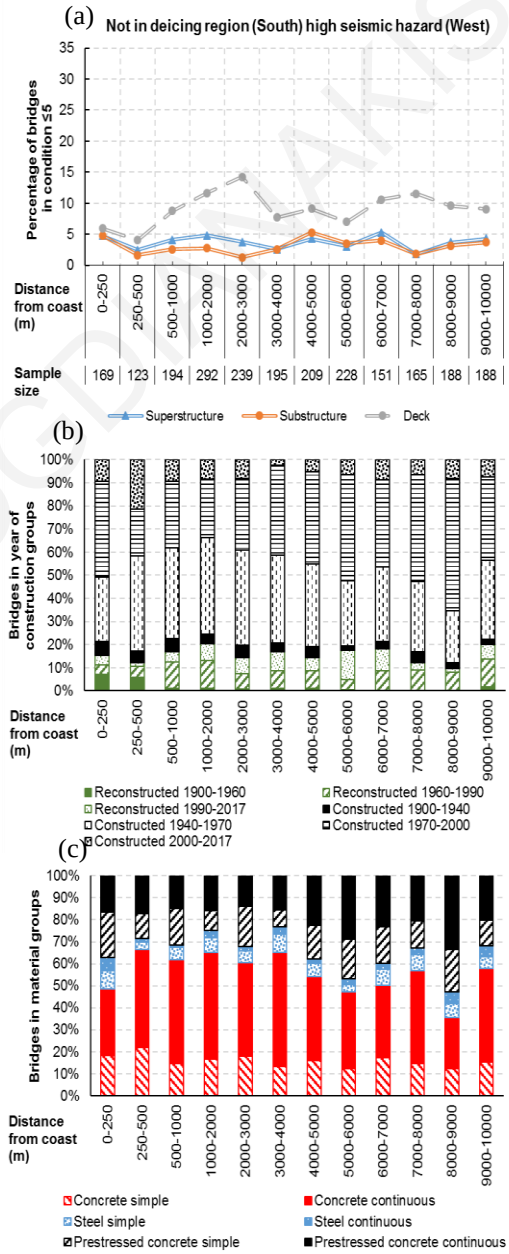

Figure 5.7: Bridges within regions of high earthquake hazard and deicing is not allowed for the different distances from coast, (a) percentage of bridges below or equal condition 5, (b) stacked column chart for years of construction and (c) stacked column chart for materials of superstructure.

evident in Figs 5.6(a) and 5.7(a) that the decks are generally in worse condition than other seismically designed structural components for both North and South parts. It appears that the seismic design requirements for substructures and superstructures in high earthquake hazard areas not only lead to higher strength and better quality structural components, but also implicitly increase their resistance to deterioration. In any case, no airborne chlorides effect can be deduced from Figs 5.6(a) and 5.7(a), as the distance from the coast does not seem to play any noticeable role in the condition of deteriorating bridges.

5.4.5 Results for Florida's coastal bridges and comparison with older inventory

Florida state was chosen for a separate analysis due to its peninsula shape with long coastline, its low elevations, as well as the adequate sample of bridges available within the coastal distance zones. Moreover, an additional analysis using the older NBI database of year 2009 was performed, in order to provide a comparison of results between the different years of evaluation and offer the capability to confirm the existence of a critical distance from the sea coast for the effect of airborne chlorides.

Before assessing the results of the two datasets, certain remarks should be made regarding their properties. Hence, there is a reduction in the 2016 sample size for the first 250m from the coast, as well as for distances of 4-5km. This could be an indication of either abandoned/demolished/replaced bridges or modifications in location coordinates. Note that for the replacement of bridges new entries are made in the inventory, while the old ones are simply deleted. The explanation of replacements could be also supported by the fact that more recently constructed bridges appear in the 2016 inventory (see Figs 5.8 (b) and 5.9(b)) and by the small change in superstructure materials for the same distance zones.

Despite the uncertainty induced by the fact that certain bridges have been reconstructed/rehabilitated between 2009 and 2016 (see also relevant discussion in Chapter 4), some remarks can be made regarding utilized superstructure materials based on Figs 5.8 (b,c) and 5.9 (b,c). Specifically, for the first 250m from the coast, older bridges built in 1940-1970 with concrete superstructures and simple spans (2009 inventory) seem to have been replaced by bridges with prestressed concrete superstructures and simple spans (2016 inventory). For the other distance zones, concrete superstructures with simple spans appear to have been replaced by continuous spans using the same material.

As regards condition ratings, these seem to be better in 2016 than in 2009 (Figs 5.8 (a) and 5.9(a)). This is justified by the evident increase in recent reconstructions in all coastal distance zones. Finally, a critical distance of 3km from the coast can be noticed in both figures for the deterioration effect from airborne chlorides.

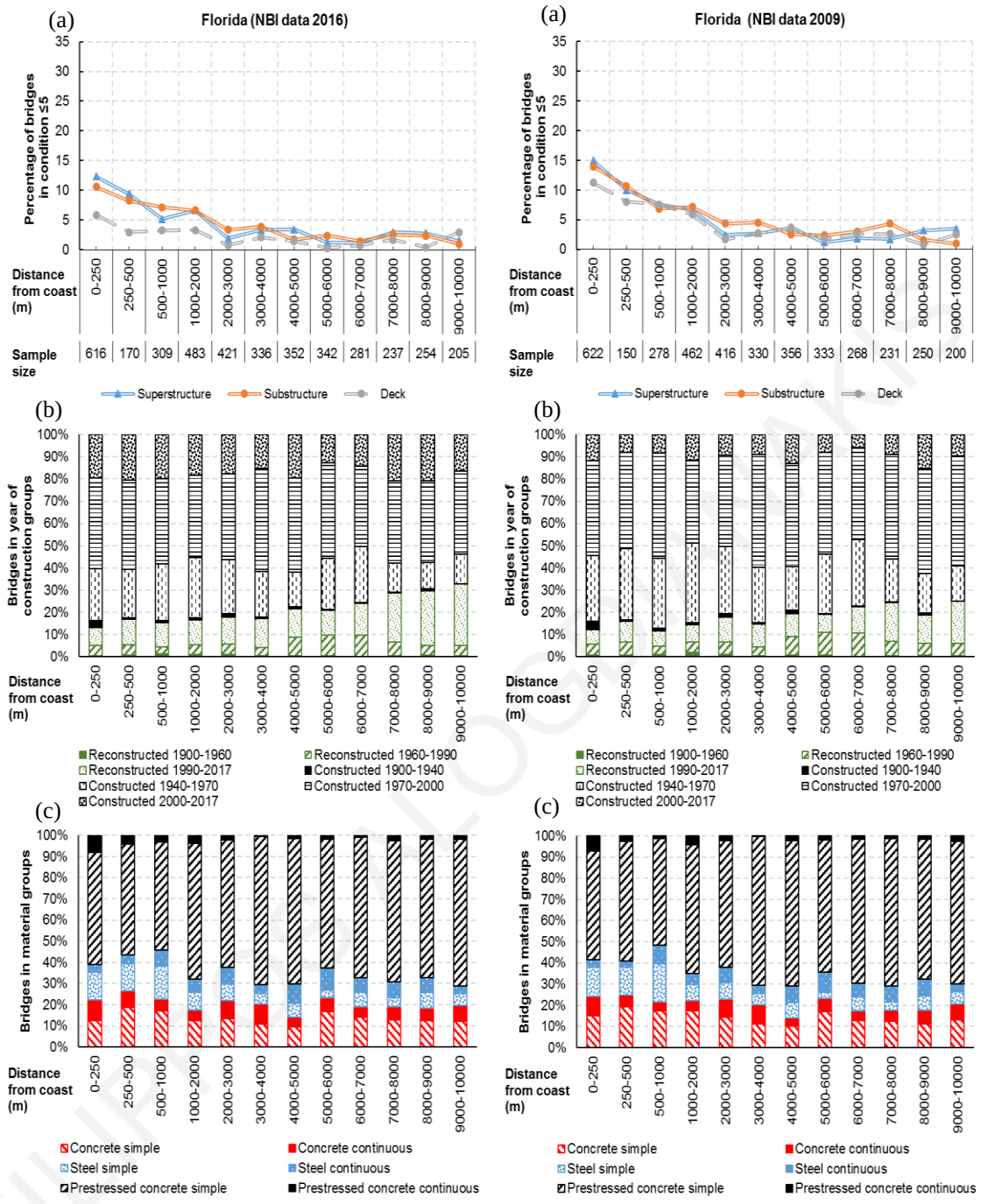

Figure 5.8: Florida's bridges as in the NBI of the year 2016, for the different distances from coast, (a) percentage of bridges below or equal condition 5, (b) stacked column chart for years of construction and (c) stacked column chart for materials of superstructure.

Figure 5.9: Florida's bridges as in the NBI of the year 2009, for the different distances from coast, (a) percentage of bridges below or equal condition 5, (b) stacked column chart for years of construction and (c) stacked column chart for materials of superstructure.

5.5 Conclusions

In this chapter the effect of airborne chlorides on the deterioration of coastal US bridges was studied using the NBI dataset. Other coexisting factors affecting bridges along or near to the coastline were also considered, in order to separate the studied coast bridges in homogenous samples and be able to distinguish the effect of airborne chlorides. The predominant other effects were confirmed to be the potential for deicing and the earthquake hazard.

The separated samples' analysis focused on the deteriorated bridges located within designated distances from the seacoast. The distribution of utilized superstructure materials in each studied area appears to be related to the factors affecting condition ratings in that area. Specifically, for the case of higher earthquake hazard ($PGA>0.2g$) and for either deicing or non-deicing regions, superstructures with continuous spans using concrete and prestressed concrete seem to be generally preferred to simple spans and structural steel. On the other hand, simple bridge types (with non-continuous spans) are most often built in areas with lower earthquake hazard ($PGA\leq0.2g$) using any of the two concrete types, especially in non-deicing regions. For the areas where deicing is used, mostly steel superstructures are encountered, but this could be attributed to the larger number of older bridges included in the bridge stock.

The inventories ratings for structural condition provided the information needed to study the effect of airborne chlorides in increments of distance inland from the sea coast. Specifically, for the locations of low earthquake hazard and no deicing, distances up to 2-3km inland showed to be affected, which was confirmed by the separate analysis for Florida state. On the other hand, in areas where deicing is applied, the airborne chlorides appear to affect distances only up to 1km inland from the coast. The smaller affected distance suggests that chloride deposition beyond 1km is dominated by deicing salts, which conceal the effect of airborne chlorides. For the locations of higher earthquake hazard, the results obtained do not show noticeable effect from airborne chlorides.

It is worth mentioning that the derived maximum distances inland from the seacoast affected by airborne chlorides correspond to the 'snapshot' of NBI-data for a particular year. The bridges included in NBI are continuously aging, while some are eventually reconstructed or replaced. Hence, larger or smaller maximum distances from the coast may be identified using a future NBI dataset, as the conclusions drawn depend to some degree on the composition of the bridge stock analyzed at any time. Despite the dynamic evolution of the studied sample with time, the general conclusions of the present work are not expected

to change, at least from a qualitative viewpoint. The conclusions are based on trends representing stock properties, therefore the effect of small sample changes are smoothened out.

6 Environmental effects on the structural deterioration of bridges

The Chapter focuses on bridge deterioration, due to corrosion, for environments defined in Chapter 4. Age and probabilities of deterioration, along with probabilities of rehabilitation are utilized to perform the analysis. The interpretation of results assists in validating the effects of the environmental exposures considered. In addition, comparison to older inventory results test the methodology's sensitivity, setting the ground for next chapter's predictions of future conditions to be performed.

6.1 Introduction

Structural deterioration is the main reason the service life of built infrastructure is suppressed and vast budgets are spent to extend it. Different parts and materials of a bridge can be susceptible to various environmental exposures, depending on the years of service. All common bridge materials (structural steel, concrete and prestressed concrete) utilize the benefits of carbon steel but are also affected by its susceptibility to corrosion. Thus, to study deterioration, apart from the prerequisites of corrosion, evaluations of built infrastructure should be taken to consideration for different materials and environments. Results from such studies can lead to optimal allocation of materials already in use but also motivate the market to develop more durable – but also more expensive – materials, such as fibre reinforced polymers.

Industrial steel corrodes to form electrochemically stable products. For corrosion to occur, an anode, a cathode and an electrolyte (such as water), which provides the medium, is needed. The main ingredient consumed during this process is iron, which bonds with oxygen, producing soluble and porous oxides at the anode (Davis, 2000). Although corrosion products have a passivating effect to the underlying steel surface, they can be easily removed if wetted or attacked by aggressive agents, such as chlorides, initiating corrosion (Davis, 2000). Different types of corrosion exist and can be categorized by environmental exposure, such as aqueous and atmospheric (Chapters 4 and 5), while other categorization refers to corrosion effect on steel and actions involved, such as uniform, pitting, crevice, stray-current etc. (Davis, 2000). Differences among them are due to variations in the ratio of anodic to cathodic area, presence of aggressive agents (pitting) or stray current, relative movement of surfaces under pressure etc. (Podolny, 1992).

Steel passivity is a desirable condition as corrosion rates drop close to zero, preventing further corrosion (Davis, 2000). Among the corrosion types mentioned, only in uniform corrosion the underlying surface can be passivated, if oxides are not removed or attacked. To

limit corrosion type variability, different passivating procedures are followed depending on steel's exposure. Thus, for steel superstructures, passivity is achieved by using materials that form more dense and durable oxides. This is performed by either selecting paint systems, whose main ingredient is zinc (Davis, 2000), or by selecting other steel types, such as weathering steel (Schweitzer, 2010; Kogler, 2015). Concrete on the other hand, provides different levels of protection to the reinforcing steel. For corrosion, protective cover provides physical protection, not only from direct exposures but also from its complex pore system and alkaline properties, which also provide chemical protection to the reinforcing steel (Jackson & Dhir, 1996). Another level of protection concerns a protective layer of dense impenetrable oxides formed at concrete steel interface, known as "passive" film (Broomfield, 2007). Its protections attributes depend on the preservation of the alkaline environment in its vicinity, providing electro-chemical protection (Jackson & Dhir, 1996).

Disruptions of the protection mechanisms in either structural steel or reinforcement promote corrosion initiation. Corrosion of structural steel has been studied for many years due its wide industrial applications. To model corrosion, the reduction of material volume due to rust formation is described through a time function, which depends on environmental conditions and steel types. Similar procedures have been followed to assess the durability of paint systems under different environmental exposures (Kallias, et al., 2017). Furthermore, corrosion of structural steel members can be visually detected and can be treated if noticed in early stages.

The same does not apply for concrete, which is the most commonly applied material of the different bridge parts. The major concern for bridges came with the use of deicing salts and their effect on concrete's and prestressed concrete's durability (Balafas & Burgoyne, 2010). Chlorides destroy the electrochemical protection of high pH environment and its ability to bond with aggressive chemicals, preventing them from reaching the reinforcing steel (Broomfield, 2007). Furthermore, no early notices are given until cracking of concrete's cover caused by inner pressures rising from volumetric increase of corrosion products (Balafas & Burgoyne, 2010). Although collapses of reinforced concrete structures due to corrosion are rare, the effect on safety of the users is not rare, because of the possibility of falling parts due to spalling (Broomfield, 2007). The main concern regards prestressed concrete, as tendon area reduction due to corrosion reduces prestressing, which is needed for the equilibrium of the structure. In addition, corrosion in prestressed structures may not give signs of distress. This is because corrosion products possess low volumes and this is due to low oxygen concentrations at the tendons depth. High strength and low permeability concrete used in such structures in combination to high cover depths limits the oxygen availability while corrosion unfolds. Evidence of corrosion in prestressed structures is sudden, limiting reaction time and leading to

disastrous collapses (Broomfield, 2007; Woodward & Williams, 1988). Corrosion consequences have led to a wide research interest to derive models for predicting the time to corrosion initiation.

Corrosion of steel in concrete is separated in to two main stages, corrosion initiation and corrosion propagation (Tuuti, 1982). The first is governed by mechanisms of transport through concrete. Chronologically, it begins from the exposure to a chloride solution and ends when the chlorides have reached the vicinity of reinforcement and surpassed a certain threshold concentration. The ingress of chlorides is usually modelled by Fick's second law of diffusion, under the assumptions that diffusion coefficient and surface chloride content are constant and concrete pores are fully saturated (Bertolini, et al., 2013). The constant variables of Fick's formula take values based on the fitting of experimental data from specimens or core-samples. Although based on several assumptions, the modelling of chloride transport through concrete has progressed during the past decades (Angst, 2018). On the other hand, the prediction capabilities for estimating the time to corrosion initiation of the mechanistic models are limited due to their sensitivity in chloride threshold and its variability (Angst, 2018). The problem mainly relates to the nature of the passive film (Angst, 2018; Hussain, 2014). Additional complications arise with the use of environmentally friendlier concrete with lower clinker consistencies, which are more prone to carbonation (Stefanoni, et al., 2018). The same applies for the propagation stage, where cracking and spalling occurs, which is generally accepted to last 4-6 years (Bentur, et al., 1997). The former duration could be prolonged to 20 years depending on environmental exposure and rust production (Balafas & Burgoyne, 2010). These limitations restrict mechanistic models of concrete materials from performing useful comparisons with steel materials regarding durability to corrosion.

Bridge parts may be exposed to various environments and, even for the same element, structural deterioration may vary due to type and duration of exposure. Wet dry cycles, freeze thaw cycles, the splash zone, high temperatures and humidity may alter the corrosion rates of steel especially in presence of aggressive agents, such as chlorides (Neville, 1995). Additional effects, such as fatigue creep and construction errors, can increase the modelling uncertainties (Melchers & Beck, 2018). To account for the variating effects taking place, studies have utilized inspection records of built infrastructure to statistically model deterioration.

Statistical deterioration models range from bridge element level to macro-elements, such as the case of NBI. Bridge Management Systems (BMS) utilize element level to assist owners in planning repairs, inspections and rehabilitations (Ryall, 2001). Their main purpose is to predict the future condition of a bridge element utilizing records of its previous conditions.

More information regarding the prediction of future conditions and methodologies used are provided in Chapter 7.

Statistical models could be utilized to address differences in structural deterioration between materials and/or environments. For the US, most studies are performed for individual States (Kim & Yoon 2010; Sobanjo et al. 2010; Bolukbasi et al. 2006; Turner, et al., 1991; Yanev & Xiaoming, 1993;Chang, et al., 2017), where most variations occur due to average daily traffic, therefore performance can be measured. In addition, the fact that different methodologies of sample selection and analysis have been used at different States forbids direct comparisons between their models. On the other hand, studies incorporating bridges of all States (Dunker & Rabbat, 1990; 1992; 1993; 1995; Farhey, 2010; 2012; 2014; 2015; Lee, 2012) show material performance that varies significantly, but alterations for environmental factors have not been taken to consideration. Furthermore, when condition data for individual states from North and South were compared (Veshosky et al. 1994), similar durability performance was observed between construction materials.

In this work the NBI database, in combination with the additional factors introduced in Chapter 4, is utilized to reveal the structural deterioration of bridge parts and materials for the conterminous US. The analysis involves comparisons between environmental exposures for the main materials of superstructure, substructure and deck. The results are furtherly interpreted based on corrosion, validating older findings and showing areas where additional research could be performed.

6.2 Methodology

The US include a variety of factors that affect structural condition. In this subsection the performed analysis and the procedures to manage the sample are presented. As seen from Chapters 4 and 5, factors that predominantly affect the structural condition of bridges are related to ‘external’ factors, i.e. earthquake hazard, deicing salts, water underneath, precipitation, as well as ‘internal’ factors, such as year of construction, year of rehabilitation, material types etc. Also, some factors contribute in condition melioration, such as the case of earthquakes due to strict design standards, while most of the other factors are related to corrosion of steel or degradation of mechanisms protecting it. This work aims to seek links between environments and corrosion. Variables that could reveal and validate the extent of deterioration are linked to the bridge age, as well as the condition rating of the examined structural part. To perform such analysis, bivariate plots were used with age in the horizontal axis and an appropriate measure was adopted to describe the deterioration at each age, representing the vertical axis. Each bridge part for each environmental factor could be analyzed in a type of time-series analysis. Thus,

meaningful segmentation should be made to the whole sample, first regarding the environmental factors and then the materials contained in each part.

6.2.1 Sample segmentation

As seen in Chapter 5, meaningful segmentations based on the condition ratings limit the averaging effect of bridges that differ in exposure. To prioritize the variables, for which the segmentations are performed, the magnitude of the most predominant variables and their interactions, similarly to Chapter 5, were utilized. The factors of peak ground acceleration, deicing water underneath and precipitation were used for the whole sample of 443,603 bridges (A-IV.1-3). Furthermore, an additional analysis of the spatial distribution of materials was carried out (A-IV.4), to investigate irregularities caused by design preferences (i.e. continuity and materials).

The results showed that the most affecting factor was peak ground acceleration, which increased condition ratings validating the results of Chapters 4 and 5. Additionally, the observations of Chapter 5 regarding preferences for continuous bridges of concrete and prestressed concrete and less steel in high seismic hazard areas ($\geq$0.2g) were confirmed. Thus, the high seismic hazard areas were excluded from the analysis, as they should be analyzed with additional criteria, possibly with further segmentations to peak ground acceleration.

The first segmentation included bridges within the deicing region, which appeared to be the second most influencing factor. For the second segmentation, the factor of water underneath was selected due to the significant differences it created for substructure. Although precipitation was not selected for main segmentation, it is considered among the factors used in further analysis and/or in explanation of results.

To achieve better sample uniformity, some exclusion were performed regarding the coastline effects of Chapter 5 and material types of decks. Specifically, bridges located within 2km from the south-east coast, where no deicing is used, and 1km for the North east coast, where deicing is used, were excluded. No further exclusions were performed for the West coast as all bridges were excluded due to high seismic hazard. It was observed that decks made of wood have poor condition ratings; due to the correlations among condition ratings found in Chapter 4, the whole bridge record and not only deck condition was excluded from the analysis for these bridges.

For the two segmentations performed, four environmental exposures were defined (Fig. 6.1) that include bridges:

- ‘no deicing, no water’: out of deicing region, not over water,
- ‘no deicing, water’: out of deicing region, built over water,

- ‘deicing, no water’: within the deicing region, not over water,
- ‘deicing, water’: within the deicing region, over water.

Confounding factors that could affect deterioration are high temperatures and precipitations for non-deicing regions. Although carbonation has not been studied herein, bridges not over water can be regarded to be more exposed. This can be also noticed from the map of carbon dioxide emissions provided in the Appendix (A-IV.5), showing that increased CO_2 emissions coincide with no water environments of Fig. 6.1 (a). Thus, air polluting chemical agents and environmental changes, although not included, can increase deterioration (Kumar & Imam, 2013). Other sources that could alter deterioration are mentioned in the main analysis (section 6.3).

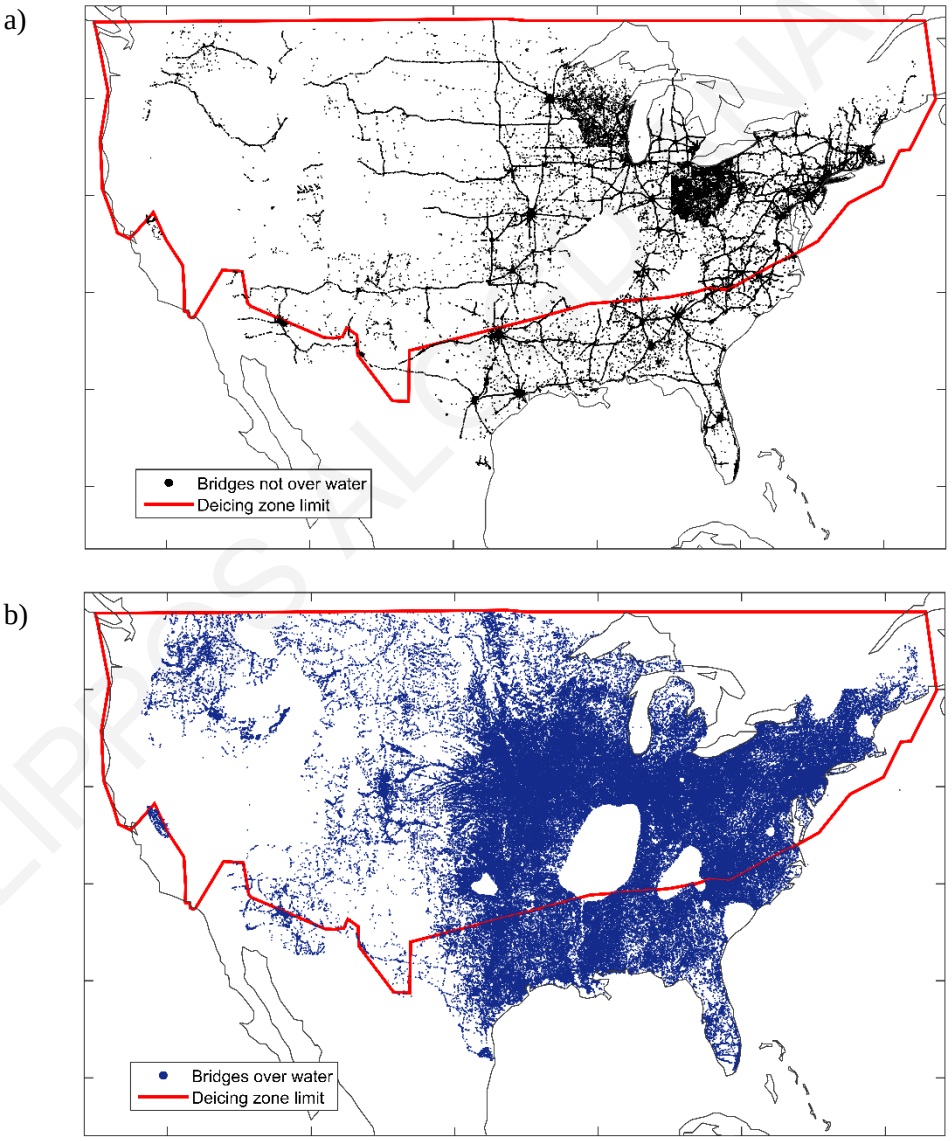

Figure 6.1: Segmentations of the sample based on the exposure of deicing salts (red line (a) and (b)) and on the existence of water underneath the bridge to no water underneath (a) and water underneath (b).

6.2.2 Non-satisfactory condition

The condition ratings of deck, superstructure and substructure were used to indicate deterioration. Condition ratings below or equal 5 were selected for the analysis, as 5 corresponds to 'fair' condition. In this condition all primary structural elements of a bridge part are sound but may have minor section loss, cracking, spalling or scour (FHWA, 1995). Lower conditions were also included as they indicated more advanced damage. Thus, bridge parts with ratings below or equal 5 were considered as being in *non-satisfactory condition*.

6.2.3 Bridge age and the issue of rehabilitated bridges

The NBI provides three time references: year of construction, reconstruction and inspection. Those can be utilized to determine the age and deal with rehabilitation issues. Year of construction and year of reconstruction correspond to the initial construction of a bridge and the last major repair work or rehabilitation that took place (FHWA, 1995). As seen in Chapters 4 and 5, both affect the condition ratings in a different way. For non-rehabilitated bridges, the year of construction signifies the years of service of each bridge. On the other hand, rehabilitated bridges are generally in better condition, but, apart from the year of reconstruction, no information has been provided in NBI regarding the repaired/rehabilitated part. The year of inspection corresponds to the last inspection constituting a reference time as to when the current condition ratings were assigned. Thus, the age of a non-rehabilitated bridge was estimated by subtracting the year of construction from the year of inspection. For rehabilitated bridges, two different ages were utilized, one to define the age of a bridge from its initial construction and the second the age from its rehabilitation. The first age was estimated similarly to non-rehabilitated bridges, while, for the second age, the year of reconstruction was subtracted from the year of inspection.

For each segmented bridge sample, an exploratory analysis of the age contents was carried out for non-rehabilitated bridges and for rehabilitated bridges utilizing both ages computed (A-IV.6-13). The results presented in the Appendix for each environmental exposure are given for continuous and simple types (based on the material categorization of superstructure). Deck and substructure results are presented together, as no segmentations are made based on material for these bridge parts and no condition ratings are used in the analysis. Segmentations are performed, however, for superstructure materials.

The analysis revealed that the vast majority of not-over-water-bridges, has been built after 1956 (age 60 in Appendix-IV. 6-13), and their locations (Fig.6.1 (a)) relate with the interstate network, whose main construction started at that same year (Weingroff, 1996). Additionally, the same category of bridges appeared to have more rehabilitations when compared to the

bridges over water. Also, attention was specifically given to prestressed concrete bridges, as this material was not used prior to the 1950s. Prestressed concrete bridges durability performance in different environments can be observed in the Appendix (A-IV.10-13), while Fig. 6.2 shows rehabilitated and non-rehabilitated prestressed bridges located in all environments. The age of rehabilitated bridges listed is computed also according to the year of initial construction and shows prestressed bridges built before 1950, when prestressing technology was not available. The same bridges, when listed by age of reconstruction, all appear to have ages younger than 60, signifying a switch in the superstructure material to prestressing during rehabilitation.

Bridges' material switching during rehabilitation, along with lack of information regarding parts rehabilitated, conditions prior to rehabilitation and reason of rehabilitation, led to the definition of a separate sample for rehabilitated bridges. Hence, rehabilitated bridges were excluded from the main analysis. On one hand, their incorporation would lead to erroneous results, on the other hand, their exclusion from the main analysis could bring rise to sample selection bias, a topic that is discussed in the following subsection.

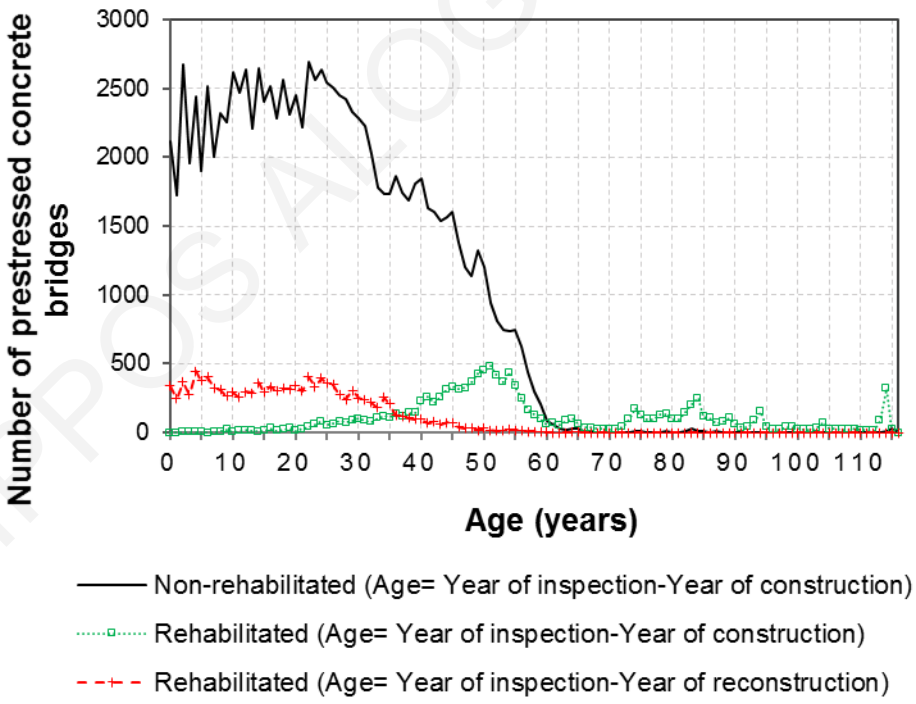

Figure 6.2: Aggregation of prestressed concrete bridges. Rehabilitated bridges (green line) that appear to have been built from prestressed concrete, when listed with regard to the age from reconstruction (red line) reveal changes in material. Also, minor variations (0.2% of the non-rehabilitated sample) noticed for non-rehabilitated bridges (black line) after 66 years are due to coding errors of year of reconstruction or material-type.

6.2.4 Cumulative Condition Probability (CCP)

The selection of a specific year's NBI dataset to study deterioration provides static information regarding the age of a bridge and its condition at the year of inspection. Thus, each bridge condition rating can be regarded as the result of the years of exposure equivalent to its age. To compare deterioration among different strata, cumulative frequency below or equal condition 5 was inappropriate due to its dependency on the size of each age group. For the same reason, Kaplan Meier estimator (Kaplan & Meier, 1958) should not be used, as the purpose of the study is not to identify the stock's problematic bridges, but to determine bridge deterioration caused by various environmental factors. Other studies have used the mean age or the mean condition rating of each age; the effects of mean condition rating for the NBI sample handled herein have already been presented in Chapter 4. Hence, the proportion of bridges being in the conditions of interest (rating ≤5) for each age was adopted as the measure analyzed, similarly to the studies of Dunker and Rabbat (1990; 1992; 1993; 1995) and Farhey (2014; 2015).

The segmented samples of the four different aforementioned environmental exposures were grouped according to their construction material and were sorted by age. For each age, the number of bridges at a particular condition (rating 0-9) varies due to its dependency on the sample of that age. Herein we are particularly interested in referring to all bridges in a condition characterized with a rating below or equal a particular threshold value. Following the frequentistic definition of probability (Faber, 2012), the proportion of bridges below or equal a threshold value at a particular age is referred to as Cumulative Condition Probability (CCP). It is computed independently for each age as follows:

$$CCP_i(t) = \frac{N_{c,i}(t)}{N_{c,tot}(t)} = \frac{\sum_{j=0}^{i} N_j(t)}{\sum_{j=0}^{9} N_j(t)} = \frac{N_0(t) + \cdots + N_i(t)}{N_0(t) + \cdots + N_9(t)} \quad (6.1)$$

where: $CCP_i(t)$ is the CCP for structural condition ≤i of the bridges at age t; $N_{c,i}(t)$ is the total number of bridges at condition ≤i at age t; $N_{c,tot}(t)$ is the total number of bridges at age t (at any condition 0-9); $N_i(t)$ is the total number of bridges at condition i at age t.

In this chapter, CCP_5 corresponding to the probability of a bridge being in non-satisfactory condition is utilized. CCPs for other condition thresholds are presented in Chapter 6. The graphs shown in this chapter present CCP_5-values calculated at various bridge ages. For each studied sample, an increasing trend of CCP_5 with time is anticipated due to aging linked with environmental exposure. The results are presented for bridge age up to 60 years, in order to have some uniformity among the effects of environmental factors (no water or water underneath) and structural materials (especially for reliably handling prestressed concrete).

Note that variations should be expected in the graphs, as CCP_5 is separately calculated for each independent age group, while the sizes of these groups are generally different.

6.3 Results and discussion

Table 6.1 provides information regarding the sample population in terms of structural materials utilized for each environmental exposure considered for the 60-year analysis. The most popular bridge material under all environmental exposures is prestressed concrete with simple (non-continuous) spans, with the exception of 'no deicing, water', in which simple-span concrete is mostly used. Moreover, there is a lower preference to continuous spans for prestressed concrete bridges in all environments, for steel in environment 'no deicing, no water' and 'deicing, water', and for concrete in environment 'no deicing, no water'. Smaller sample sizes indicate that higher variations in the results should be expected, which can be furtherly justified by the sample for each individual age (Appendix A-IV.6-9). For decks and substructures, since there is no material categorizations, sample segmentations were performed for the existence of construction joints, which were seen to affect substructure and superstructure condition in Chapter 5. Thus, all samples including bridges with simple spans are aggregated to form the overall sample signifying construction joint presence and, similarly, continuous spans for construction joint absence.

Table 6.1: Sample size for each environmental exposure analyzed.

Material/Environment	**Deicing, no water**	**Deicing, water**	**No deicing, no water**	**No deicing, water**
Concrete simple	7%	11%	7%	42%
Concrete continuous	9%	12%	7%	4%
Steel simple	23%	25%	13%	10%
Steel continuous	25%	9%	17%	4%
Prestressed concrete simple	26%	37%	48%	36%
Prestressed concrete continuous	9%	6%	9%	4%
Sample size	50,376	144,688	18,490	52,036

In the remainder of this section, the sample selection bias is first addressed. Then, the main analysis results are given separately for bridge decks, superstructures and substructures. An additional analysis to compare the current prestressed concrete superstructures to those of an older inventory is reported.

6.3.1 Sample selection bias

This section addresses the issue of bias imposed during the selection of the samples analyzed. Since bridge materials after rehabilitation may have been changed and there is no clarification in NBI regarding materials in the bridge's initial state (before rehabilitation), rehabilitated bridges are categorized only according to the environmental exposures. Most rehabilitations performed are related to bridges exposed to 'deicing, no water' (20% of the overall sample for this environmental exposure), followed by 'no deicing, no water' (11%), 'deicing, water' (8%) and 'no deicing, water' (6%). The mean age of rehabilitated bridges shows small variations around 50 years for all environments (A-IV.6-13).

In this work, the CCPs were computed for non-rehabilitated bridges. The fact that rehabilitated bridges have been removed from the main samples analyzed may impose a selection bias producing misleading results. If there was information to keep rehabilitated bridges in the samples, it is expected that higher CCP-values would be obtained than the ones computed herein. Since segmentations based on structural material cannot be performed, an indication of the magnitude of the selection bias can only regard environmental factors. To account for this bias, rehabilitated bridges were listed by their age corresponding to the year of construction and aligned with the non-rehabilitated bridges. Then, following the frequentistic approach, the number of reconstructed bridges for each age group was divided with the total sample population for that age, which included non-rehabilitated and rehabilitated bridges, in order to calculate the corresponding Rehabilitation Probability (PR):

$$PR(t) = \frac{N_R\,(t)}{N_{NR}(t) + N_R(t)} \qquad (6.2)$$

In the above equation, *PR* is the probability of rehabilitation for a bridge of age *t*, N_{NR} is number of non-rehabilitated bridges at age *t* and N_R is the number of rehabilitated bridges at age *t*. The *PR*-values shown herein provide information regarding the magnitude of the bias introduced by removing rehabilitated bridges from the samples analyzed.

The selection bias is examined through the *PR*-plot of Fig. 6.3. In this figure, the probabilities of rehabilitation have an increasing tendency with age, as expected. Similar probabilities of rehabilitation for different environmental exposures indicate similar biases introduced in the corresponding samples. This appears to be the case for 'no deicing, water', 'deicing, water' and 'no deicing, no water'. The higher variations of the graph noticed for 'no deicing, no water' can be attributed to the smaller sample size available (see Table 6.1). The percentage of rehabilitated bridges removed from the 3 aforementioned samples and the

corresponding bias introduced are deemed acceptable for the age range of 0-60 years considered herein.

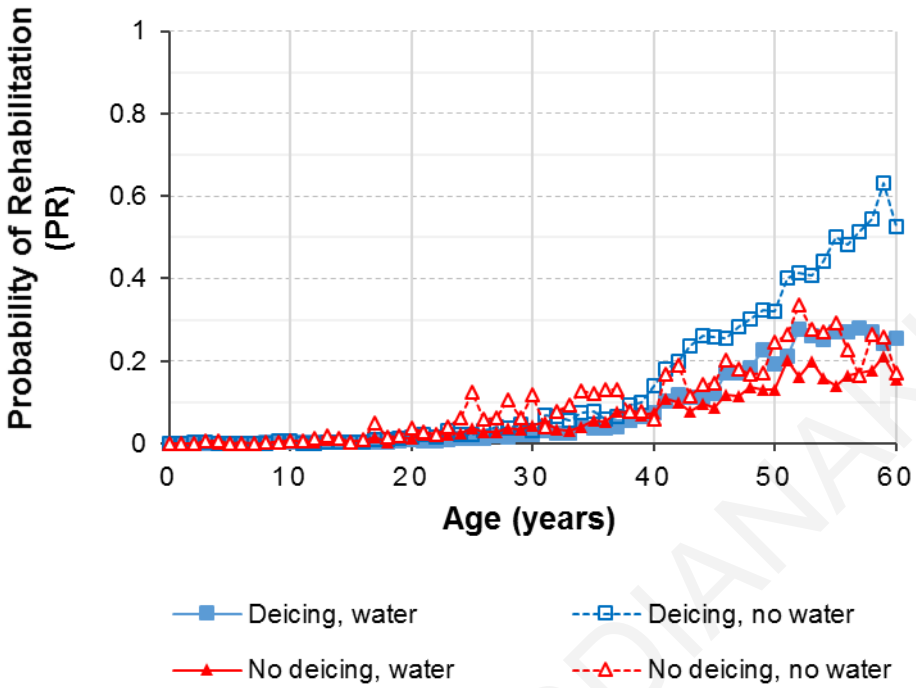

Figure 6.3: Probability of rehabilitation for each age of the corresponding environments (Figures 6.4 to 6.7)

Regarding 'deicing, no water', the probabilities of rehabilitation obtained are higher than in the other environments. Specifically, there is an increase after the age of 40 years, which induces higher uncertainties in the interpretation of results. To resolve this issue in a 'fair' way, comparisons of results among 'deicing, no water' and the other 3 samples were limited to the age range 0-40 years.

6.3.2 Concrete decks

The deck surface comprises of a large area exposed to thermal loads, traffic, as well as the effects of aggressive factors, such as deicing salts, to ensure traffic safety. Inspection ratings in NBI do not refer to the wearing surface, but to the main structure of the deck (FHWA, 1995). Deicing chemicals sprayed in winter months on the deck surface can affect the main structure, the effect on which can be increased by damages imposed to the wearing surface by deicers and disruptions of protective membranes. Additionally, construction joints could be another source of chlorides, as they provide easier access to the underlying concrete. Furthermore, deicing salts can become airborne by splashing from traveling vehicles and can find their way either to the structure's sides or below the deck, driven by wind or turbulence generated from passing

vehicles underneath the bridge (Radomski, 2002). Freeze thaw cycles and wet dry cycles can affect the condition of a deck, especially when drainage details are of poor design (Azizinamini, et al., 2014).

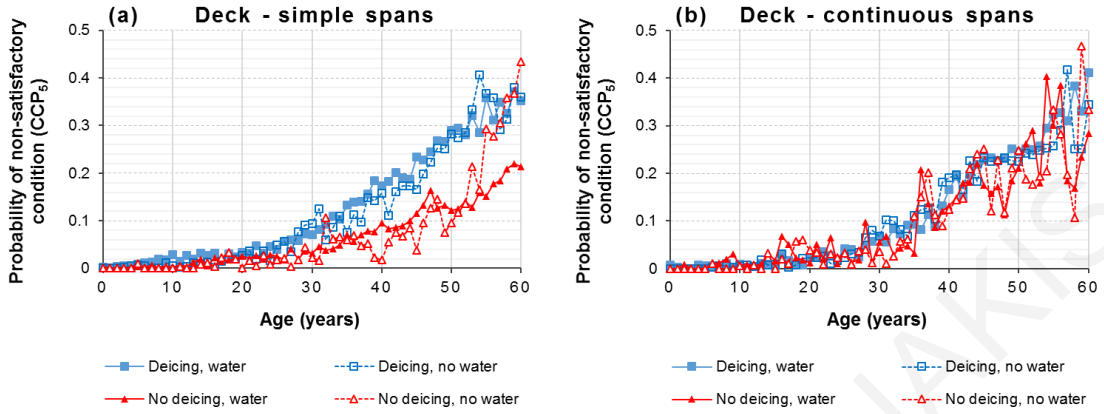

Figure 6.4: Probability of non-satisfactory condition for concrete decks of simple (a) and continuous (b) spans for a 60-year analysis.

The results of the 60-year analysis show two different deterioration patterns for simple (Fig. 6.4(a)) and continuous spans (Fig. 6.4(b)). In Fig. 6.4(a), deterioration for simple-span decks appears to be greater in deicing than in non-deicing regions. The largest variations in CCP-values appear for areas of 'no deicing, no water' and 'deicing, no water' due to the smaller sample sizes. Specifically, for the case of 'no deicing, no water', a sudden increase in probabilities for ages of 55-60 years can be seen, which can be attributed again to the smaller sample size at these ages (Appendix A-IV.10-13). Furthermore, a rise can be noticed in the in CCP-values for environment 'deicing, water' from young ages up to 16 years. After 18 years of age, other exposures also reach the same probabilities and all environments can be considered to have equal effect up to 22 years. Then, the difference between two groups increases, with the probabilities of non-satisfactory condition for deicing environments being about double than those of non-deicing ones. For continuous spans, there is no actual difference in effects among the different environmental exposures. Thus, it can be concluded that deicing salts affect slightly less decks with continuous than with simple spans, while the probabilities for no deicing environments are elevated in comparison to simple spans.

Hence, the presence of deicing salts appears to affect more bridges with simple spans (presence of structural joints) due to the concrete's vulnerability and increased exposed deck area. An explanation for the increased probabilities for 'deicing, water' environment in the first 16 years could be linked to the presence of increased humidity due to water presence. Increased humidity at the pores fuels reinforcement corrosion due to higher chloride transports and causes

damage through freeze-thaw cycles. This was not noticed for continuous spans, as structural continuity eliminates joints and hence reduces surface chlorides concentrations due to joint leakages. After the age of 22 years, the 'deicing, water' and 'deicing, no water' environments appear to have similar tendencies regarding deterioration rates, although the 'deicing, no water' environment shows slightly lower probabilities. Such generalization cannot be made after the age of 40 years due to increased selection bias for this environment.

For decks with continuous spans, high probabilities of non-satisfactory condition can be noticed also where no deicing is used. This can be attributed to the higher temperatures in these environments, which may cause cracks due to joint absence. An additional effect that could also play a significant role is the increased annual precipitation at those areas, which, after cracking, could increase humidity content in the pores and, along with effects of carbonation, lead to depassivation of the embedded steel. Also, the absence of structural joints may be responsible for the decrease in deterioration when deicing is used.

To conclude, decks are mostly affected by the presence of deicing salts and an increase of deterioration is expected, when structural joints are present. On the other hand, continuous bridges could be more effective in colder regions, where deicing is used, while in warmer areas, absence of joints could lead to increased deterioration.

6.3.3 Substructures

The substructure consists of a wider range of materials that have to be rated, such as piers, abutments, piles, footings, among others (FHWA, 1995). Through the segmentation performed, substructures can be in direct contact with the water underneath the structures. Thus, wet-dry cycles affect both regions with use of deicing and no deicing. Problems related to wet-dry cycles include the accumulation of contaminants from the surrounding water on the substructure's surface, where absorption can promote adequate transport, combined with oxygen and temperature adequacy, which can accelerate corrosion. Also, in deicing regions, chlorides can reach the substructures' surfaces through leakages of structural joints and washing out of the chloride contaminated surface during rainy seasons. Accumulation of chlorides can also occur from the airborne chlorides generated from deck vehicles, leakages from deck draining systems, as well as water with chloride content due to deicing activity. Furthermore, freeze-thaw cycles can generate cracks, assisting chlorides to penetrate in deeper concrete depths, especially in deicing regions.

For the cases of no deicing and no water presence underneath the structure, only rainwater can cause wet-dry cycles. Also, since coastal regions have been excluded from the analysis, only contaminants within rainwater or deck surface can reach the substructure. On the other

hand, in the deicing region, chlorides may reach the substructure surfaces as airborne, while larger quantities could be applied through direct splashing either from travelling vehicles or from deicers. Extensive damage has been observed for cases where snow has been piled in contact to substructures' surfaces from deicers clearing the road surface (Ainge,2012). The packed snow is contaminated with chlorides from the road surface and prolonged saturated conditions can promote chloride transfer. Additionally, damage can be caused from freeze thaw cycles and wet-dry cycles during the warmer months, similarly as above.

The results of the 60-year analysis in Fig. 6.5 show reduced probabilities of non-satisfactory condition for substructures supporting continuous spans (Fig. 6.5(b)) in comparison to simple spans (Fig. 6.5(a)) for all environmental exposures. For both types of substructure, 'no deicing, water' appears to give the highest probabilities for all environmental exposures. Quite similar probabilities can be observed for deicing environments. For simple spans, substructures appear to be affected slightly more during the first 20 years in 'deicing, water', while, after that age range, 'no deicing, water' seems to be worse. Moreover, higher differences in probabilities can be noticed for substructures of bridges with continuous spans (Fig. 6.5(b)) among the 'no deicing, water' and 'deicing, water' environments, if compared to the substructures of simple-span bridges. The environment that appears to affect the substructure rating the least in both cases is 'no deicing, no water' for all ages (except after 50 years due to small sample size).

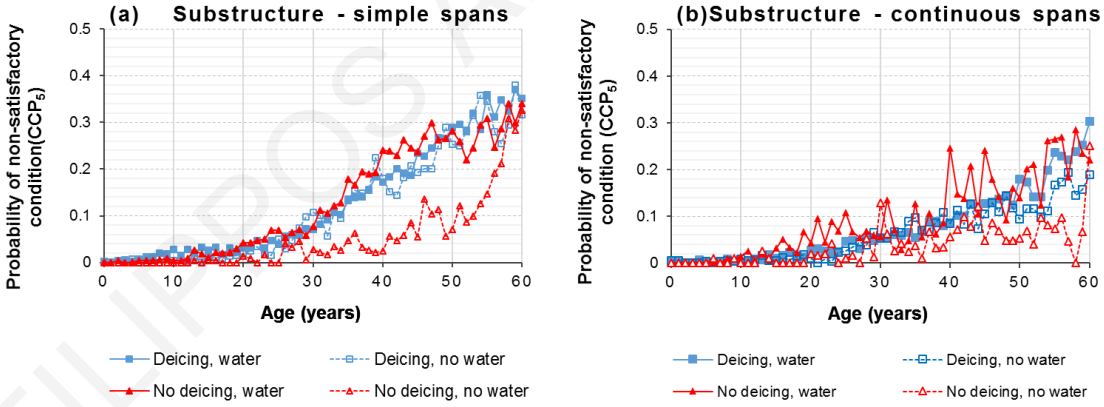

Figure 6.5: Probability of non-satisfactory condition for substructures of bridges with simple (a) and continuous (b) spans for a 60-year analysis.

For simple spans (Fig. 6.5(a)), leaking joints in combination with wet-dry and freeze-thaw cycles may cause increased deteriorations in the 'deicing, water' environment for early bridge ages. Afterwards, any environmental exposure that includes deicing appears to affect the substructure similarly. Also, the exposure 'no deicing, water' appears to affect both substructure types similarly. Regarding the presence of water, a possible explanation for its corrosive effect

lies in the increased humidity it creates; additional effects may include alkali-silica reactions or bio-deterioration, which are expected to be higher in those areas. Overall, the differences observed for continuous and simple span bridges could be attributed to problems arising by the leakages in construction joints of simple spans.

Wet-dry cycles and extra chlorides from leaking joints appear to affect structures from early ages. Occasional splashing and leaking joints effects appear to increase probabilities after the first 10 years. Older ages appear to have similar probabilities of non-satisfactory condition, for both environments where deicing is used. On the other hand, for continuous spans (Fig. 6.5(b)), deicing environments have similar deterioration effects for all ages. Such notice could be an indication that wet-dry and freeze-thaw cycles are comparable to the occasional splashing of chloride contaminated water, from traffic. This could mean an equal chloride deposition for the two environments.

In conclusion, bridges over water in more temperate areas and lack of deicing salts appear to be equally or even more susceptible to deterioration than areas where deicing is used. Interpretations only due to corrosion were taken into consideration herein, however scour hazard may be more critical not only for substructure condition, but also for structural integrity of the whole bridge (Imam & Chrysanthopoulos, 2012; Kallias & Imam, 2015). The presence of deicing salts with or without the presence of water appears to have a similar effect when structural joints are not present. In simple-span bridges, accelerated corrosion appears at early ages, when both deicing and water are present.

6.3.4 Superstructures

Superstructures are affected by the presence of joints through leakages, whose effect can be more aggressive when contaminants, such as deicing salts, are present. Additionally, airborne chlorides can reach their surface at the deck or below the bridge traffic. Similarly, the effect of wet-dry and freeze-thaw cycles can enhance chloride transport. In the Appendix (A-IV.14), graphs comparing structural material performance for each environmental exposure are provided separately for simple and continuous-span superstructures. These graphs show similar probabilities of non-satisfactory condition among all environmental exposures for the different materials and span types. This does not apply for exposure ‘no deicing, water’, for which steel superstructures with both simple and continuous spans show increased deterioration rates. In general, it could be stated that, among the structural materials studied, small differences in probabilities of non-satisfactory superstructure condition are observed. Macroscopically, prestressed concrete gave the best performance among them, followed by concrete and steel.

To assess superstructure performance for various structural materials, separate comparisons for the different environmental exposures are shown in Fig. 6.6. Increased variations can be noticed in certain cases due to small sample size (Table 1). Because of these variations, only trends of deterioration rates should be observed in Fig. 6.6 rather than numbers. In cases of very high variations, not even trends can be observed, therefore transparent lines have been used, in order not to eliminate these lines from the graphs and provide complete results.

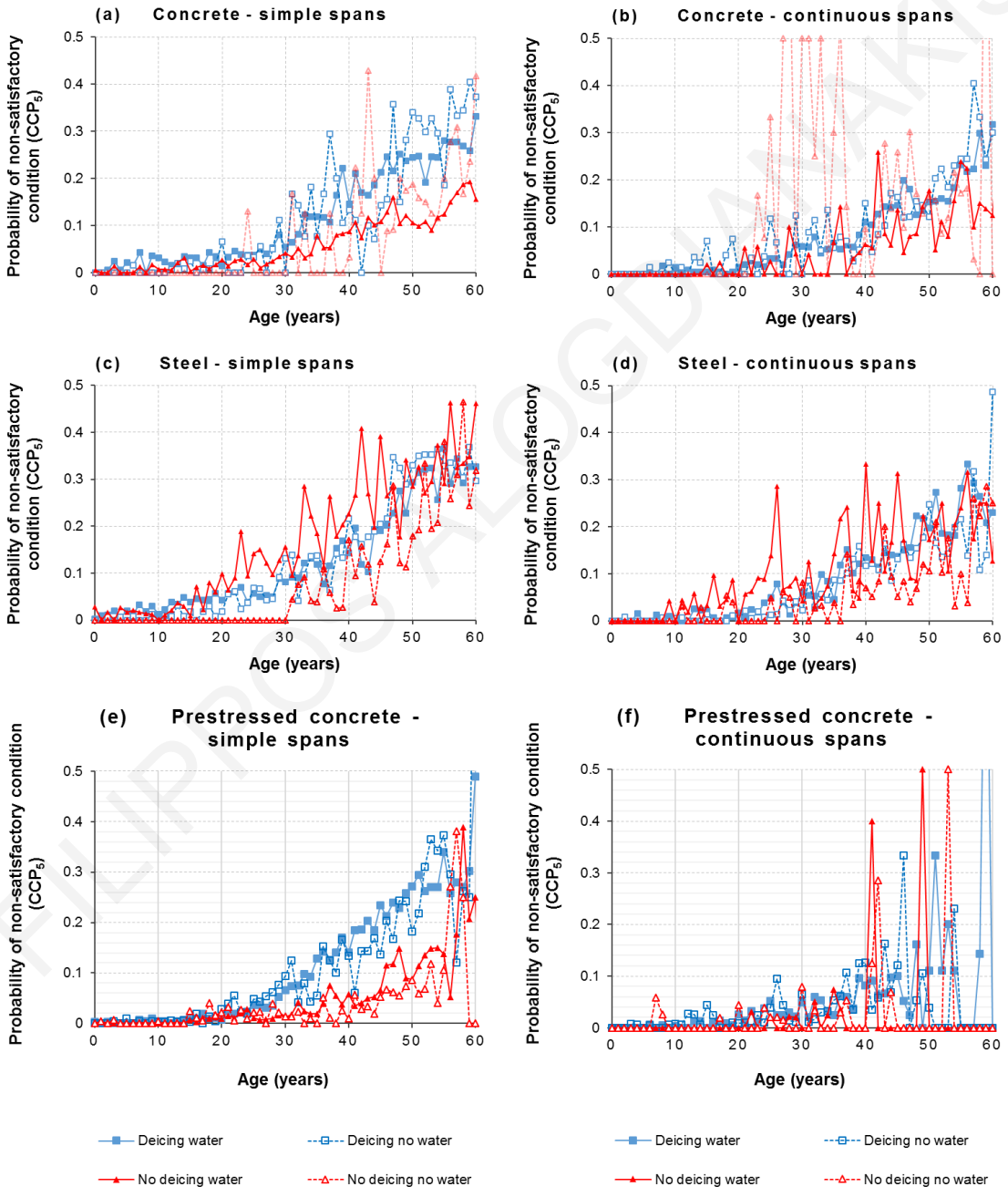

Figure 6.6: Probability of non-satisfactory condition for superstructures of concrete, steel or prestressed concrete materials of bridges with simple or continuous spans. Transparent lines have been used for results with high variations.

6.3.4.1 Concrete superstructures

For the 60-year analysis of concrete superstructures with simple spans (Fig. 6.6(a)), increased probabilities of non-satisfactory condition appear in deicing environments. The presence of water underneath appears to increase the probabilities at younger ages. Despite the occasional large variations due to small sample size, the environments of 'no deicing, water' and 'no deicing, no water' seem to have similar effect on concrete superstructures, lower than environments where deicing is used. Similar observations can be made for continuous spans (Fig. 6.6(b)), although smaller differences are observed when deicing is used or not. Also, at young ages, concrete superstructures appear to be more affected by presence of traffic underneath than by water.

Simple-span bridges exposed to deicing salts are greatly affected by chlorides due to leakages occurring at the construction joints. For continuous bridges, the small difference observed in probabilities among deicing and no deicing environments could be attributed to airborne chlorides generated from the deck area or/and traffic underneath the bridge. Simple-span superstructures at younger ages are significantly affected when in a 'deicing, water' environment, probably due to high humidity and structural joints, however this is not noticed for continuous spans. On the contrary, bridges of older ages seem to be affected more by the presence of traffic underneath (Fig. 6.6(b)). As such observation was not made in the analysis regarding decks (Fig. 6.4(b)), this may be attributed to the superstructure geometry. Concrete I-section beams are normally used; the web plus the top and bottom flanges form a barrier that captures and accommodates airborne chlorides. Thus, chlorides generated from both deck and road (under the bridge) surfaces land on the beams of the bridge's superstructure due to the generated air flows from traffic vehicles, especially from taller vehicles, such as trucks. Also, the smaller differences between probabilities for simple and continuous bridges in no-deicing environments show that the absence of structural joints in warmer environments does not affect concrete superstructures as much as it affects decks. This could be explained by the increased surface of the deck exposed to thermal deformation, in comparison to the smaller exposed surface area of superstructures.

In conclusion, deicing salts are more corrosive for the case of simple spans. Increased humidity can lead to earlier superstructure deterioration, provided that chlorides and joints are present. Continuous superstructures have lower deterioration rates in deicing environments, and similar ones to simple spans in no-deicing conditions.

6.3.4.2 Steel superstructures

Steel superstructures are formed in various geometries and shapes, as they can be located either over or under the decks in the form of beams or trusses. Also, their detailing may be complex regarding connections (fixed or pinned connections among beams or with decks, stiffeners, etc.) or cross-sectional shapes. The main issues affecting steel are the time of wetness and contaminants that could activate pitting corrosion where discontinuities of the paint exist (Davis, 2000). Crevice and fretting corrosion can also take place depending on structural details, especially in the areas of connections, and along with fatigue they can impose a very destructive combination. Additionally, since the deck is typically made of concrete, condensation of humidity has been documented to be generated at the interface of the steel superstructure and the deck's concrete (Azizinamini, et al., 2014).

For the 60-year analysis for both simple (Fig. 6.6(c)) and continuous spans (Fig. 6.6(d)), higher probabilities of non-satisfactory superstructure condition are noticed when water is present underneath the bridge and no deicing is used. Lower probabilities are generally noticed for continuous rather than simple span bridges. Simple-span bridges at younger ages are more affected when water is underneath the structure irrespective of the presence or absence of deicing salts. This effect is also evident at a lower degree for young continuous bridges. Deicing environments appear to be the second most corrosive conditions, while the least affected bridges were those exposed to 'no deicing, no water' conditions.

An inclination change of the probability lines is observed for bridges older than 46 years of age (Figs 6.6(c) and (d)). This could be attributed to a modification of design standards for brittle connections in bridges before the 1970's (Azizinamini, et al., 2014). Thus, the probabilities of non-satisfactory condition for superstructures older than 46 years correspond to bridges with brittle joints and show another case of selection bias due to rehabilitation. Consequently, for the case of steel superstructures, all comparisons are made up to the age of 46 years.

The higher probabilities in 'no deicing, water' environments (Figs 6.6(c) and (d)) could be attributed to the increased humidity levels generated by water presence. Also, this effect in warmer areas can be due to the higher temperatures that correspond to higher dew point temperatures, which govern the volume of water that can be retained in the atmosphere. Thus, increased condensation occurring at the superstructure-deck interface could be expected in southern regions. Moreover, structural joints appear to increase the probabilities in all studied environments. An additional confounding variable linked to water corrosivity is the increased population of birds and animals in warmer areas, where no deicing is allowed. Additionally,

higher temperatures combined with increased rainfall and no deicing induce also wet-dry cycles, which affect corrosion (Stratmann, 1990).

The presence of joints appears to affect in all cases, which can be attributed, as for other bridge components, to joint leakages due to water from rainfall or melting ice contaminated with chlorides (deicing regions). The difference between 'no deicing, water' and 'no deicing, no water' environments for both span types, could be attributed to decrease in humidity levels due to absence of water underneath the bridge. Although the results for steel superstructures have larger variations due to smaller sample sizes, certain variations for continuous spans could also be linked to the increased probabilities of non-satisfactory deck condition noticed for continuous spans in subsection 6.3.2. Specifically, in that subsection, probabilities for continuous decks increase for 'no deicing, water' and 'no deicing, no water' environments to reach similar levels to those observed for simple-span decks.

In conclusion, steel bridges seem to be affected more by humidity levels, either with the presence of structural joints and direct water contact or by condensation of water due to changes in dew point temperatures. Although the presence of aggressive agents is considered to be very corrosive, lower temperatures appear to decrease the agents' effect. On the other hand, other confounding variables such as rainwater, scour etc., of 'no deicing, water' environment, should also be furtherly investigated.

6.3.4.3 Prestressed concrete superstructures

Prestressed concrete bridges can be posttensioned (tendons are placed in ducts) or pretensioned (tendons bonded directly with concrete), with the latter performing better under corrosive conditions than the former (Wallbank,, 1989). High concrete strength is normally used to avoid loss of prestress due to creep. Lack of cracks in service and concrete's low permeability prevent chlorides to drive through cover and cause reinforcing steel corrosion. However, low permeability and thick cover delimit oxygen presence, therefore low volume corrosion products are generated, which cannot crack the cover and hence prevent visual detection. This can have severe consequences and lead to catastrophic collapses without warning (Woodward & Williams, 1988).

For the 60-year analysis of prestressed concrete superstructures, simple spans (Fig. 6.6(e)) appear to induce a similar deterioration rate pattern with concrete superstructures and decks, with a more distinct difference between deicing and no deicing environments. Signs of early deterioration cannot be noticed, as is the case in other concrete structural parts. This can be noticed also when comparing continuous prestressed concrete bridges (Fig. 6.6(f)) and continuous concrete bridges (Fig. 6.6(b)), despite the increased variations in probabilities due

to small sample sizes. Bridges built just after the introduction of prestressed technology (mid 1950s) show today rather high probabilities of non-satisfactory superstructure condition. This can be attributed to lack of knowledge in design and construction of prestressing in the early applications of this technology, as well as to problems that were addressed in later years (Podolny, 1992; Schupack, 1982; Szilard 1969).

As in reinforced concrete bridges, simple-span prestressed concrete superstructures gave higher levels of deterioration compared to continuous ones. The absence of early deterioration could be attributed to the adequate standards of prestressed concrete mix design, to achieve the high compressive strengths needed, which can also provide enhanced chloride protection, as seen in Chapter 5. In conclusion, deterioration in simple span prestressed bridges is increased when deicing salts are used under high humidity conditions. The deterioration rates are halved for continuous prestressed bridges.

6.3.4.4 Comparisons between NBIs of different years

To test the consistency of the analysis procedure used in this chapter, the reliability of NBI ratings and the sensitivity of results, a comparative assessment was performed for two inventory databases: the one of 2016 and an older, the one of 2009. The samples of prestressed concrete superstructures were chosen to validate the results, with both simple and continuous-span bridges included in the analyses.

Clearly, the 60-year analyses for the data of the two inventories correspond to different time periods. The analysis for the inventory of 2016 refers to the period 1956-2016, while for the inventory of 2009 to the period 1949-2009. Thus, the bridges of a certain age are represented by different year-samples in the two sets of results obtained. Moreover, to examine the deterioration rate of the same bridges in time, a 7-year difference in bridge age has to be taken into account between the two inventories. E.g., the 30-years old bridges of the 2016-database are actually the 23-years old bridges of the 2009-database; the corresponding sample sizes of the two inventories are not necessarily the same.

The results for the 60-year analyses providing probabilities of non-satisfactory superstructure condition are illustrated in Fig. 6.7. In the time axes, instead of bridge age, the equivalent year of construction was used. This was determined by subtracting each bridge age from the inventory year. This way, the different bridge stock years could be traced between both inventories. Small differences observed in the year of construction can be attributed to the 24-month inspection interval, which can affect the age calculated. Certain points have been marked in the graphs to show the progression of deterioration for individual year-samples.

Hence, samples corresponding to ages of 30, 40, 45 and 50 years have been marked to facilitate comparisons of probabilities among inventories.

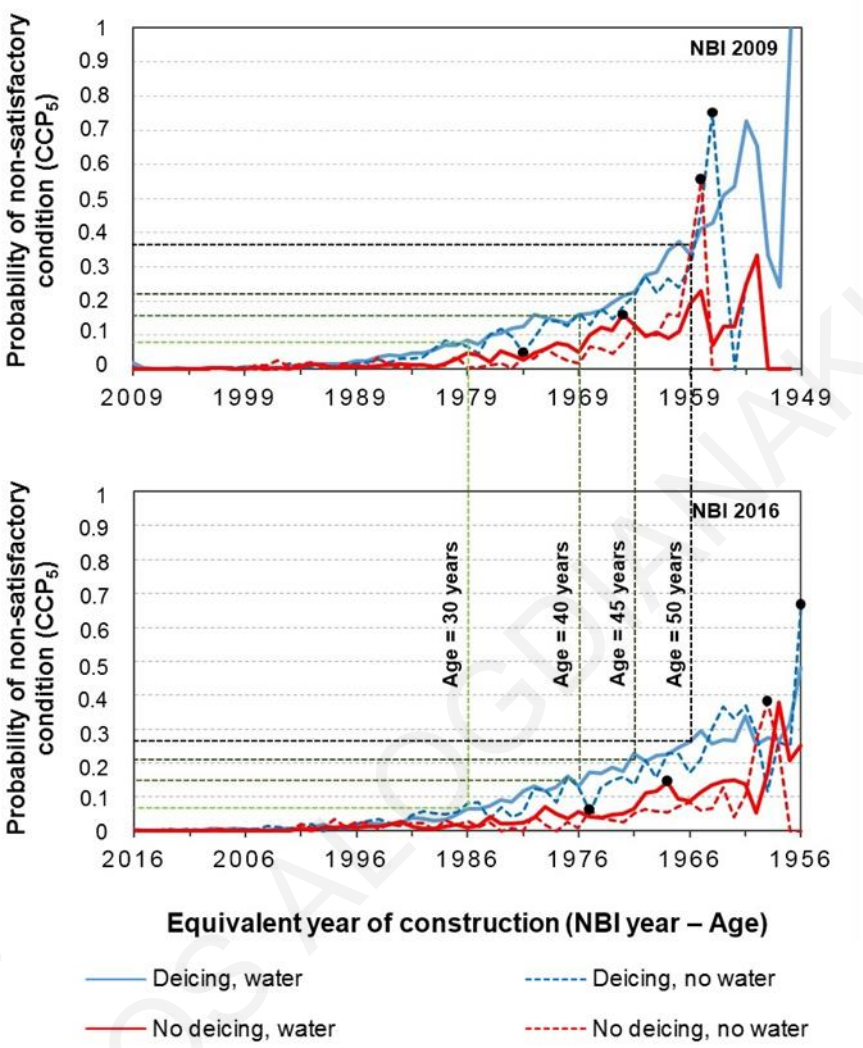

Figure 6.7: Comparison between inventories of different years for prestressed concrete superstructures.

Figure 6.7 shows that both inventories lead to similar probabilities of non-satisfactory condition for ages up to 45 years. Hence, observations made regarding environmental factors affecting superstructures of prestressed concrete are confirmed also for the case of 2009 inventory. On the other hand, in the 2009 inventory an increase in probabilities is observed for years of construction between 1950 and 1960 (after 45 years of age), which cannot be noticed in the 2016 inventory for the same equivalent years of construction. This increase could be attributed to the first ten years of the newly applied material in the US and the flaws commented in section 6.3.4.3. While, differences among inventories, indicate that rehabilitations have taken place (after 2009), leaving only well performing bridges, corresponding to lower probabilities (in the 2016 inventory).

In conclusion utilizing NBI data with the methodology followed appears to be independent of the year collected. Furthermore, robustness of the results can be assumed, provided no major changes in construction standards have been made.

6.4 Conclusions

A sample of US bridges was used to study bridge deterioration under various conditions. Meaningful sample segmentations were performed to distinguish environmental exposures affecting differently various bridge parts. The analysis results indicated that:

- For concrete decks, deicing appears to be the most corrosive factor. The presence of water increases probabilities of non-satisfactory condition when chlorides are present due to deicing. For the case of structural joints, the mentioned environment affects the structural condition of the deck in younger ages, while the same does not apply for the case of continuous spans. Absence of structural joints, on the other hand, lowers probabilities for deicing environments, but increases probabilities for warmer environments.
- For substructures, environments, in which no deicing is used and water is present, have the highest probabilities of non-satisfactory condition, followed by environments, in which deicing is used regardless of water presence. The presence of structural joints in simple-span bridges increases the probabilities for all environmental exposures, while deicing affects younger ages.
- For simple spans, concrete superstructures are affected more by deicing in young ages, when also water is underneath the bridge. For continuous spans, lower probabilities of non-satisfactory condition are obtained, however, concrete superstructures are again affected more by deicing salts, but younger bridges are affected more by traffic presence in areas where deicing is used.
- Steel superstructures deteriorate substantially in humid environments without deicing. Lower probabilities of non-satisfactory condition were noticed at deicing environments regardless of water presence. Structural joints to form simple spans increase the probabilities forall environmental exposures. Especially young, simple-span bridges are vulnerable under humid and deicing conditions.
- Prestressed concrete superstructures in deicing environments are affected similarly to concrete ones. The main difference is the lack of early deterioration for simple-span bridges in the simultaneous presence of water underneath the bridge and deicing. However, early deterioration was noticed, similarly to reinforced concrete bridges in areas where deicing is used and traffic exists under the bridge.

Similar deterioration rates were observed between all studied superstructure materials under the same environmental exposures and span types (simple or continuous). An exception is the case of steel in ‘no deicing, water’ environment for both span types, where increased deterioration can be observed. A closer look at the results indicated a better performance of prestressed concrete, followed by concrete and steel.

The absence of structural joints in integral bridges leads to better performance for superstructures, but may be problematic for decks (Chen & Duan, 1999). As shown in Chapter 5, bridges located at costal California, where the vast majority of superstructures are continuous, appear to have their decks in worse condition under deicing (North) and no-deicing conditions (South).

The analysis methodology using probabilities showed a robustness regarding the year of inventory used, from which the above conclusions were made.

7 A method to probabilistically estimate the deterioration rate of aging bridges

The processes performed in previous chapters have led to segmented samples of bridges for various environmental factors and materials, with cumulative condition probabilities to reveal deterioration within the age range of the different bridge stocks. In this chapter, these probabilities are utilized and a novel method is developed to estimate the time-to-rehabilitation where no data are available. The method adjusts techniques applied for accelerated experiments and exploits properties of the cumulative condition probabilities to calibrate the process. The method is validated using various samples of bridges under various environments.

7.1 Introduction

During the last decades vast budgets have been spent to maintain aging infrastructures all over the world. The 20th century's increased construction activity has led, in particular, to the accumulation of bridges, forming stocks, which are deteriorating with age. Aging bridges need continuous interventions either in the form of maintenance or major rehabilitation. Reliably estimating the deterioration rate and the lifetime of bridges are essential aspects in determining optimal programs regarding maintenance and/or rehabilitation. This could assist decision makers in both elongating the useful life of bridges and controlling their structural safety in a cost-effective manner. However, the structural performance of bridges in time is governed by high uncertainties, which need to be quantitatively treated in order to enable rational decision-making regarding maintenance and rehabilitation.

An essential step toward the effective handling of such uncertainties is the gathering and exploitation of respective data. Typically, the data collected refer to current bridge conditions and are used in conjunction with Bridge Management Systems (BMS) to decide on the necessity and degree of priority of any potential intervention and to allocate corresponding funds (Ryall 2001). Frequent inspections ensure that the BMS is up-to-date regarding the structural condition of the stock. However, in order to estimate future needs and optimally allocate available budgets, models to predict the future stock condition are essential.

Various deterioration models exist and can be categorized based on the information/knowledge used to mechanistic (Stewart & Rosowsky, 1998) or to statistical

models, where only inspection data are utilized. Hybrid models have been proposed, which use both statistical and mechanistic approaches to model deterioration from the macroscopic to microscopic level (Lounis & Madanat, 2002). As mechanistic models and their shortcomings to modelling time to corrosion initiation in concrete were already discussed in the previous chapter, this chapter emphasises more in statistical deterioration modelling. Relevant techniques vary from regression models (Fitzpatrick et al. 1981; Veshosky et al, 1994) to stochastic approaches, such as Markov Chains, and their purpose is to link the evaluated condition of infrastructure to affecting surrounding measurable factors.

Stochastic models can be divided into discrete-time state based and discrete-time time based (Mauch & Madannat, 2001). The state based models predict the probability that a facility will undergo a change in condition at a given time (Mauch & Madannat, 2001), whereas, time based models predict the probability distribution of the time taken by infrastructure facility to change condition state (Mauch & Madannat, 2001). Thus, both types of models utilize different inspection years to track changes in condition.

The most frequently used, discrete-time state based models are Markov and semi-Markov processes (Wu, et al., 2016). The appropriateness of the Markovian process to model bridge deterioration has been shown by Madanat & Ibrahim, 1995. These deterioration models use previous years' structural condition data to trace condition changes and estimate the probability of transition from one condition rating to another. The evolution of the models include the estimation of the transition probabilities. Some of the methods used include regression-based approaches (Ceasare, 1994), Poisson regression (Madanat & Ibahim, 1995), multinomial (Morcous, 2001), probit logit models (Madanat et.al 1997), Kaplan and Meier methods (De Stefano & Grivas, 2001), as well as hidden Markov models (Kobayashi, et al., 2012).

Other methods used to model deterioration, include Weibull sojourn times (Sobanjo, 2010), Artificial Neural Networks (Huang, 2010) and Dynamic Bayesian Belief Networks (Rafiq et al., 2015), Weibull analysis (Agrawal et.al, 2010; Nasrollahi, 2015) and duration models (Mauch and Madanat, 2001). All mentioned methods are dependent on many years of previous inspection records whose reliability can be questionable. Furthermore, the way the data is used can only provide partial validation, as mentioned in Chapter 2. Thus, actually only short-term validation can be achieved by future inspection results that will be available.

In the present work, a novel macroscopic method is presented to probabilistically estimate the future structural condition of a bridge. For this purpose, real data maintained by the Federal Highway Administration (FHWA) for USA bridges are exploited. The method utilizes the database of a single year's evaluation to calibrate a probabilistic model for

predicting the structural condition of a bridge over time. Thus, all bridges in the data-stock processed are used, based on their ages, to represent the condition of a single bridge during its lifetime. This way, curves relating bridge age with cumulative probability for each structural condition can be assembled. Certain time-shifts and scalings are then applied to achieve predictions for bridge ages not covered by available data.

The proposed method is illustrated on a sample of 26,764 concrete bridges of various ages exposed to 'deicing, water' environmental conditions. The predictions derived from the method are presented and compared to corresponding existing data, which span a century for the illustrated sample and additional test cases, offering insight for its long-term validation results.

7.2 Deterioration modelling perspectives and the new method's main assumption

Bridges age at various rates, depending on internal and external factors. Internal factors include structural materials and the overall quality embodied through the construction process. External factors, such as deicing salts, humidity, earthquakes etc., can cause bridge condition to deteriorate. The effects of both internal and external factors are functions of time. Bridges age and deteriorate due to the duration of exposure to those factors. On the other hand, maintenance can decelerate deterioration. As the scope of a deterioration model is to describe a generalized aging-deterioration relation, the selection of a proper sample is crucial.

To visualise the perspectives of deterioration modelling, a three-dimensional graph is presented in Fig. 7.1. Two axes of time are used to indicate the year of completion and the year of inspection for each bridge stock. Bridge stocks are placed on the plane created from these axes as spheres according to their year of completion (year built) and their first year of inspection. The spheres of the figure vary in size to indicate differences in total number of bridges built in that year or a year's bridge stock. The z-axis indicates the number of bridges below or equal a certain condition; frequency is actually used to achieve uniformity between the different bridge stocks. The frequency has a tendency to increase over the years if no corrective action is performed on the different bridge stocks.

A bridge is built following certain constructional characteristics depending on age. Performed inspections evaluate the condition of the structure to present criteria. Hypothetically, if inspection data existed since 1900, then bridge deterioration evolution with age could be described by condition distributions of bridges with similar age. Additionally, the duration of a bridge being at a certain condition could be estimated and transition distributions could then be described. Unfortunately, inspection standards in NBIS

(FHWA 1995) change throughout the years. Additionally, no records can be found before the establishment of the NBI in 1978. Both reasons reveal the necessity of certain assumptions to be made for the study of deterioration.

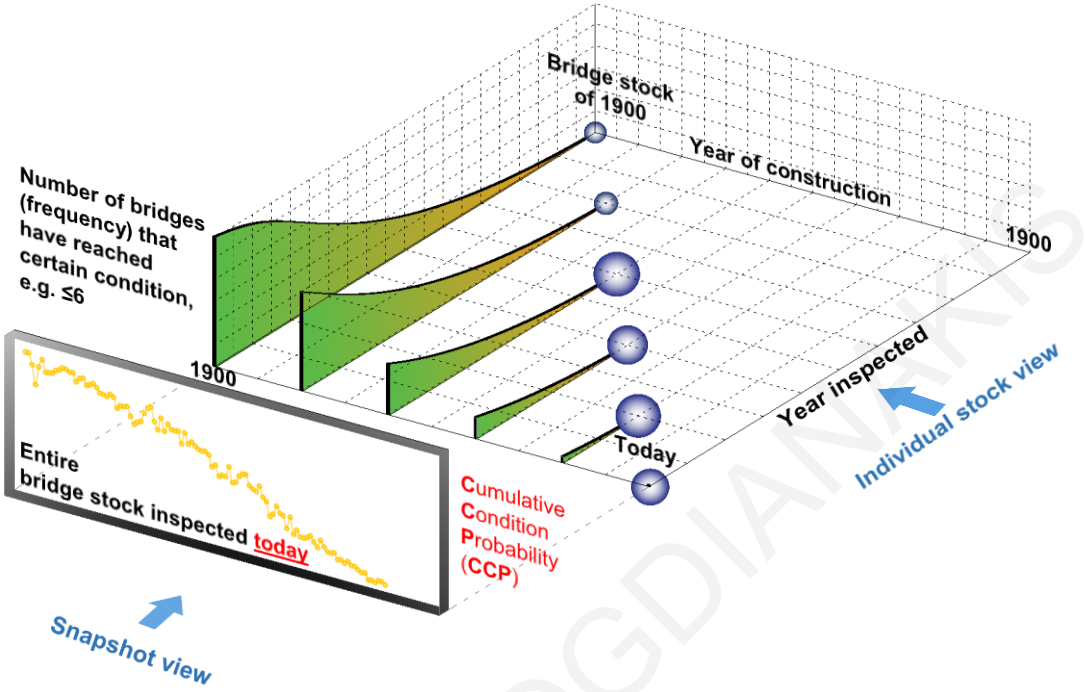

Figure 7.1: Bridge deterioration modeling and the two perspectives used to tackle it. In this study the snapshot view is proposed, where bridge deterioration data of one year of the latest inspections is used today (2016). The snapshot reveals how bridges of each stock are performing today. The CCPs observed show a mirror view of the ones seen in the previous chapter, as year of construction is used instead of age.

The most common perspective of analysis is the 'individual stock view' (Fig. 7.1), where condition changes from all inspection years are used for both time-based and state-based approaches. Thus, if a region was studied where *N* bridges had been inspected for *L* years, the maximum sample size would derive from the number of the different inspections (*N x L*). The advantage of such assumption lies in the enrichment of the sample due to multiple inspections. The disadvantage of this approach is the reliability of the inadequate data used, as well as assumptions regarding the way a bridge transitions from one condition to the other.

As seen in Chapter 3, changes in NBIS may mean change in the inspection procedures, as well as in the evaluations derived. In all reviewed work, a basic step before proceeding to probability calculations is filtering among the inspection data of different years for each bridge. In many cases data have been excluded due to errors in coding or due to inappropriate evaluations for deterioration modelling. Specifically, in many cases condition ratings of non-

rehabilitated bridges have been noticed to rise from year to year (Agrawal et.al, 2010). These errors can be attributed to human factor, errors performed during inspection procedure or minor rehabilitation work that has been performed. Furthermore, a 2001 survey conducted to assess the reliability of visual inspections of the NBI revealed that 95% of the examined sample was found to vary plus or minus 2 condition ratings (in the 10-scale evaluation program), 68% of which were found to vary plus or minus 1 condition rating (Phares et.al, 2004). Such observations render information of older inspections dubious and, therefore, filtering of untrusted inspections may result in selection biases, which are not traceable afterwards.

In the present work, it is assumed that the NBIS are kept frozen, leaving only the inspectors' subjectivity and minor repair work to create data anomalies. This is achieved by using a single reliable annual inspection database that reveals the snapshot view (Fig. 7.1). Although this perspective has been used by studies investigating deterioration or material performance mentioned in chapter 4, the difference of the present study lies in the probabilities, which are used under the main assumption that all bridges in the processed data-stock are used, based on their ages, to represent the condition of a single bridge during its lifetime. The validity of such assumption was illustrated for the case of prestressed concrete (chapter 6), where different years of inspections were compared. The 'snapshot view' provides the advantage of utilizing the latest most advanced and accurate inspections, while its disadvantage regards data limitations caused by segmentations performed to achieve sample uniformity. As seen in chapter 6, small sample sizes increase probability variations between different ages, while for certain ages no sample is available.

7.3 The proposed method

To probabilistically predict the time to a future condition, the proposed methodology utilizes Cumulative Condition Probabilities (CCPs) of segmented samples of bridges. Sample segmentations regarding materials and environments are required to achieve sample uniformity, which is necessary for the main assumption to hold. To both describe and validate a method a specific segmented sample is used, whose purpose is to increase the accuracy of the CDF, when only limited data are available. Thus, only part of the available data are utilized to describe the method, while the rest of the data are used to validate the method's predictions. The validation process of the method is extended by varying the number of available data used. The same procedure is followed for other samples to provide additional validation results.

7.3.1 Selection of segmented samples

Segmentation of a sample would include a data analysis processes similar to chapter 4, to identify predominant sources of deterioration. As the purpose of this chapter is to illustrate and later validate the method, an 'ideal' segmented sample was sought among the ones used in chapter 6. An 'ideal' sample should include low variations among computed CCPs for different ages, thus the first criterion was based on the number of bridges in each age. Second, it should include an age range wide enough to provide adequate data for validating the method's predictions. Thirdly, the imposed selection bias due to rehabilitations should be kept to a low level, in order to avoid misleading lower probabilities affecting the method's validation.

Based on these criteria, bridge superstructures with simple spans in 'deicing, water' environment (chapter 6) were selected, as they had the highest sample populations, both regarding the number of bridges built per year, as well as after the age of 60 years (Appendix Chapter 6 A-IV. 10). Among the structural materials of the category, prestressed concrete did not contain data after 66 years of age and, thus, the selection was based on the material with the least rehabilitated bridges, which was concrete. Hence, simple-span concrete superstructures in 'deicing, water' environment are used for the method's illustration in this section. Additional validations for the method have been included in section 7.6 for the samples of concrete superstructures with continuous spans in 'deicing, water' environment and concrete superstructures with simple spans in 'no deicing, water, environment.

7.3.2 Calculation of cumulative condition probabilities based on NBI data

The CCPs of the stratified sample used in this section are calculated using Eq. (7.1). The calculated value reveals the probability of a bridge at a certain age to be in a condition equal or below a certain threshold. In Fig. 7.2, CCPs for conditions 8, 7, 6 and 5 are only displayed, as CCP_9 is always equal to 1 and CCPs for conditions below 5 (i.e. 4, 3, 2, 1, 0) correspond to conditions signifying the need for rehabilitation. As noticed from chapter 6, the CCPs calculated are not monotonic, but vary within a range, which tends to widen as the bridge sub-stock becomes older. This can be attributed to the smaller samples of constructed bridges available for older years (Fig. 7.2). Also, an overall tendency of the probabilities to rise and reach the value of one can be noticed.

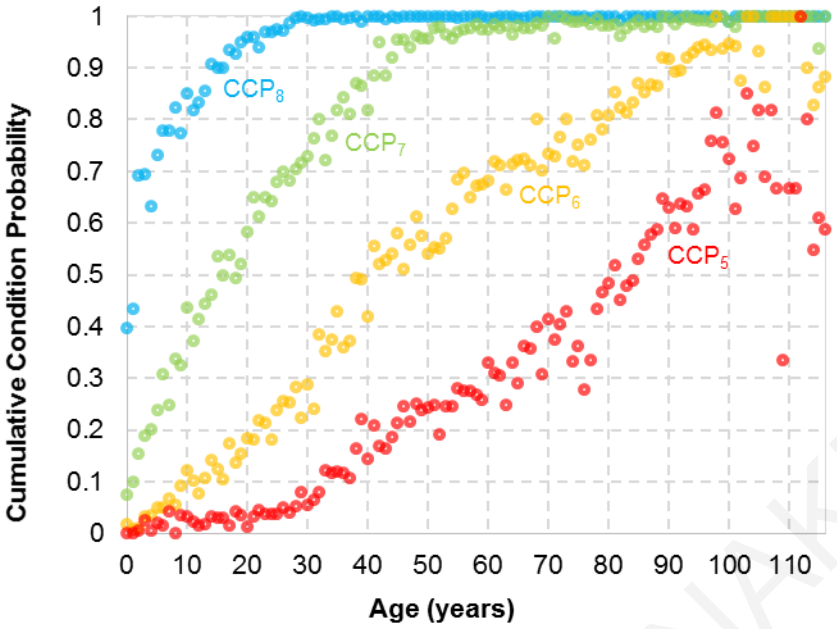

Figure 7.2: Calculated CCPs for concrete superstructures exposed to 'deicing, water' environment.

7.3.2.1 Bridge aging process within the scope of CCPs

In chapter 6, CCPs were initially introduced to express the probability of bridges in deteriorated condition at each particular age (defined by the bridge stock). As seen from chapter 6, but also from Fig. 7.2, the differences among the different bridge stocks for each age are responsible for variations of CCPs. Rehabilitations performed tend to remove bridges in worse condition, leaving in the samples only bridges that are performing well. Thus, despite the fact that rehabilitated bridges are not taken to consideration, the selection bias increases with increase in rehabilitations.

Hypothetically, if each age sample was rich enough, variations noticed in chapter 6 would be radically reduced. Moreover, if no corrective action was allowed, but instead bridges were left to deteriorate until failure (condition 0), the cumulative condition ratings could be qualitatively presented by a figure of the form of Fig. 7.2. Then, the Condition Probabilities (CPs) for any age can be calculated by:

$$CP_i(t) = \frac{N_i(t)}{N_{c,tot}(t)} = \frac{N_i(t)}{N_0(t) + \cdots + N_9(t)} \quad (7.1)$$

where $CP_i(t)$ is the CP for structural condition $=i$ of the bridges at age t; $N_i(t)$ is the total number of bridges at condition $=i$ at age t. Thus, CPs reveal information about the probability of a bridge at certain age to be in a specific condition.

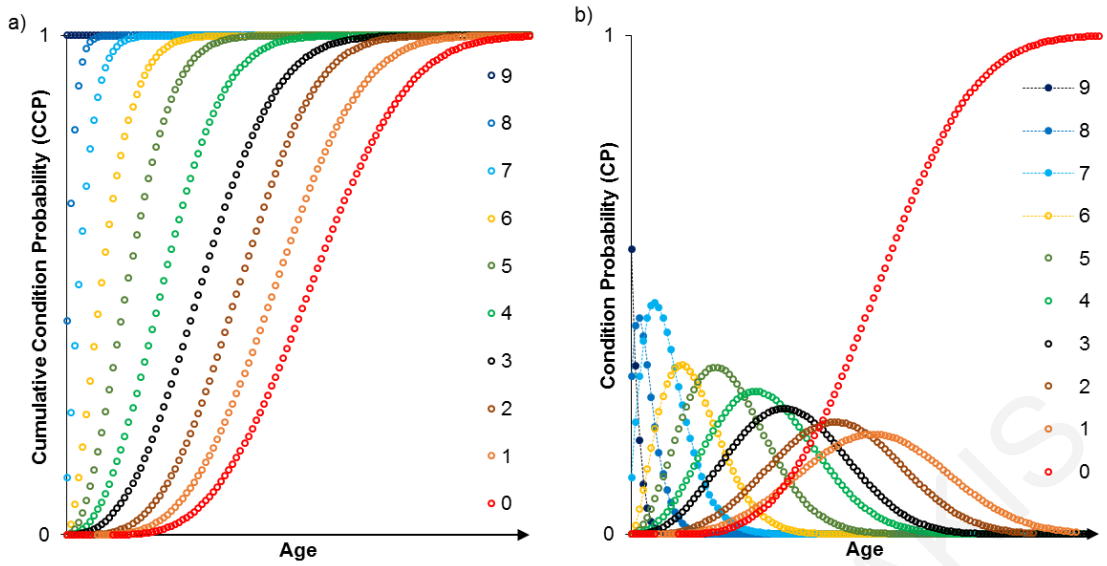

Figure 7.3: The aging process from the scope of CCPs (a) and CPs (b) under the hypothesis that no corrective action (maintenance or rehabilitation) is performed.

Figure 7.3 provides the probability of one bridge to be in each condition throughout its lifetime. The CPs of Fig. 7.3 appear to have a shape similar to a probability density function, while failed condition (=0) appears to have a shape of a cumulative distribution function.

The shape of CPs can be explained by the dynamic process of aging, where lower structural condition ratings are more likely, as a bridge gets older. Furthermore, as lower conditions than failure (=0) have not been assigned, the bridge will eventually reach failure and thus a cumulative effect is evident. Another useful observation from Eq. (6.1), but also from Fig. 7.3, is that for each age the sum of the different CPs is equal to the certain event (probability=1). Thus, CCPs, which are the sum of all CPs below or equal a particular condition, present all information included in the dynamic aging process in compact form, which can be modelled by using CDFs.

In reality, bridges are rehabilitated and rarely left to fail, also each age has a limited sample, which, as seen in chapter 4, depends on various socioeconomic, as well as technological aspects. Furthermore, for certain environments or materials (such as prestressed concrete), data are not available for all ages. All mentioned reasons limit the hypothetical bridge's probabilities to a certain age. As the NBI database for only one year has been utilized herein, Markov chains or survival analysis procedures cannot be used to predict the hypothetical bridge's future conditions. Moreover, since explanatory variables have already been used to segment samples, resulting in a bridge aging process that can be described by a CDF, the appropriate fits to the data have to be found.

7.3.3 Finding an appropriate fit to the data

A necessary procedure for predicting the time to rehabilitation, but also assist the validation process, is to have an objectively trusted original sample. This means ruling out the objectively untrusted probabilities, by noticing the tendency and variations of Fig. 7.3. It is evident that after 98 years of age all calculated CCPs usually have increased variations and a tendency to achieve lower values. Both can be linked to the very low sample sizes for the corresponding years of construction Appendix (A-IV). It is worth mentioning that attention should be given in selecting the trusted sample by considering outliers in the probabilities calculated. To do so, additional information should be sought regarding rehabilitations, sample sizes, as well as changes in construction standards.

Most commonly used lifetime distributions for reliability analysis are the exponential, Weibull, gamma, log-normal, logistic, Pareto and extreme value (Pham, 2006). For each CCP-curve, a regression was performed to determine each distribution's parameters and produce a non-linear-least-squares fit for each of these candidate CDF. The purpose of this step is to achieve a fit that best describes the data for the range of the trusted sample. The selection was based on three different goodness of fit tests. The first is the two sample Kolmogorov-Smirnov (KS) test (Pratt & Gibbons , 1981) at a 5% level of confidence, where the maximum distance between samples is measured and is more effective around the mean. Also, two general goodness of fit measures based on residuals were used: the Mean Square Error (MSE) (Hyndman & Koehler, 2006) and the coefficient of determination R^2.

Table 7.1 reports results for the goodness of fit tests. Regarding the p-values of the KS test given, higher values reveal higher confidence of the null Hypothesis (no significant difference among CCPs and candidate distribution). Larger MSE reveals increased differences among the fit and the data, while higher R^2 values indicate better fits. Based on the results of Table 7.1, the three parameter Weibull distribution was chosen. Its CDF and PDF are (Johnson et.al., 1994):

$$F(t) = 1 - e^{-\left(\frac{t-t_0}{a}\right)^{\beta}}, t \geq 0 \qquad (7.2)$$

$$f(t) = \frac{\beta}{\alpha} \cdot \left(\frac{t-t_o}{a}\right)^{\beta-1} \cdot e^{-\left(\frac{t-t_o}{a}\right)^{\beta}}, t \geq 0 \qquad (7.3)$$

where α>0 is the scale parameter (or according to (Abernethy, 2000), a product's characteristic life), which has the same unit as t, t_o is the time free of failures, which has the same unit as t, while β>0 is the unit-less shape parameter (according to (Abernethy, 2000), β<1 indicates infant mortality, β=1 random failure and β>1 wear out failure).

Table 7.1: Results of goodness of fit tests for the estimated parameters for each distribution examined. The parameters are named based on Matlab's notation. All hypothesis tests were performed on the 0.05 significant level failing to reject the H_o (no significant difference among CCP and the candidate distribution), apart from cases noted with (*).

Results for CCP_8

Distribution name	Estimates of parameterers			KS p-value	MSE	R^2
Log-Normal	$\mu = 0.29$	$\sigma = 1.86$		0.109	0.0068	0.70
Gamma	$a = 0.29$	$b = 17.02$		0.537	0.0063	0.72
Weibull	$t_o = -1.53$	$\alpha = 4.35$	$\beta = 0.65$	0.537	0.0012	0.95
Logistic	$\mu = -0.01$	$\sigma = 6.26$		0.936	0.0019	0.92
Pareto	$\sigma = 1.11$	$\theta = 1.36$		0.055	0.0071	0.69
Extreme Value	$\mu = 3.29$	$\sigma = 12.91$		0.342	0.0025	0.89
Exponential	$\mu = 3.69$			* 0.005	0.0137	0.41

Results for CCP_7 data

Distribution name	Estimates of parameterers			KS p-value	MSE	R^2
Log-Normal	$\mu = 2.59$	$\sigma = 0.97$		*0.020	0.0030	0.96
Gamma	$a = 1.04$	$b = 18.95$		0.540	0.0013	0.98
Weibull	$t_o = -6.09$	$\alpha = 27.12$	$\beta = 1.42$	1.000	0.0006	0.99
Logistic	$\mu = 16.10$	$\sigma = 11.02$		0.937	0.0011	0.98
Pareto	$\sigma = -0.13$	$\theta = 21.79$		0.989	0.0011	0.98
Extreme Value	$\mu = 23.47$	$\sigma = 17.59$		*0.020	0.0022	0.97
Exponential	$\mu = 19.73$			0.405	0.0013	0.98

Results for CCP_6 data

Distribution name	Estimates of parameterers			KS pvalue	MSE	R^2
Log-Normal	$\mu = 3.76$	$\sigma = 0.70$		0.356	0.0021	0.98
Gamma	$a = 2.22$	$b = 23.22$		0.804	0.0014	0.98
Weibull	$t_o = 0$	$\alpha = 56.38$	$\beta = 1.61$	0.964	0.0012	0.99
Logistic	$\mu = 47.32$	$\sigma = 18.80$		0.804	0.0018	0.98
Pareto	$\sigma = -0.83$	$\theta = 87.67$		0.964	0.0017	0.98
Extreme Value	$\mu = 60.14$	$\sigma = 28.15$		0.202	0.0036	0.96
Exponential	$\mu = 57.50$			* 0.015	0.0073	0.92

Results for CCP_5 data

Distribution name	Estimates of parameterers			KS p-value	MSE	R^2
Log-Normal	$\mu = 4.36$	$\sigma = 0.574$		0.148	0.0022	0.96
Gamma	$a = 3.75$	$b = 22.98$		0.456	0.0018	0.97
Weibull	$t_o = 0$	$\alpha = 92.04$	$\beta = 2.33$	0.804	0.0011	0.97
Logistic	$\mu = 79.59$	$\sigma = 21.33$		0.271	0.0014	0.97
Pareto	$\sigma = -2.43$	$\theta = 249.53$		0.202	0.0023	0.96
Extreme Value	$\mu = 90.65$	$\sigma = 27.01$		* 0.022	0.0017	0.97
Exponential	$\mu = 135.56$			* 0.022	0.0107	0.8

The fitted Weibull CDFs are presented in Fig. 7.4. Negative values of age implied in the figure, but also from Table 7.1, indicate that the deterioration process of newly built bridges did not start from the perfect condition 9.

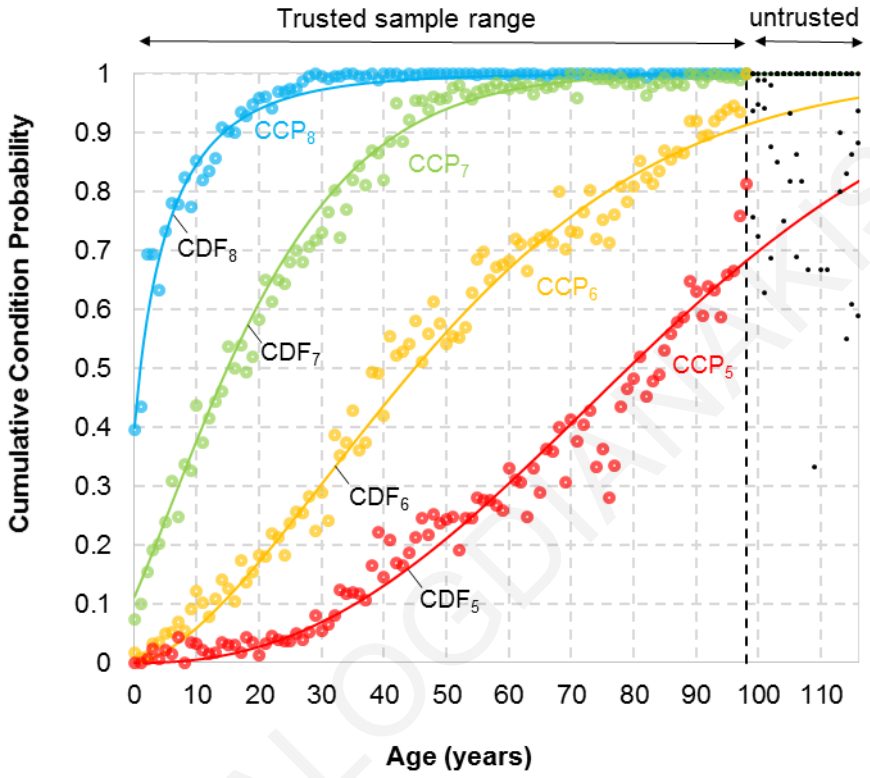

Figure 7.4: Trusted and untrusted sample regions based on the maximum trusted sample (98 years) and fitted Weibull CDFs for each CCP-curve.

7.3.4 Method development preliminaries

To illustrate the proposed method, the NBI data of concrete bridges in 'deicing, water' environment are used. Although a total spectrum of 98 years would be normally used as input to derive predictions, to describe and validate a prediction outcome of the method, only part of the known data are used, while the rest are used to validate the prediction outcome. Thus, an age limit defined as 'cutting age' (t_{cut}) is imposed, separating the data to a 'known range' and an 'unknown range' (Fig. 7.5). Only data from the 'known range' would be utilized to predict the data within the considered as 'unknown range', which would be then checked in the validation process (subsection 7.3.7).

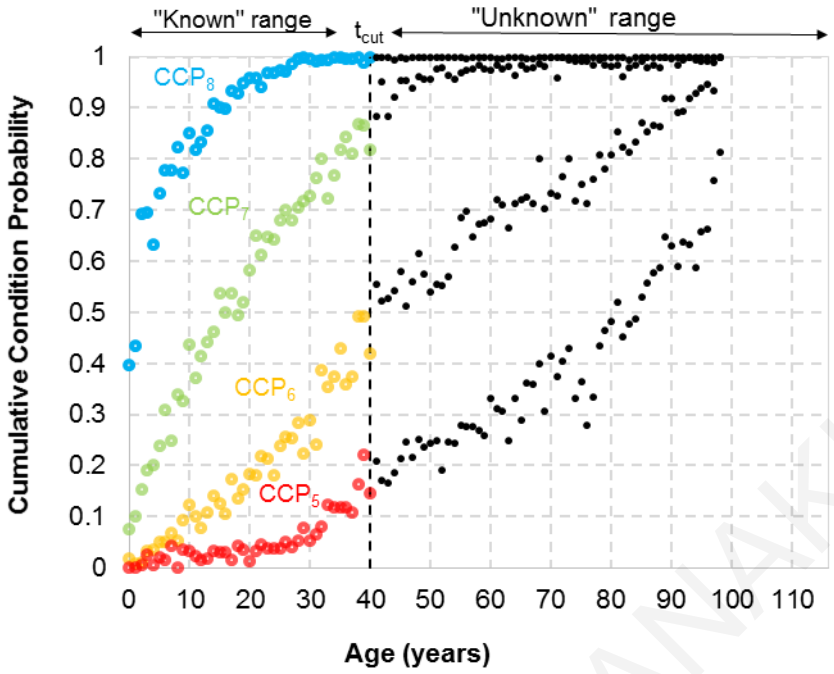

Figure 7.5: Definition of t_{cut} as the limit of the 'known'data to be used, which are then validated using the supposedly 'unknown' data.

The prediction of the failure of a bridge with deterioration rate following an appropriate CDF could produce realistic results (i.e. approaching the original data) provided that few data are missing, corresponding to older cutting ages, where increased probability values are also anticipated. For the case of a Weibull CDF, more accurate predictions can be anticipated for t_{cut} greater than the characteristic life (parameter α), corresponding to probabilities greater than 0.632 (Abernethy, 2000). As this could not be the case for CCP_6 and CCP_5 for this particular sample's whole range of 98 years, greater errors are anticipated for low cutting ages, such as t_{cut}=40 years of Fig. 7.5. Thus, the method developed aims in generating additional data points to assist the selected distribution in achieving better predictions.

7.3.5 Accelerated Creep Tests and the concept of data shifting

Accelerated tests are generally carried out when the actual testing time of a product would be impractical or even impossible. The basic idea of these methods is to carry out experiments with calibrated increments of severity to derive accelerated fracture or wear-out models. The generated models are then scaled based on material properties to represent the lifetime of the product under normal use (Bagdonavicius & Nikulin, 2002).

A good example of accelerated tests concerns polymer materials, known to be prone to creep-rupture under long-term, low-stress loading. Although their creep-rupture behavior

has to be experimentally studied for their application in the construction industry, conventional creep tests require many years to complete. Hence, accelerated creep tests are performed.

Creep is accelerated as the polymer is exposed to increased temperature, humidity or stress. When the acceleration factor is chosen, e.g. temperature, then a number of specimens are tested at constant but increased temperatures (Fig. 7.6). Care is taken for other acceleration factors not to interfere, i.e. if temperature is to be accelerating creep, all tests are performed at constant levels of humidity and stress. The creep rupture curves have similar shapes; the increase of temperature has the effect of displacing the creep curve to the left, or else contracting the time scale, hence creep accelerates (Markovitz, 1975).

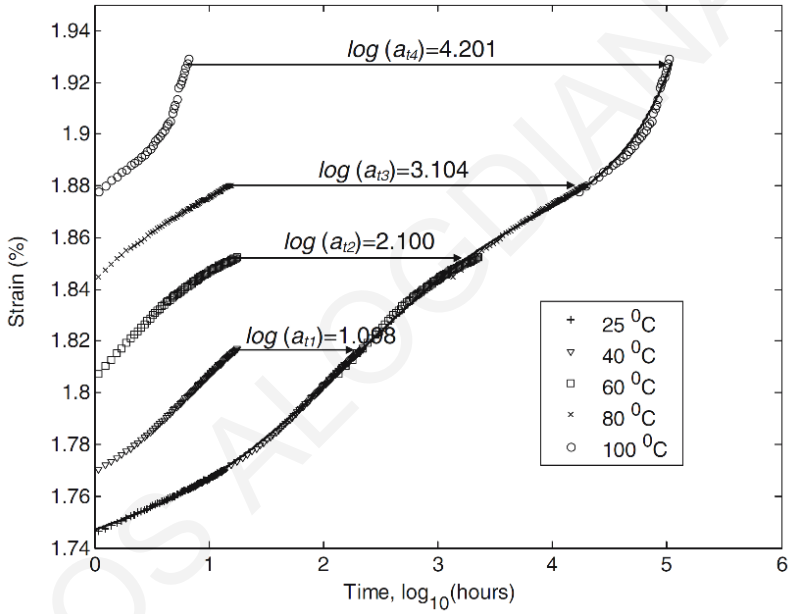

Figure 7.6: Creep curves for tests performed on specimens at various temperatures; horizontal shifting is applied to assemble the creep master curve and the acceleration factors to perform shifting. Figure taken from (Alwis, 2006).

The recorded creep data can then be used to predict the 'creep master curve', or else the complete creep curve, at a given temperature level. As creep is a thermally activated process, a kinetic rate theory can be assumed to be followed, i.e. Arrhenius equation (for temperatures below glass transition). If temperature is the only mechanism to accelerate creep, then they can be shifted horizontally to the right by using appropriate shifting factors, for the assumed kinetic theory to be followed by the deterioration mechanisms. In other words, the time scale is increased, obeying the assumed deterioration law, and horizontal shifting can then be performed.

If two acceleration mechanisms occur simultaneously, a replacement to the Arrhenius law needs to be formed for horizontal shifting to take place. If such a law is not available,

and Arrhenius is to be used, then vertical shifting needs to be performed as well as horizontal, which reduces credibility in the predictions.

If temperature is the acceleration factor, then the horizontal shifting is performed on a logarithmic time scale. Such a horizontal shifting is shown in Fig. 7.6 with the appropriate shifting factors. The data refer to accelerated creep tests performed at aramid yarns at elevated temperatures, which are shifted horizontally to complete a smooth master curve at 25° (Alwis, 2006).

7.3.6 The Shifting Scaling Data Regression (SSDR) method

7.3.6.1 Analogies between SSDR and accelerated creep tests

A bridge is expected herein to be reconstructed when its condition is below 5, a case in which CCPs are typically not completed. The concept of shifting is shown in Fig. 7.6, where an incomplete creep curve at a typical average annual environmental temperature (≈25°C) is completed by shifting data from other creep curves at elevated temperatures (40°-100°C). Similarly, in the case of bridge condition prediction, the CCPs for conditions 8, 7 and 6 may be used to complete the incomplete CCP_5. This could be performed under the main assumption that the CCPs represent the lifetime of a single bridge. Furthermore, as temperature was used as the acceleration factor for aramid fibres, condition evaluation can be used for bridges. Specifically, as seen in 6.3.3, the higher a condition rating is, the less likely it is for a bridge to be in that condition in the future and the smaller is the corresponding age range. In other words, higher CCP's could be considered as accelerated data, from which lower CCPs can be produced.

Although the concept of shifting is simple, complications arise regarding the axis, on which horizontal shifting is to be performed. Such axis would be linked to the deterioration mechanism, which could be described by a law. The practical use of that law would give the time scale factor for condition data to be spread in the future. In the case of a bridge deteriorating due to aging, many factors contribute, i.e. increased temperature, humidity, loading, among others, which occur simultaneously. It is considered difficult to derive such a deterioration law under so many deterioration mechanisms. Despite that, it should be mentioned that shifting and superposition are methodologies whose outcomes cannot be proven (Markovitz, 1975) even for cases where they are extensively used, such as the case of creep testing. On the other hand, for the case of the method developed, despite the absence of a controlled physical means, such as temperature, to derive an acceleration factor for shifting to be applied, enough data exists to validate for the CCPs considered.

7.3.6.2 Shifting of the data

The concept of shifting is used to complete the missing data of CCP-curves by copying data from the previous, completed CCP-curve to the next, incomplete one. Fig. 7.7 demonstrates the shifting process as applied to CCP_7 that is completed with CCP_8-data beyond the threshold age t_{cut}. A preliminary CDF is fitted (F_{aux}) to the incomplete CCP-curves to assist in reducing the variations of the data and facilitate the shifting procedure. For the case of the particular sample studied, auxiliary Weibull CDFs have been fitted, in order to determine data points A and B that are then used instead of the original data points of CCP_7 and CCP_8, respectively (Fig. 7.7). Hence, point A corresponds to the fitted CDF value for CCP_7 at age $t=t_{cut}$ (F_{aux_7} (t_{cut})) and by drawing a line parallel to the age axis from point *A* toward the higher CCP-curve, point *B* is determined. Point B has probability $F_8(t_{e8})=F_{aux\_7}(t_{cut})$ at age $t=t_{e8}$, thus the age t_{e8} can be calculated (obviously, $t_{e8}<t_{cut}$). Then, the actual points of the higher CCP-curve from point B and beyond are horizontally shifted to the lower CCP-curve at point A, i.e. the aforementioned part of the higher CCP-curve is copied toward the lower CCP-curve by t_{cut}-t_{e8}, as shown by the arrows in Fig. 7.7. After performing the required shift, the incomplete curve must have reached probability value of one.

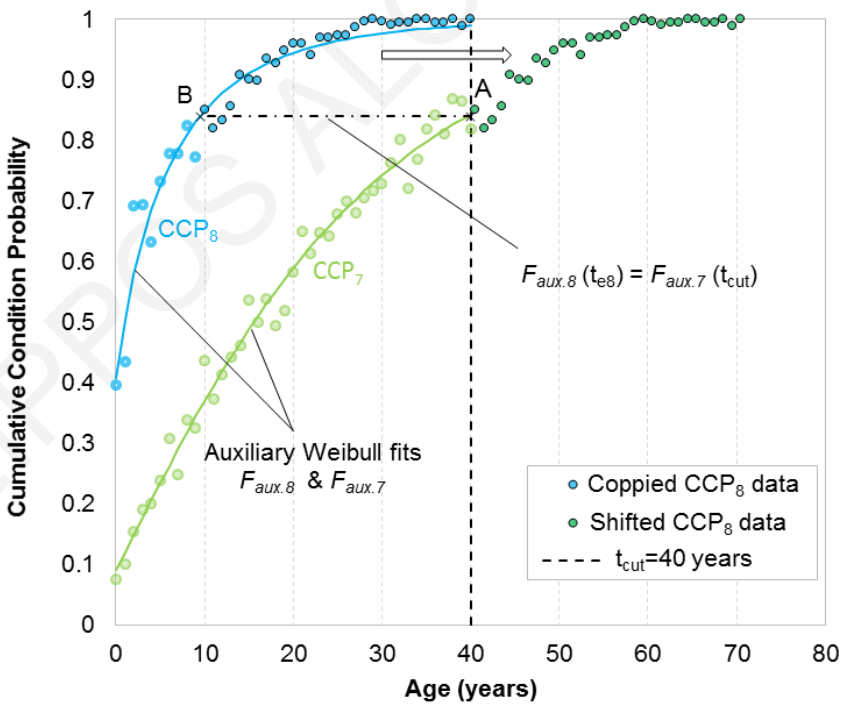

Figure 7.7: Data of CCP_8 are coppied from point B and tranfered to point A of CCP_7 (shifted from B to A); points A and B are determined using the auxiliary Weibull fits.

7.3.6.3 Scaling of the data

As can be verified from Figs 7.4 and 7.5, the inclinations of different CCP-curves cannot be the same, because they describe bridge deterioration at different conditions. Normally, lower inclinations are generally expected for lower CCP-curves than for higher CCP-curves. However, with the shifting of the previous subsection, curve-parts with the same inclination are generated for different CCP-curves. Shifting without scaling the age axis, as performed in the study of Balafas (2003), led to pessimistic results (i.e. prediction for unrealistically fast deterioration) due to the accelerated form of the copied, higher CCPs. On the other hand, changing the age axis to logarithmic and then performing similar shifts would lead to optimistic scalings (i.e. excessive stretching predicting unrealistically slow deterioration). Hence, the shifting procedure was decided to be performed with the age axis as is; the shifted data are then adjusted using an appropriate coefficient to achieve the appropriate spread (Fig. 7.8).

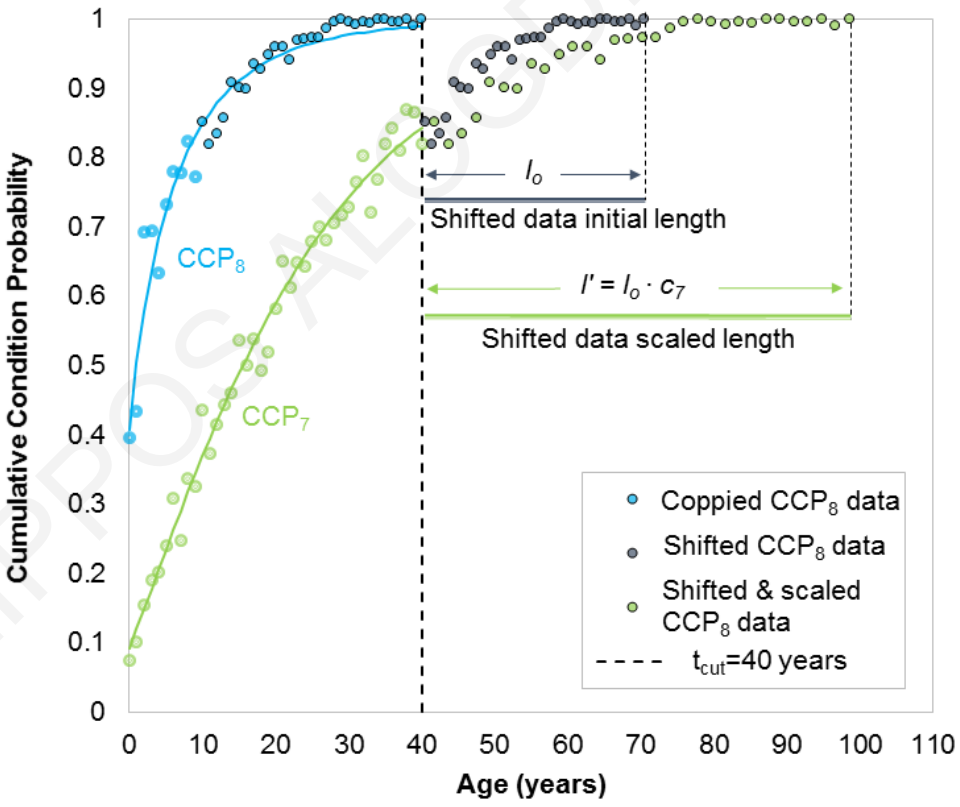

Figure 7.8: Shifted data are spread using the scaling coefficient c_i, the data are spread at equal distances so that the initial shifted data length (l_o) is transformed to the shifted and scaled data length (l').

To find an appropriate scaling coefficient, a number of attempts have been made to utilize properties of the auxiliary CDF fits. These attempts included slopes, hazard functions

or combinations of various geometric properties, which did not lead to adequate predictions. The best performing scaling procedure included a scaling coefficient (c_i) estimated using the Coefficients of Variation (CoV) of two successive CCP-curves:

$$c_i = \frac{CoV_{i+1}}{CoV_i} \qquad (7.4)$$

where c_i is the scaling coefficient for CCP_i data, CoV_{i+1} and CoV_i are the coefficients of variation for CCP_{i+1} (complete) and CCP_i (incomplete) curved, respectively. In general, the coefficients of variation can be calculated as follows:

$$CoV = \frac{\sigma}{\mu} \quad (6.5)$$

$$\sigma = \sqrt{(\int_0^\infty t^2 \cdot f(t)dt - \mu^2)} \quad (7.6)$$

$$\mu = \int_0^\infty t \cdot f(t)dt \qquad (7.7)$$

where σ is the standard deviation, μ is the mean time to failure and f is the probability density function of the corresponding CDF (Eq. (7.3)).

For cases where the 2-parameter Weibull distribution (t_o=0 in Eqs (7.3) and (7.4)) is used for two CCP-curves, the coefficients of variation can be directly calculated as:

$$CoV = \sqrt{\frac{\Gamma\left(1+\frac{2}{\beta}\right)}{\Gamma(1+\frac{1}{\beta})^2} - 1} \qquad (7.8)$$

where Γ is the gamma function and β is the Weibull scale parameter. As parameter β is directly linked to the dispersion of data, greater β values correspond to higher age failure and lower CoV (Jiang & Murthy, 2011). Furthermore, if the 2-parameter Weibull CDF is used, good prediction results can be also anticipated by using directly the fraction of the shape parameters to obtain the scaling coefficient:

$$c_i = \beta_i/\beta_{i+1} \qquad (7.9)$$

where β_i is the shape parameter of the CDF fitted to CCP_i data and β_{i+1} is the shape parameter of the CDF fitted to CCP_{i+1} data.

Apart from its good performance, the CoV-based coefficient of Eq. (7.4) was preferred, as it provides a dimensionless comparison of dispersion between sets of data that vary in magnitude, provided three requirements (Shechtman, 2013) are met:

- Data describe continuous variables of a ratio scale.
- Data compared should vary in magnitudes.
- The mean and standard deviation change proportionally.

Scales are rules of measurement, assisting in assigning numerals to properties of objects or events (Stevens, 1951) and specifying relationships between empirical relational

structures and numerical relational structures (Musvoto & Gouws, 2010). A ratio scale has quantitative nature, incorporating attributes of classification (nominal scale), extent of the property measured (ordinal scale), equality reflected between successive intervals (interval scale) and a meaningful starting point at 0. The data for each *CCP* curve correspond to bridge age, which is defined as a ratio scale variable. Moreover, to avoid the violation of the ratio scale requirement regarding the existence of a meaningful zero value, Eqs. (7.5) and (7.6) are integrated from age t=0. The selection of this limit was based on the fact that no negative ages of a bridge exist and the first inspection/evaluation is performed when a bridge is delivered at age t=0.

Regarding differences in magnitudes between the fitted curves to be compared, each *CDF* has a different mean and a different standard deviation, as can be observed from the form of the curves of Figure 7.5. Additionally, different age values are always anticipated between different *CCP curves*, because each curve corresponds to different condition states. Thus, more bridges of younger ages are anticipated to be in 'perfect' condition, corresponding to lower mean age and a smaller standard deviation. On the other hand, lower ratings correspond to older mean ages and greater standard deviations. Furthermore, an indication of proportionality can be given by linearly regressing the data points defined by the computed mean and standard deviation of each *CCP* curve. This is illustrated in Fig. 7.9 for the *CCPs* of the sample studied herein, for which an R^2 value of 0.97 suggests a strong linear relationship. As all three aforementioned requirements were met, COVs could be utilized to provide meaningful comparisons between the *CCP curves*.

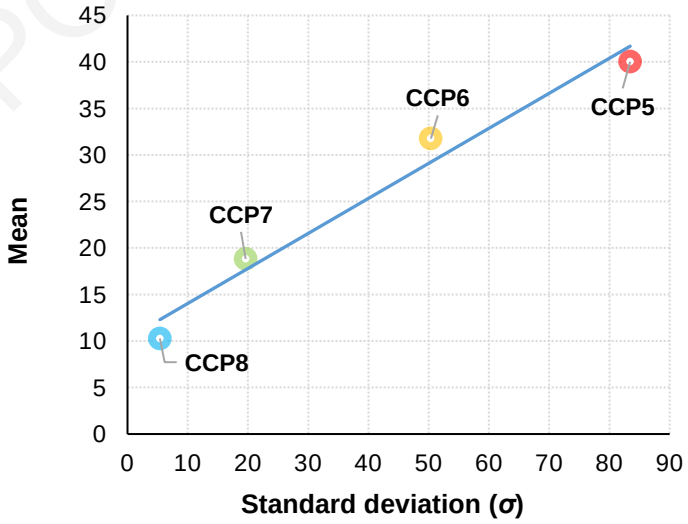

Figure 7.9: Results of linear regression of mean and standard deviation for each CCP curve.

7.3.6.4 Fitting a CDF to complete data and iterating to complete lower CCPs

After having completed the CCP_7 data using shifting and scaling, the appropriate 3-parameter Weibull is fitted. Similarly, the data of lower CCPs are completed by repeating the steps of subsections 7.3.6.2 to 7.3.6.4. When the CCP-data for the prespecified condition of interest are completed (in this case, when CCP_5 data are complete), then all CCP-data can be replaced by the corresponding fitted Weibull curves, as shown in Fig. 7.10.

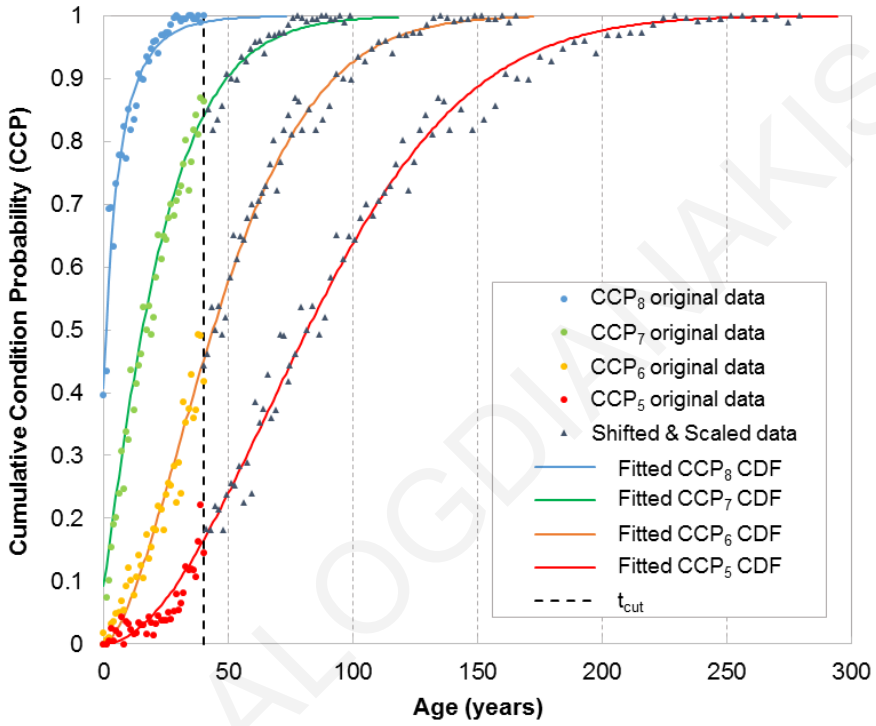

Figure 7.10: Results of the SSDR method after perfroming shifting, scaling and fitting for successive CCPs.

For the cutting age adopted, Table 7.2 presents the Weibull parameter values calculated, as well as the coefficient of determination R^2 attained by applying the fitting procedure to the properly completed CCP-data for bridge conditions ≤7, ≤6 and ≤5. The very high R^2-values reported indicate that a very good fit has been achieved between Eq. (7.3) and the available data (see also Fig. 7.10). The CDFs in Fig. 7.10 are graphical representations of Eq. (7.3) using the Weibull parameter values of Table 7.1. These successful CDF-fits are due to the adequate size of the utilized sample, which exhibits low variation of the available data. In other cases employing lower-quality data, lower R^2-values were observed.

Table 7.2: Weibull parameter values for t_{cut}=40 years.

CCP	t_o (years)	α (years)	B	R^2
8	-1.92	4.84	0.70	0.957
7	-3.60	26.14	1.18	0.992
6	0	55.01	1.61	0.994
5	0	87.79	2.19	0.996

7.3.7 Statistical validation of the proposed method for t_{cut}=40 years

The SSDR method uses recorded, trusted data to predict future condition probabilities. The selection of a cutting age t_{cut} is a subjective decision, which specifies the 'known' part of the available data ($t \leq t_{cut}$), but also creates the need to predict the condition probabilities for $t>t_{cut}$. In this subsection, the effectiveness of the proposed method is assessed with respect to the selected value of t_{cut}, to illustrate the validation process. In section 7.4, various t_{cut} -values are used.

To validate the method proposed, the final fits of subsection 7.3.6.4 have to be compared with the original data known also beyond the age t_{cut}. In this method, when a t_{cut}-value is chosen, the data recorded for $t>t_{cut}$ are excluded from the analysis. Thus, age t_{cut} represents the 'new' present and the excluded data represent the 'unknown' future. The method's CCP-predictions for $t>t_{cut}$ can then be compared with the respective original data, which were excluded from the analysis. Hence, for each t_{cut}-value considered, the SSDR method is applied to obtain a Weibull CDF for each of bridge conditions ≤7, ≤6 and ≤5. The CDF attained for all initial data (ages 0-t_{cut}) is provided as a supplemental comparative prediction. As this fit corresponds to the fitted auxiliary CDF (section 7.3.6.2), the same notation is used (F_{aux}).

To assess the performance of both SSDR and F_{aux}, two validation tests are carried out, one regarding the overall fit of the produced CDF (either SSDR or F_{aux}) to the whole data range (ignoring t_{cut}) and a second regarding the consistency of the produced predictions. It is important to bear in mind, when comparing results of the two methods, that SSDR has the inherent advantage of incorporating also newly generated data points, in contrast to F_{aux} that utilizes only existing ones. The effect of this uneven situation concerning data input can be better observed for lower conditions (≤6, ≤5) where the data utilized by F_{aux} correspond to lower probabilities.

7.3.7.1 Goodness of fit tests

Goodness of fit tests reveal how appropriate a fit is for the available data. The coefficient of determination reported herein is a common way to evaluate the goodness of a fit. It's values range from 0 to 1, with 0 revealing no fit to the data and 1 a perfect fit. Two coefficients of determination are calculated to evaluate the goodness-of-fit achieved. The first coefficient of determination, R^2, compares the attained Weibull CDF with the original data for $t \leq t_{cut}$ and the shifted/scaled data for $t>t_{cut}$; such R^2-value for t_{cut}=40 years was reported in Table 7.2 and calculated as follows:

$$R^2 = 1 - \frac{\sum_i (y_i - F_i)^2}{\sum_i (y_i - \bar{y}_i)^2} \qquad (7.10)$$

where i is indicator of the data of a sample of size n; y_i is the CCP-value of the data and F_i is the value of the fitted Weibull CDF for indicator i; $\bar{y}$ is the mean for all values y_i, i=1,2,…,n.

As the first coefficient of determination of Eq. (7.10) is actually utilized as an objective function by the estimator (in this case nonlinear least squares) to achieve the fit, it is not appropriate for assessing the new method's performance. Thus, a modified coefficient of determination R_m^2 is introduced to compare the attained Weibull CDF (for the t_{cut}-value considered) with all original data (before shifting/scaling) for $t \leq 98$ years (i.e. for $t_{cut} \rightarrow \infty$). Hence, for y_i in Eq. (7.10), the original data of all 98 years (99 points including the one for age 0) are used instead of the shifted and calibrated data. This way, the comparison with the method's attained Weibull CDF is performed using: (a) the shifted/scaled data actually used to calculate the fitted Weibull parameter values (coefficient R^2) or (b) the original unshifted/unscaled data (coefficient R_m^2). In general, higher values for R^2 than for R_m^2 are expected. The same applies for the simple regression prediction F_{aux}.

Under real circumstances, there is no meaning in calculating R_m^2, because all trusted data should be exploited by the SSDR method, therefore $R_m^2 = R^2$. The sample processed in this section includes rich data that are of acceptable quality over the whole range of bridge ages. Thus, by selecting various values for t_{cut}, we can compare the resulting CDFs with original *trusted* data for bridge ages up to 98 years. In other words, although predictions of bridge condition probabilities are derived for ages from t_{cut} up to 98 years, we have actual *trusted* data beyond the age t_{cut} to compare against and can therefore calculate a meaningful coefficient R_m^2, as reported in Fig. 7.11. This allows an objective assessment of the method proposed in the present chapter.

7.3.7.2 Consistency test

The SSDR method and the simple regression F_{aux} can be evaluated also with respect to the consistency of their results by focusing on a specific probability value $F(t)$ to reach a bridge condition. In Fig. 7.11, the attained CDFs (F_{aux}, F_{SSDR} and the red line representing a fit to the whole range of data) are illustrated for t_{cut}=40 years. The consistency tests illustrated regard values for $F(t)$=95% and $F(t)$=70%; at these CCP-values, the corresponding age is found for the 3 different CDFs. The value of the fitted CDF corresponding to all known data can be considered as the most accurate one, thus all other values found are compared with it

(Fig. 7.11). Hence, for the case of $F(t)$=95%, F_{aux} appears to produce a conservative prediction (t=109 years) in comparison to the 'actual' value (t=149 years), while the attained value of F_{SSDR} appears to be more optimistic (t=178 years). Thus, F_{SSDR} is closer to the actual prediction and this is confirmed by the modified goodness of fit test.

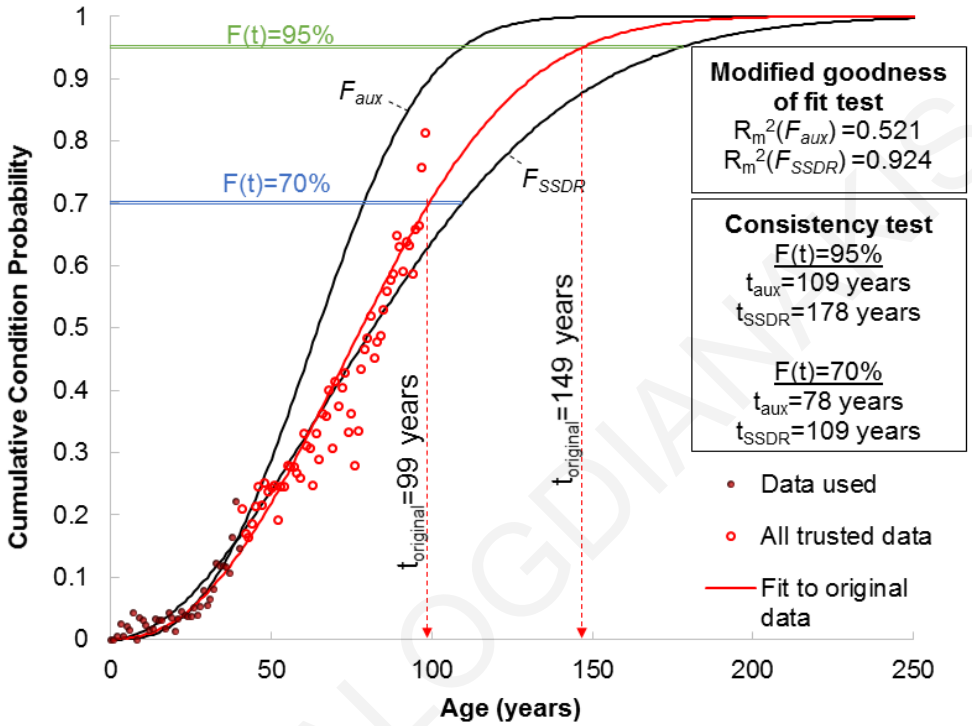

Figure 7.11: Illustration of the validation process on CCP_5 performed for the indicative t_{cut} value selected (t_{cut}=40 years).

In the same figure, the attained predictions (F_{aux}, F_{SSDR}) can be graphically compared to the fit using the whole range of the data (red line). For F_{SSDR}, R^2=0.97 (see Table 7.1); the R^2_m values corresponding to SSDR and F_{aux} are 0.924 and 0.521, respectively. These results indicate that the prediction of SSDR performs much better than simple regression for t_{cut}=40 years. The same process is performed for various t_{cut} values in the next section, where the results for all corresponding R^2_m values and consistency tests are displayed.

7.4 Results and discussion

In this section, the results for various t_{cut} values are presented starting from an initial age of t_{cut}=34 years and successively adding one year of age data to complete the whole range of the trusted sample (up to t_{cut}=98 years). First, the new method's parameters are assessed for each t_{cut} value and then follows the validation process.

7.4.1 SSDR's parameters estimation

For each t_{cut} value, data are initially shifted from CCP_8 to CCP_7, a scaling coefficient c_7 is calculated, the shifted CCP_8-data are scaled and a new Weibull fit is obtained. The same process is successively performed for lower CCPs. In Fig. 7.12(a), the numbers of data points (CCPs) copied from higher CCPs to the immediate lower ones are presented for the different t_{cut} values. Also, for each t_{cut} value, the calculated scaling coefficients (c_7, c_6, c_5) are provided in Fig 7.12(b). In both figures, the number of CCP_8 points shifted to CCP_7, as well as the corresponding scaling coefficient c_7, stop at t_{cut}=69 years, because CCP_7 is completed after that age, thus the new method is not used.

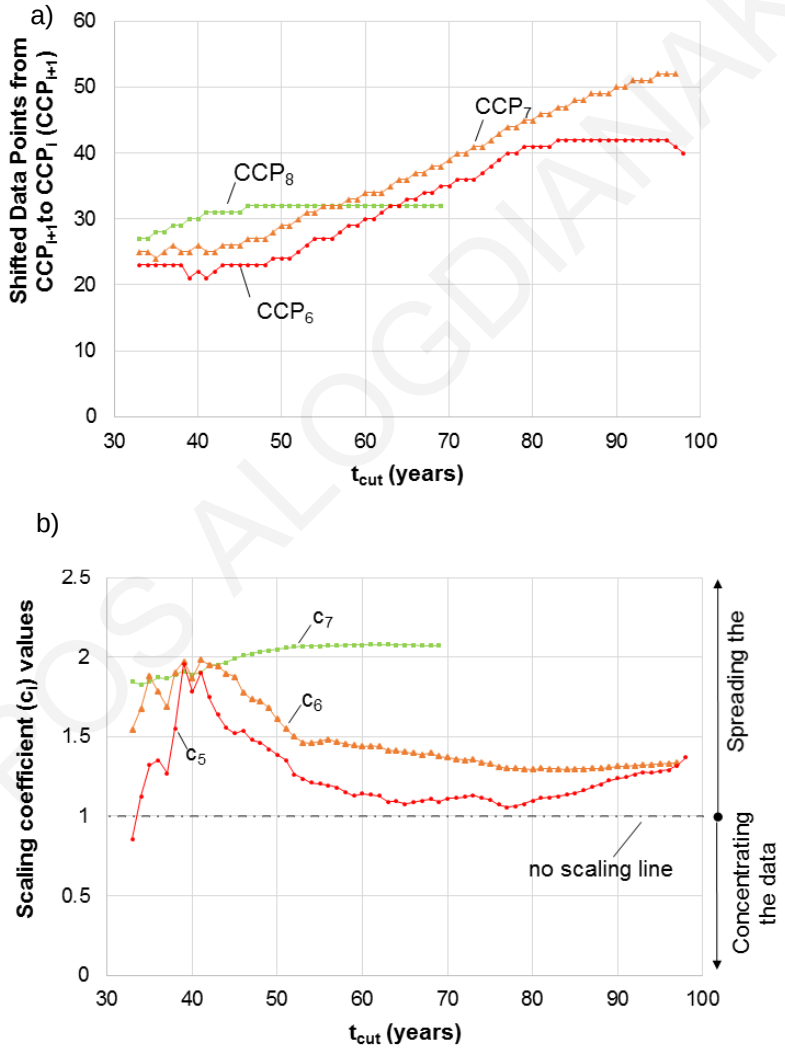

Figure 7.12: Shifted data points from higher to lower CCPs (a) and scaling coefficients of the SSDR method for increasing t_{cut} values (b).

The values of Fig. 7.12 calculated for a selected t_{cut} can be used to present a calibrated (scaled) age axis, where data from higher CCPs can be shifted. Such axis would indicate an equivalent 'law' mentioned in subsection 7.3.6.1, as to how the data should be shifted. The new method proposed performs successive shifts and scalings from higher to lower CCPs.

Specifically, shifted data from curve CCP_8 to CCP_7 (Fig. 7.12(a)) are scaled by multiplying bridge age with c_7 (Fig. 7.12(b)), then the same data as part of the completed CCP_7 curve are shifted to curve CCP_6 and scaled again using c_6, while in the end they are shifted to curve CCP_5 and scaled again using c_5. Thus, the initial data shifted from curve CCP_8 to CCP_5 are overall scaled using a coefficient equal to the product of the successive scaling coefficients used (i.e. $c_7 \cdot c_6 \cdot c_5$). Similar overall coefficients can be calculated for shifting CCP_7 and CCP_6 data to complete the CCP_5 curve. These overall coefficients actually specify the shifting 'law' to appropriately copy data from a CCP curve to another for different t_{cut} values. Hence, the equivalent age axes for shifting to CCP_6 and CCP_5 curves are presented for 3 different t_{cut} values in Figs 7.13 (a) and (b), respectively. As can be seen from these figures, shifts originating from higher CCPs have slopes deflecting more from the 'no scaling line' in comparison to shifts from the immediately previous CCP, which do not deflect as much. The peaks of each line for a different t_{cut}, where slope changes, are points separating data shifted from different CCP curves. The slope changes are due to different overall coefficients applied for the scaling of corresponding data. For example, for completing curve CCP_5 in the case of t_{cut}=35 years (Fig. 7.13(b)), the shifted data originate from CCP_8 (overall scaling coefficient $c_7 \cdot c_6 \cdot c_5$), CCP_7 (overall scaling coefficient $c_6 \cdot c_5$) and CCP_6 (overall scaling coefficient c_5), justifying the 3 different slopes observed.

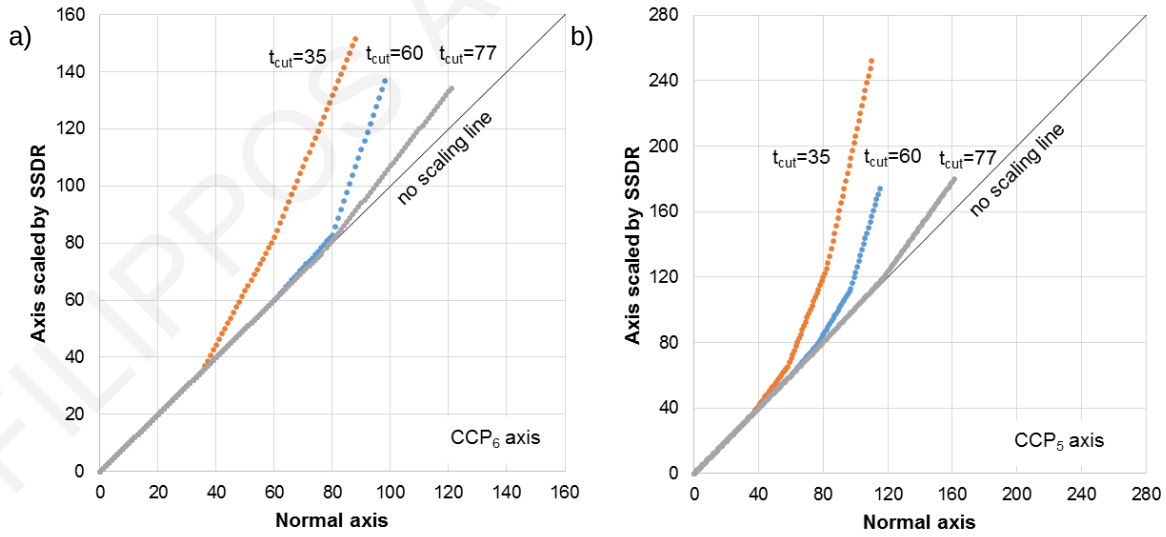

Figure 7.13: Scaling performed to axis on the shifted data for (a) CCP_6 and (b) CCP_5.

7.4.2 Validation results

The SSDR method is based on the concept of shifting and scaling of successive CCPs. Hence, the errors from the whole process are anticipated to be accumulated in the smaller

CCP (CCP_5 for this chapter's case). On the other hand, simple regression utilizes all available data points to fit a CCP curve. Thus, the process of validation, apart from testing the SSDR method's effectiveness, can also reveal when simple regression (based on Weibull for this case) using all available data points should be preferred.

The results are presented in Figs 7.14-7.16 for each CCP curve obtained. In each figure, first the R^2_m values are plotted for the t_{cut} values considered; then, two consistency tests are performed for $F(t)$=95% and $F(t)$=70%. The good effectiveness of either method (SSDR and simple regression) is indicated in the results, when increasing R^2_m and smaller variations of age values in consistency tests are observed for increasing t_{cut} values.

In each consistency test the 'actual' value (from the fit achieved utilizing all data, i.e. t_{cut}=98 years) is provided to compare against each prediction. Furthermore, as the results of only two *F*-values are presented (95% and 70%), results for additional *F*-values are given to compare the overall consistency of both methodologies. The results of consistency tests, ranging from a low probability (10%) to an extreme (99.9%), are organized using boxplots for each CCP curve in Fig. 7.17.

Regarding CCP_7, Fig. 7.14 shows that both SSDR and simple Weibull regression perform very well, as both methods, for $t_{cut}\geq$50 years, reach a high R^2_m (>0.99) and the 'actual' age corresponding to the two *F*-values of 95% and 70%. In the consistency tests (Fig. 7.14(b, c)), the SSDR method appears to have slightly increased variations, especially for the case of $F(t)$=70%. This can be attributed to the fact that CCP_7 is anyway close to being completed (trusted points reach CCP values higher than 0.632, see Fig. 7.2), which means that the available data are adequate for a successful fit using simple regression. For the lower t_{cut} values, the SSDR method slightly distorts the results with the additional data generated. Nevertheless, the results show that both approaches can be used for cases with data that are near to being complete.

Regarding CCP_6, Fig. 7.15(a) shows much better R^2_m results for SSDR in comparison to simple regression for the lower t_{cut} values (≤50 years). Similar observation is made for the consistency tests (Figs 7.15(b, c)), where simple regression (F_{aux}) produces unrealistically conservative predictions for both *F*-levels examined, while the SSDR method produces age results that vary within a range of only 15 years. For t_{cut}>50 years, the performance of simple regression is enhanced due to the high CCP values available in the input data. Although for these higher t_{cut} values both methods appear to be performing equally well, the SSDR method can be considered more robust for the whole range of t_{cut} values and thus more preferable to simple regression (especially for $t_{cut}\leq$50).

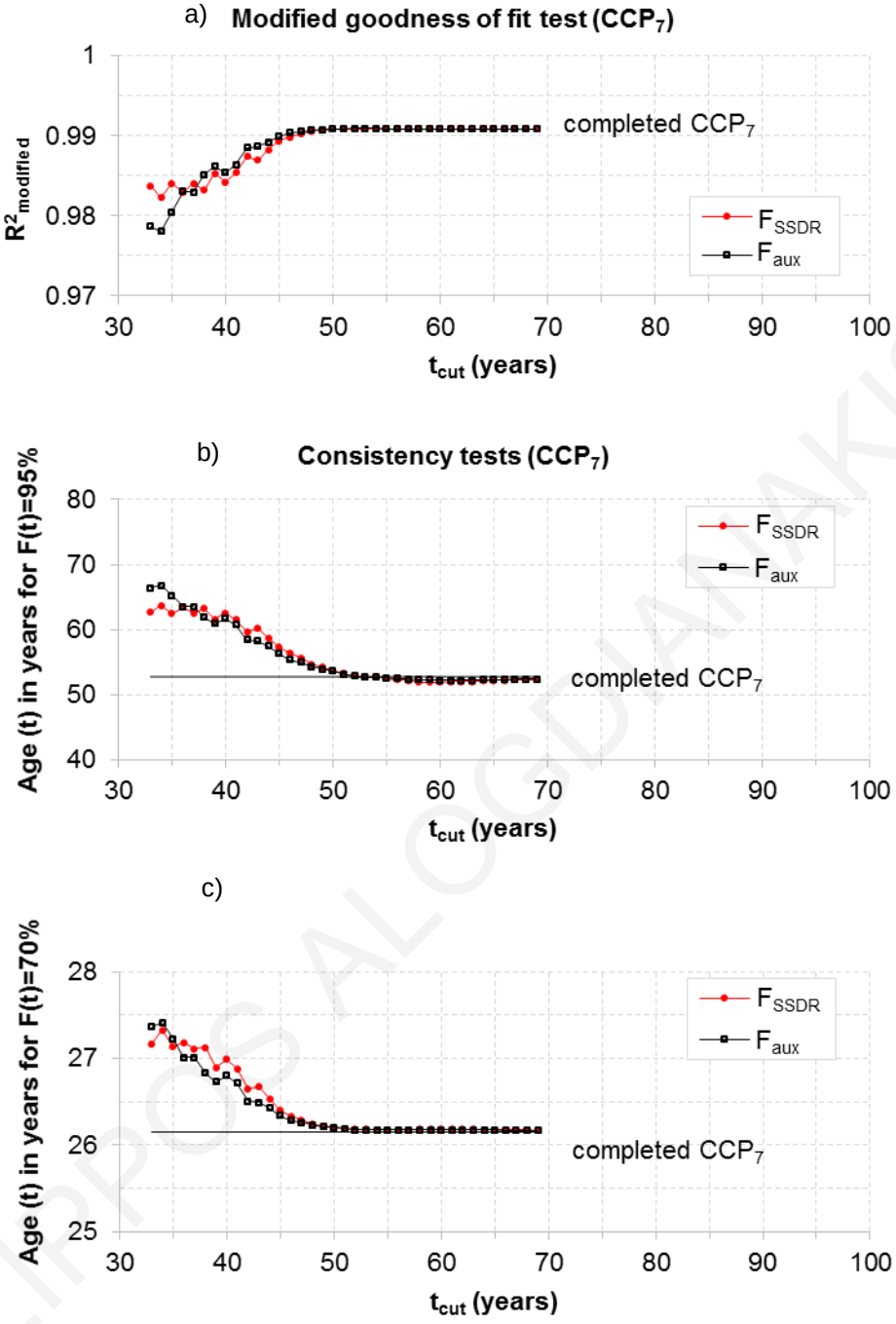

Figure 7.14: Validation results for CCP7: modified goodness of fit test (a), consistency tests for F(t)=95% (b) and F(t)=70% (c).

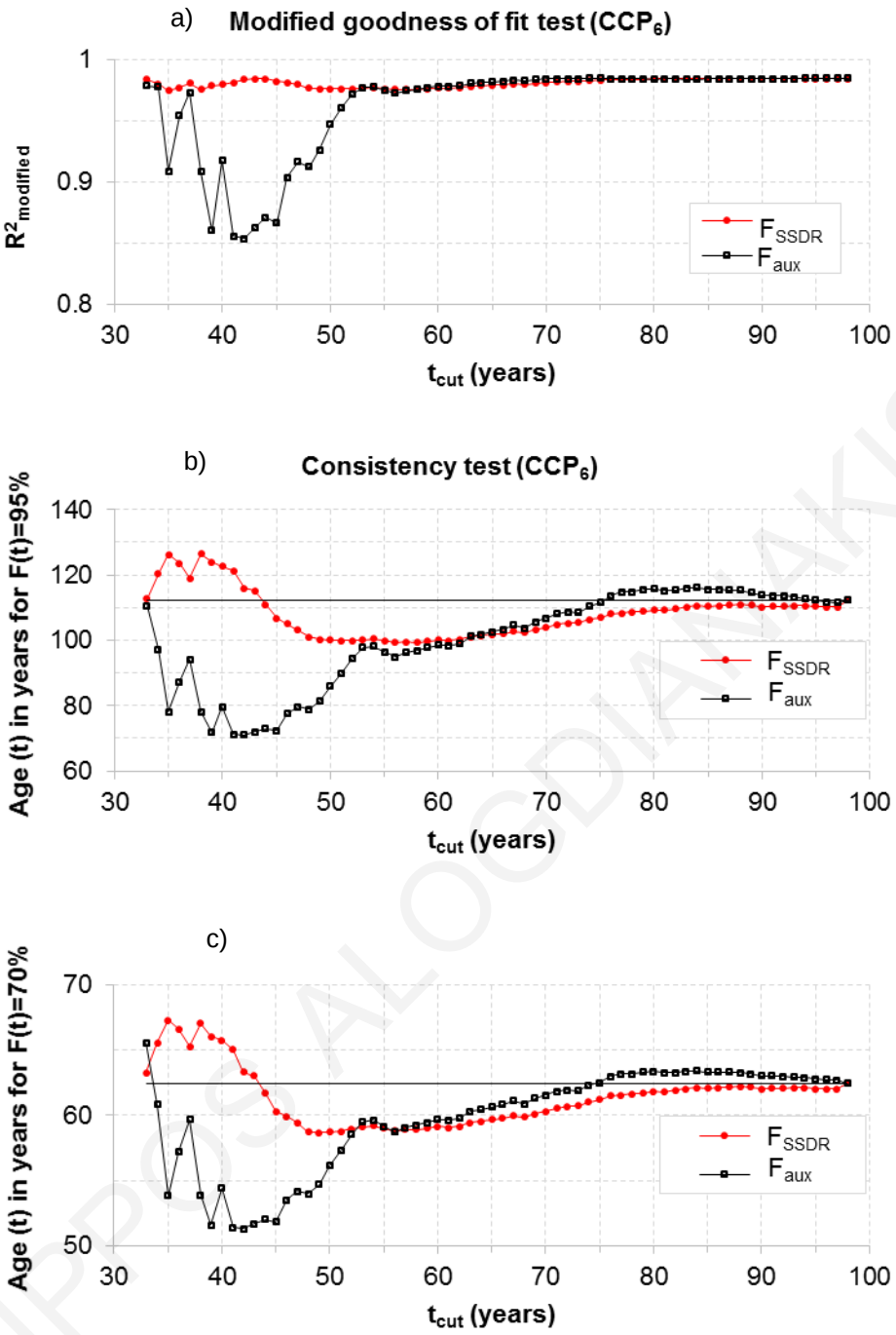

Figure 7.15: Validation results for CCP_6: modified goodness of fit test (a), consistency tests for F(t)=95% (b) and F(t)=70% (c).

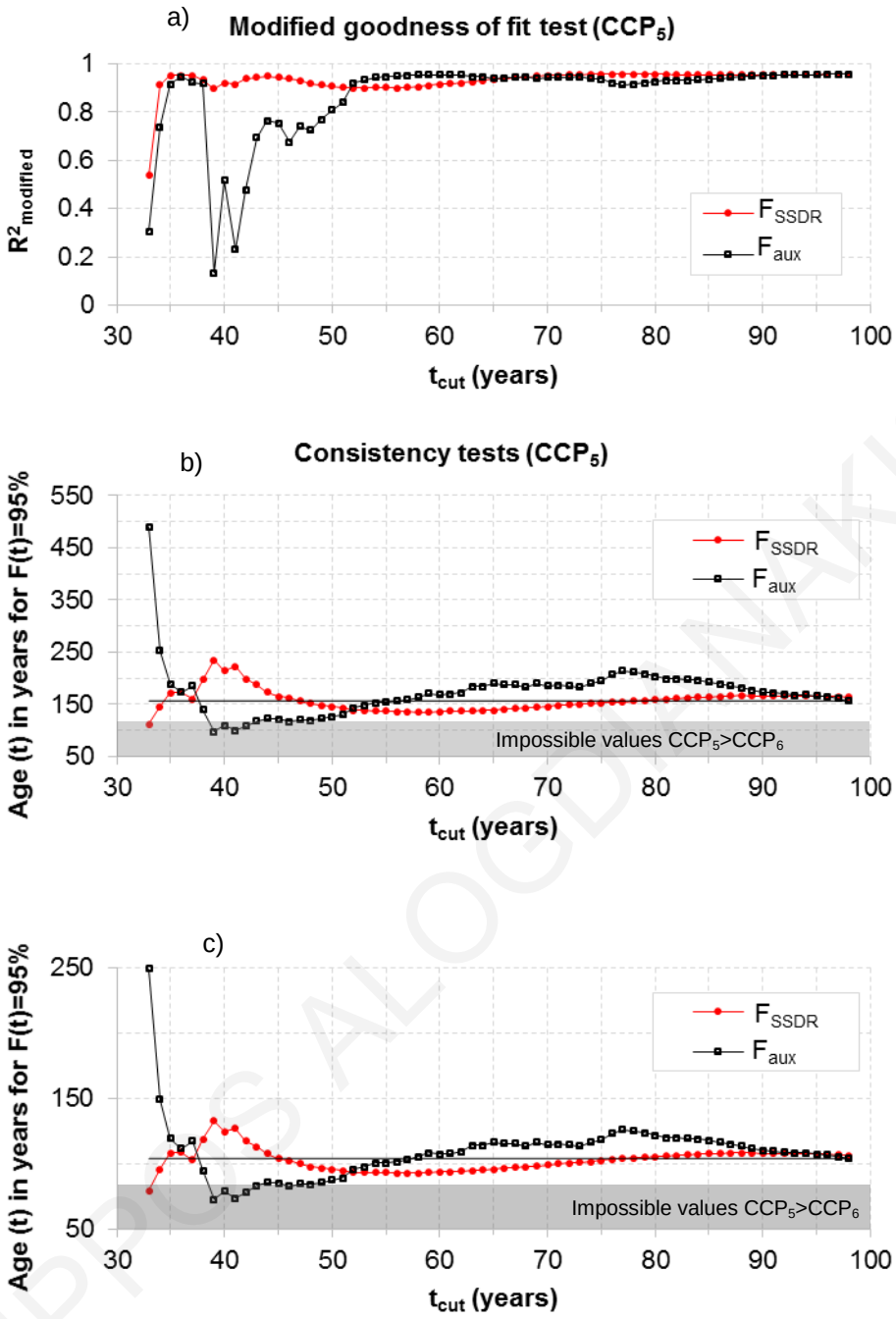

Figure 7.16: Validation results for CCP_5: modified goodness of fit test (a), consistency tests for F(t)=95% (b) and F(t)=70% (c).

The SSDR method was mainly developed to predict CCP_5 (and even lower CCP curves), where the simple regression would not have adequate data to perform reliable predictions. According to Fig. 7.16(a), both predictions do not perform well for t_{cut}=34 years. This is due to the fact that, for certain age values, the CCP_5 values are similar with a slight decreasing tendency (Fig. 7.2), creating over-dispersed predictions for the simple regression (F_{aux}). As described in the steps of the SSDR method, the regression values are used to

calculate the scaling coefficient of Eq. (7.4), which leads to unrealistic results (concentration of data instead of spreading).

The results attained can be further evaluated for their validity by utilizing the definition of CCPs, which forbids the case of a CCP curve including a higher CCP value than its a higher CCP for the same age (i.e. CCP curves cannot intersect). This restriction prohibits a bridge to deteriorate until it is first in a lower condition rating and then to a higher one, which is not possible without rehabilitation. This led to the definition of 'impossible values', which indicate that a result in the consistency test is erroneous due to intersecting CCP curves. Furthermore, due to their sigmoid shape, CCP curves that are close to intersecting indicate unrealistic results.

According to Fig. 7.16(a), for t_{cut} >34 years, the SSDR method appears to achieve very good fits for CCP_5. The same is not observed for F_{aux} for cutting ages up to 50 years. Although from the consistency tests (Figs. 7.16(b, c)) the variations of both methods appear to be comparable, simple regression leads to unrealistic or even impossible results for several t_{cut} values up to 50 years. Furthermore, for t_{cut}>43 years, SSDR appears to have a very robust performance with a maximum variation of 22 years around the 'actual' value. For simple regression, the variation of age results exceeds 50 years (even for t_{cut}>70 years).

Figure 7.17 presents analogous consistency test results in the form of boxplots for various $F(t)$-values (from 10% to 99.9%). Hence, for each $F(t)$-value and for all t_{cut}-values considered, the variation of the bridge age to reach condition ≤7, ≤6 or ≤5 is illustrated. It is interesting to note that a non-symmetric distribution of age predictions is yielded for each $F(t)$-value. In general, a higher prediction variation is associated with a higher probability $F(t)$. Nevertheless, the selected t_{cut}-value does not seem to excessively influence the calculated age predictions for $F(t)$-values of practical interest (e.g. up to 90%). A direct comparison with the simple Weibull regression reveals that the SSDR method is more robust and leads to lower variation of results (especially to less distant outliers) with respect to t_{cut} values.

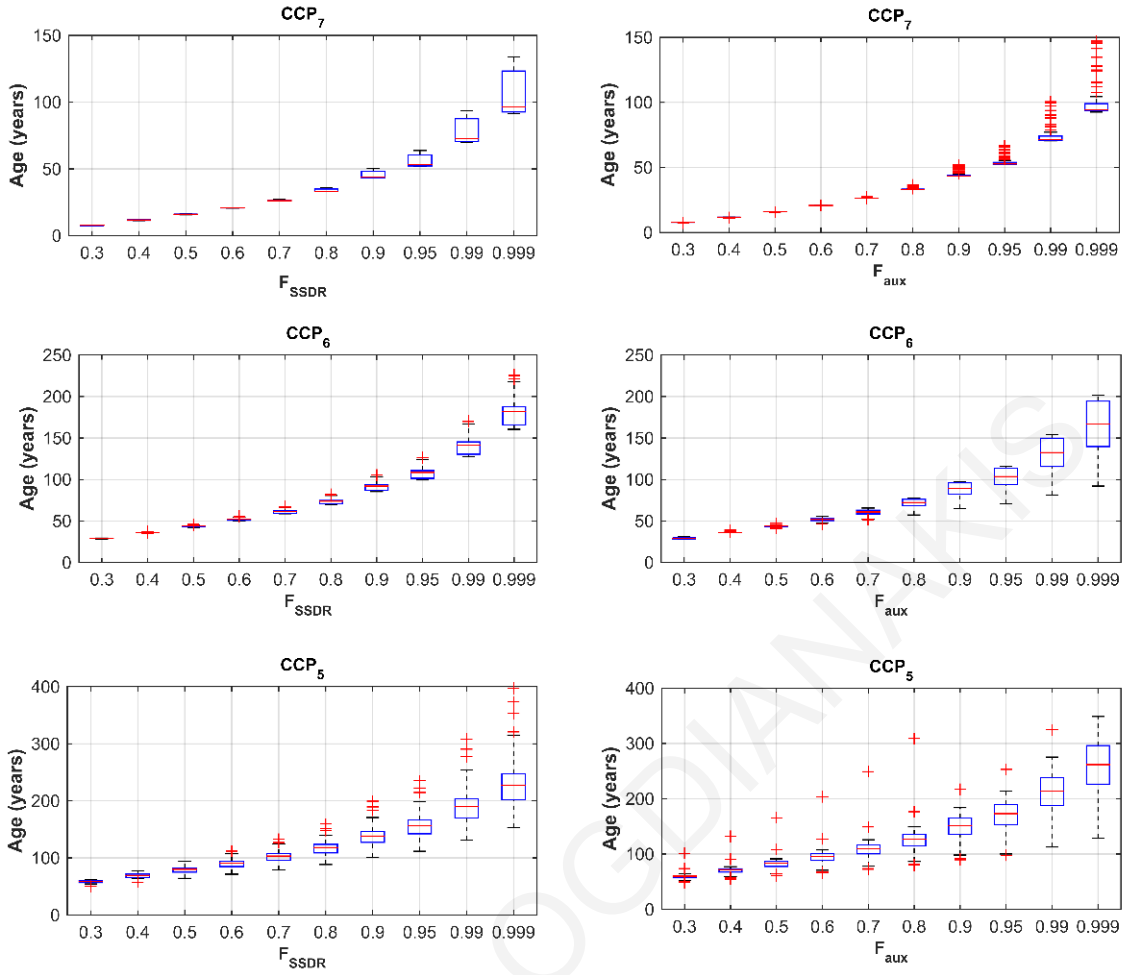

Figure 7.17: Multiple consistency tests for different values of probability F(t) for CCPs using the SSDR method (F_{SSDR}) and simple regression (F_{aux}).

7.5 Additional validation cases

In this section, two additional samples of concrete superstructures are used to validate the SSDR method. The first case refers to concrete continuous bridges in 'deicing, water' environment and the second concrete simple bridges in 'no deicing, water' environment. As noticed from the results of the first sample used for validation in the previous section (concrete simple bridges in 'deicing, water' environment), to be able to validate the predictions of the SSDR method, trusted data points have to exist above probability value 0.632, as the Weibull function produces more accurate results. Thus, for the case of concrete continuous bridges in 'deicing, water' environment, CCPs for conditions ≤7, ≤6 and ≤5 are presented (Figs. 7.18-20). For concrete simple bridges in 'no deicing, water' environment, only CCPs for conditions ≤7 and ≤6 are presented (Figs. 7.21 and 7.22), as probability values of CCP_5 did not reach the mentioned limit (0.632).

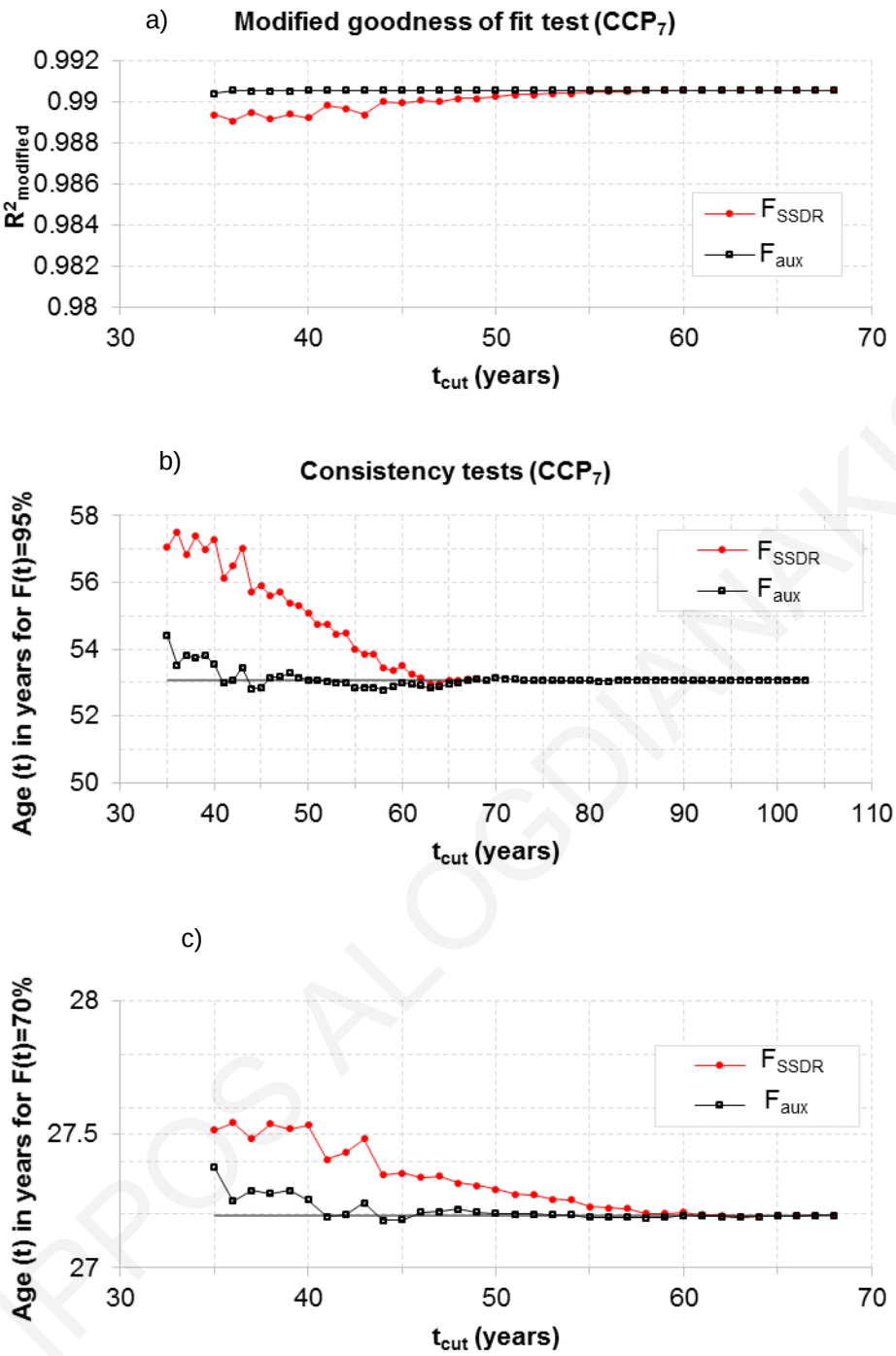

Figure 7.18: Validation results for CCP_7 for concrete continuous spans in 'deicing, water'" environment: modified goodness of fit test (a), consistency tests for F(t)=95% (b) and F(t)=70% (c).

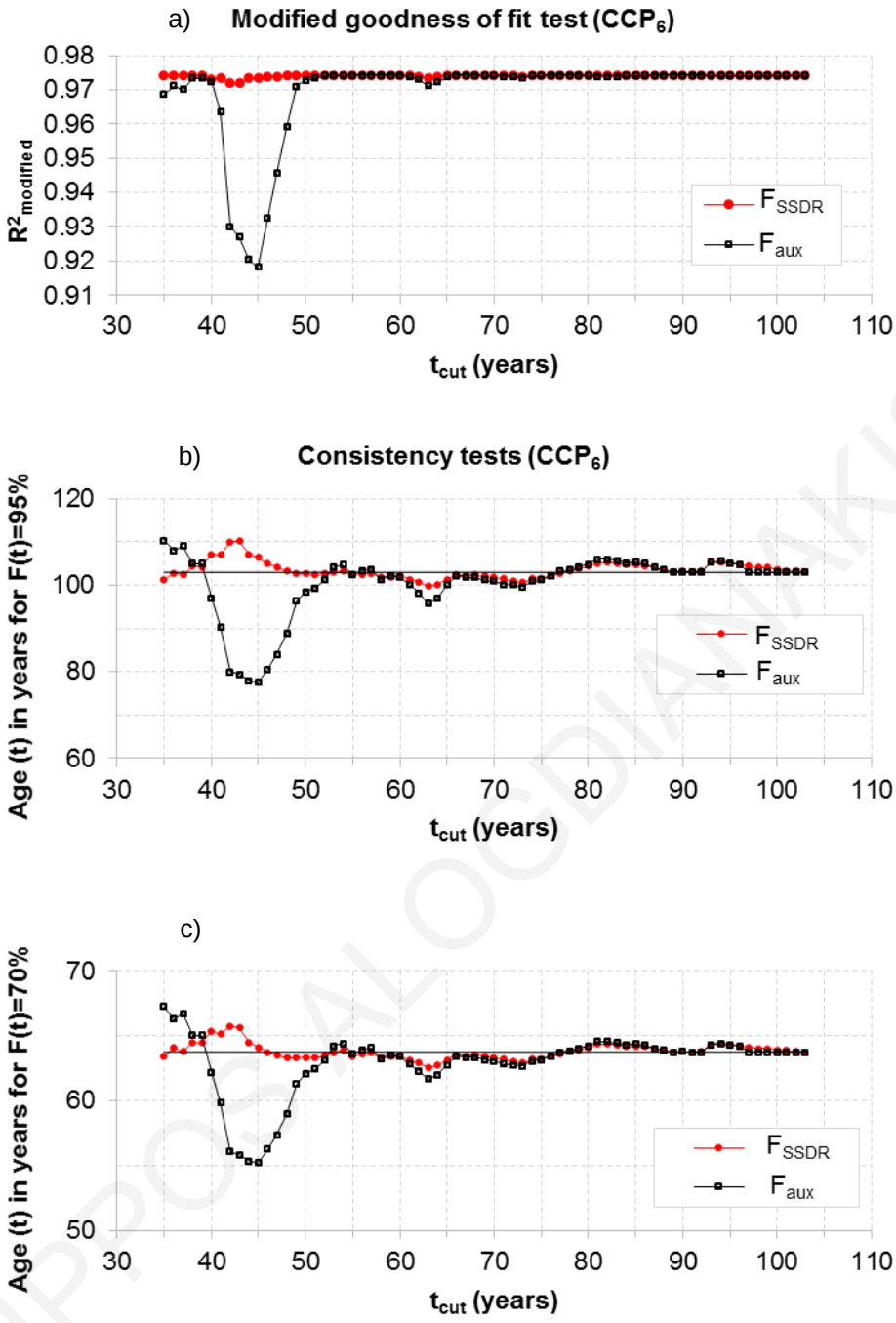

Figure 7.19: Validation results for CCP_6 for concrete continuous spans in 'deicing, water' environment: modified goodness of fit test (a), consistency tests for F(t)=95% (b) and F(t)=70% (c).

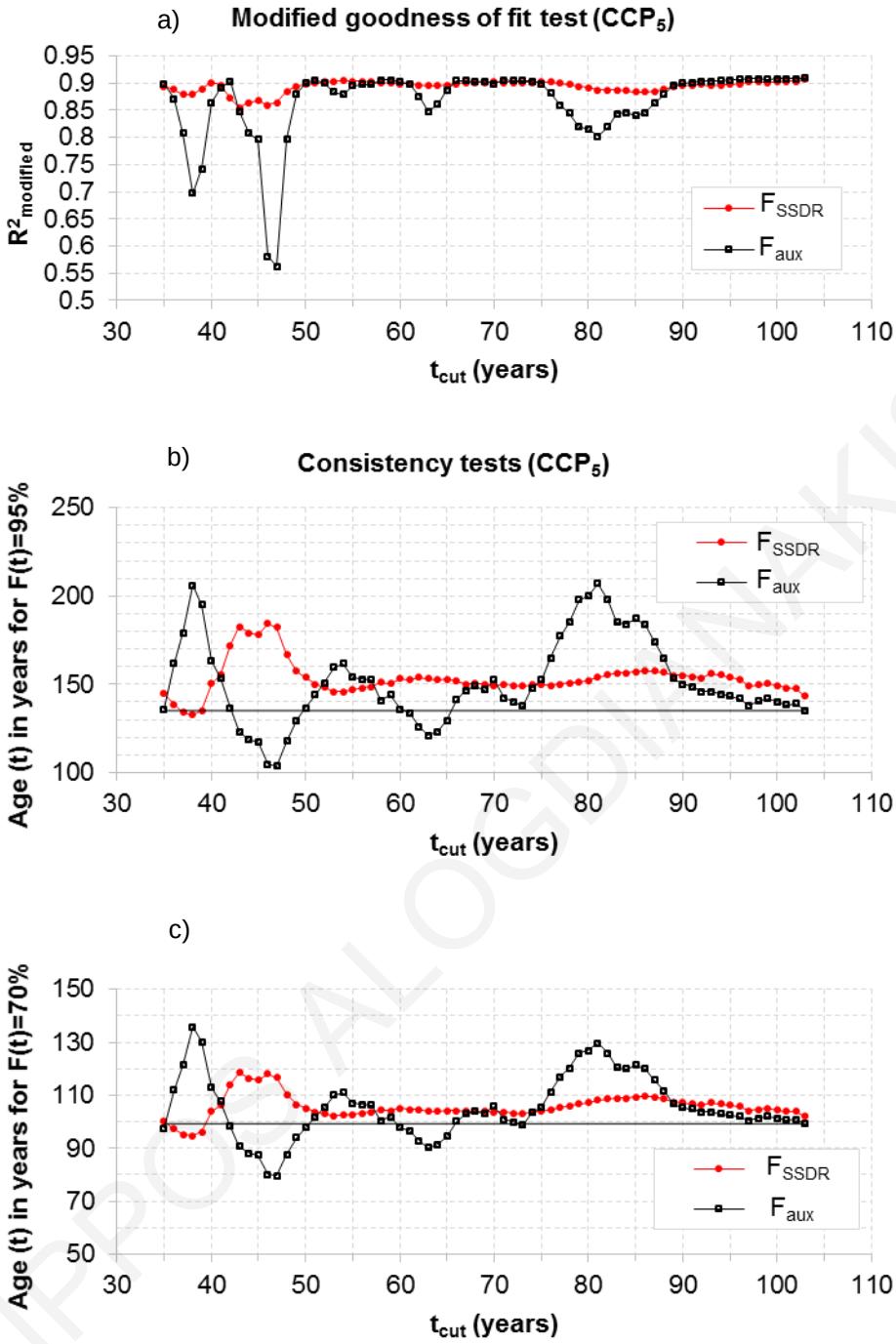

Figure 7.20: Validation results for CCP_5 for concrete continuous spans in 'deicing, water' environment: modified goodness of fit test (a), consistency tests for F(t)=95% (b) and F(t)=70% (c).

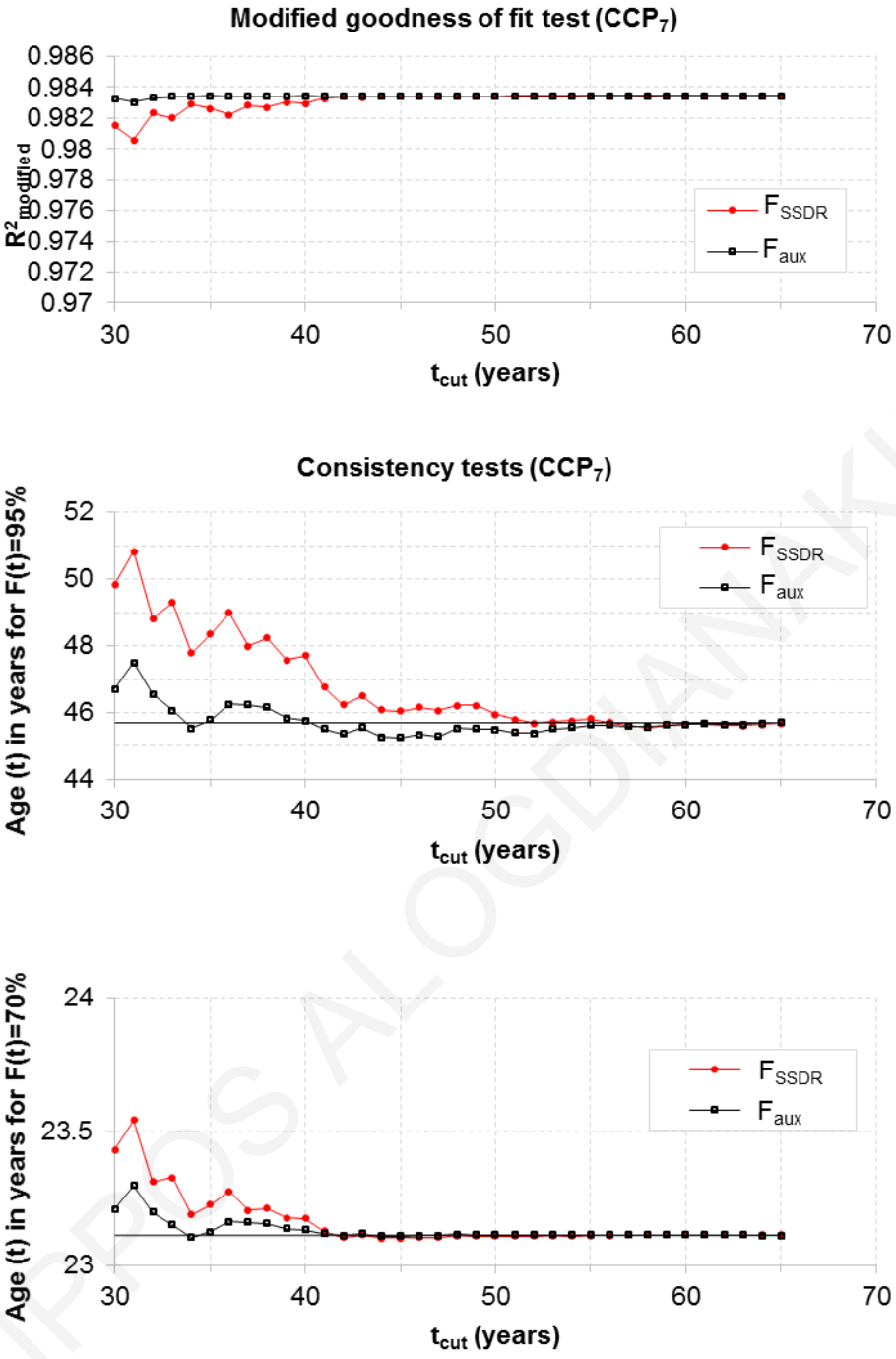

Figure 7.21: Validation results for CCP_7 for concrete simple spans in 'no deicing, water'" environment: modified goodness of fit test (a), consistency tests for F(t)=95% (b) and F(t)=70% (c).

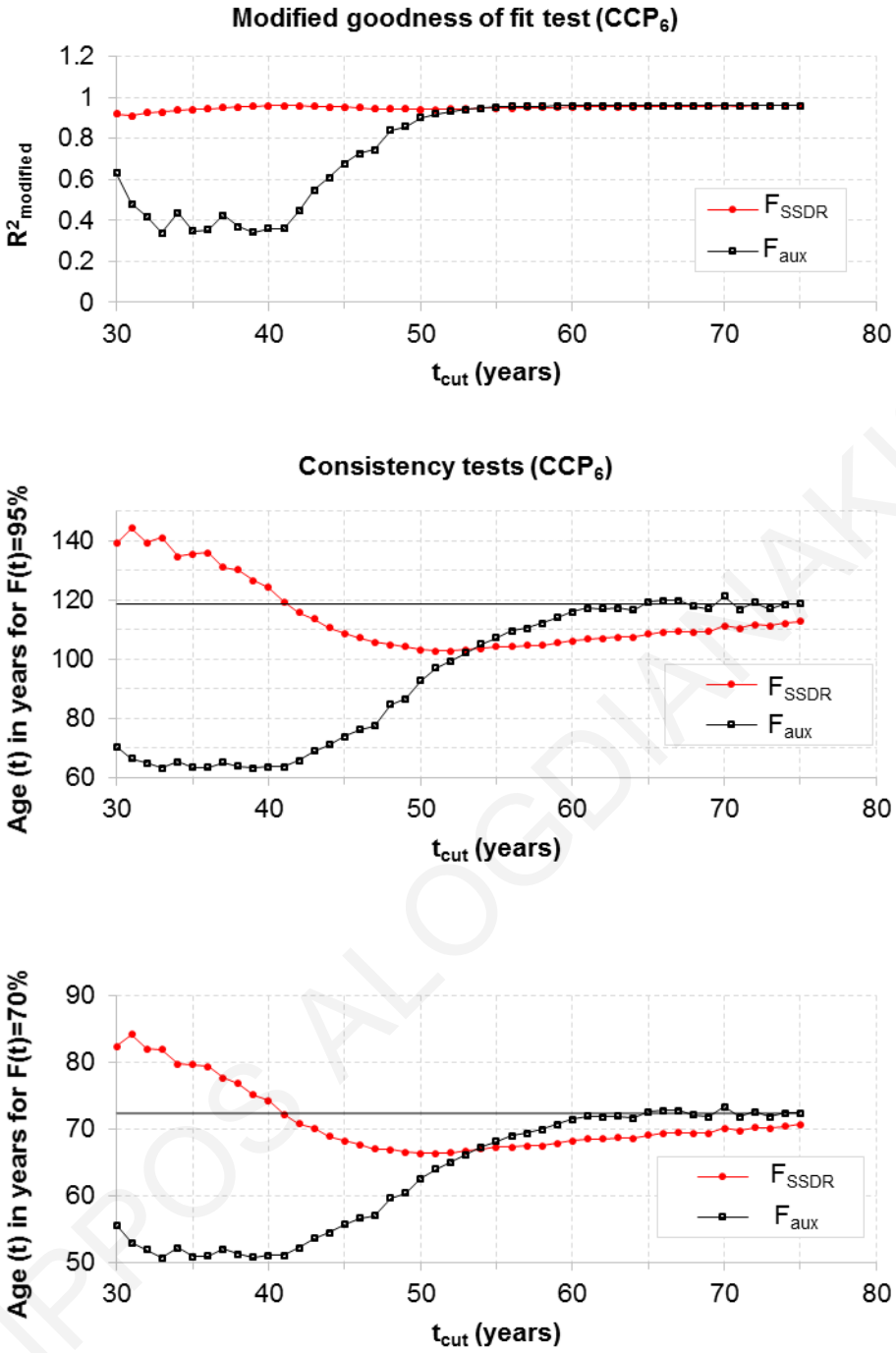

Figure 7.22: Validation results for CCP_6 for concrete simple spans in 'no deicing, water' environment: modified goodness of fit test (a), consistency tests for F(t)=95% (b) and F(t)=70% (c).

From the additional cases presented, analogous observations as in the previous section can be made regarding the performance of the SSDR method. Hence, when probability values above 0.632 have been reached, a simple Weibull regression (if this is the CDF followed by the data) is adequate; this is typically the case for CCP_7. If, however, lower probability values are reached due to unavailable data, the SSDR method is much more accurate and consistent than a simple regression.

7.6 Application of the SSDR method to other samples

The validated SSDR method was applied to other data samples for superstructures of various materials in 'deicing, water' environment and the results are presented in Table 7.3. For each case considered, the attained Weibull parameters of the CCP curves are given. The t_{cut} value denoted in each case indicates the size of the trusted sample utilized by the method. The separation of the probabilities of trusted years from those of untrusted years was determined where increased variations were observed. Attention was given to which data points are handled as outliers. Information that assisted in selecting t_{cut} values were:

i) the sample size at each particular age (increased variations were observed for low sample sizes);

ii) the probabilities of rehabilitation (PR) (see Chapter 6); increased probabilities of rehabilitation intensify the selection bias and produce misleadingly lower CCP-values due to the sample bridges in better condition that are kept for analysis;

iii) knowledge regarding changes to construction standards or practices for the material studied that could have affected its deterioration (see steel superstructures, Chapter 6).

Table 7.3: Attained Weibull fits utilizing the SSDR method for environmental exposure 'deicing, water'.

Materials & data used from sample (t_{cut})	CCP curve	Weibull Parameters		
		t_o	α	B
Steel Continuous Spans, t_{cut}=39 years	8	-0.59	1.89	0.52
	7	-0.80	20.10	1.06
	6	0	55.43	1.75
	5	0	103.2	2.05
Steel Simple Spans, t_{cut}=49 years	8	-2.28	3.03	0.66
	7	-4.49	21.67	1.00
	6	0	55.78	1.41
	5	0	100.66	1.87
Concrete Simple Spans, t_{cut}=98 years	8	-1.53	4.35	0.65
	7	-6.09	27.12	1.42
	6	0	55.40	1.55
	5	0	97.61	2.09
Concrete Continuous Spans, t_{cut}=89 years	8	-0.80	2.35	0.61
	7	-6.14	29.65	1.59
	6	0	57.80	1.90
	5	0	99.72	2.48
Prestressed concrete Simple Spans, t_{cut}=43 years	8	-1.26	2.37	0.53
	7	-3.96	30.44	1.14
	6	0	76.53	1.89
	5	0	105.30	2.53
Prestressed Concrete Continuous Spans, t_{cut}=41 years	8	-1,78	4.37	0.77
	7	-10.20	37.23	1.90
	6	0	55.44	1.92
	5	0	96.01	1.97

7.7 Probabilistic estimation of the time-to-rehabilitation

Using the SSDR method's final fit to the set of trusted CCP-points available for bridge condition ≤5, the time-to- rehabilitation can be probabilistically estimated. That is, any time-to-critical-condition given is accompanied by a probability for the bridge considered to have reached condition ≤5, which is assumed to induce the need for rehabilitation.

The Weibull CDF for bridge condition ≤5 (Table 7.2, Fig. 7.10) provides the sought probabilistic information for the time-to-rehabilitation of a concrete bridge exposed to deicing salts and humidity due to the presence of water underneath: by selecting a probability of reaching bridge condition ≤5, the respective time-to-critical-condition for the bridge is determined. Figure 7.23 and Table 7.4 give the time-to-rehabilitation for selected probability-values. Note that, as the term 'time-to- rehabilitation' is used herein, it counts from the year a bridge is built, i.e. this is the 'age-to-rehabilitation'. The actual time-to-critical-condition is easily calculated by subtracting the current age of a bridge from its 'age-to-rehabilitation'. Using such information, a decision maker can make a rational schedule for bridge rehabilitations, which takes into account not only available or anticipated funds, but also risks associated with the uncertain deterioration rate of bridges.

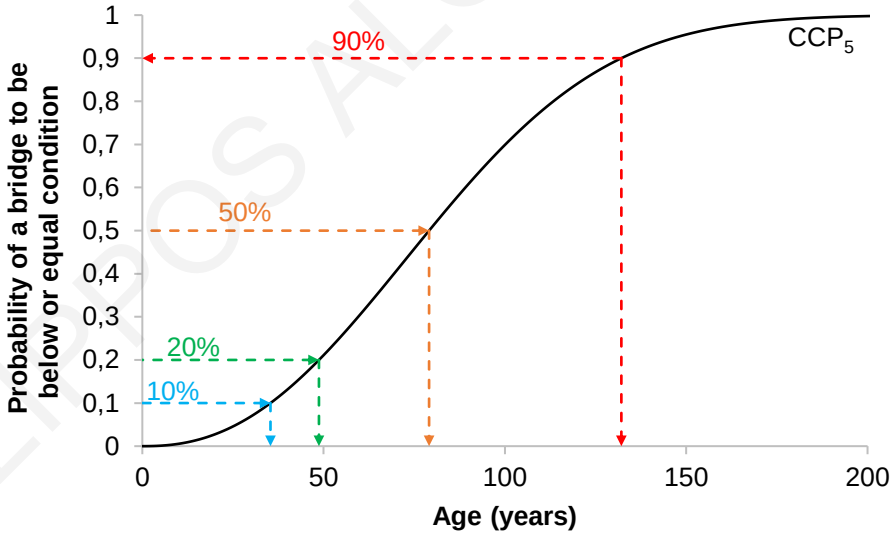

Figure 7.23: Estimation of age to rehabilitation for different levels of probability.

Table 7.4: Estimation of age-to-rehabilitation, values corresponding to Figure 7.22.

Probability	90%	50%	20%	10%
Age to rehabilitation	132	79	49	35

7.8 Conclusions

In this chapter, real condition data from the NBI database of USA' FHWA were utilized for predicting the deterioration rate of bridges. Specifically, probabilistic results were obtained for concrete bridges exposed to deicing salts and humidity that allow the quantitative estimation of the time-to-rehabilitation. To accomplish this task, a new method was presented for identifying a reliable probabilistic description of bridge deterioration over time. In general, small deviations between actual data and data predicted with the new method were observed for a large number of test configurations considered.

The new method utilizes only one year of inspection results to perform probabilistic predictions, whereas other methodologies utilize inspection results of many past years, which in many cases were proven to be unreliable. In contrast to other methodologies, a validation process was followed for the long-term prediction results of the SSDR, showing that the new method is robust. This was possible due to the use of one year of inspection results, the 'snapshot view' of deterioration and the new method's main assumption.

The procedure followed herein can be applied also to other types of bridges exposed to different environmental effects, provided that respective trusted data are available.

8 Scheduling bridge rehabilitations based on probabilistic structural condition model, risk attitude and life cycle cost

Being able to reliably assess and select among rehabilitation schedules for an aging bridge is a major issue in cost-effectively maintaining it in safe and operational condition. This task is seriously hindered by the high uncertainties that govern the deterioration rate over the lifetime of bridges. Work of previous chapters regarding segmented samples (chapter 6) and the method developed (chapter 6) are utilized in this chapter to provide a case study. Specifically, a simple-span concrete bridge in 'deicing, water' environment with certain life-cycle costs is supposed. The SSDR method is used to attain and extend the Weibull distributions that provide structural condition probabilities over the bridges lifetime. Based on these distributions, the risk attitude and preference of the decision maker, the time-to-rehabilitation can be probabilistically estimated and a respective rehabilitation schedule can be specified. In the framework of life cycle management of a bridge, various rehabilitation schedules are comparatively assessed with respect to the expected total rehabilitation cost induced, as well as the expected cost due to the possible need for bridge replacement.

8.1 Introduction

Aging bridges need continuous interventions either in the form of maintenance or major rehabilitation demanding vast budgets. Estimating the deterioration rate and the lifetime of bridges are essential aspects in determining optimal schedules, regarding maintenance and/or rehabilitation. Such information can greatly assist decision makers in both elongating the useful life of bridges and controlling their structural safety in a cost-effective manner. However, the structural performance of bridges in time is governed by high uncertainties, which need to be quantitatively treated, in order to be able to make rational predictions and decisions regarding any intervention. In this respect, various reliability and risk-based approaches have been developed, to effectively handle the process of deciding, under uncertainty, when to maintain/rehabilitate individual bridges or bridge components, bridge stocks/networks and infrastructure assets in general (e.g. Kleiner, 2001; Liu & Frangopol, 2006; Lounis & Daigle, 2008; Orcesi & Cremona, 2010; Orabi & El-Rayes, 2012; Frangopol & Bocchini, 2012; Salem et al., 2013; Saad et al., 2016; Tamvakis & Xenidis,2013; Xenidis & Angelides,2005; Xenidis & Stavrakas,2013;).

In the present chapter, the SSDR method is employed to estimate the future structural condition of a bridge taking into account uncertainty in its deterioration with time. Hence,

using real data maintained by the Federal Highway Administration (FHWA) for USA bridges, a macroscopic probabilistic model for the structural performance of an aging concrete bridge of simple spans exposed to deicing salts and elevated humidity is calibrated. This model is then exploited in the framework of life cycle management of the bridge. In particular, the required rehabilitations of the bridge within a span of 150 years are scheduled based on various attitudes of the decision maker toward risk. Following the risk preferences of the decision maker, risk-based cost estimations of the specified rehabilitation schedules are determined, which allow for objective comparative assessments.

8.2 Probabilistic model for life cycle structural condition of bridges

The focus herein is on concrete bridges deteriorating with age, e.g. due to corrosion. Deicing salts are known to accelerate deterioration, especially in combination with humidity (chapter 6). Thus, the segmented sample of chapter 6 containing 26,764 concrete bridges was utilized, which included age and structural condition data for all bridges at a particular inspection year.

The SSDR method uses NBI data of a single year to calibrate a probabilistic model for predicting the structural condition of a bridge over time. Thus, all bridges in the data-stock processed are used, based on their ages, to represent the condition of a single bridge during its lifetime. Hence, the portion of bridges being in a certain age and condition represent the probability of the bridge under study to be in the same condition at that age. This way, curves relating bridge age with cumulative probability for each structural condition can be assembled. Certain time-shifts and scalings are then applied to achieve predictions for bridge ages not covered by available data. By fitting Weibull distribution functions to the original and shifted data and specifying some criteria for deciding bridge rehabilitation, the time left for a bridge until it reaches a structural condition, that induces a need for rehabilitation, can be probabilistically evaluated.

The application of this method to the above described sample of 26,764 concrete bridges yields the macroscopic probabilistic deterioration model of Fig. 8.1. In this figure, Weibull curves relating bridge age with Cumulative Condition Probability (CCP) are provided. As an example of using the probabilistic model of Fig. 8.1, the age of a bridge with probability $P(\text{Condition}\leq 4)=0.2$ can be estimated from CCP_4 as 85.4 years.

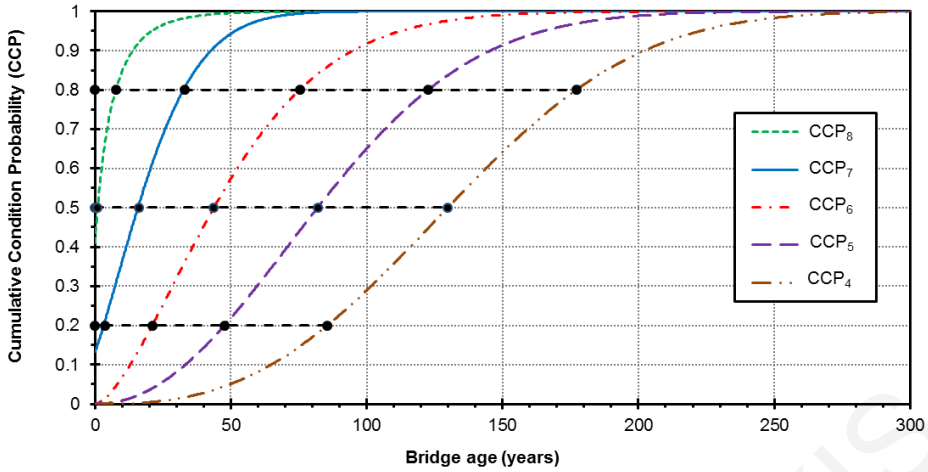

Figure 8.1: Probabilistic model for life cycle structural condition of concrete bridges exposed to deicing salts and elevated humidity: Cumulative Condition Probability (CCP) versus bridge age for structural conditions $\leq i$, i=8,7,6,5,4.

8.3 Life cycle management: scheduling bridge rehabilitations based on risk preference

The CCP-curves of Fig. 8.1 reveal the probabilistic deterioration rate of a bridge, as they provide the probability and the corresponding duration needed to reach each structural condition ≤8 to ≤4. This probability is a measure of uncertainty that can be taken into account when scheduling bridge rehabilitations. An example is given in this section to illustrate the exploitation of the probabilistic model of the previous section in life cycle management of bridges under uncertainty.

In this regard, certain assumptions are made. The initial structural condition of a bridge, from which it starts to deteriorate with time, is a crucial input information for a life cycle analysis. Bridges of the same age or era delivered may have a very different life cycle cost due to different initial structural conditions. To facilitate the demonstration of this section, an initial condition 9 (‘excellent’) is assumed for a hypothetical concrete bridge considered as an example. Moreover, a rehabilitation is assumed to fully restore the bridge in its initial state, i.e. condition 9 is reestablished. Hence, contractors and constructors perform any construction/rehabilitation phase with no flaws, while the duration of bridge construction/rehabilitation is ignored. Once the bridge is constructed/rehabilitated, successive condition drops occur as time passes: condition 8 succeeds 9, 7 succeeds 8, etc.

Three different CCP-levels (20%, 50% and 80%) are considered, which are assumed to represent the risk preferences resulting from the attitudes of 3 different decision makers toward risk (Hillson & Murray-Webster, 2005): from a risk-averse (CCP-level of 20%) to a risk-seeking (or risk-loving) preference (CCP-level of 80%). Table 8.1 presents 6 different

rehabilitation schedules based on these risk preferences. The time-to-rehabilitation reported is the duration for a bridge starting from condition 9 to reach structural conditions ≤5 or ≤4 for the 3 aforementioned CCP-levels and is easily determined from the Weibull curves of Figure 8.1. Hence, revisiting the example of the previous section for Figure 8.1, a bridge needs to be rehabilitated at the age of 85.4 years for a CCP-level of 20%.

Table 8.1: Time-to-rehabilitation and number of required rehabilitations within a span of 150 years for 6 different rehabilitation schedules corresponding to various probability (CCP) levels.

Rehabilitation schedule	Probability-level	Time-to-rehabilitation (years)	Required rehabilitations
1	$P(\text{Condition}\leq 4)=0.2$	85.4	1
2	$P(\text{Condition}\leq 5)=0.2$	47.6	3
3	$P(\text{Condition}\leq 4)=0.5$	129.8	1
4	$P(\text{Condition}\leq 5)=0.5$	81.9	1
5	$P(\text{Condition}\leq 4)=0.8$	177.1	0
6	$P(\text{Condition}\leq 5)=0.8$	122.6	1

Table 8.1 provides valuable for a decision maker probabilistic information regarding bridge deterioration with time. Hence, assuming that condition ≤5 (i.e. bridge condition is 'fair' or worse) signifies the need for rehabilitation, a risk averser would schedule an early intervention, at about 48 years after the construction of the bridge (although the probability that the bridge will actually reach condition ≤5 is only 20%). A risk seeker, on the other hand, would schedule a late upgrade, at about 123 years after construction, when the probability that the bridge will actually reach condition ≤5 is 80% and also the probability to reach condition ≤4 is relatively high (>40%). A decision maker with a more balanced attitude toward risk (CCP-level of 50%) would schedule an upgrade at about 82 years after bridge construction. If it is assumed that condition ≤4 (i.e. bridge condition is 'poor' or worse) induces the need for rehabilitation, longer times can be tolerated before any intervention takes place. Thus, rehabilitation would be scheduled at the bridge age of about 85 years by a risk averser, 177 years by a risk seeker and 130 years by a decision maker exhibiting an intermediate risk tolerance.

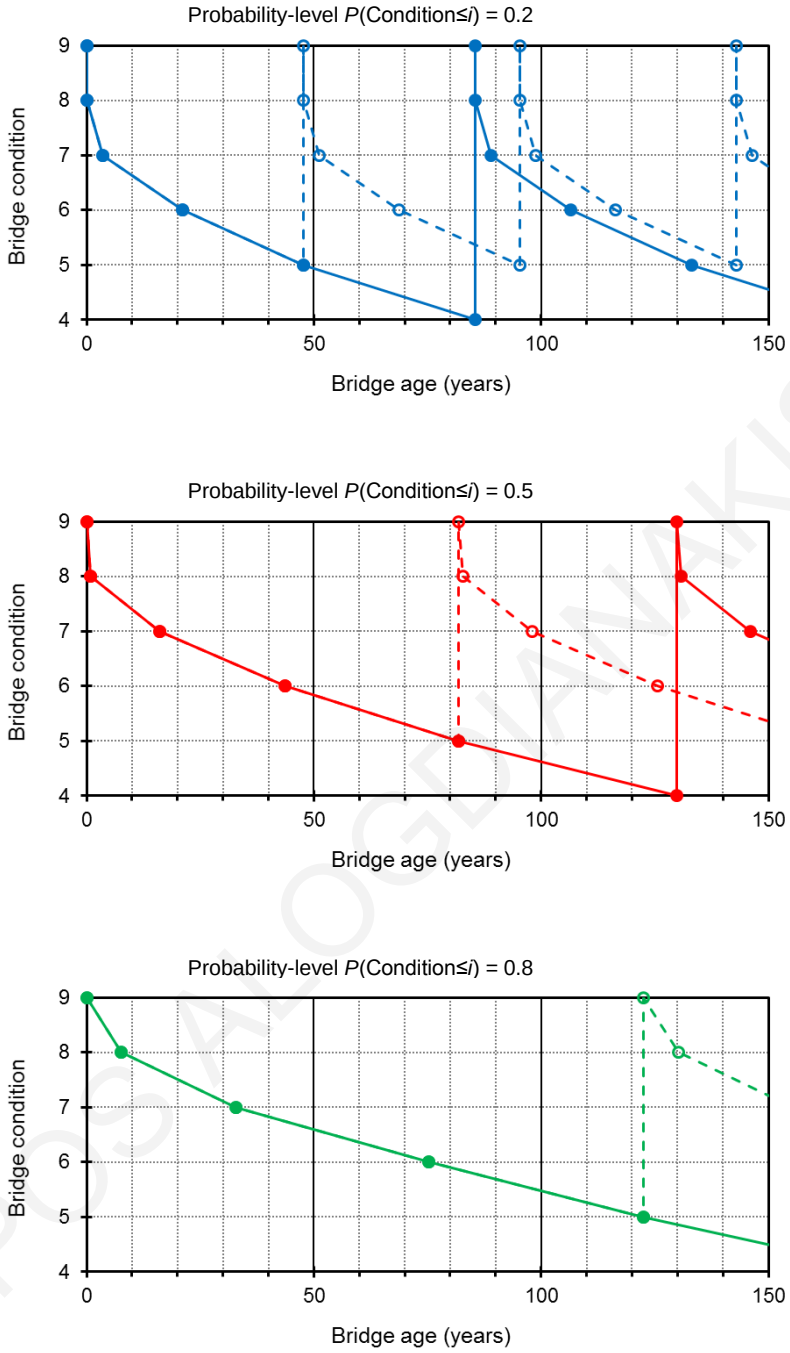

Figure 8.2: Life cycle management for a bridge considering 3 different risk attitudes corresponding to probability-levels $P(\text{Condition} \leq i)$ = 20%, 50% and 80% (i=8,7,6,5 or 4). Rehabilitation takes place when the bridge is expected to reach condition ≤4 (solid lines) or ≤5 (dashed lines) for each probability-level considered.

Figure 8.2 illustrates the effect of the 3 risk attitudes in the context of life cycle management for maintaining a bridge in good and operational condition by scheduling regular interventions. In this figure, we consider a newly constructed bridge that is delivered at age 0 in excellent condition (code 9) and starts deteriorating. Depending on the CCP-level adopted, successive condition drops are predicted at certain bridge ages determined through

the CCP-curves of Fig. 8.1. A rehabilitation is scheduled at the age the bridge is predicted to reach condition ≤5 or ≤4 for the particular CCP-level (Table 8.1). It is assumed that a rehabilitation fully restores the bridge condition to code 9. Then, deterioration starts again, which causes once more successive condition drops that may lead to a new rehabilitation according to the respective time of Table 8.1 and so on. The same risk preference of the decision maker is presumed for the life cycle of the bridge, i.e. the adopted CCP-level remains unaltered.

According to the life cycle setting specified above, a series of bridge rehabilitations need to be scheduled within a certain time frame (indicatively taken herein as 150 years), depending on the CCP-level adopted. This results in the 6 aforementioned schedules with required rehabilitations that are evident in Fig. 8.2 and summed up in Table 8.1.

Hence, assuming that any interventions are decided by monitoring the event of the bridge condition being ≤5, a risk averser (CCP-level of 20%) would schedule 3 rehabilitations within 150 years, because a rehabilitation is required every about 48 years. Accordingly, a risk seeker (CCP-level of 80%) would schedule just one rehabilitation at the age of about 123 years, while the intermediate risk preference (CCP-level of 50%) induces the need for 1 rehabilitations within 150 years (every about 82 years). If the event of the bridge condition being ≤4 would shape the decision for rehabilitation, a risk seeker would not schedule any intervention within 150 years. A risk averser, however, would still schedule 1 rehabilitations within this time frame (every about 85.4 years), while the intermediate risk preference would lead to a single rehabilitation at the age of about 114 years.

A small number of upgrades over the life cycle of the bridge translates to a low overall anticipated rehabilitation cost, but also to a high risk associated with the bridge condition reaching code 5 or 4 earlier than expected or even dropping below it. This could induce additional, non-scheduled direct and indirect costs, compromise the safety and operational availability of the bridge and possibly force decision makers to partially or even fully replace it. Such issues are further investigated in the next section.

8.4 Expected life cycle cost estimation and comparative assessment of rehabilitation schedules

In order to be able to make a rational decision regarding the most favourable rehabilitation schedule of a bridge, the expected total cost over the time frame of study needs to be estimated for every choice identified. Thus, an overall rehabilitation cost is calculated

for each schedule specified in Table 8.1 by taking into account the number of interventions planned and the bridge ages, at which they are intended to take place (Fig. 8.2). Moreover, an overall expected cost for bridge replacement is determined, which refers to the risk of the bridge dropping to such a condition that rehabilitation is not a suitable choice anymore. Replacement of the bridge may be dictated by extensive failure that renders uneconomical the repairs required, partial/full collapse, dropping of the safety level provided below an acceptable/tolerable threshold, etc.

The initial cost to construct at time t=0 the hypothetical concrete bridge studied in the present work is designated as C_0. All costs given in this section are expressed with respect to the initial cost C_0. Using the study of (Ehlen, 1997), the fraction of rehabilitation cost of superstructure elements was estimated and attributed to the cost of restoring to condition 9 from condition 5 (C_{R5}=0.4C_0). As this cost included both construction and user costs (due to delays, increased travel expenses, increased accident rates, inconvenience, etc.), the corresponding cost allocations were estimated from the same study (Ehlen, 1997). Thus, lower construction costs would be anticipated for restoring from higher condition ratings and user costs would be assumed negligible, while for lower conditions increased user and construction costs would be assumed. Moreover, regarding higher superstructure conditions, rational fractions were estimated for restoring to condition 9 by considering the unit cost estimates of Pontis BMS studies (Adams & Juni, 2003; Milligan, et al., 2006). Hence, the cost of rehabilitation (i.e. of restoring condition 9) from condition 8 is taken herein as C_{R8}=0.005C_0. Accordingly, the rehabilitation costs from conditions 7, 6, 5, ≤4 are set to C_{R7}=0.01C_0, C_{R6}=0.03C_0, C_{R5}=0.1C_0, C_{R4}=0.4C_0, respectively. It is assumed that a rehabilitation from conditions 5 and ≤4 is also associated with user costs because of works needing the bridge to be closed for 0.1 and 0.5 months, respectively. User costs during rehabilitation are taken as 3C_0 per month of bridge closure. Thus, the costs for rehabilitation from conditions 5 and ≤4 are increased to C_{R5}=0.4C_0 and C_{R4}=1.9C_0, respectively. The expected rehabilitation cost of the bridge at time t is then given by:

$$C_{Reh}(t)=\sum_i [P(\text{Condition}=i)\times C_{Ri}]+P(\text{Condition}\leq 4)\times C_{R4},\ i=8,7,6,5. \qquad (8.1)$$

The probabilities P(Condition=i) with time are given in Fig. 8.3. These are easily calculated from the probabilities P(Condition≤i) of Figure 8.1, e.g. P(Condition=7)=P(Condition≤7)-P(Condition≤6) at any age t.

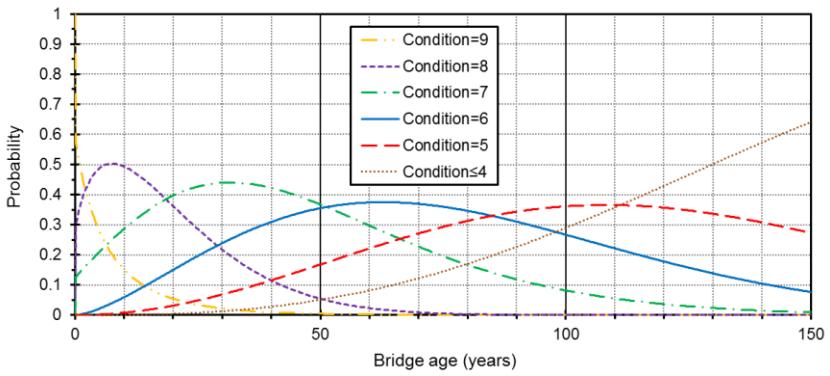

Figure 8.3: Probabilities $P(\text{Condition}=i)$, i=9,8,7,6,5, and $P(\text{Condition}\leq 4)$ versus bridge age.

The bridge replacement cost at any time t is taken as $1.2C_0$. This includes the amount of $0.2C_0$ for the removal of the old bridge (Ehlen, 1997), as well as the amount of C_0 for the construction of the new one. It is assumed that all replacement actions (removal of old bridge, establishment of detour, design/bidding/construction of new bridge, etc.) are carried out within 12 months, during which the bridge is closed. User costs during replacement works are taken as $5C_0$ per month of bridge closure. This results in a total replacement cost at time t of $61.2C_0$. Due to lack of data, it is simply assumed that the replacement probability at any time t is $P_{\text{Rep}}=0.2\times P(\text{Condition}\leq 4)$. Then, the expected replacement cost of the bridge at time t is given by $C_{\text{Rep}}(t)=P_{\text{Rep}}\times 61.2C_0$.

The above-mentioned costs $C_{\text{Reh}}(t)$ and $C_{\text{Rep}}(t)$ refer to Future Values (FV), since these are costs to be paid at various instances t within the period of study (150 years). Any FV at time t can be transferred to time t=0 by discounting it to the corresponding Present Value (PV) according to the formula: $\text{PV}=\text{FV}/(1+r)^t$, where r is the discount rate adopted (assumed to remain constant over the period of study).

Assuming 4 different discount rates, Fig. 8.4 presents the total expected cost of each of the 6 rehabilitation schedules for the period of 150 years. This cost includes the total expected rehabilitation cost of each schedule, which is calculated as $PV[C_{Reh}(t_1)]+PV[C_{Reh}(t_2)]+\ldots$ for the planned rehabilitations at bridge ages $t_1,t_2,\ldots$ according to this schedule. The total expected cost includes also the expected replacement cost, which is set as the average over all years $0\leq t\leq 150$ of the costs $PV[C_{Rep}(t)]$.

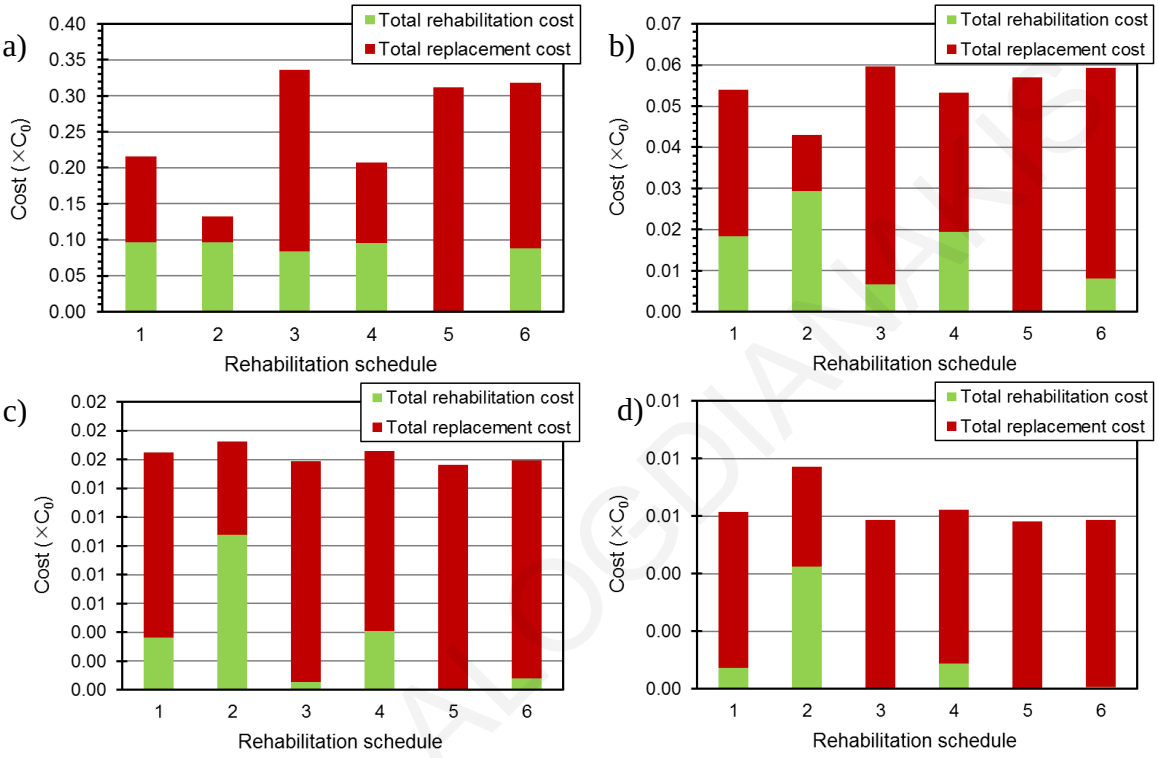

Figure 8.4: Total expected cost and its allocation to expected rehabilitation and replacement costs for the 6 bridge rehabilitation schedules, considering a discount rate of a) r=2%, b) r=4%, c) r=6% and d) r=8% (bottom).

Figure 8.4 demonstrates the interplay between the contributions of the rehabilitation and replacement costs in the total life cycle cost. The overall cost resulting from a schedule with frequent rehabilitations (e.g. schedule 2), which is typically adopted by a risk averser, is clearly governed by rehabilitation costs. On the other hand, expected replacement costs are the major concern in case of infrequent or no rehabilitations (e.g. schedules 5, 6) in the framework of risk seeking decisions regarding the life cycle management of the bridge. The discount rate considered decisively influences the cost-effectiveness and the comparative assessment of the rehabilitation schedules and actually dictates the choice to make.

8.5 Conclusions

Scheduling rehabilitations for an aging bridge within a highly uncertain deterioration setting in a cost-effective manner is a great challenge. Rational decisions can be made by, first of all, acquiring probabilistic data regarding the deterioration rate and the failure potential of the bridge. Then, any rehabilitation schedule can be quantitatively assessed with respect to the expected life cycle cost it induces. In this respect, the gathering and estimation of reliable economic data (mainly including rehabilitation, replacement and user costs, as well as the discount rate) and the risk preference of the decision maker are crucial aspects. Hence, the process of life cycle cost assessment and management of a deteriorating bridge may be cumbersome and demanding, but it is an essential step toward the effective handling of highly important bridge stocks and networks.

9 Concluding remarks and future work

This chapter presents the Thesis's main contribution to research and discusses its transferability. The main assumptions adopted in the study are summarized, as well as the concluding remarks of each Chapter. In the end, suggestions for future work and research plans are presented.

9.1 Main contribution to research

In this thesis, a data-driven approach was developed exploiting bridge inspection data, through which the following main contributions were made:

- the predominant deterioration factors for bridge components were identified,
- the qualitative and quantitative effects of bridge deterioration factors were determined and
- a novel method for probabilistic prediction of bridge deterioration with time was developed and validated.

9.2 Transferability

The US inventory was utilized for achieving the Thesis objectives due to its public disclosure and the unavailability of similar inventories from other countries. Additionally, utilizing bridges located in the US provided adequate data to model deterioration for different types of exposures. This is due to the large sample of bridges available, as well as the variety of the deterioration factors existing in the US territory. This section presents the transferability of the study's framework and results for cases, where many bridges exist with inspection records containing similar information, as well as for cases with small number of bridges and inadequate or even no data.

9.2.1 Application to other inventories

The SSDR method can be applied to inventories of other countries, which also use condition ratings, even in different scales. To do so, the whole framework of the study should be followed, identifying the predominant factors of deterioration and then calculating the probabilities corresponding to bridge ages.

Although a large initial sample was used in this study, many different factors existed within the US territory, which lead to certain segmentations. Hence, due to segmentations performed, the initial 615.000 records could not be used as one sample, therefore the method was developed and validated using 4% of the initial sample (25500 bridges with age range

of 116 years). The validation process showed that robust predictions can be achieved utilizing much smaller age ranges (minimum 0-35 years), corresponding to only 1.2% of the whole sample (7500). Furthermore, it is not essential to utilize successive ages, if the probabilities calculated have large variations among them due to low sample sizes.

9.2.2 Application of deterioration curves to countries with small samples

This work's framework utilizes independent probabilities calculated for each age, disengaging deterioration from the number of bridges existing at that particular age (stock). Thus, the CDFs derived for various environments and materials are transferable. Hence, in cases where only a small number of bridges with similar exposures exist in a country, the corresponding deterioration curve derived from the US inventory can be utilized. It is worth mentioning that such application should be performed after considering differences regarding design standards and material properties.

9.3 Main assumptions of the study

The National Bridge Inventory of the US was utilized to conduct a macroscopic study of bridge deterioration within different environmental exposures. The Thesis was conducted in a number stages, starting with a data analysis process to determine the predominant environmental effects, then probabilities were utilized to compare the performance of different environments and a novel method was developed to utilize the former probabilities and perform predictions for future years. To meet these objectives, certain assumptions had to be made, specifically:

- Bridge condition evaluations are regarded as being hazard-driven rather than State-dependent (chapter 4).
- Rehabilitated bridges had to be excluded due to missing information regarding material switch and condition rating prior to rehabilitation (Chapter 6).
- The calculated probabilities of the bridge stock studied, arranged based on the age of each bridge, represent the probabilities of one bridge to be in a specific condition at various ages (Chapter 7).

Each of these assumptions is adopted in the mentioned chapter and applies for the rest of the study.

It is also important to bear in mind that an updated database should be used to incorporate important technological and/or constructional changes or significant changes in inspection standards that could affect the condition ratings. Such updates are not expected to be required every few years, as the methodologies applied combined with the type and

amount of exploited data produced results that were found to be relatively insensitive to data changes with time.

9.4 Summary of conclusions

Based on the analyses performed and the results obtained, the following macroscopic remarks can be made:

- The NBI, which included the 2016 inspection recordings, was used, as it provided the most recent and most accurate inventory of the US. In the study, results of 2016 inspections were checked for their consistency to earlier years and were found to have small differences. Thus, studying one inventory using the 'snapshot view' can be regarded as a robust way of analysis to attain macroscopic information for the bridge sample.
- The data analysis process revealed that the most significant factor linked to structural condition and deterioration is the age of the structure. The structural material of superstructures and decks significantly affect the corresponding condition ratings, while geometric variables, such as length, maximum span and deck width, seem to play a less significant role. Average daily traffic and average daily truck traffic also appeared to have a small effect on all condition ratings.
- Using the bridge coordinates provided in NBI and information from the weather stations and from the US geological survey, weather and earthquake variables were introduced. Among them, peak ground acceleration appeared to have a predominant meliorating effect on all structural condition ratings, mostly for superstructures and substructures. The deicing region, water underneath the bridge and annual precipitation also appear to have a significant decreasing effect in condition ratings.
- The effect of airborne chlorides was studied utilizing increments of bridge distance away from the coast. Sample segmentations were performed based on the predominant effects within the coastline. For the locations of low earthquake hazard and no deicing, distances up to 2km showed to be affected. This effect was noticed to be extended up to 1km inland for the case of low elevations and the formation of a peninsula (Florida). On the other hand, the places where deicing policies are used, the airborne chlorides appear to affect distances up to 1km away from the coast. This difference could be attributed to the fact that chloride deposition in north areas is more affected by the deicing procedures. High earthquake hazard areas could not be analyzed due to variations in year of construction/reconstruction content, but similar limits of the coastline can be anticipated.

- Segmentations of the initial sample were performed and probabilities were calculated to compare the performance of decks, superstructures and substructures in different environments.
- For Concrete decks, deicing appeared to be the most corrosive factor. The existence of joints in deicing environment affected more the structural condition of the deck in younger ages, while the same did not apply for the case of continuous spans. Absence of structural joints lowered probabilities of deterioration for deicing environments, but increased the probability of deterioration for warmer environments.
- For substructures, environments, where no deicing is used and water is present, have the highest deterioration probabilities, followed by environments where deicing is used regardless of water presence. The presence of structural joints in simple spans increases the probabilities of deterioration for all environments, while deicing environments affect younger ages.
- For superstructure materials, similar probabilities were noticed for the same environmental exposures and span types (simple or continuous). A closer look at the results indicated a better performance of prestressed concrete, followed by concrete and steel. An exception is the case of steel in environment of water and no deicing for both span types, where increased deterioration can be observed.
- Concrete superstructures are affected more by deicing environments in young ages, when also water is underneath for simple spans. Although continuous spans have lower probabilities of deterioration and are affected more by deicing salts, younger ages are affected more by traffic presence in areas where deicing are used.
- Steel superstructures are substantially deteriorating at humid environments without deicing sources. Lower deterioration probabilities were noticed at deicing environments regardless of water presence. The presence of structural joints to form simple spans increased the probabilities of deterioration compared to the other environmental exposures. Especially young simple span bridges are vulnerable under humid and deicing conditions.
- Prestressed concrete superstructures are affected by deicing environments similarly to concrete. The main difference is the lack of early deterioration for simple span bridges in the simultaneous presence of water underneath and deicing. But early deterioration was noticed, similarly to RC-bridges, in areas where deicing is used and traffic exists under the bridge.

- Absence of structural joints in integral bridges performs well in the superstructure, but may be problematic for the decks.
- A novel method was developed and validated appropriately to probabilistically estimate the deterioration rate and the time-to-rehabilitation of aging bridges. The method utilized cumulative condition probabilities of segmented samples and techniques used in accelerated experiments were modified to perform forecasts. The method was found to have small prediction errors and performed well, even under rather limited data availability.
- The method was applied for different materials on a selected environmental exposure and was utilized in a decision-making process regarding scheduling rehabilitation for a concrete bridge.

9.5 Future research

This work included a variety of factors which could affect structural deterioration of superstructures, substructures and decks. Additional sources of deterioration could be also investigated, such as drought, CO_2/SO_2 and other emissions related to atmospheric pollution for the structural parts studied. Furthermore, other segmentations could be performed to investigate the probabilities of non-satisfactory condition, such as the case of annual precipitation.

Additional data analysis processes such as Cox Regression can be utilized to analyze the factors affecting deterioration and cluster analysis could be performed to investigate the State effect. Also, following the same framework, other available ratings, such as the ones concerning scour, could be utilized to identify their predominant deterioration factors, segment samples and perform predictions.

The new SSDR method can be applied to the rest of the segmented samples of this work. Additional effort may be required to tackle extremely low sample sizes for specific ages, such as the case of the coastline. Moreover, the method can be applied to a generalized local level, where no organized inventory existed and efforts are currently made to do so. Such is the case of the East Mediterranean area, including Cyprus. On the other hand, the method can be applied at a European level, where inspection records existed, but homogenization of inspections is currently on the verge and the goal of COST action TU-1406, which is funded by the European Union.

The SSDR method could be applied to accelerated creep experiments instead of utilizing the log-shifting of the Arhenius model, which may render more optimistic results. This model is applicable also in other applications of deteriorating infrastructure, like in

pavements, water/gas supply networks, etc. Furthermore, the method could also be utilized to complete cumulative condition probabilities and calibrate a Markov chain, which could be used for comparisons with other models. An additional application of such model could be the use of the derived distribution as a prior, which is to be updated with the additional collected data.

References

Adarkwa, O. & Attoh-Okine, N., 2016. Prediction of structural deficiency ratio of bridges based on multiway data factorization. *ASCE-ASME Journal of Risk and Uncertainty in Engineering Systems, Part A: Civil Engineering,* December, 2(4), pp. F4016002-(1:7).

Adams, T. M. & Juni, E., 2003. *Element unit and failure costs and functional improvement costs for use in the Mn/DOT Pontis Bridge Management System,* St. Paul: Minnesota Department of Transportation.

Abernethy, R. B. (2000). The New Weibull Handbook. (4th ed.) Florida, US: A.B. Abernethy.

Agrawal, A. K., Xu, X. & Chen, Z., 2011. *Bridge-Vehicle Impact Assessment,* New York: New York State Department of Transportation.

Agrawal, A.K., Kawaguchi, A., Chen, Z. 2010. Deterioration rates of typical bridge elements in New York. *ASCE Journal of Bridge Engineering* 15:419-429.

Ainge, Steven W., 2012 *Repair and Strengthening of Bridge Substructures*. Master's Theses. Paper 173.

Alhozaimy, A., Hussain, R. R., Al-Zaid, R. & Al-Neghe, A., 2012. Coupled effect of ambient high relative humidity and varying temperature marine environment on corrosion of reinforced concrete. *Elsevier: Construction and Building Materials,* Volume 28, pp. 670–679.

Alwis, K. B. C., 2006. Time-temperature superposition to determine the stress rupture of aramid fibres. *Journal of Materials Science,* pp. Vol 13, 249-264.

Ambler, H. R. & Bain, A. A., 1955. Corrosion of metals in the tropics. *Journal of Applied Chemistry,* Volume 5, pp. 437-467.

Andric, J. M. & Lu, D.-G., 2016. Risk assessment of bridges under multiple hazards in operation period. Elsevier: Safety Science, Volume 83, pp. 80–92.

Angst, U. M. & Elsener, B., 2017. The size effect in corrosion greatly influences the predicted lifespan of concrete infrastructure. *Science advances,* Volume 3, pp. e1700751 (1-8).

Angst, U. M., 2018. Challenges and opportunities in corrosion of steel in concrete. *Materials and structures,* 51(4), pp. 1-20.

ASCE, 2017. *Infrastructure Report Card.* [Online]
Available at:
https://www.infrastructurereportcard.org/wpcontent/uploads/2017/01/Bridges-Final.pdf. Accessed [3-7-2018].

ASCE. 2010. *Minimum Design Loads for Buildings and Other Structures*. ASCE/SEI Standard 7-10.

Avramenko, Y., Nystrom, L. & Kraslawsk, A., 2002. Selection of internals for reactive distillation column - Case-based Reasoning approach. Elsevier Science: European Symposium on Computer Aided Process Engineering - 12 , pp. 157-162.

Azizinamini, A. et al., 2014. *Design Guide for Bridges for Service Life*. Washington D.C.: Transportation Research Board.

Bagdonavicius, V. & Nikulin, M., 2002. *Accelerated life models (modeling and statistical analysis).* Boca Raton London, US: Chapman & Hall/CRC.

Balafas, I. & Burgoyne, C. J., 2010. Environmental effects on cover cracking due to corrosion. *Cement and concrete research*, 40(9), pp. 1429-1440.

Balafas, I., 2003. *Fibre-reinforced-polymers vs Steel in Concrete Bridges: Structural Design and Economic Viability*. PhD thesis, University of Cambridge.

Baron, R. M. & Kenny, D. A., 1986. The moderator-mediator variable distinction in social psychological research: Conceptual, strategic, and statistical considerations. *Journal of personality and social psychology,* Volume 51, pp. 1173-1182.

Bentur, A., Diamond, S. & Berke, N. S., 1997. *Steel corrosion in concrete.* London: E&FN Spon.

Bertolini, L., Elsener, B., Radaeli, E. & Polder, R., 2013. *Corrosion of steel in concrete (prevension, diagnosis, repair).* 2nd ed. Weinheim, Germany: Wiley-VCH Verlag GmbH & Co. KGaA.

Biau, D. J., Jolles, B. M. & Porcher, R., 2009. p value and the theory of hypothesis testing: An explanation for new Researchers. *Clinical Orthopedics and Related Research Springer,* Issue 468, p. 885–892.

Billington, P. N., Billington, D. P. & Shirley-Smith, H., 2017. *Encyclopedia Britannica.* [Online] https://www.britannica.com/. Accessed [3-7-2018].

Blanchard, D. C. & Woodcock, A. H., 1980. The production, concentration and vertical distribution of the seasalt aerosol. *Annals New York Academy of Sciences,* Volume 338, pp. 330-347.

Bolukbasi, M., Mohammadi, J. & Arditi, D., 2004. Estimating the Future Condition of Highway Bridge Components Using National Bridge Inventory Data. *Practice Periodical on Structural Design and Construction*, 9(1), pp.16–25.

Bolukbasi, M.M., Arditi, D. & Mohammadi, J., 2006. Deterioration of reconstructed bridge decks. *Structure and Infrastructure Engineering*, 2(1), pp.23–31.

Broomfield, J. P., 2007. *Corrosion of steel in concrete.* 2nd ed. Oxon, UK: Taylor & Francis.

Brown, E. et al., 1995. *Seawater: its composition, properties and behavior.* Oxford, UK: Pergamon.

Bu, G.P. et al., 2014. Prediction of Long-Term Bridge Performance: An Integrated Deterioration Approach with Case Studies. *Journal of Performance of Constructed Facilities*, 29(3), p.140206155953003.

Bullard, S. G. et al., 2012. *The Silver Bridge Disaster of 1967 (Images of America).* Charleston, South Corolina: Arcadia Publishing.

Ceasare, M. A., Santamarina, C., Turkstra, C., Vanmarke, E. H. 1994. Modelling bridge deterioration with Markov chains. *ASCE: Journal of Transportation Engineering*. 118(6): 56-62.

Chang, M., Maguire, M. & Sun, Y., 2017. Framework for mitigating human bias in selection of explanatory variables for bridge deterioration modeling. *Journal of infrastructure systems ASCE,* 23(3), pp. 04017002(1-11).

Chase, S.B. & Gaspar, L., 2000. Modeling the reduction in load capacity of highway bridges with age. *ASCE: Journal of bridge engineering*, 5(4), pp.331–336.

Chen, W.-F. & Duan, L., 2014. *Bridge engineering handbook: Seismic Design 2*nd ed. Boca Raton, Florida, USA: CRC Press.

Chen, W.-F., & Duan, L. (1999). Bridge engineering handbook (1st ed.). Boca Raton: CRC Press.

Chen, Y.-S.et al., 2013. The correlation between air-borne salt and chlorides cumulated on the concrete surface in the marine atmospere zone in north Taiwan. *Elsevier: Journal of Marine Science and Technology*, 21(1), pp. 24-34.

CHNEP, 2017. *Charlotte Harbor Wateratlas.* [Online]
Available at: http://www.chnep.wateratlas.usf.edu/. Accessed [25-9-2016].

Cole, I. S. & Paterson, D. A., 2004a. Holistic model for atmospheric corrosion Part 5- Factors controlling deposition of salt aerosol on candles plates and buildings. *Corrosion Engineering, Science and Technology*, 39(2), pp. 125-130.

Cole, I. S. et al., 2003b. Holistic model for atmospheric corrosion: Part 2- Experimental measurement of deposition of marine salts in a number of long-range studies. *Corrosion Engineering, Science and Technology*, 38(4), pp. 259-266.

Cole, I. S. et al., 2003c. Holistic model for atmospheric corrosion: Part 3- Effect of natural and manmade landforms on deposition of marine salts in Australia and southeast Asia. *Corrosion Engineering, Science and Technology*, 38(4), pp. 267-274.

Cole, I. S., Lau, D. & Paterson, D. A., 2004b. Holistic model of atmospheric corrosion Part 6- From wet aerosol to salt deposit. *Corrosion Engineering Science and Technology*, 39(3), pp. 209-218.

Cole, I. S., Paterson, D. A. & Ganther, W. D., 2003a. Holistic model for atmospheric corrosion: Part 1- Theoretical framework, transportation and deposition of marine salts. *Corrosion engineering, Science and Technology*, 38(2), pp. 129-134.

Cole, I. S., Trinidad, G. S. & Paterson, D. A., 2004. Holistic model for atmospheric corrosion Part 4- Geographic information system for predicting airborne salinity. *Corrosion Engineering, Science and Technology*, 39(1), pp. 89-91.

Crowe D., Feinberg A. 2001. *Design for Reliability*. Fl. US: CRC Press.

Curtis, L. E. & Irvine, T., 2015. A review of spectral methods for variable amplitude fatigue prediction and new results. Elsevier: Procedia Engineering 101: 3rd International Conference on Material and Component Performance, VAL2015, pp. 243 – 250.

Davis, J. R., 2000. *Corrosion understanding the basics.* Materials Park: ASM International.

DeStefano, P. D. & Grivas, D. A., 1998. Method for estimating transition probability in bridge deterioration models. *ASCE: Journal of Infrastructure Systems,* 4(2), pp. 56-62.

Dimitriou, G., Savva, P. & Petrou, M. F., 2018. Enhancing mechanical and durability properties of recycled aggregate concrete. *Construction and Building Materials,* Volume 158, pp. 228-235.

Dimitriou, L. & Stathopoulos, A., 2016. Capturing system-wide magnitude of earthquakes' effects on urban traffic networks. *ScienceDirect: IFAC (International Federation of Automatic Control) papers online,* 49(3), pp. 243-248.

Dimitriou, L., Marinelli, M. & Fragkakis, N., 2017. Early bill-of-quantities estimation of concrete road bridges: An artificial intelligence-based application. *Public Works Management & Policy,* 23(2), pp. 127-149.

Din, Z.U. et al., 2016. Automatic logical inconsistency detection in the National Bridge Inventory. *Procedia Engineering*, 145, pp.729–737.

DOT, Department of Transportation, 1977. *America's highways, 1776-1976: a history of the Federal-aid program.* Washington: US Department of Transportation & Federal Highway Administration.

Dunker, K. F. & Rabbat, B. G., 1990. Highway Bridge Type and Performance Patterns. *ASCE: Journal of Performance of Constructed Facilities,* 4(3), pp. 161-173.

Dunker, K. F. & Rabbat, B. G., 1993. Why Americas bridges are crumbling. *Scientific American,* 268(3), pp. 66-72.

Dunker, K.F. & Rabbat, B.G., 1992. Performance of Prestressed Concrete Highway Bridges in the United States - The First 40 Years. *Precast/Prestressed Concrete Institute,* 37(3), pp.48–64.

Dunker, K.F., Rabbat, B.G. 1995. Assessing infrastructure deficiencies: The case of highway bridges. *ASCE Journal of Infrastructure Systems* 1(2):100-119.

Ehlen, M. A., 1997. Life-cycle cost of new construction materials. *ASCE: Journal of Infrastructure Systems,* 3(4), pp. 129-133.

Encyclopedia Britanica, 2017. *Encyclopedia Britannica.* [Online]
Available at: https://www.britannica.com/technology/concrete-building-material. . Accessed [4-7-2018].

Enright, M.P. & Frangopol, D.M., 1998. Failure Time Prediction of Deteriorating Fail-Safe Structures. *Journal of Structural Engineering*, 124(12), pp.1448–1457.

Faber, M. H., 2012. *Statistics and probability theory.* Dordrecht, Netherlands: Springer.

Farhey, D. N., 2014. Operational structural performances of bridge materials by deterioration trends. *ASCE: Journal of Performance of Constructed Facilities,* 28(1), pp. 168-177.

Farhey, D. N., 2015. Deterioration trends and structural performances of bridge types using deck areas. *Journal of Performance of Constructed Facilities,* 30(3), pp. 04015044.

Farhey, D., 2013. Operational Structural performance of Bridge Types by Areas. *Journal of Performance of Constructed Facilities*, 27(3), pp.303–318.

Farhey, D.N., 2010. Performance of Bridge Materials by Structural Deficiency Analysis. Journal of Performance of Constructed Facilities, 24(1), pp.345–352.

Farhey, D.N., 2012. Operational Structural Performances of Bridge Materials by Areas. *Journal of Performance of Constructed Facilities*, 26(1), pp.453-461.

Farny, J. A. & Kerkhoff, B., 2017. *Diagnosis and control of alkali-aggregate reactions in concrete.* Skokie, IL: IS413 Portland Cement Association.

Federal Highway Administration (FHWA). 2014. *Office of inspector general audit report: FHWA has not implemented all MAP-21 provisions and prior OIG recommendations*, Report No. MH-2014-089, Washington D.C.: U.S. Department of Transportation.

Feliu, S., Morcillo, M. & Chico, B., 1999. Effect of distance from sea on atmospheric corrosion rate. *Corrosion,* 55(9), pp. 883-891.

FHWA, 2014. *OIG Audit Report: FHWA has not fully implemented all MAP-21 bridge provision and prior OIG recommendations. Report No: MH-2014-089,* Washington D.C.: Department of Transportation.

FHWA, 2017. *FHWA: Road weather management program.* [Online] Available at: https://ops.fhwa.dot.gov/weather/weather_events/snow_ice.htm. Accessed [5-2-2017].

FHWA & DOT, 2014. National Bridge Inspection Standards review process Notice. *Federal Register,* 12 May, Volume 79, pp. 27032-27040.

FHWA, Federal Highway Administration, 1995. *Recording and coding guide for the structure inventory and appraisal of the nation's bridges,* Washington D.C.: Department of Transportation.

FHWA, Federal Highway Administration, 2009. *National bridge inspection program: Assessment of FHWA's implementation of data-driven, risk-based oversight. Report N.: MH-2009-013,* Washington D.C.: U.S. Department of Transportation.

FHWA, Federal Highway Administration, 2011. *Bridge Preservation Guide*, Washington: U.S. Department of Transportation.

FHWA, Federal Highway Administration, 2012. [Online] Available at: www.fhwa.dot.gov. Accessed [5-9-2016].

FHWA, Federal Highway Administration, 2013. *Metrics for the oversight of the National Bridge Inspection Program,* Washington: U.S. Department of Transportation.

Fitzpatrick, M.W., Law, D.A., Dixon W.C. 1981. Deterioration of New York State highway structures. *60th Annual Meeting of the Transportation Research Board*, Washington D.C., USA, pp. 1-8.

Frangopol, D.M. and Bocchini, P., 2012. Bridge network performance, maintenance and optimization under uncertainty: accomplishments and challenges. *Structure and Infrastructure Engineering*, Vol. 8, No. 4, pp. 341-356.

Frangopol, D. M., Dong, Y. & Sabatino, S., 2017. Bridge life-cycle performance and cost: analysis, prediction, optimization and decision-making. Structure and Infrastructure Engineering, 13(10), pp. 1239-1257.

Fulmer, J. E., 2009. What in the world is infrastructure. *Infrastructure Investor*, pp. 30-32.

Gaito, J., 1980. Measurement scales and statistics: Resurgence of an old misconception. *Psychological bulettin*, 87(3), pp. 564-567.

Gamst, G., Meyers, L. S. & Guarino, A. J., 2008. *Analysis of variance designs: a conceptual and computational approach with SPSS and SAS.* New York: Cambridge University Press.

GAO, 1988. *Bridge condition assessment: Inaccurate data may cause inequities in the apportionment of Federal-Aid funds*, Washington: United States General Accounting Office.

Ghobarah, A., Murat, S. & Ioan, N., 2006. The impact of the 26 December 2004 earthquake and tsunami on structures and infrastructure. *Elsevier: Engineering Structures*, Volume 28, pp. 312-326.

Ghosn, M. & Moses, F., 2000. Effect of changing truck weight regulations on US bridge network. *ASCE: Journal of bridge engineering*, 5(4), pp. 304-310.

Golson, J., It's time to fix America's infrastructure, 2015 [Online]
Available at: www.wired.com. Accessed [12-6-2018].

Goovaerts, P., 1997. *Geostatistics for natural resources evaluation*. New York: Oxford.

Hachem, Y., Zografos, K. & Soltani, M., 1991. Bridge Inspection Strategies. *ASCE: Journal of performance of constructed facilities*, 5(1), pp.37–56.

Hartkamp, A.D. & de Beurs, Kirsten & Stein, Alfred & White, Jeffrey. (1999). Interpolation techniques for Climate variables. *Geographic Information Systems Series* 99-01. International Maize and Wheat Improvement Center (CIMMYT), Mexico 1999. ISSN: 1405-7484.

Hearn, G. & Shim, H., 1998. Integration of Bridge Management Systems and Nondestructive Evaluations. *Journal of Infrastructure Systems*, 4(2), pp.49–55.

Hilbe, J. M., 2011. *Negative binomial distribution.* 2nd ed. Cambridge: Cambridge university press.

Hillson, D. and Murray-Webster, R. 2005, *Understanding and managing risk attitude*. Gower, England.

Holz, J., Akin, H. & Jamieson, K. H., 2016. *Presidential debates: What's Behind the Numbers?*. White Paper edit.. s.l.: The Annenberg public policy center university of Pennsylvania.

Hosain, K. M. A., Eesa, S. M. & Lachemi, m., 2009. Evaluation of the effect of marine salts on urban built infrastructure. *Elsevier: Building and environment*, 44(1), pp. 713-722.

Hosmer, D. D., Lemeshow, S. & Sturdivant, R. X., 2013. *Applied logistic regression.* 3rd ed. Hoboken, New Jersey: John Wiley and sons.

Huang, Y.-H., 2010. Artificial neural network model of bridge deterioration. *ASCE: Journal of Performance of Constructed Facilities,* 24 (6), pp. 597-602.

Hussain, R. R., 2014. Passive layer development and corrosion of steel in concrete at the nano-scale. *Journal of Civil & Environmental Engineering,* 4(3), pp. e116 (1-4).

Hyndman, R. J. & Koehler, A. B., 2006. Another look at measures of forecast accuracy. *International Journal of Forecasting,* Issue 22, pp. 679– 688.

Hyman, W. A. & Hughes, D. J., 1983. Computer model for life cycle cost analysis of statewide bridge repair and replacement needs. Transportation Research Board, Issue 899, pp. 52-61.

Imam, B. M. & Chrysanthopoulos, M. K., 2012. Causes and consequences of metallic bridge failures. *Structural Engineering International*, Volume 22, pp. 93-98.

Jackson, N. & Dhir, R. K., 1996. *Civil engineering materials.* 5th ed. N.Y.: Palgrave.

Jiang R., Murthy D.N.P. 2011. A study of Weibull shape parameter: properties and significance. *Reliability Engineering and System Safety* 96 (12): 1619-1626.

Jiang, Y. & Sinha, K. C., 1989. Bridge service life prediction model using the Markov chain. *Transportation Research Board, Transportation Research Record No. 1223, Bridge Design and Performance and Composite Materials.,* Issue 1223, pp. 24-30.

Johnson N. L., Kotz S., N. Balakrishnan. 1994. *Continuous univariate distributions*. New York, USA Wiley 1994

Jolliffe, I. T., 2010. *Principal Component Analysis.* 2nd ed. New York, US: Springer.

Jones, C.J., Johnson, P.A. & ASCE, 2015. Risk Assessment for Stream Modification Projects in Urban Settings. *Journal of Risk and Uncertainty in Engineering Systems*, 1(2), pp.4015001-1-415001–8.

Kallias, A. N. & Imam, B., 2015. Probabilistic estimation of local scour in bridge piers under changing environmental conditions. *Structure and Infrastructure Engineering,* 12(9), pp. 1228-1241.

Kallias, A. N., Imam, B. & Chryssanthopoulos, M. K., 2017. Performance profiles of metallic bridges subject to coating degradation and atmospheric corrosion. *Structure and Infrastructure Engineering,* 13(4), pp. 440-553.

Kaplan, E. L., & Meier, P., 1958. Nonparametric estimation from incomplete observations. *Journal of American Statistical Association*, 53(282), pp. 457–481.

Kim Yail, J. & Yoon, D. K., 2010. Identifying critical sources of bridge deterioration in cold regions through the constructed bridges in North Dakota. *ASCE: Journal of Bridge Engineering,* 15(5), pp. 542-552.

Kleiner, Y. (2001) Scheduling inspection and renewal of large infrastructure assets. *ASCE Journal of Infrastructure Systems,* Vol. 7, No. 4, pp. 136-143.

Klink, K., 1999. Climatological mean and interannual variance of United States surface wind speed, direction and velocity. *International Journal of climatology,* Issue 19, pp. 471-488.

Kobayashi, K., Kaito, K. & Lethanh, N., 2012. A statistical deterioration forecasting method using hidden Markov model for infrastructure management. *Transportation Research Part B,* Volume 46, pp. 544-561.

Kogler, R., 2015. *Steel Bridge Design Handbook Report No: FHWA-HIF-16-002 - Vol.19,* Springfield, VA, USA: FHWA (Federal Highway Administration).

Kroft, S., 2012. *CBS news.* [Online]
Available at: https://www.cbsnews.com/news/falling-apart-america-neglected-infrastructure/. Accessed [11-6-2018].

Kumar, P. & Imam, B., 2013. Footprints of air pollution and changing environment on the sutainability of built infrastructures. *Elsevier: Science of the Total Environment,* Volume 444, pp. 85-101.

Kutz, M., 2004. *Handbook of Transportation Engineeging.* NY: McGraw-Hil.

Labate, V., 2016. *Roman Engineering.* [Online]
Available at: https://www.ancient.eu. Accessed [10-6-2018].

Lawrence, M. G., 2005. The Relationship between Relative Humidity and the Dewpoint Temperature in Moist Air: A Simple Conversion and Applications. *Bulletin of the American Meteorological Society (BAMS).*, 86(2), 225-233.

Lee, J. et al., 2008. Improving the reliability of a Bridge Management System (BMS) using an ANN-based Backward Prediction Model (BPM). *Automation in Construction,* 17(6), pp.758–772.

Lee, S.-K., 2012. Current state of bridge deterioration in the US. *NACE International: Materials Selection and Design* , 51(1). pp. 62-67.

LePatner, B. B., 2010. *Too Big to Fall: America's Failing Infrastructure and the Way Forward.* New England: Foster Pub.

Li, Z. & Burgueno, R., 2010. Using soft computing to analyze inspection results for bridge evaluation and management. ASCE: Journal of Bridge Engineering, 15(4), pp. 430-438.

Lichtenstein, G.A., 1994. The Silver bridge collapse recounted. *ASCE: Journal of performance of constructed facilities*, 7(4), pp. 249–261.

Liu, H. & Madanat, S., 2014. Adaptive optimization methods in system-level bridge management. *Structure and Infrastructure Engineering*, 11(7), pp. 884–896.

Liu, M. and Frangopol, D.M. (2006) Optimizing bridge network maintenance management under uncertainty with conflicting criteria: life-cycle maintenance, failure, and user costs. *ASCE Journal of Structural Engineering*, Vol. 132, No. 11, pp. 1835-1845.

Liu, T. & Weyers, R. W., 1998. MODELING THE DYNAMIC CORROSION PROCESS IN CHLORIDE CONTAMINATED CONCRETE STRUCTURES. Elsevier: Cement and Concrete Research, 28(3), pp. 365–379.

Longley, P. A., Goodchild, M. F., Maguire, D. J. & Rhind, D. W., 2005. *Geographical information systems: principles techniques and applications.* 2nd ed. Hoboken, NJ, USA: Wiley.

Lounis, Z. & Madanat, S. M., 2002. Integrating mechanistic and statistical deterioration for effective bridge management. *Seventh international conference on Applications of Advanced Technologies in Transportation*, pp. 513-520.

Lounis, Z. and Daigle, L. 2008. Reliability-based decision support tool for life cycle design and management of highway bridge decks. In: *Proceedings of Annual Conference of the Transportation Association of Canada (TAC)*, Toronto, Ontario, Canada, pp. 1-19.

Lwin, M. M., 2007. *FHWA, Federal Highway Administration US DOT, Department of Transportation.*[Online] Available at: www.fhwa.dot.gov. Accessed [5-1-2016].

Madanat, M.S., Karlaftis, G.M. & McCarthy, S.P., 1997. Probabilistic infrastructure deterioration models with panel data. *ASCE: Journal of infrastructure systems*, 3(1), pp. 4–9.

Madanat, S. & Ibrahim, W.H.W., 1995. Poisson regression models of infrastructure transition probabilities. *Journal of Transportation Engineering*, 121(3), pp. 267–272.

Madanat, S., Mishalani, R. & Ibrahim, W.H., 1995. Estimation of Infrastructure Transition Probabilities from Condition Rating Data. *ASCE: Journal of infrastructure systems*, 1(2), pp.120–125.

Mair, A. and Fares, A., 2011. Comparison of rainfall interpolation methods in a mountainous region of a tropical island. *Journal of Hydrologic Engineering*, 16(4), pp. 371-383.

Markovitz, H., 1975. Supperposition in rheology. *Journal polymer science*.: Symposium No. 50 431-456.

Martinez, W. L. & Martinez, A. R., 2005. *Exploratory data analysis with Matlab.* London (UK): Chapman & Hall/CRC Press.

Mauch, M. & Madanat, S., 2001. Semiparametric hazard rate models of reinforced concrete bridge deck deterioration. *ASCE: Journal of infrastructure systems*, 7(2), pp.49–57.

Mc Gee, R., 2000. *Modelling of chloride ingress in Tasmanian bridges, Testing and Modelling the Chloride Ingress into Concrete, Proceedings of the 2nd international RILEM Workshop.* Cachan, France, RILEM.

Medeiros, M. H., Gobbi, A., Reus, G. C. & Helene, P., 2013. Reinforced concrete in a marine environment: Effect of wetting and drying cycles, height and positioning in relation to the sea shore. *Elsevier: Construction and building materials,* Volume 44, pp. 452-457.

Meira, G. R. et al., 2010. Durability of concrete structures in marine atmosphere zones-The use of chloride deposition rate on wet candle as an environmental indicator. *Elsevier: Cement and Concrete Composites,* 32(6), pp. 427-435.

Melchers, R. E. & Beck, A. T., 2018. *Structural Reliability: Analysis and Prediction.* 3 ed. Hoboken, NJ, US: Wiley & Sons Ltd.

Milligan, J. H., Nielsen, R. J. & Schmeckpeper, E. R., 2006. Short and long term effects of element costs and failure costs in Pontis. *ASCE: Journal of Bridge Engineering*, 11(5), pp. 626-632.

Mishalani, R.G. & Madanat, S.M., 2002. Computation of Infrastructure Transition Probabilities Using Stochastic Duration Models. *Journal of Infrastructure Systems*, 8(4), pp.139–148.

Mishikawa, K. & Tanaka, Y., 1993. *A nation-wide investigation of air-borne salt content (IV),* s.l.: Division of Bridge Structures of Institute of Civil Engineering, Ministry of Construction.

Moore, M. et al., 2001. *Reliability of visual inspections. Report No:FHWA-RD-01-020,* Washington,D.C: U.S. Department of Transportation.

Morcillo, M., Chico, B., Mariaca, L. & Otero, E., 2000. Salinity in marine atmospheric corrosion: its dependence on the wind regime existing in the site. *Corrosion Science,* Volume 42, pp. 91-104.

Morcous, G., Rivard, H. & Hanna, A. M., 2002. Modeling bridge deterioration using Case-Based Reasoning. ASCE: Journal of Infrastructure Systems, 8(3), pp. 86-95.

Mustafa, M. A. & Yusof, K. M., 1994. Atmospheric chloride penetration into concrete in semitropical marine environment. *Elsevier Science: Cement and concrete research*, 24(4), pp. 661-670.

Musvoto, S. W. & Gouws, D. G., 2010. The concept of a scale in accounting measurements. *South African Journal of Economic and Management Sciences (SAJEMS)*, 13(4), pp. 424-436.

Nasrollahi, M., Washer, G. 2015. Estimating inspection intervals for bridges based on statistical analysis of National Bridge Inventory data. ASCE Journal of Bridge Engineering. 1(1):1-11.

National Research Council, 1984. *Perspective on urban infrastructure.* Washington, D.C.: National Academy Press.

Neville, A., 1995. Chloride attack on reinforced concrete: an overview. *Materials and Structures,* Volume 28, pp. 63-70.

Nickless, K. & Atadero, R. A., 2018. Mechanistic deterioration modeling on bridge design and management. ASCE: Journal of bridge engineering, 23(5), pp. (04018018) 1 - 14.

NOAA, 2017a. *Coastline extractor for Global Self-consistent, Hierarchical, High-resolution Geography Database.* [Online]
Available at: https://obs-vlfr.fr/. Accessed [10-3-2016].

NOAA, 2017 b. *National Oceanic and Atmospheric Administration.* [Online]
Available at: http://www.noaa.gov. Accessed [5-3-2016].

Orabi, W. and El-Rayes, K., 2012. Optimizing the rehabilitation efforts of aging transportation networks. *ASCE Journal of Construction Engineering and Management*, Vol. 138, No. 4, pp. 529-539.

Orcesi, A.D. and Cremona, C.F., 2010. A bridge network maintenance framework for Pareto optimization of stakeholders/users costs. *Reliability Engineering and System Safety*, Vol. 95, pp. 1230-1243.

Orchard Ltd., 2004. *The prevention of corrosion on structural steelwork.* [Online]
Available at:
http://resource.npl.co.uk/docs/science_technology/materials/life_management_of_materials/publications/online_guides/pdf/structural_steelwork.pdf. Accessed [5-3-2018].

Padgett, J. et al., 2008. Bridge damage and repair costs from hurricane Katrina. *ASCE: journal of bridge engineering*, 13(1), pp. 6-14.

Penn, A., 2018. *CNN.* [Online]
Available at: https://edition.cnn.com/2018/03/15/us/bridge-collapse-history-trnd/index.html. Accessed [15-6-2018].

Pereira, F., Antoniou, C. & Dimitriou, L., 2018. Social network analysis in future transportation systems: contributions on observability, behavior and structure. *Transportation Research Part C: Emerging Technologies*, 91(1), pp. 369-370.

Pham, H. 2006. *Handbook of Engineering Statistics*. New Jersey USA: Springer.

Phares, B. M. et al., 2004. Routine highway bridge inspection condition documentation accuracy and reliability. *ASCE Journal of Bridge Engineering*, 9(4), pp. 403-413.

Podolny, W. J., 1992. Corrosion of prestressing steels and its mitigation. *PCI journal*, 37(5), pp. 34-55.

Pontes, R. B., Monteiro, E. B., de Oliveira, R. A. & de Paiva, S. C., 2009. *Chloride ion propagation in onshore structures.* Cape Town, CRC Press, pp. 449-454.

Pratt, J. W. & Gibbons, J. D., 1981. *Concepts of Nonparametric Theory.* New York: Springer-Verlag.

Qin, C., Wang, L., Zhao, H. & Douglass, S. L., 2007. Prediction of storm surges and wind waves on coastal highways in hurricane prone areas. *Journal of coastal research*, Volume 235, pp. 1304-1317.

Radomski, W., 2002. *Bridge rehabilitation.* 1st ed. London: Imperial College Press.

Radovic, M., Ghonima, O. & Schumacher, T., 2016. Data Mining of Bridge Concrete Deck Parameters in the National Bridge Inventory by Two-Step Cluster Analysis.

ASCE-ASME Journal of Risk and Uncertainty in Engineering Systems, Part A: Civil Engineering, pp. 1–9.

Rafiq, M.I., Chryssanthopoulos, M.K., Sathananthan, S. 2015. Bridge condition modelling and prediction using dynamic Bayesian belief networks. *Structure and Infrastructure Engineering* 11(1): 38-50.

Ramey, E.G. & Wright, L.R., 1997. Bridge deterioration rates and durability/longevity performance. *ASCE:Practice periodical on structural design and construction*, 2(3), pp. 98–104.

Russel, S., 1995. Artificial Inteligence. New Jersey: Prentice-Hall, Inc.

Ryall, M. J., 2001. *Bridge Management.* Oxford: Butterwood-Heinemann.

Saad, L., Aissani, A., Chateauneuf, A. and Raphael, W., 2016. Reliability-based optimization of direct and indirect LCC of RC bridge elements under coupled fatigue-corrosion deterioration processes. *Engineering Failure Analysis*, Vol. 59, pp. 570-587.

Salem, O.M., Miller, R.A., Deshpande, A.S. and Arurkar, T.P., 2013. Multi-criteria decision-making system for selecting an effective plan for bridge rehabilitation. *Structure and Infrastructure Engineering*, Vol. 9, No. 8, pp. 806-816.

Sanabra-Loewe, M. & Capellà-Llovera, J., 2014. The four ages of early prestressed concrete structures. *PCI*, 59 (4), pp. 93-121.

Sawyer, S. F., 2009. Analysis of Variance: The Fundamental Concepts. *Journal of Manual & Manipulative Therapy*, 17 (2), pp. 27E-38E.

Schechtman O., 2013. *Epidimiology and Public Health*. Berlin Germany: Springer.

Schmider, E. και συν., 2010. Is it really robust: Reinvestigating the robustness of ANOVA against violations of the normality assumption. *Methodology European Journal of Research Methods for the Behavioral and Social Sciences*, 6(4), pp. 147-151.

Schupack, M. & Suarez, M. G., 1982. Some recent corrosion embrittlement faillures of prestressing systems in the United States. *PCI journal*, 27(2), pp. 38-55.

Schweitzer, P. A., 2010. *Fundamentals of corrosion.* Boca Raton, Florida: CRC Press.

Simonoff, J. S., 2003. *Analyzing categorical data.* New York: Springer-Verlag.

Sluiter, R., 2009. *Interpolation methods for climatic data literature review*. De Bilt: KNMI, R&D Information and Observation Technology.

Sobanjo, J., Mtenga, P. & Rambo-Roddenberry, M., 2010. Reliability-Based Modeling of Bridge Deterioration Hazards. *ASCE: Journal of bridge engineering*, 15(6), pp. 671-683.

Song, H.-W., Lee, C.-H. & Ann, K. Y., 2008. Factors influencing chloride transport in concrete sttructures exposed to marine environments. *Elsevier: Cement and Concrete Composites*, Volume 30, pp. 113-121.

Stefanoni, M., Angst, U. & Elsener, B., 2018. Corrosion rate of carbon steel in carbonated concrete - a critical review. *Cement and Concrete Research,* Volume 103, pp. 53-48.

Stein, S.M. et al., 1999. Prioritizing scour vulnerable bridges using risk. *ASCE: Journal of infrastructure systems,* 5(3), pp. 95–101.

Stewart, M. G. & Rosowsky, D. V., 1998. Time dependent reliability of deteriorating reinforced concrete bridge decks. *Elsevier Science: Structural Safety,* Volume 20, pp. 91-109.

Stevens, S. S., 1951. *Mathematics, measurement and psychophysics in Handbook of experimental in Handbook of experimental psychology*. New York: Wiley.

Stratmann, M., 1990. The Atmospheric Corrosion of Iron - A Discussion of the Physico-Chemical Fundamentals of this Omnipresent Corrosion Process Invited Review. *Ber. Bunsenges. Phys. Chem,* Volume 94, pp. 626-639.

Szilard, R., 1969. Servey on durability of prestressed concrete structures in the United States, Canada and Pacific and Eastern countries. *PCI journal*, 14(5), pp. 62-73.

Tabatabai, H. et al., 2011. Reliability of Bridge Decks in Wisconsin. *Journal of Bridge Engineering*, 16 (February), pp. 53–62.

Tamvakis, P. & Xenidis, Y., 2013. Comparative Evaluation of Resilience Quantification. *Elsevier Science: Procedia - Social and Behavioral Sciences,* Issue 74, pp. 339 – 348.

Tanaka, Y., Kawano, H., Watanabe, H. & Nakajo, T., 2006. Study on cover depth for prestressed concrete bridges in airborne Chloride environments. *Precast Concrete Institute (PCI),* 51(2), pp. 42-53.

Thompson, P. D. & Michael, J. B., 2005. Markovian bridge deterioration: developing models from historical data. Structure and Infrastructure Engineering, 1(1), pp. 85 – 91.

Tobler, W. R., 1970. A Computer Movie Simulating Urban Growth in the Detroit Region. *Economic Geography*, Volume 46, pp. 234-240.

Tolliver, D. & Lu, P., 2011. Analysis of bridge deterioration rates: A case study of the Northern Plains Region. *Transportation Research Forum,* 50(2), pp. 87-100.

Transportation for America, 2013. *Transportation for America.* [Online] Available at: http://t4america.org. Accessed [15-6-2018].

Triola, M.F., 2015. *Essentials of Statistics.* 7th edit.. Boston: Pearson.

Tukey, J. W., 1977. *Exploratory data analysis.* Reading, Massachusetts, USA: Addison-Wesley Longman, Inc.

Turner, D. S., Richardson, J. A. & Wong, K. S., 1991. *Development of bridge deterioration models for the ABIMS Interim Rep. No. 3 Bureau of Engrg. Rep. 548-39,* Tuscaloosa, Ala.: Univ. of Alabama.

Tuuti, K., 1982. *Corrosion of steel in concrete. Dissertation.* Sweden: Lund University.

USGS, 2017. *United States Geological Survey.* [Online]
Available at: https://www.usgs.gov. Accessed [20-3-2017].

Veshosky, D., Beidleman, C.R., Buetow, G.W., Demir, M. 1994. Comparative analysis of Bridge Superstructure Deterioration. *ASCE Journal of Structural Engineering*. 120(7): 2123-2136

Wallbank, E. J., 1989. *The performance of concrete bridges: A survey of 200 highway bridges*., s.l.: HSMO, London, Department of Transport, UK - G. Mauncell & Partners.

Wan, B., Petrou, M. F. & Harries, K. A., 2006. The Effect of the presence of water on the durability of bond between CFRP and concrete. *Journal of Reinforced Plastics and Composites,* 25(8), pp. 875-890.

Weingroff, R. F., 1996. Federal-aid highway act of 1956, creating the interstate system. *Public Roads. Federal Highway Administration,* 60(1).

Weissmann, J., Harrison, R., and Leonard, J., 1993. Estimating load impacts on highway structures using the national bridge inventory database, *Proceedings of the 4th International Conference on Microcomputers in Transportation*.

Wesley , C., Barr, P. J., & Halling, M. W. 2014. Bridge failure rate. ASCE: Journal of Performance of Constructed Facilities, 29(3), pp:1-8.

White, S. P., Thornes, J. E. & Chapman, L., 2006. *A Guide to Road Weather Information Systems,* London: SIRWEC.

Wilcox, R.R., 2009. *Basic statistics (Understanding Conventional Methods).* Oxford New York: Oxford university press.

Woodward, R. J. & Williams, F. W., 1988. Collapse of Ynys-y-Gwas bridge, West Glamorgan. *Proceedings Institute of Civil Engineers*, 84(1), pp. 635-669.

World Economic Forum, 2016. *World Economic Forum.* [Online]
Available at: https://www.weforum.org/reports/the-global-competitiveness-report-2016-2017-1. Accessed [27-6-2018].

Wu, D., Yuan, C., Kumfer, W. & Liu, H., 2016. A life cycle optimization model using semi-markov process for highway bridge maintenance. *Elsevier Science: Applied Mathematical Modelling*, Volume:43, pp. 1-16.

Xenidis, Y. & Angelides, D., 2005. The financial risks in build-operate-transfer projects. *Construction Management and Economics,* Issue 23, pp. 431–441.

Xenidis, Y. & Stavrakas, E., 2013. Risk Based Budgeting of Infrastructure Projects. *Elsevier Science : Procedia - Social and Behavioral Sciences* , Issue 74, pp. 478 – 487.

Yanev, B. S. & Xiaoming, C., 1993. Life cycle performance of bridges of New York City bridges. *Transportation Research Record: Innovations in Construction,* Issue 1389, pp. 17-24.

Zambon, I. et al., 2017. Comparison of stochastic prediction models based on visual inspections of bridge decks. Journal of civil engineering and management, 23(5), pp. 553–561.

Zhou, S., Rizos, D. C. & Petrou, M. F., 2004. Effects of superstructure flexibility on strength of reinforced concrete bridge decks. *Elsevier Science: Computers and Structures*, 82(1), pp. 13–23.

Author's Publications

Charmpis, D.C., Dimitriou, L., Balafas, I. & F. Alogdianakis. 2014. Optimal Bridges' Upgrade Programming under Technical, Economical and Social Considerations. *OPT-i, an International Conference on Engineering and Applied Sciences Optimization*, Kos Island, Greece.

Alogdianakis, F., I. Balafas, I. & Charmpis D. C., 2014. Environmental effects on bridges: Statistical durability study based on existing inspection data. *IBSBI, 2nd International Conference on Bridges: Innovations on Bridges and Soil-Bridge Interaction*, Athens, Greece. pp.161-168.

Alogdianakis, F., Charmpis D. C. & Balafas, I., 2015. Probabilistic estimation of the time-to-rehabilitation for deteriorating bridges, Uncecomp, 1st International Conference on Uncertainty Quantification in Computational Sciences and Engineering, Crete Island, Greece. pp.407-416.

Alogdianakis, F., Charmpis D. C. & Balafas, I., 2015, Using inspection data to probabilistically estimate the time-to-rehabilitation for deteriorating bridges. COST Action TU1406, Quality specifications for roadway bridges, standardization at a European level, eBook of the 1st Workshop Meeting, Geneva, ETH-Zürich.

Alogdianakis, F., Charmpis D. C. & Balafas, I., 2016. Using existing inspection data to probabilistically estimate the time-to-rehabilitation for concrete bridges exposed to deicing salts and humidity, *ICCRRR an International Conference on Concrete Repair, Rehabilitation and Retrofit*. Leipzig, Germany. pp. 949-957.

Alogdianakis, F., I. Balafas, I. & Charmpis D. C., 2016. Environmental effects on bridge durability based on existing inspection data. *COST Action TU1406, Quality specifications for roadway bridges, standardization at a European level, eBook of the 2nd Workshop Meeting, Belgrade*. Faculty of Civil Engineering, University of Belgrade, Serbia.

Charmpis D. C., Alogdianakis, F. & Balafas, I., 2016. Scheduling bridge rehabilitations based on probabilistic life cycle condition information. *COST Action TU1406, Quality specifications for roadway bridges, standardization at a European level, eBook of the 2nd Workshop Meeting*, Belgrade. Faculty of Civil Engineering, University of Belgrade, Serbia.

Alogdianakis, F., Charmpis D. C. & Balafas, I., 2016. Using calibrated probabilistic deterioration information to optimize the rehabilitation schedule of bridges. *IABMAS, International Association for Bridge Management and Safety*, Foz do Iguaçu, Brazil. pp. 2387-2394.

Balafas, I. , Alogdianakis, F. & Charmpis D. C., 2016. A method to predict bridge conditions based on recorded bridge inspection data. *51st ESReDA, Seminar on Maintenance and Life Cycle Assessment of Structures and Industrial Systems*, Clermont-Ferrand, France.

Charmpis D. C., Alogdianakis, F. & Balafas, I., 2016. Scheduling bridge rehabilitations based on probabilistic structural condition model, risk attitude and life cycle cost. *51st ESReDA, Seminar on Maintenance and Life Cycle Assessment of Structures and Industrial Systems*, Clermont-Ferrand, France.

Alogdianakis, F., Charmpis D. C. & Balafas, I., 2019. The effect of distance from seacoast on bridge deterioration - Statistical assessment based on structural condition recordings. *Structure and Infrastructure engineering*. (submitted for review)

Alogdianakis, F., I. Balafas, I. & Charmpis D. C., 2019. Environmental effects on the structural deterioration of bridges. *ASCE: Journal of Performance of Constructed Facilities.* (submitted for review)

APPENDICES

A-I.1 Appendix Chapter 4: Database handling

A-I.1 Introduction

The NBI database contains 116 Items some of which are subdivided depending on the type of information provided. Each bridge record corresponds to a line while the Item information are placed in columns. The content of the Items may vary from location to structural condition, the name of the main route or the km point of the inventory route, thus both numeric and letter inputs can be found. The length of each information is provided by the guide (FHWA, 1995) and is registered starting from a specific column. Information regarding the columns and lengths of Items can be found in FHWA's website (www.fhwa.dot.gov/bridge/nbi/format.cfm), where additional Items or change in Item lengths can be found.

The NBI has certain peculiarities in contrast to other databases. Specifically, the coded form dictated by the guide allows blank records, and some numeric values may correspond to maximums or may be indications of lack of information. Furthermore, combinations of coded values of different Items included in the database may correspond to specific structures such as culverts or arch bridges. Thus, the Items to be incorporated should be carefully selected after advising the guide to seek dependencies that may alter the individual Item information.

For this study, code was written in Matlab R2014b to retrieve, combine and check the provided information. In this part the main functions of the code are presented. To run the code for a different inventory, changes in the positions of the items should be taken to account from FHWA's website.

A-I.1.1 Item selection

A total number of 68 Items and sub-Items (indicated with capital letters) were selected (Table A1) based on the information provided in the coding guide (FHWA, 1995). This selection was based on dependencies mentioned in the guide which would allow the identification of errors, cleaning of the data, and correcting the data. Examples of such dependencies regarded:

- Condition Ratings of Culverts (62), Deck (58), Superstructure (59) and Substructure (60). Culverts should have numeric item for item 62 while all other condition ratings should be coded with (N) corresponding to not applicable. On the other hand arched bridges should be coded with (N) for Item 62 as they are not culverts and (N) for

Item (58) as they do not include a separate deck according to the guide, while condition ratings of superstructure and substructure should have a numeric value.

Table AI.1. Selected Items: the number of each items is indicated in the parenthesis, capital letters indicate sub-Items

CATEGORY	ITEM NAME & (code) from the coding guide	
Bridge ID	Record Type (5A)	Structure Number (8)
Location	State Code (1) Longitude (17)	Latitude (16)
Water Underneath	Navigation Control (38)	Scour Critical Bridges (113)
Dimensions & Clearances	Number of Spans in Main Unit (45) Structure Length (49) NBIS Bridge Length (112) Minimum Vertical Underclear. Ref. feature (54A) Minimum Lateral Undercl. Ref. feature t (55A) Minimum Lateral Undercl. on Left (56)	Length of Maximum Span (48) Deck Width, Out-to-Out (52) Minimum Vertical Clear. Over Bridge Roadway (53) Minimum Vertical Undercl. (54B) Minimum Lateral Undercl on Right (55B) Inventory Route, Minimum Vertical Clear. (10)
Information of usage and ownership	Designated Level of Service (5C) Toll (20) Owner (22)	Base Highway Network (12) Maintenance Responsibility (21)
Classification	Functional Classification of Inventory Route (26) STRAHNET Highway Designation (100)	Historical Significance (37) Federal Lands Highway (105)
Traffic	Lanes on the structure (28A) Average Daily Traffic (29) Design load (31) Type of service on the bridge (42A) Direction of Traffic (102) Average Daily Truck Traffic (109) Year of Future Average Daily Traffic (115)	Lanes under the structure (28B) Year of Average Daily Traffic (30) Structure Open, Posted or Closed to Traffic (41) Type of service under the bridge (42B) Temporary Structure Designation(103) Future Average Daily Traffic (114)
Materials	Kind of material, Main (43A) Deck Structure Type (107) Type of Membrane (108B)	Type of Design, Main (43B) Type of Wearing Surface (108A) Deck Protection (108C)
Structural Condition Ratings	CR Deck (58) CR Substructure (60) Appraisal structural rating (67)	CR Superstructure (59) CR Culverts (62) Sufficiency rating (-)
Age	Year Built (27)	Year Reconstructed (106)
Inspection Information	Inspection Date (90)	Designated Inspection Frequency (61)
Cost	Bypass, Detour Length (19) Length of Structure Improvement (76) Roadway Improvement Cost (95) Total Project Cost (97)	Type of Work (75A) Bridge Improvement Cost (94) Total Project Cost (96)

- Water underneath is indicated if Navigation control (38) is coded with 0 or 1 while at the same time Scour critical (113) coded with numeric value and Type of service under the bridge (42) with value 5.
- Coordinates, Longitude (17) and Latitude (16) in combination with State code (1), which would reveal if each bridges coordinates are located within the respective State's territory.

Additional Items were also considered to extend the study for rehabilitation costs presented in the category of Cost (Table AI.1).

A-I.1.2 Matlab code

The basic concept of the code written in Matlab was to assist in extracting the different data types of the inventory and processing them to identify blanks and errors based on the guide (FHWA, 1995). The code read separately the characters of each considered Item, translated the extracted information to digits, recombined the digits to provide the Item information and checked it for errors (fig A1). The information was saved in a specific column of one Total matrix containing all Items considered (fig A1). In the end all Items were placed in the Total Matrix and a data cleaning process would be performed to check the errors of the combined information (fig A1). In the next part the basic functions utilized in Matlab are presented with indicative examples of specific Items.

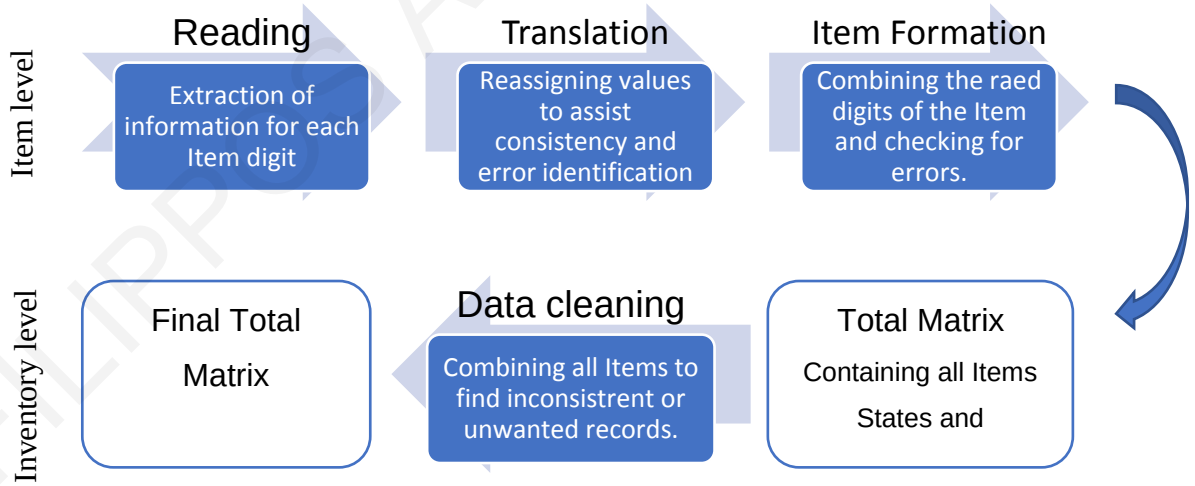

Figure A-I.1: Processes performed by the written code starting from Item level and reading of the NBI file to the formation of an error free Final Total Matrix to be used for analysis purposes.

A-I.1.2.1 Reading process

The initial data are in .txt format (Figure A-I.2) with lines corresponding to bridges and columns to items. As can be seen from the figure the different Items are not separated instead all 434 characters are placed next to each other. To be able to identify errors within

each Item, characters of each Item were read separately. Each Item's number of characters and their column position within the NBI .txt file was found from FHWA's web page http://nationalbridges.com/nbiDesc.html, where changes in record format are updated every time a new inventory is uploaded. In Matab the *fscanf* function was utilized to read the .txt

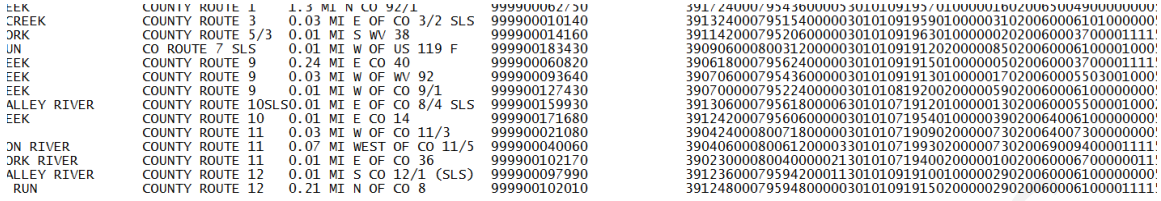

Figure A-I.2: NBI .txt file format

characters. The function's option of printing to characters is preferred to the option of digits as in the latter option if characters are read the function terminates. This preference lead also the reading of one character at a time as each character would be easier to be reassigned to a digit. For each character the number of characters to skip from the start should be defined, the number of characters to read and the number of characters to skip to read the next record. An exception to this procedure regarded Item 1 corresponding to the State code where all 3 digits are read as such, to provide the needed dimensions of the *fscanf* function to all the following Items. The Matlab code regarding State code (Item 1) and Owner (Item 22) are

```
fprintf('ITEM 1 - State code \n') %Print the phrase within '' on Matlab's
                                  command window

fid = fopen('2013_all.txt'); %opening txt file
I_1=fscanf(fid,'%3d%*432c\n');  %reading txt file and saving it in a
                                  matrix I_1
fclose(fid); %closing txt file

%Defining the matrix number of lines
M=length(I_1);

fprintf('ITEM 22 - Owner \n') %Print the phrase within '' on Matlab's
                                  command window

fid = fopen('2013_all.txt'); %opening txt file
C1=fscanf(fid,'%*152c%1c%*282c\n',[M 1]); %reading txt file and saving
                                                it in a matrix C1 of 1
                                                column and M number of
                                                lines
fclose(fid); %closing txt file
fid = fopen('2013_all.txt'); %opening txt file
C1(:,2)=fscanf(fid,'%*153c%1c%*281c\n',[M 1]); %reading txt file and
                                                saving it in C1 Matrix's
                                                of 2nd column and M number
                                                of lines
fclose(fid); %closing txt file

Translator; %Translation function
I_22; %Item function
```

Figure A-I.3: Matlab code for reading the .txt file; the green letters beginning with % sign correspond to comments explaining what each line of code performs. The last two lines show the other two functions that are used for translating and forming the data for each Item as shown in fig. AI.2

provided in Figure AI.3. Also, the two last lines provided call the two next functions for Owner (Item 22) that needs to be translated and checked.

A-I.1.2.2 Translation Function

This function reads the characters of the matrix C (Fig. AI.3) and assigns them numeric values. Its name, "Translation", refers to the way it works, as each character of the database is read from the txt file and translated to a mat file. Mat-files can be further used for analyses as they contain all the translated data. If the character read is numeric then the corresponding numeric character. If on the other hand, the character read is a letter or a sign, then decimal values smaller than 1 are assigned, for example 'A' is 0.01, 'B' is 0.02, 'Z' is 0.26, '-' is 0.27, '.' is 0.28, '&' is 0.29 and '*' is 0.30. Blank characters are assigned with value -2000 while other characters with value -1000. This way distinction can be for the information provided.

```
for i=1:1:M;% loop repeated from 1 with step 1 to M (number of records)
            if C1(i,1)=='0'; %If C1 is character 0
               D1(i,1)=0; %Assign value0 to D1
            elseif C1(i,1)=='1';
            D1(i,1)=1;
               .
               .
               .
            elseif C1(i,1)=='9';
            D1(i,1)=9
            elseif C1(i,1)=='A';
            D1(i,1)=0.01
               .
               .
               .
            elseif C1(i,1)=='*';
                    D1(i,1)=0.30
            elseif C1(i,1)=='';
                    D1(i,1)=-2000
            else D1(i,1)=-1000
            end % end of if else command
end % end of for loop after M records have been processed
```

Figure A-I:4: Translation function

A-I.1.2.3 Item function

This function uses one or more translated columns and manipulates them according to the guide (FHWA, 1995) to form an individual Item. This means that in case a certain precision is denoted by the coding guide the corresponding digits are multiplied by powers of ten and added accordingly. It also checks the data for errors and plots them on Matlab's

command window (Fig. A-I.5). In the end it creates a matrix with the manipulated data named after the Item number.

```
%Item 22 corresponds to 2digit number
for i=1:M; ; %loop repeated from 1 with step 1 to M (number of records)

    if (D(i,1)>=1||D(i,1)==0) &&(D(i,2)>=1||D(i,2)==0)%If the values
                                                       are not
                                                       character inputs
                                                       or blanks
        D(i,3)=D(i,1)*10+D(i,2); )%Multiply with 10 and sum
    else
        fprintf('Problem in line %d \n',i)%print on the command window
                                          the line of error
    end% end of if command
end% end of loop after M records have been processed


I_22=D(:,3); %Assign the value to matrix I_22
```

Figure A-I.6: Item function for Owner (Item 22)

The item function was very useful as corrections could made regarding mistakes in the codes and tracking errors or missing records for all Items. Among all Items Longitude (Item 17) and Latitude (Item 16) had many errors due to lower precision adopted. Specifically, although the precision required by the guide was 9 and 8 digits respectively lower precision records were registered beginning with 0 value. This created blank areas within certain States (fig. A-I.6 a). The pattern of such errors was identified and was taken to account to the Item function of the coordinate Items. Thus, corrections were performed by neglecting 0 values in the beginning of either Longitude or Latitude (fig. AI.6 b).

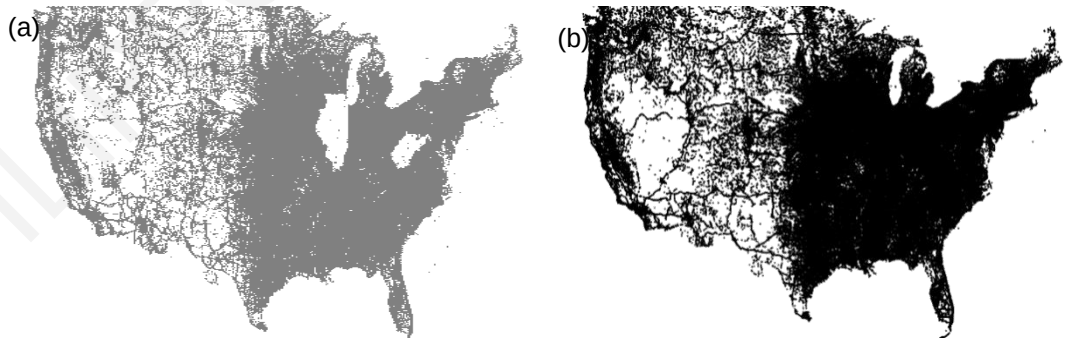

Figure A-I.7: NBI coordinates a) before corrections and b) after corrections

A-I.1.3 Data Cleaning of the Total matrix

After all individual Items were placed in the Total matrix *tabulate* function of Matlab was used to count the total numbers of errors for each Item. Furthermore, additional code was written to perform logical error checks utilizing different Items for each bridge record

(A-I.1.1). Results and description of the process were reported to FHWA followed by an Excel file to locate every inconsistent record.

A-I.1.3.1 Report to FHWA

Inconsistencies found in NBI 2016 file

Abstract: The NBI 2016 file that included all State information was used and 68 items were checked for inconsistencies with the actual NBI form from blanks, typos and different types of logical errors. This brief report explains the main errors that are listed in the Excel file that includes the line within the NBI .txt file of each error found, the State code (item 1) and the type of error.

Errors in the .txt format

Regarding the format of the NBI, a repeated error pattern was found in the lines 78840, 240965, 243224, 288628, 288671, 302081, 307308, 406967, 409114, 614387and 611845 as shown in **Figure A-I.7**.

000000000000000000	0	0N2	000000NNNN020	Y800022820370000NN	160321BZ	0*09690G
000000000000000000	0	0N2	0000001000030	YU00008220370000NN1170509	160321BK* 117000102809	0 10000G
000000000000000000	0	0N2	000000N9NN020	Y800024120370000NN	160321BZ	0*09990F
000000000000000000	0	0N2	0000002000030	YU00052220370000NN11701009	160321BK* 1170001015	0 09980G
000000000000000000	0	0N3	0000008000010	YU00014320370000NN	160321BA	2 06702G
000000000000000000	0	0N3	0000008700000	YU00011720370000NN	160321BA	2 07912F
000000000000000000	0	0N3	0000008700020	YU00024220370000NN	160321BA	2 06762G
000000000000000000	0	0N2	000000NNNN010	Y800071320370000NN	160321BZ	0*09650F
000000000000000000	0	0N3	0000008700010	YU00026720370000NN	160321BA	2 06972F
000000000000000000	0	0N2	0000001000010	Y300029220370000NN	160321BZ	0 09800F
000000000000000000	0	0N3	0000008700010	YU00002520370000NN	160321BZ	0 05750G
	0	0N2	0000001000030	Y800008020370000NN	160321BZ	0 10000G
	0	0N3	0000008700050	Y800032120370000NN	160321BA	2 05742G
	0	0N2	000000NNNN030	Y500029120370000NNH110008	160321BK* H11888872011	0*09880G
	0	0N2	000000NNNN030	Y500029120370000NNH110008	160321BK* H11888872011	0*09980G
	0	0N2	0000001000201	Y800021120330000NN	160321BZ	0 10000G
	0	0N2	0000001100080	Y800060020380000NN	160321BZ	0 09970G
	0	0N2	000000NNNN050	Y800031220370000NN	160321BZ	0*09940G
	0	0N2	000000NNNN050	Y800031220370000NN	160321BZ	0*09940G
		0N2	000000NNNN1401	Y800034720380000NN	160321BZ	0 09890G
	0	0N2	0000001000100	Y800067820370000NN	160321BZ	0 09750G
	0	0N2	0000001000010	Y800067820370000NN	160321BZ	0 09750G
	0	0N2	0000001188010	Y800067820370000NN	160321BZ	0 09750G
	0	0N2	0000001100020	Y800012520380000NN	160321BZ	0 10000G
	0	0N2	0000001100020	Y800012520380000NN	160321BZ	0 10000G
	0	0N2	000000NN00010	YU00039520350000NN	160321BZ	0*09580G
000000000000000000	0	0N2	000000NNNN100	Y800062520350000NN	160321BZ	0*09570F
000000000000000000	0	0N2	0000001600100	Y800060020360000NN	160321BZ	0 06900G
000000000000000000	0	0N2	0000001000100	Y800309620350000NN	160321BA	2 06542G
000000000000000000	0	0N2	00000026001503	Y800125020350000NN	160321BA	2 01012F
000000000000000000	0	0N2	000000NNNN050	Y800013220360000NN	160321BZ	0*09980G
000000000000000000	0	0N2	100000NNNN200	Y201006320350000NN	160321BZ	0*09190F
000000000000000000	0	0N2	000000NNNN020	Y800026420350000NN	160321BZ	0*09830G
000000000000000000	0	0N2	000000NNNN200	Y800055620360000NN	160321BZ	0*09830G
000000000000000000	0	0N2	101988NNNN190	Y800815520350000NN	160321BZ	0*08760G
000000000000000000	0	0N2	100000NNNN200	Y801006320350000NN	160321BZ	0*09650G
000086000009000095	0	0N2	1000001600200	Y701006320350000NN	160321BA	2 06902F
000000000000000000	0	0N2	100000NN00200	Y801006320350000NN	160321BZ	0*09240G
000000000000000000	0	0N2	1000001600200	Y501006320350000NN	160321BA	2 06872F

FigureA-I. 8: Extra spaces in columns 402 and 429.

Errors and inconsistencies within items

The items checked for inconsistencies were 68 in number (1, 5A, 8, 16, 17, 49, 112, 45, 48, 52, 53, 54A, 54B, 55A,55B, 56, 10, 5C, 12, 20, 22, 21, 26, 37, 100, 105, 29, 30, 109, 114, 115, 28A, 28B, 42A, 42B, 102, 41, 103, 38, 113, 43A, 43B, 31, 107, 108A, 108B, 108C, 58, 59, 60, 62, 67, 10 year rule, without 10 year rule, 27, 106, 90, 91, 19, 75A, 76, 94, 95, 96, 97, SR). In this report eight types of errors were found that are explained and presented in **Table A-I. 2**.

All Blank: refers to the error of absence of any character within the limits of each item.

- **Blank_1**: corresponds to the existence of 1 blank space within the item. It is mostly found in items 16, 17 (Latitude, Longitude) and 30 (ADT). Accordingly for **Blank_2**, **Blank_3**, **Blank_4**.
- **Typo**: Typographical error has been tracked in item 41 (structure open or posted to traffic) line 550191 where a lower case p exists instead of "P".
- **Logical errors:** such as year of future ADT estimate (item 115) greater than 2040; Year reconstructed values such as 1, 2, 7 or greater than 2017; Inspection dates greater than January 2017 etc.
- **Mixed type blank:** an error that includes the use of both "-" dash and blanks within a coding.

Table A-I.2.All inconsistencies found in the inventory categorized in Items and Types of Errors. Last column sums the columns of each line; Last line sums the lines of each column.

NBI ITEM	Error Types								Total errors (Item)
	All Blank	Blank_1	Blank_2	Blank_3	Blank_4	Logic errors	Mixed type blank	Typo	
10	2	0	0	0	0	0	0	0	**2**
16	1934	33	1921	18	1	0	0	0	**3907**
17	2013	10	41	1915	22	0	4	0	**4005**
20	1	0	0	0	0	0	0	0	**1**
26	1	0	0	0	0	0	0	0	**1**
28A	5	0	0	0	0	19	0	0	**24**
30	2	13	16	2898	0	0	2	0	**2931**
31	1	0	0	0	0	0	0	0	**1**
41	1	0	0	0	0	0	0	1	**2**
52	3	0	0	0	0	0	0	0	**3**
54A	1	0	0	0	0	0	0	0	**1**
54B	1	0	0	0	0	0	0	0	**1**
55	1	0	0	0	0	0	0	0	**1**
62	3	0	0	0	0	0	0	0	**3**
90	19	0	0	0	0	3	0	0	**22**
91	21	0	0	0	0	0	0	0	**21**
105	1	0	0	0	0	0	0	0	**1**
106	0	0	0	0	0	63	0	0	**63**
107	1	0	0	0	0	0	0	0	**1**
108A	1	0	0	0	0	0	0	0	**1**
108B	2	0	0	0	0	0	0	0	**2**
108C	3	0	0	0	0	0	0	0	**3**
115	0	6	122	1113	0	166	0	0	**1407**
Total errors (Type)	**4017**	**62**	**2100**	**5944**	**23**	**251**	**6**	**1**	**12404**

Other logical errors

Another type of logical errors relates to the combination of coded items of condition ratings (Deck (item 59), Superstructure (item 60), Substructure (item 61) and Culverts (item 62)) were found. Specifically based on the coding guide (FHWA, 1995) a Superstructure condition rating is to be coded as N-not applicable when a Culvert is coded. Similarly, Deck is to be coded with N-not applicable when culvert or if referring to a filled arch bridge. Using these restrictions, 364 logical errors were found. The lines and States codes of the mentioned errors can be found in the excel file in the worksheet named "Logical Errors from Conditions". Additionally year of improvement cost estimate (item 97), has been found to contain 1941 cases of years greater than 2016.

Errors not listed in the excel

A notable count of blanks were also counted for other items listed in **Table A-I.3**. A strange coding also appeared within the Appraisal rating (item 67) with a star symbol "*", which was not found in the guide (FHWA, 1995). Further details for these errors have not been provided within the excel since an alternative explanation may exist.

Table A-I. 3: Items with blanks or unknown coding.

Not listed		
Item	**Explanation**	**count**
12	Base Highway Network	54373
114	Average Daily Truck Traffic	61560
115	Year of Future Average Daily Traffic	1119
106	Year Reconstructed	48061
67	Appraisal rating (coded as **"*"**)	4368

Reference:

FHWA, Federal Highway Administration, 1995. *Recording and coding guide for the structure inventory and appraisal of the nation's bridges*, Washington D.C.: Department of Transportation.

A-II Appendix Chapter 4: Data Analysis

A-II.1 Kriging semivariogram models

The models used for Kriging interpolation are presented in Table A1. Three additional models were used to chose among for the best fit solution. The selected models provided the best fit solution. In the same table the annotation of a semivariogram is presented.

NOAA data	Variogram model selected	Parameters			R^2
		Nugget (N)	Sill (h)	Range (a)	
Min. Temperature S (°C)	Exponential	0.25	305.825	0.5883	0.883
Diurnal Temp. range S (°C)	Exponential	0.3	2.05	0.085	0.81
Snow depth greater than 1 inch (days)	Exponential	0	261	0.55	0.59
Precipitation (in)	Exponential	0.1	35.9	0.5	0.94
Dew point temp.(°C)	Gaussian	0	17.17	2.323	0.64
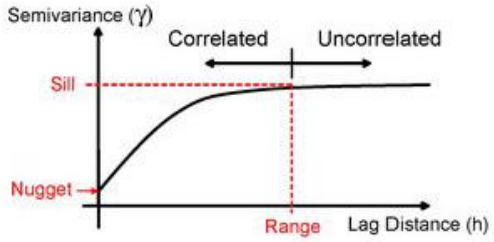		$Z_{exponential}(\gamma) = N + h \cdot \left(1 - e^{-\frac{\gamma}{\alpha}}\right)$			
		$Z_{Gaussian}(\gamma)N + h \cdot \left(1 - e^{-\frac{\gamma^2}{\alpha^2}}\right)$			

A-II.2 Peak ground acceleration

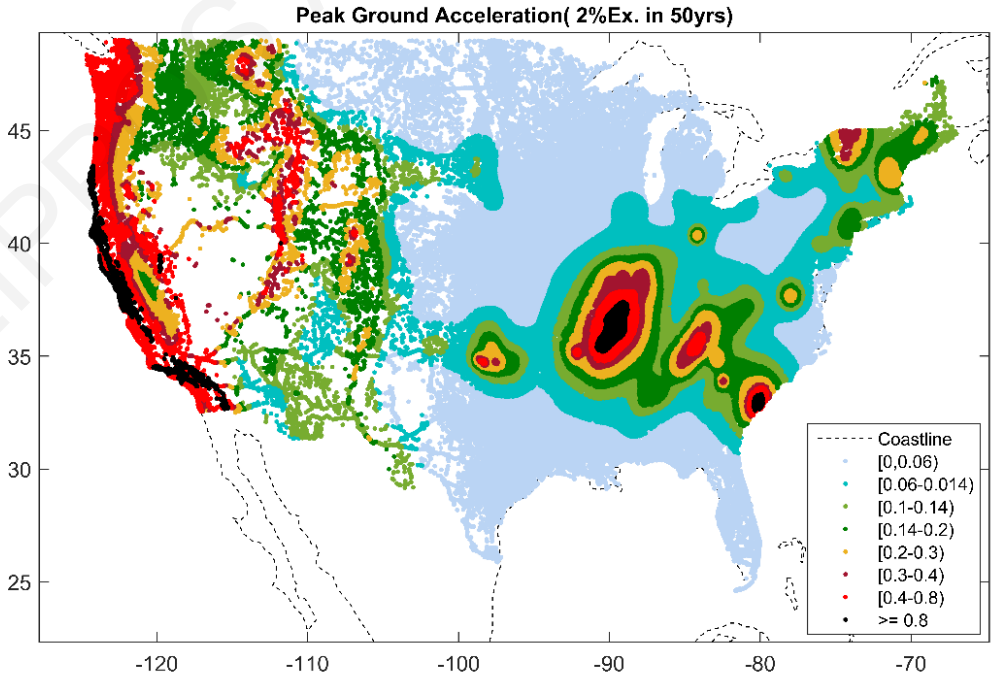

A-II.3 Average minimum Temperature

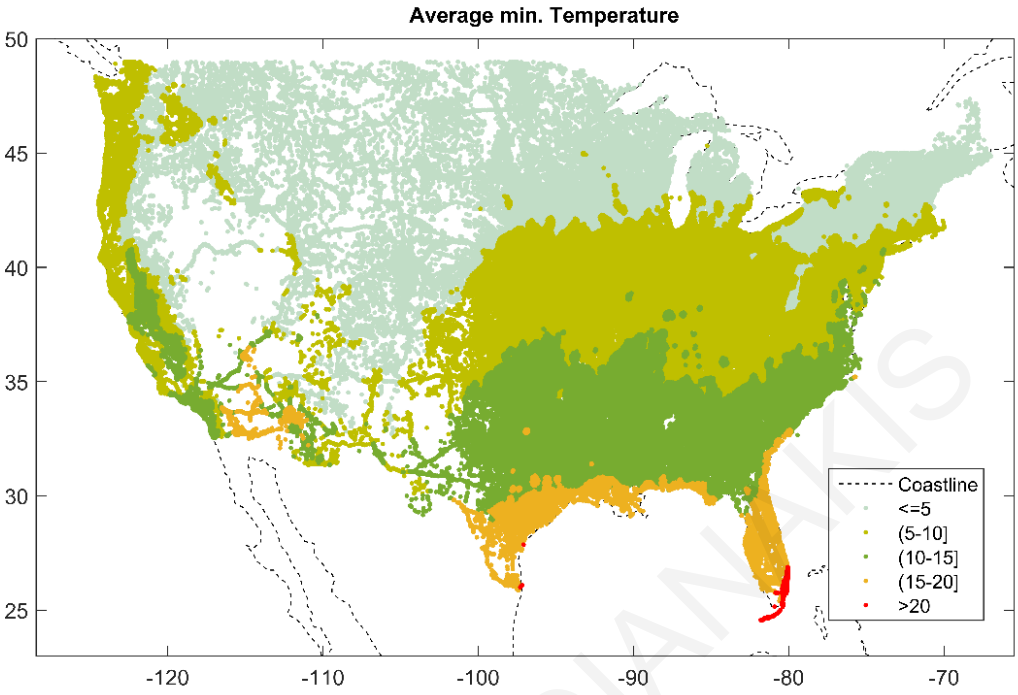

A-II.4 Diurnal temperature range

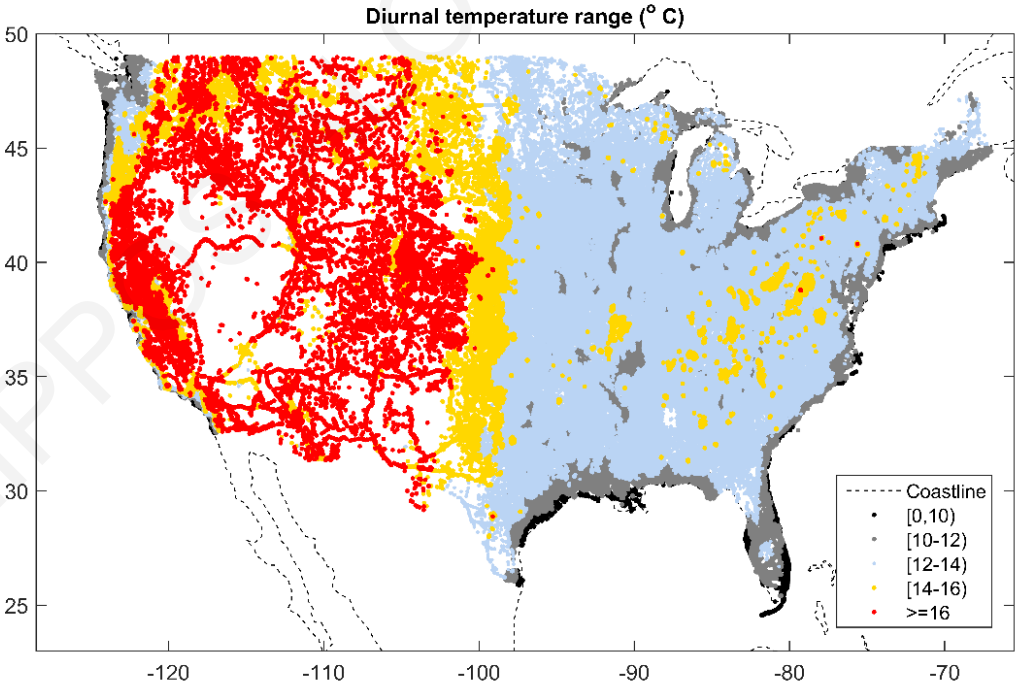

A-II.5 Snow depth days above 1inch & deicing regions

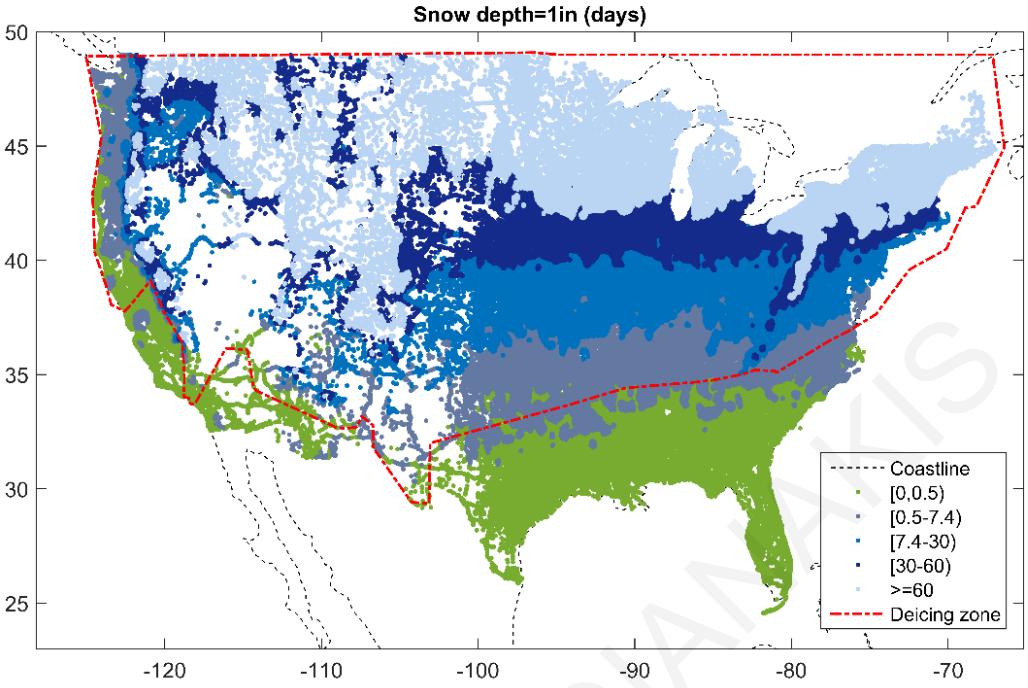

A-II.6 Precipitation

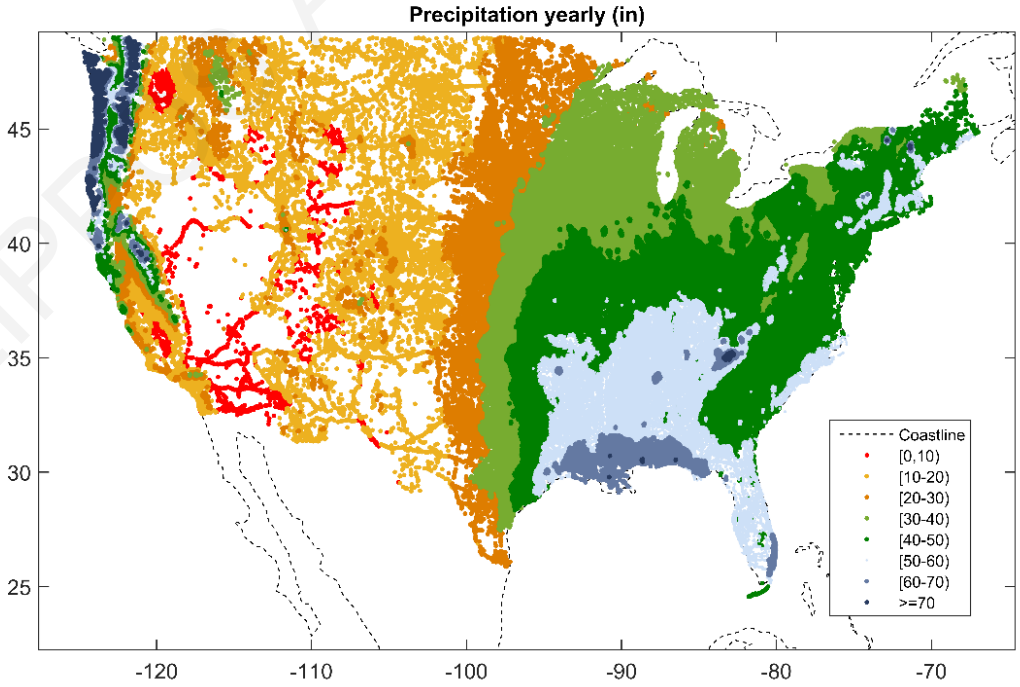

A-II.7 Dew point temperature

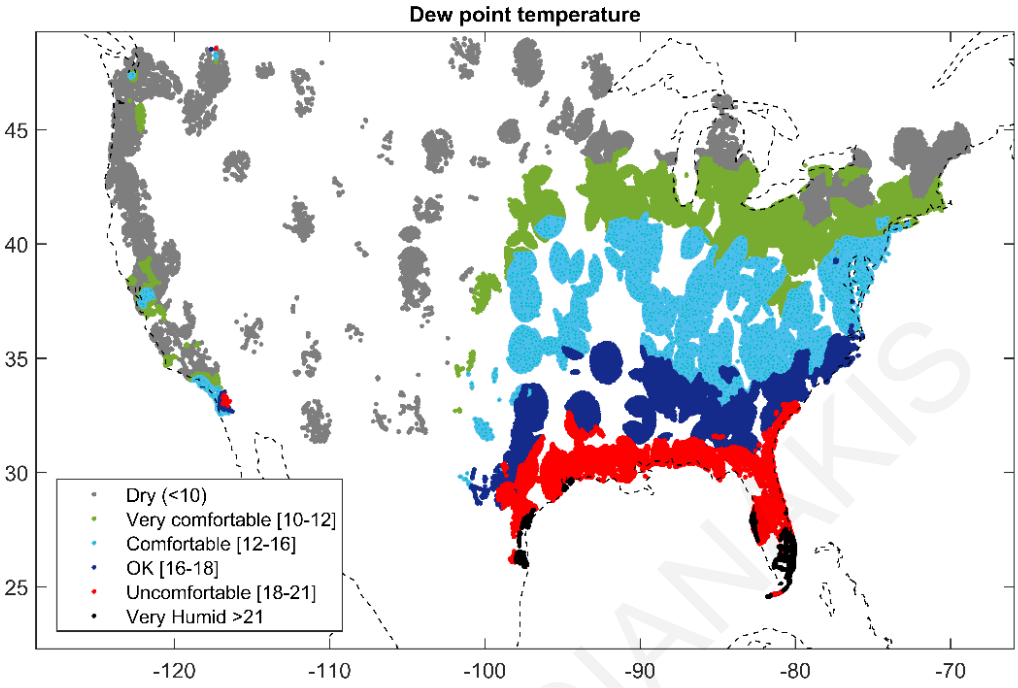

A-II.8 Humidity

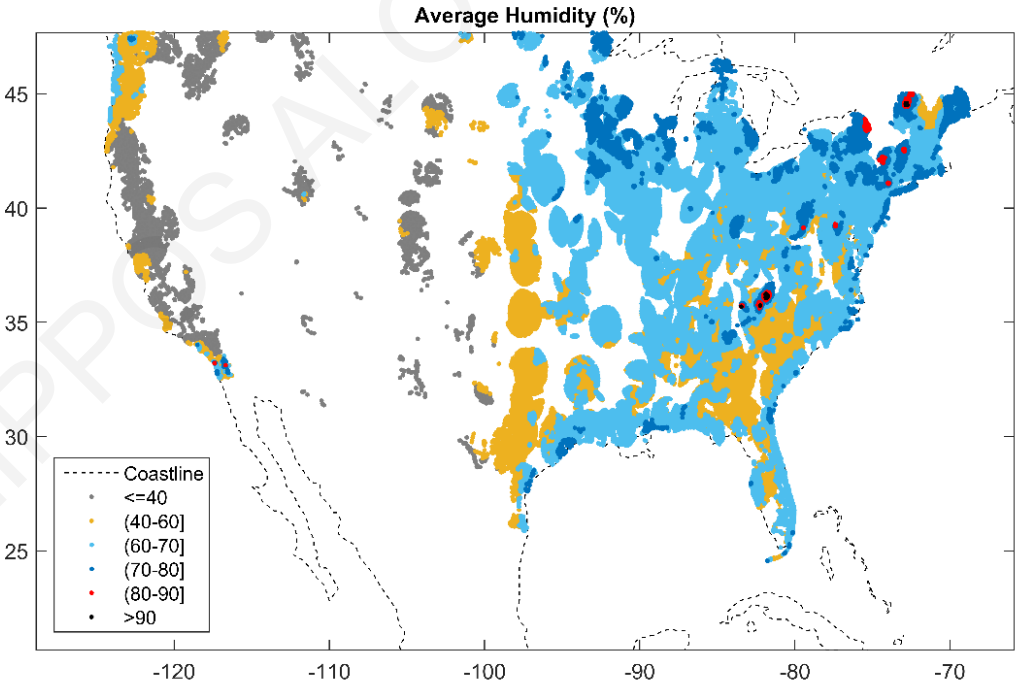

A-II.9 EDA Response Variables

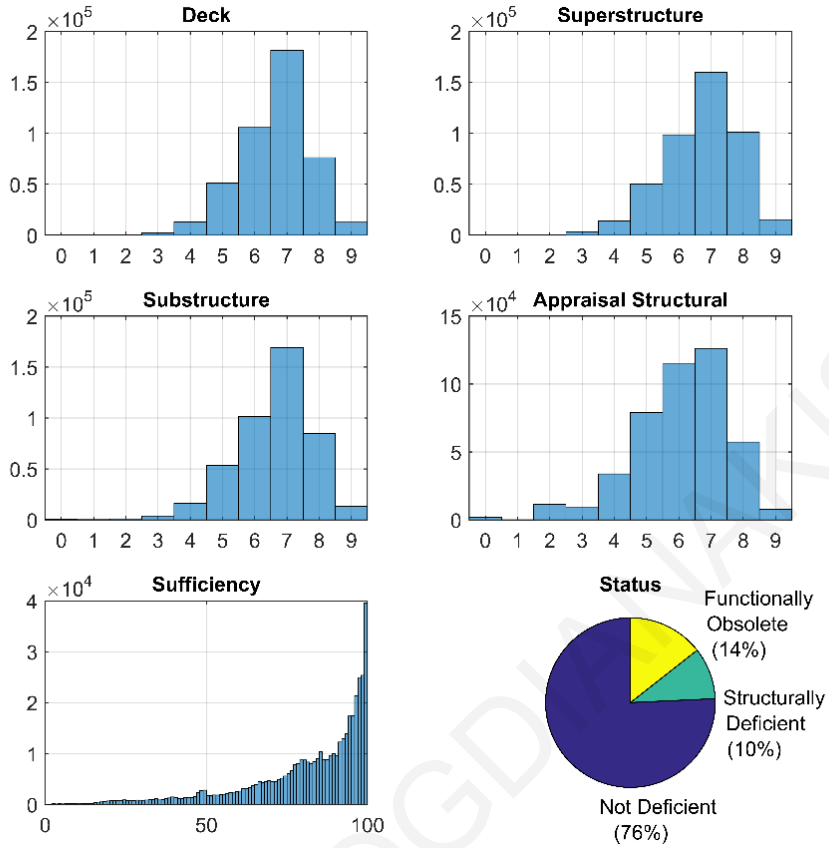

Structural Deficiency (**SD**) status

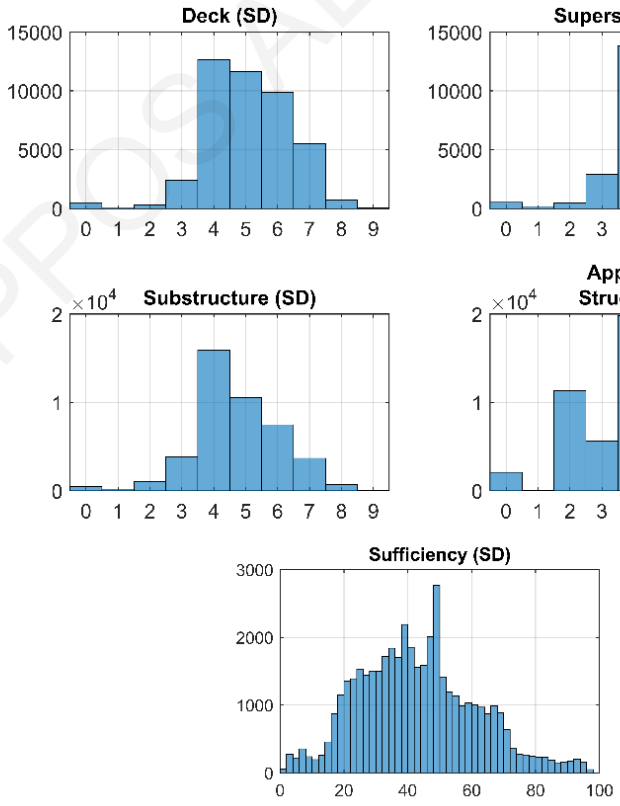

Functionally Obsolete status

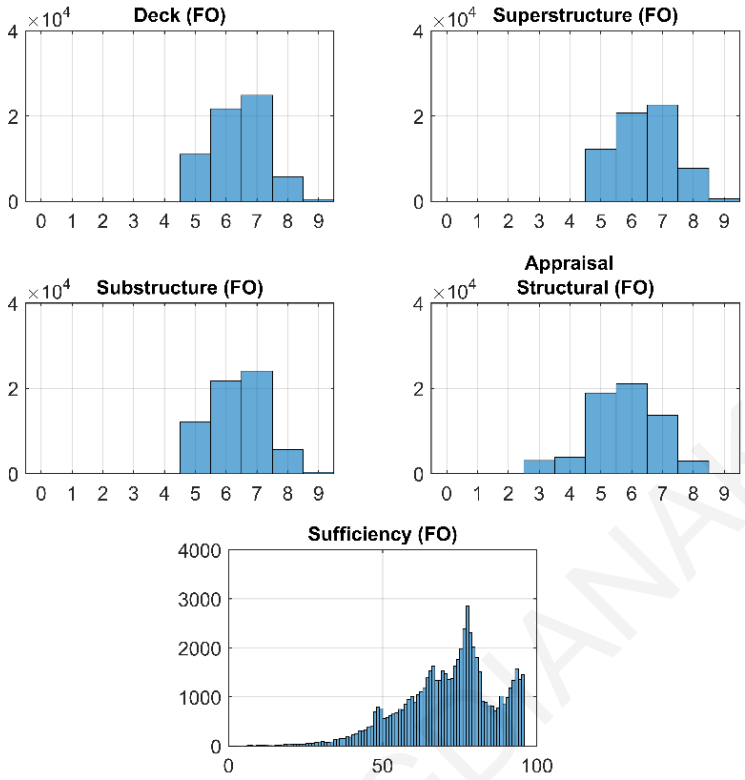

Bridges with No Deficiency (ND)

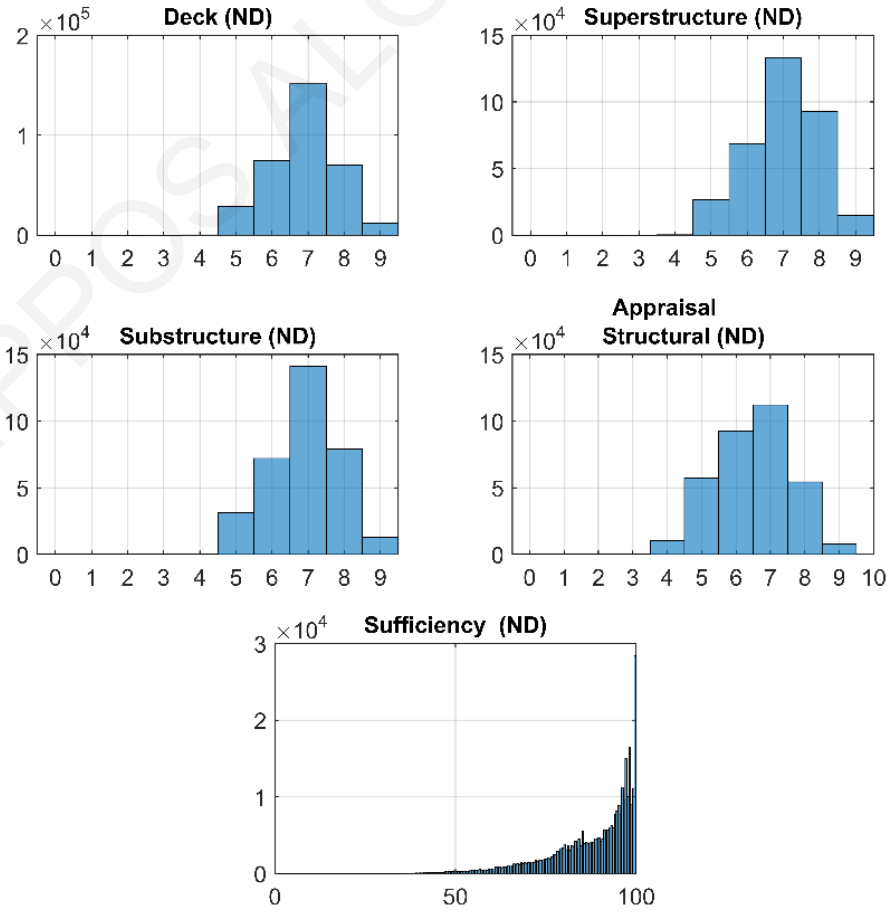

A-II.10 Dependent variables numeric

1 The outliers were ruled out only for plotting the histograms but were included in the analysis. All histograms were created without outliers apart from the ones with (*).

Variable	Min	Max	Mean	Median	Skew	Standard Variation
Length (m)	6,10	38421,6	56,33	30,50	73,56	178,90
Number of spans ()	0,00	771	2,78	2,00	57,14	5,28
Length of max. span (m)	0,00	999,9*	18,50	14,90	9,69	14,97
Deck Width out to out (m)	0,80	388.4**	11,75	9,80	15,01	7,58
Detour Length (km)	0,00	199***	21,14	5,00	9,67	63,39
Min. Vert. Clear. over (m)	0,30	30	5,90	5,03	4,89	3,89
Min.Vert. Cl. Under (m)	0,02	30	5,54	5,08	5,30	1,65
Min. Lateral Clearance left and Right (m)	0,10	30	3,79	3,00	2,11	2,82
Inventory Route min. Vertical clearance (m)	0,28	30	5,70	5,18	4,47	2,25
Average daily traffic (vehilces)	0,00	806650	8279,23	942	6,19	21831,45
Average daily truck traffic (%)	0,00	99	8,14	6,00	2,42	8,63
Lanes on (-)	1,00	82	2,24	2,0	6,19	1,11
Lanes under (-)	0,00	99	0,91	0,0	6,28	2,42
Year Built	1900	2016	1973,76	1974	-0,49	25,01
Year Reconstructed	1911	2016	1989,91	1992	-0,82	16,51
Sufficiency Rating (%)	0,00	100	81,13	87	-1,42	19,03

*the value was left as is, as there are bridges grater

**value for dead end roads NaN was used for that value so that it didn't get mixed. Not for the case of ANOVA where a category was used for this coding.

*** The value 999.9 was found the value presented has been verified using coordinates.

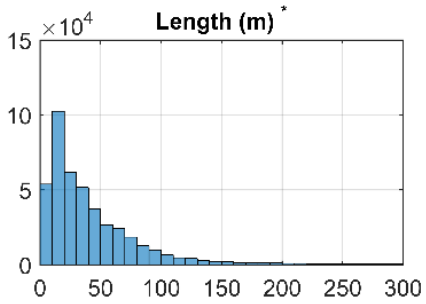

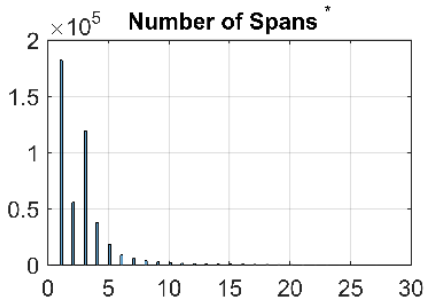

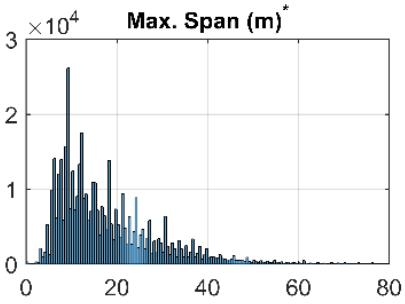

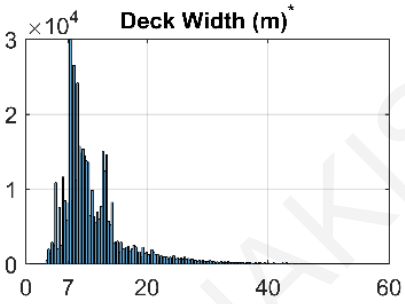

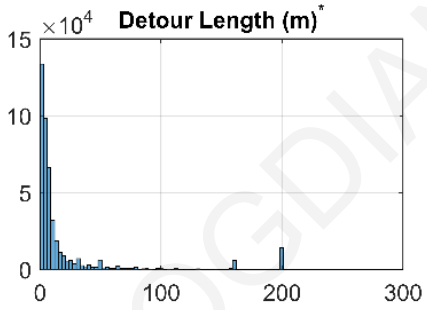

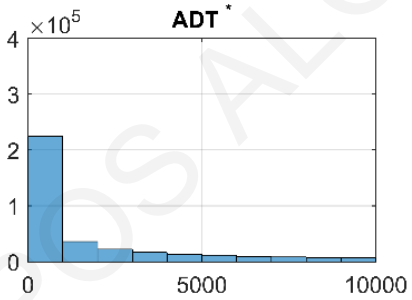

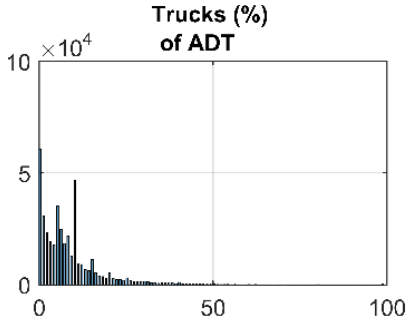

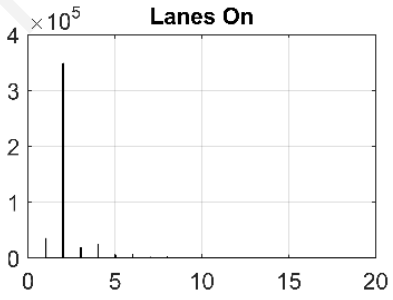

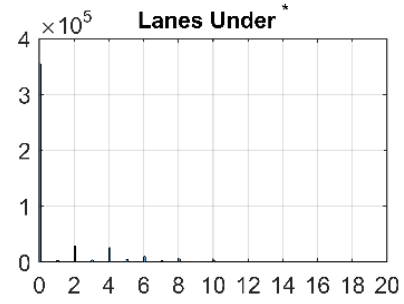

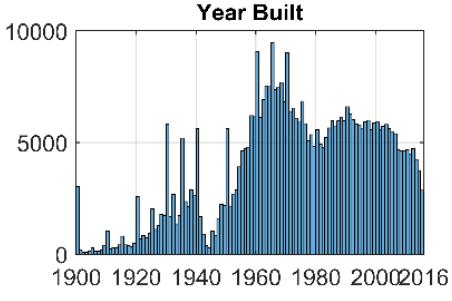

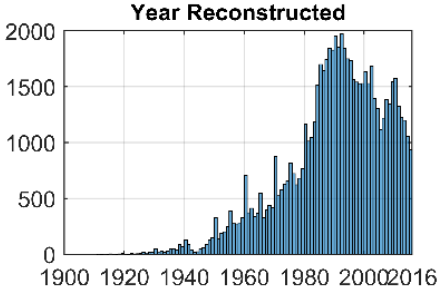

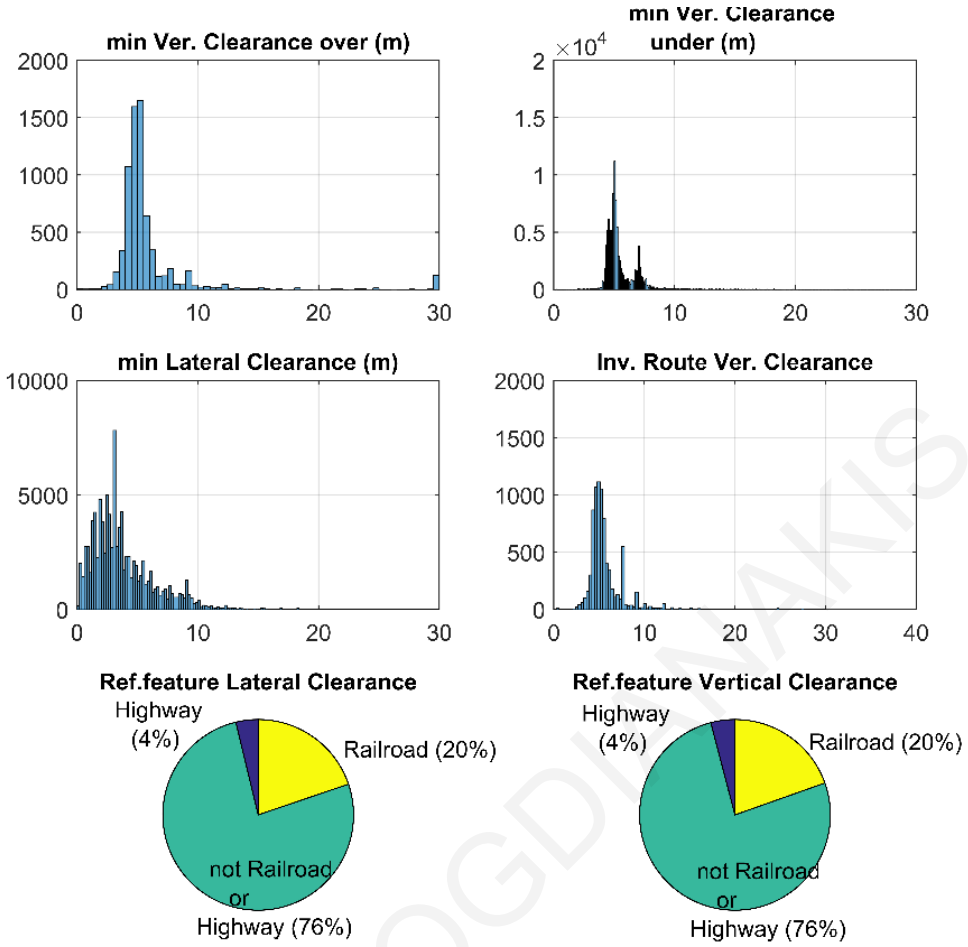

A-II.11 Environmental variables

Variable	Min	Max	Mean	Median	Skew	Standard Variation
Peak ground acceleration g (m/s^2)	0,011	2,07	0,14	0,074	3,64	0,20
Precipitation (inch)	2,61	125,81	40,02	41,32	-0,40	12,62
Snow (days above 1 inch)	0	197,02	27,03	15,96	1,26	31,09
min.Temp.(°C)	-6,31	23,22	8,18	7,62	0,36	4,11
Max. Temp.(°C)	7,87	34,82	21,06	20,55	0,30	3,83
Diurnal Range Temp.(°C)	5,28	23,86	12,88	12,65	0,99	1,75
Dew Point Temp. (°C)	-4,46	22,77	12,90	12,39	-0,033	3,66
Humidity (%)	0,014	98,25	59,25	62,09	-2,61	12,43

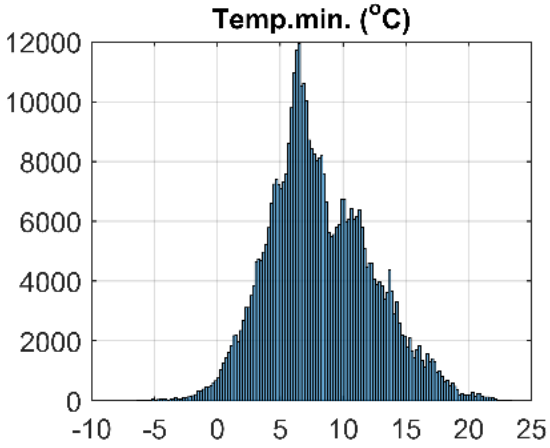

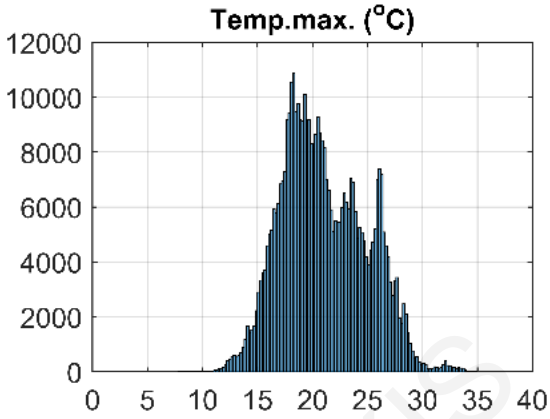

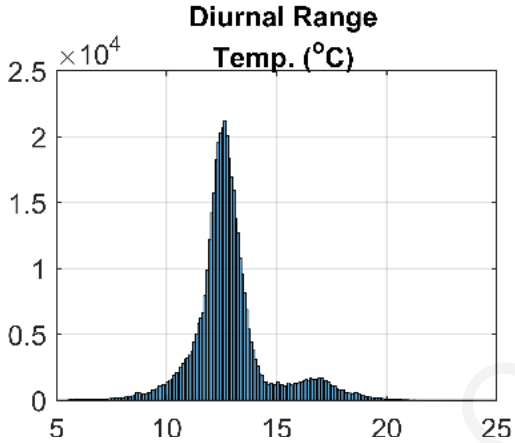

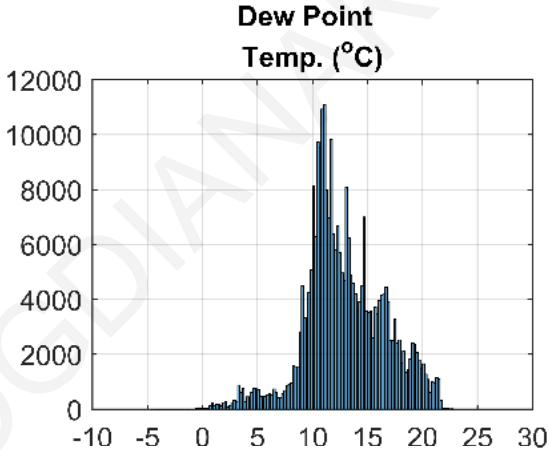

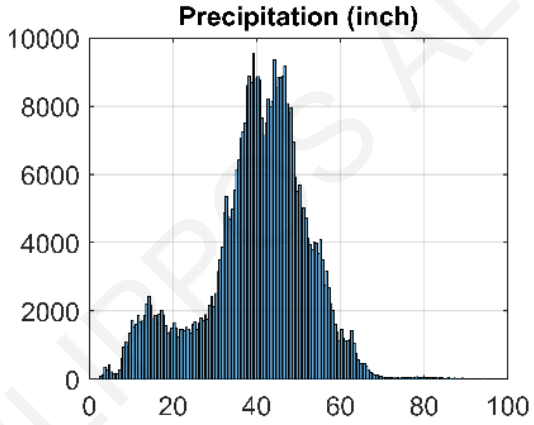

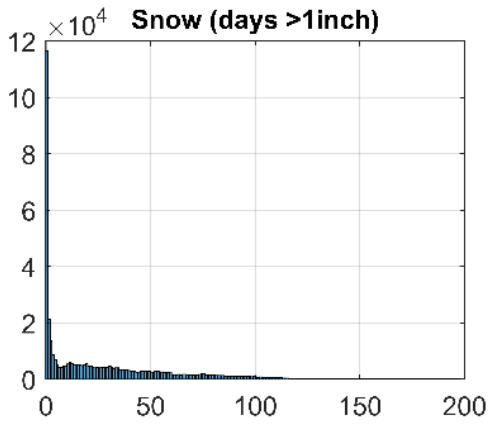

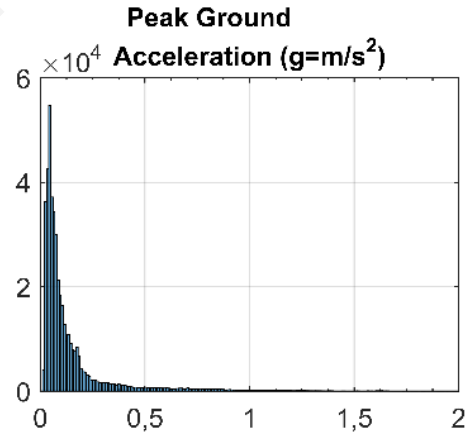

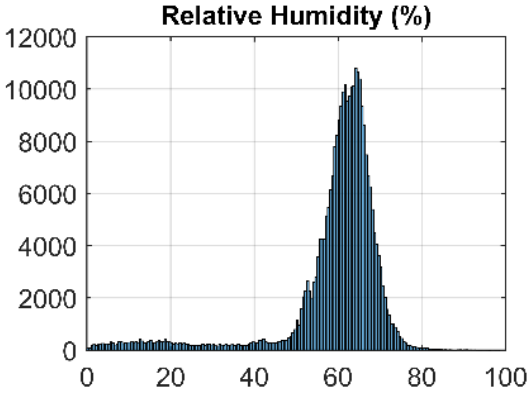

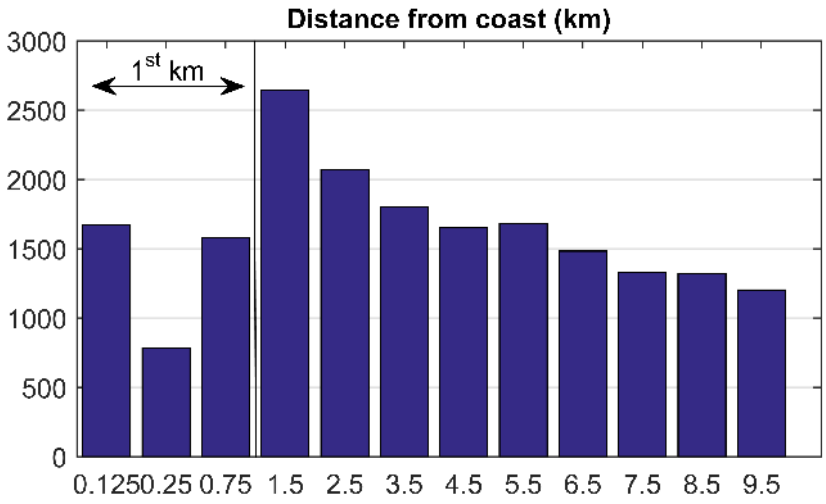

A-II.12 Categorical variables

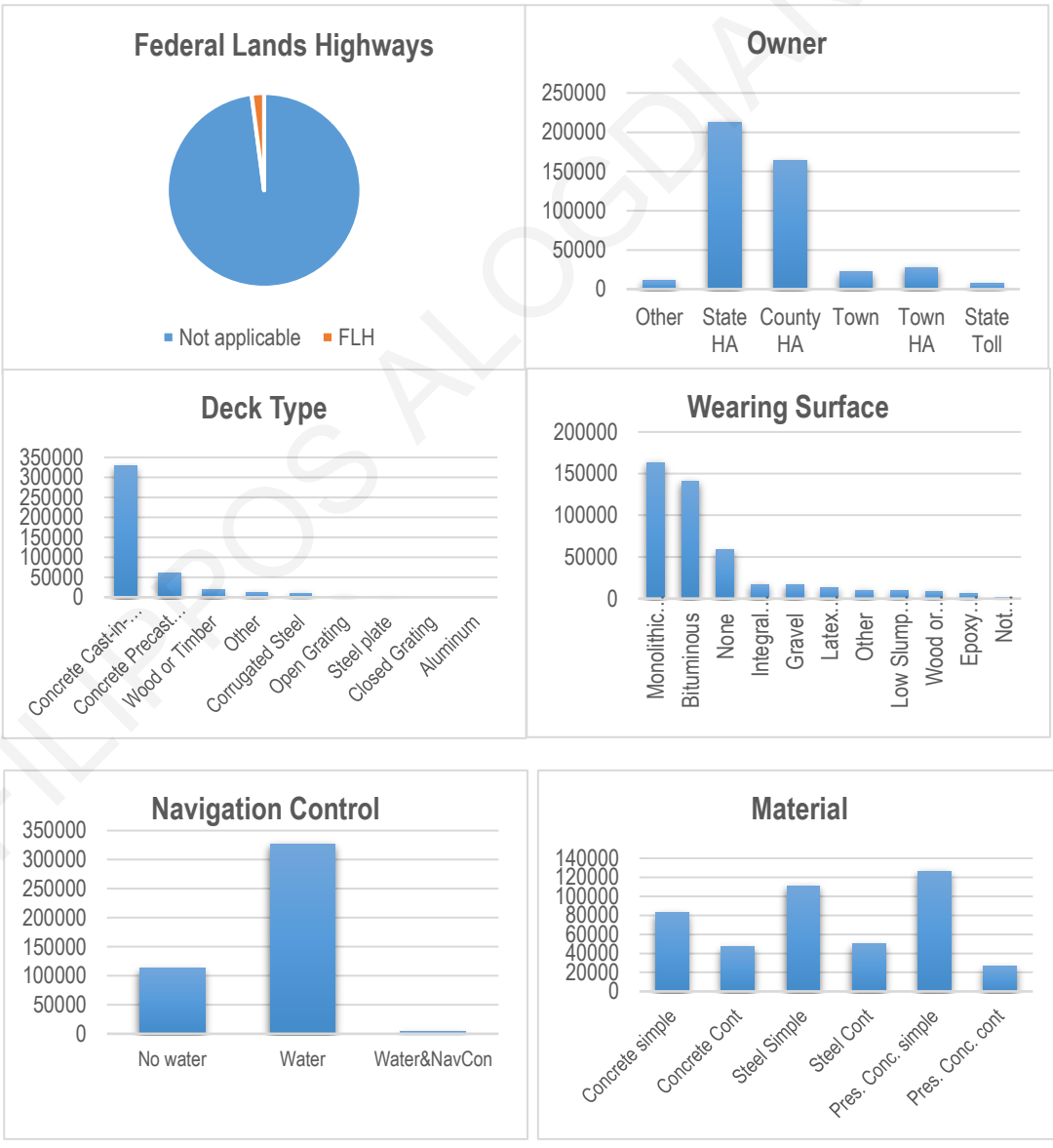

A-II.13 ANOVA Superstructure condition

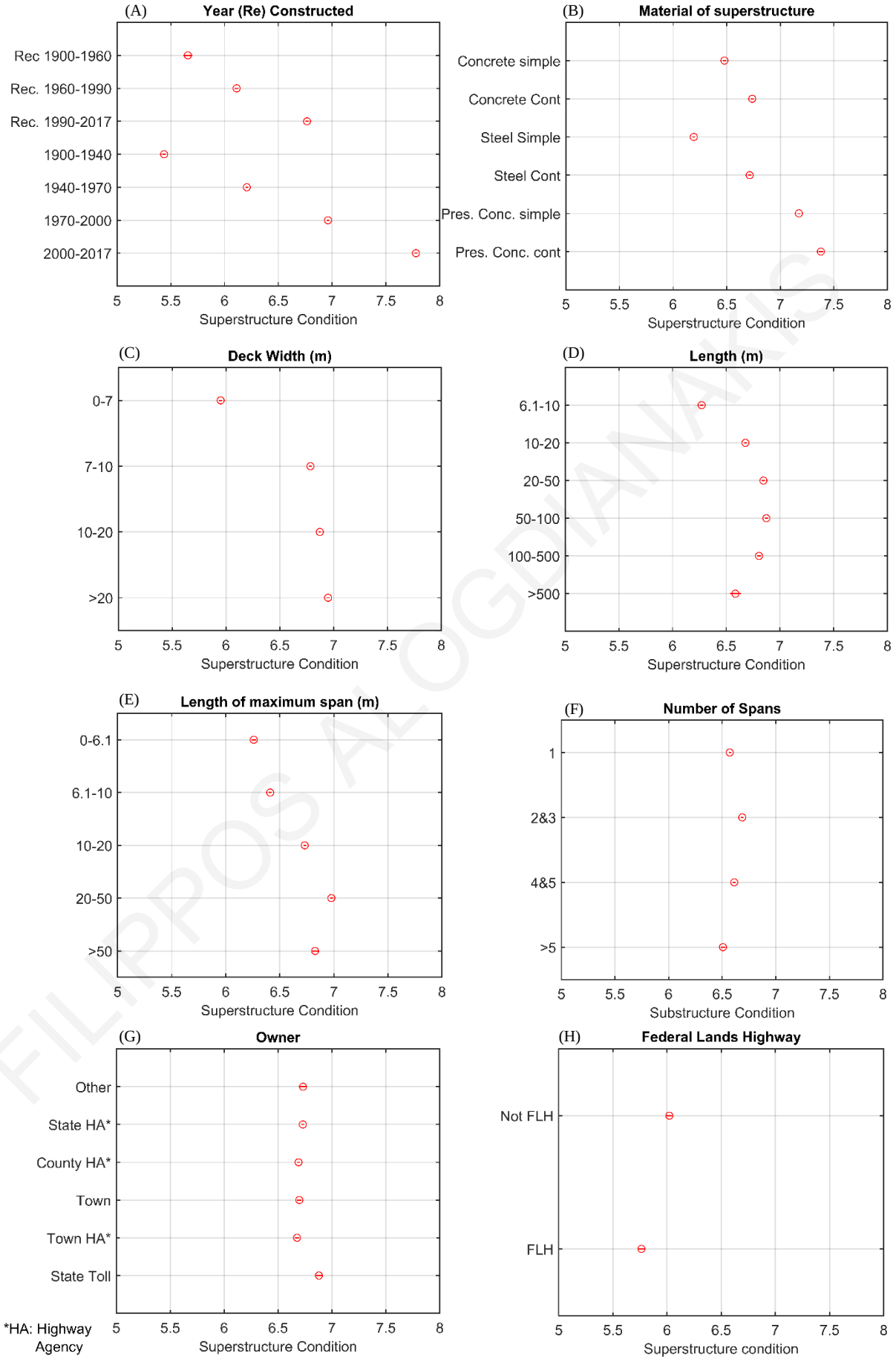

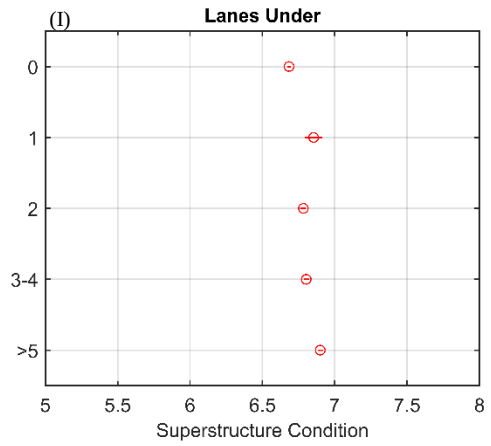

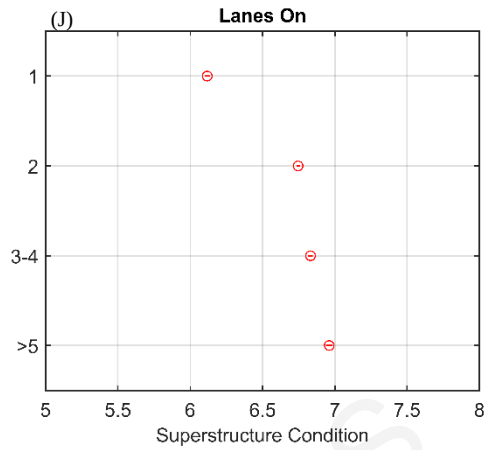

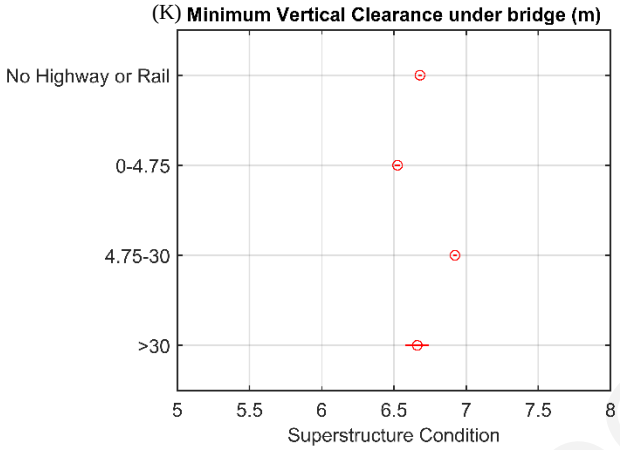

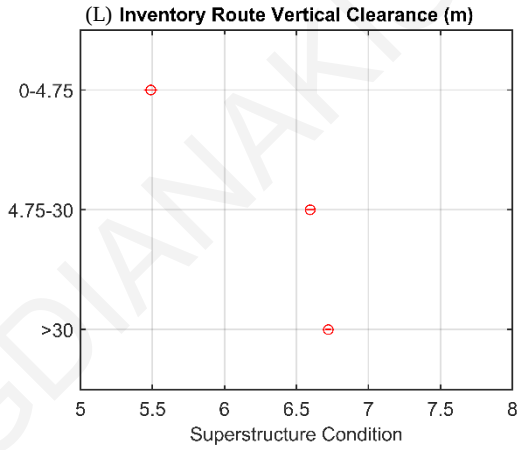

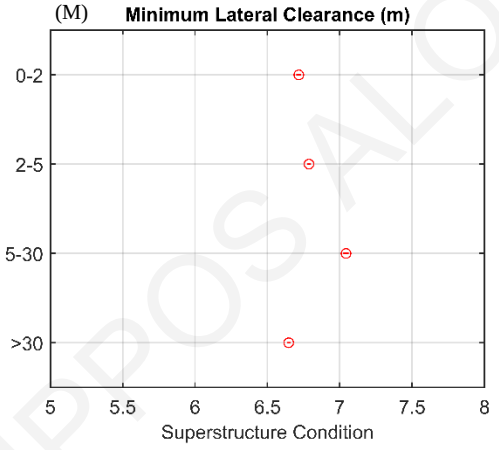

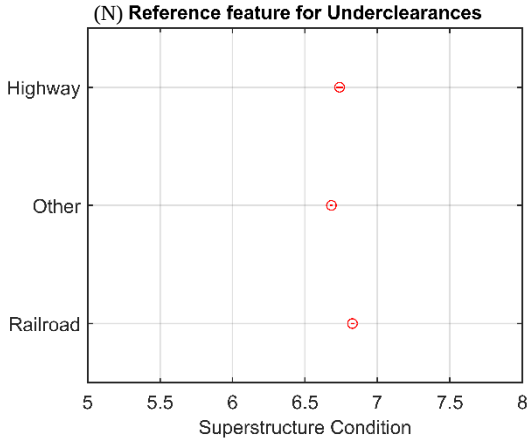

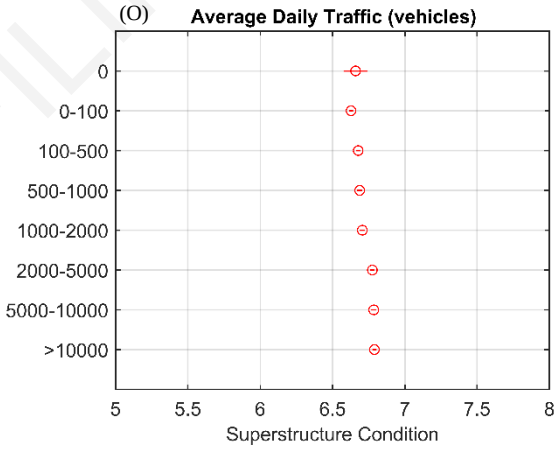

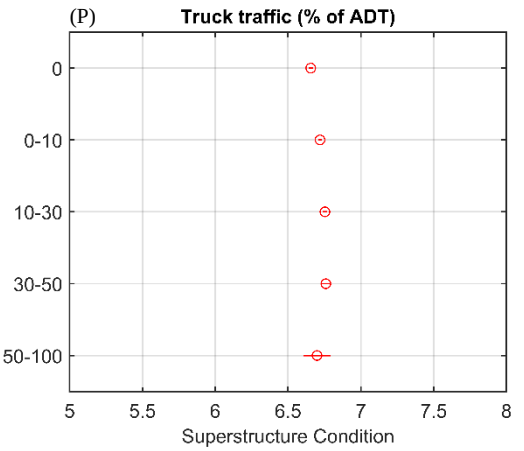

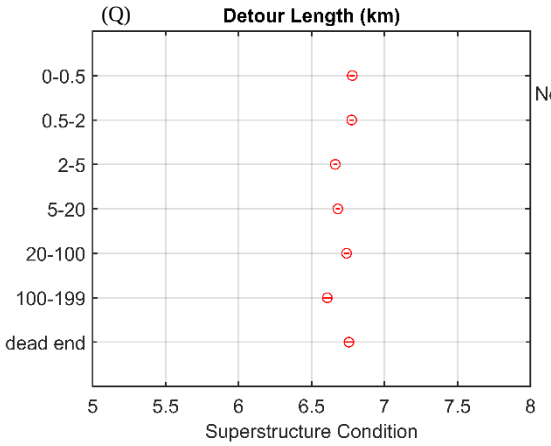

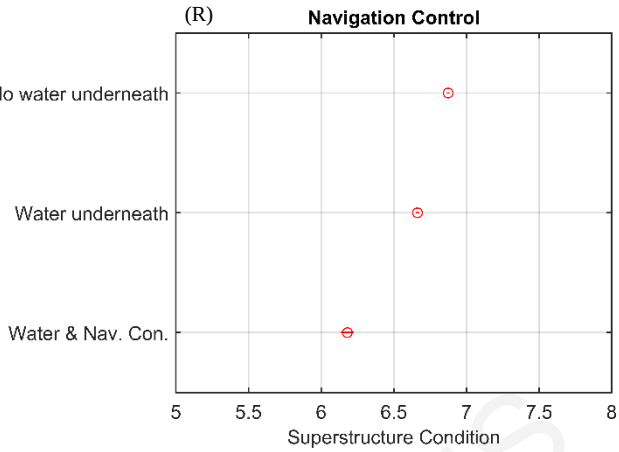

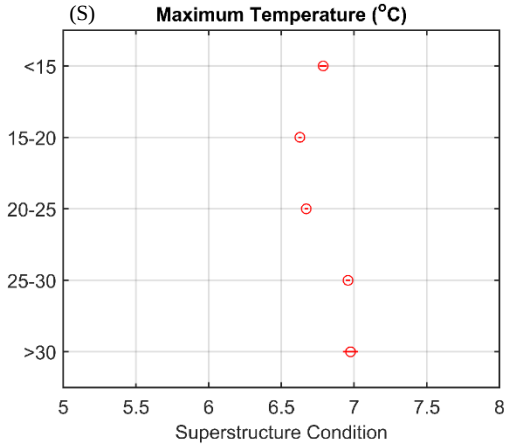

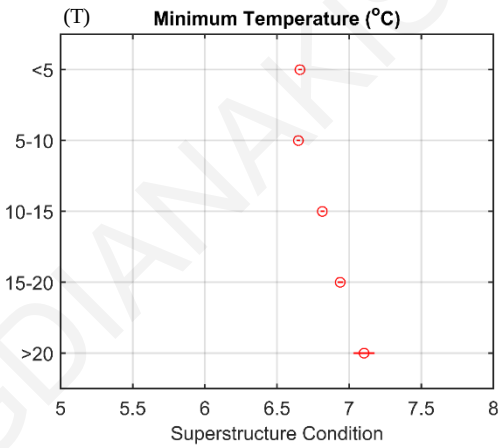

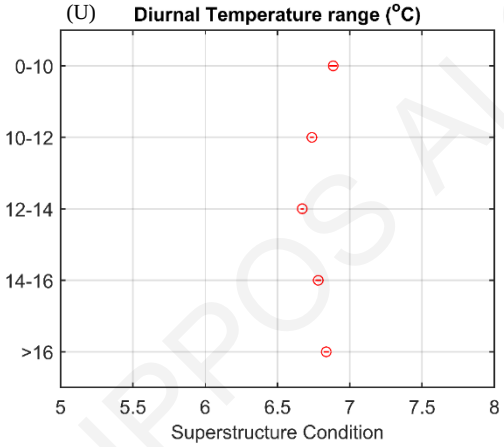

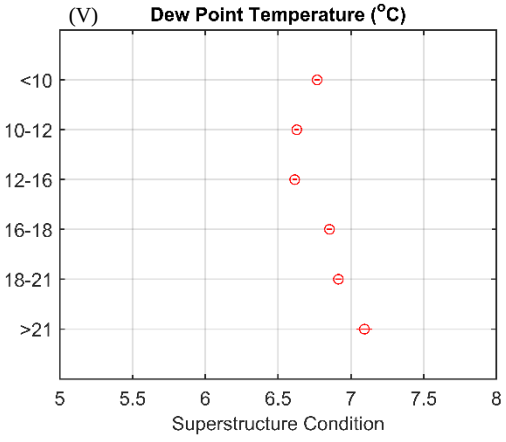

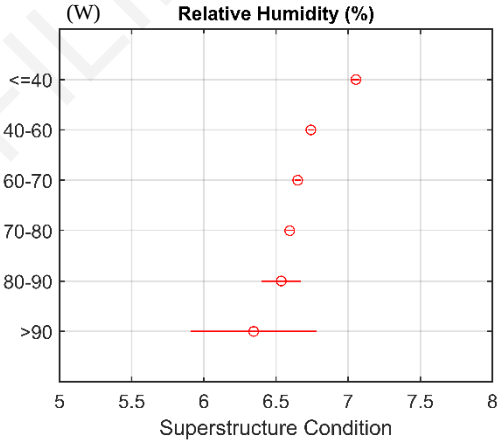

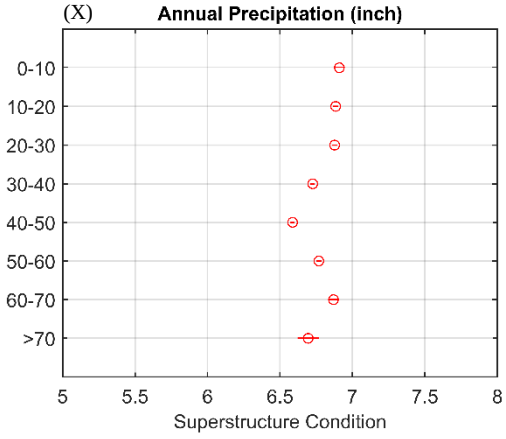

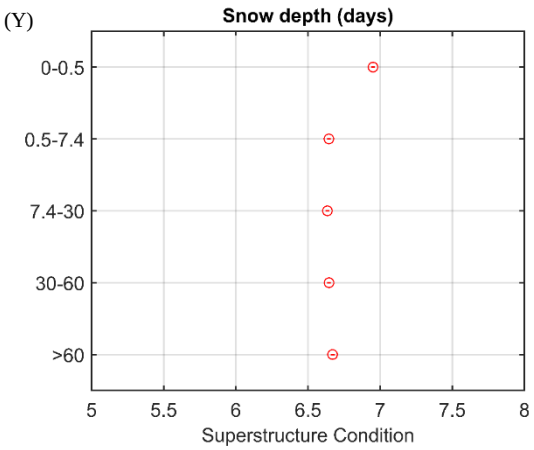

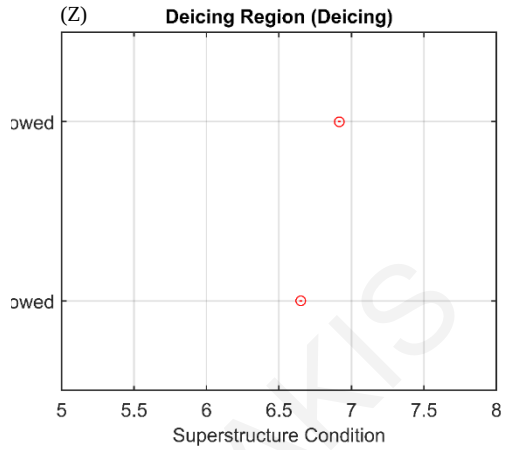

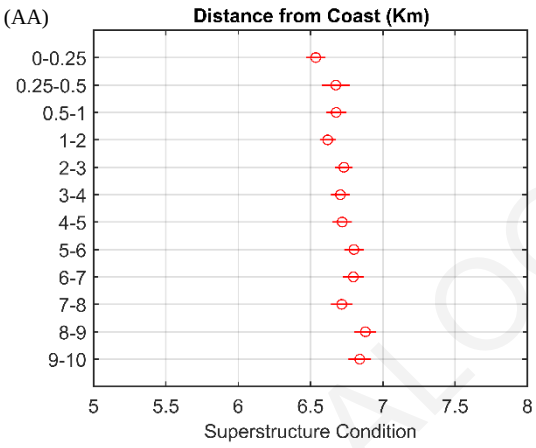

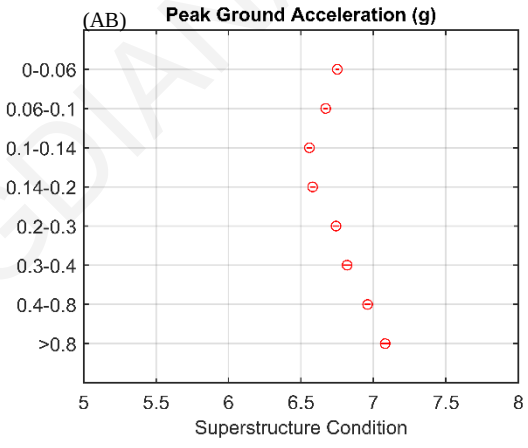

A-II.14 ANOVA Deck condition

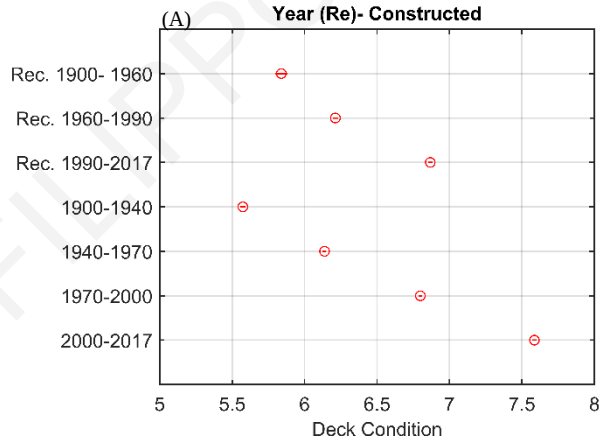

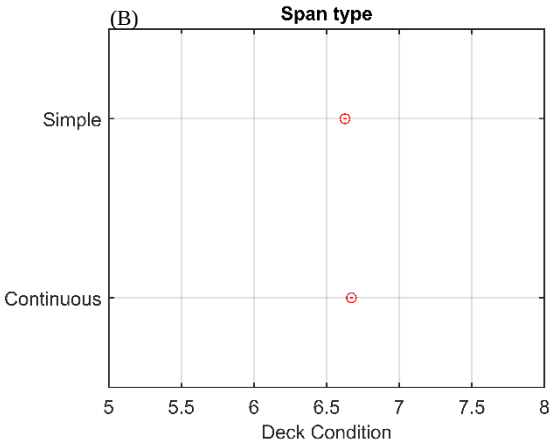

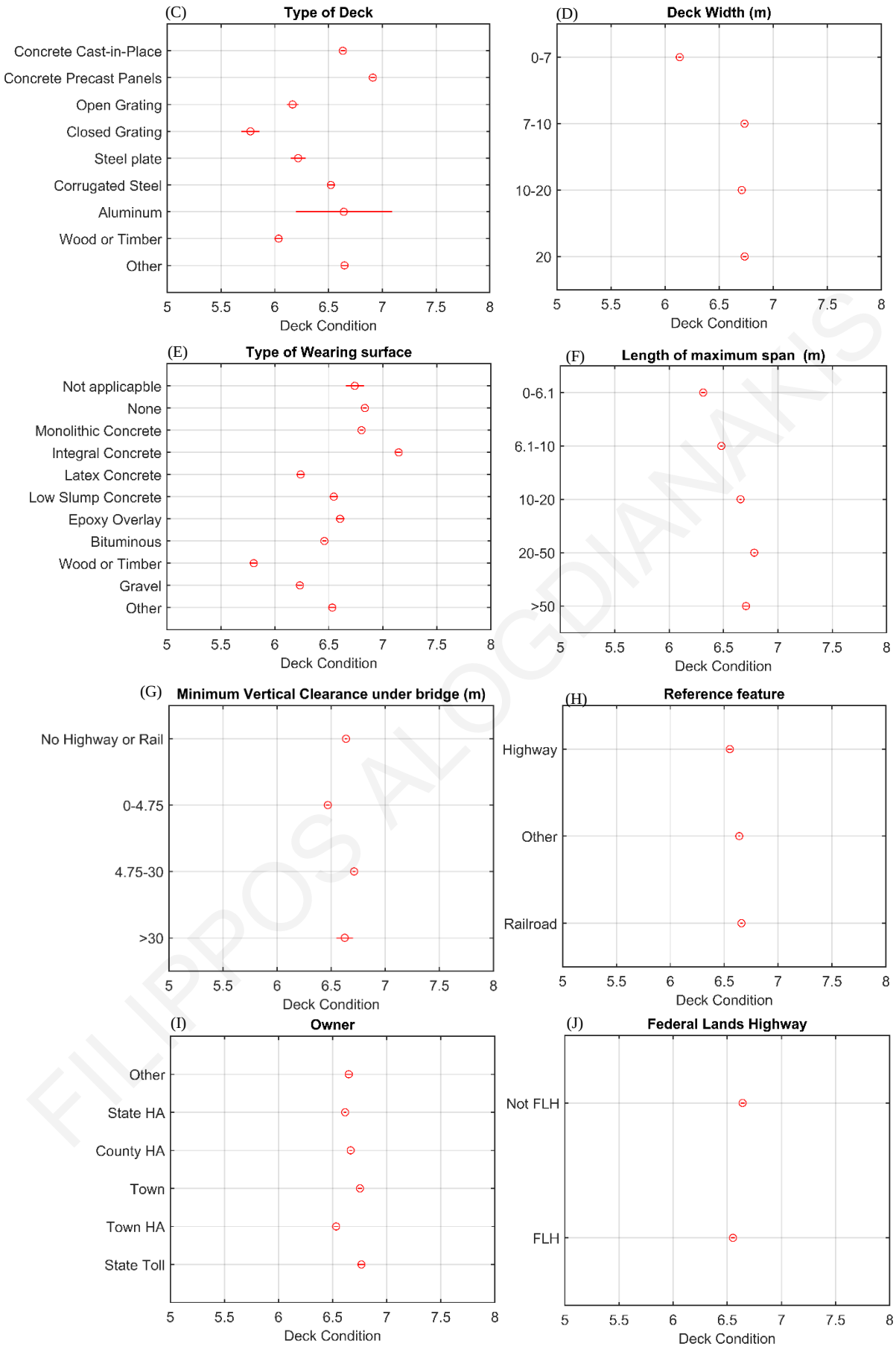

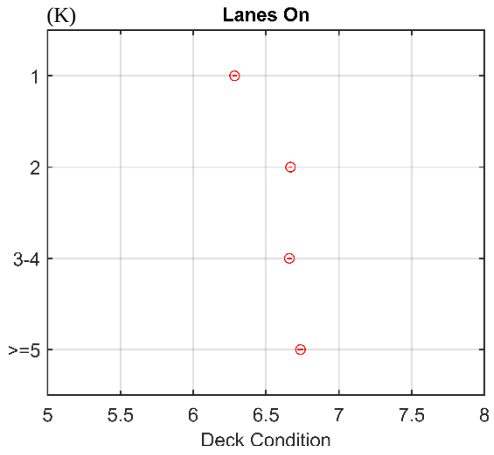

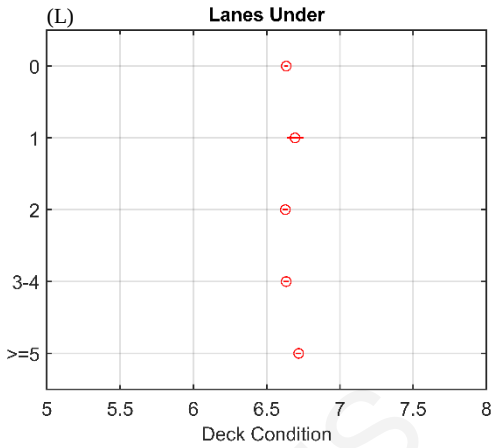

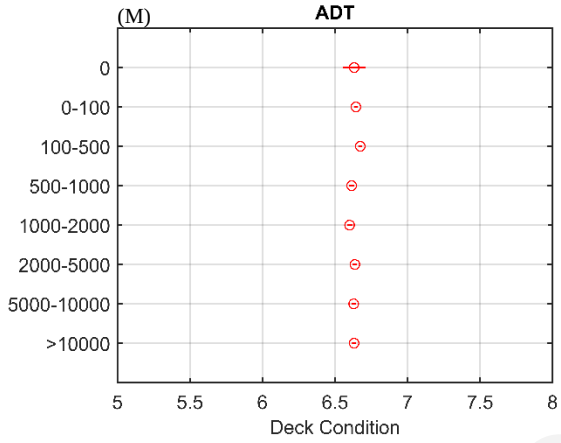

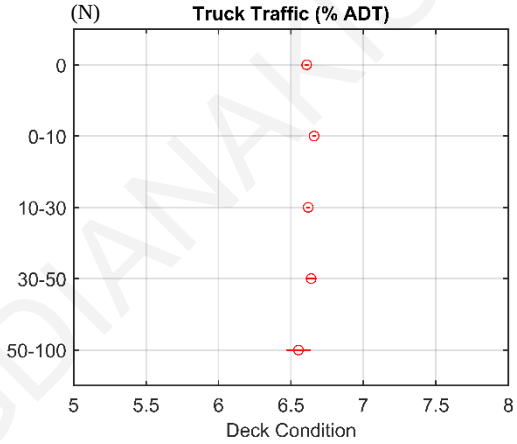

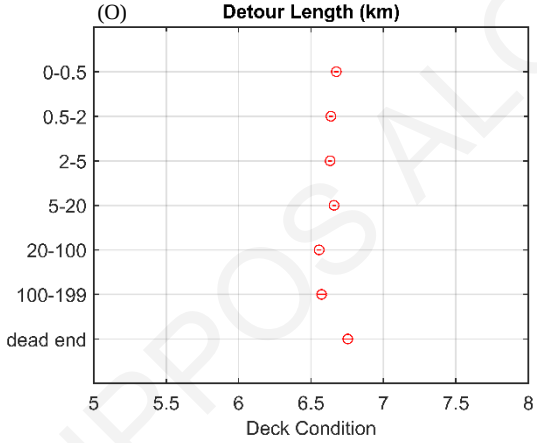

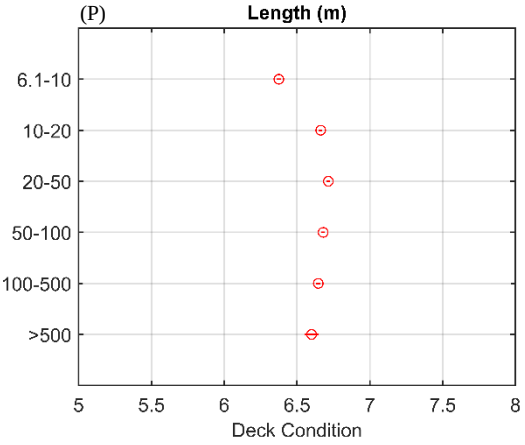

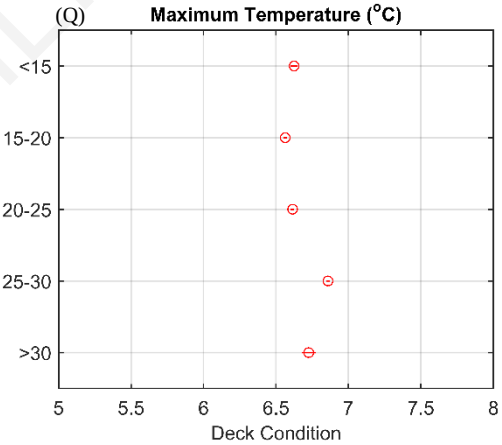

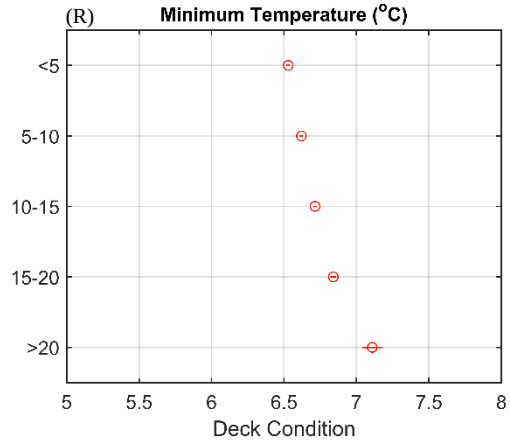

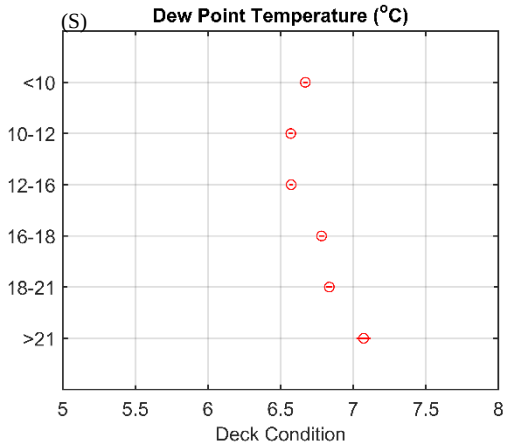

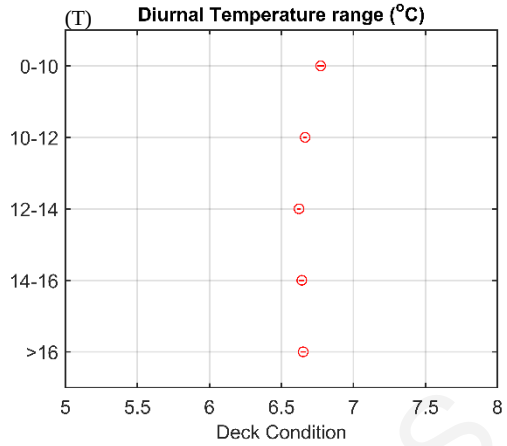

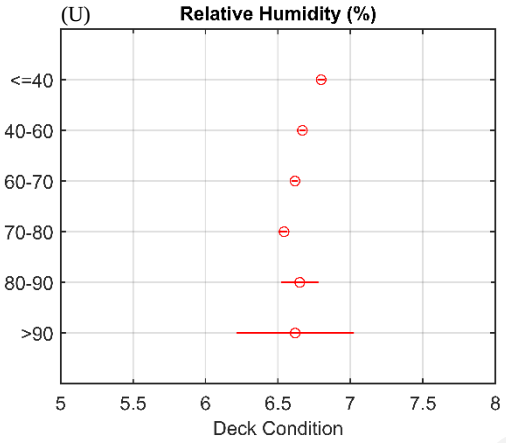

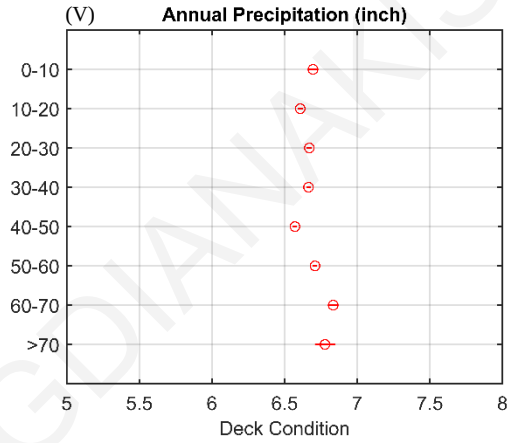

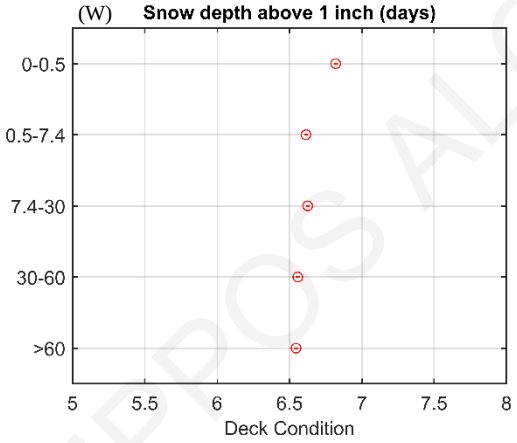

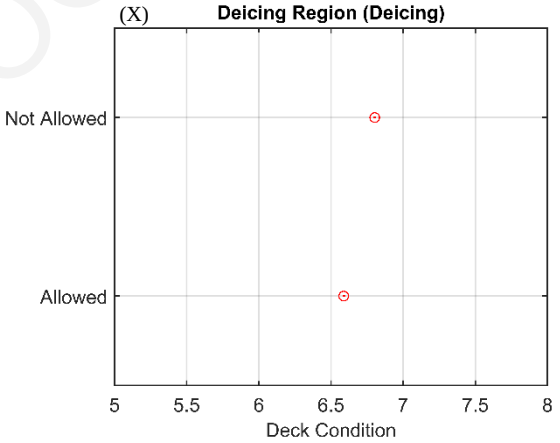

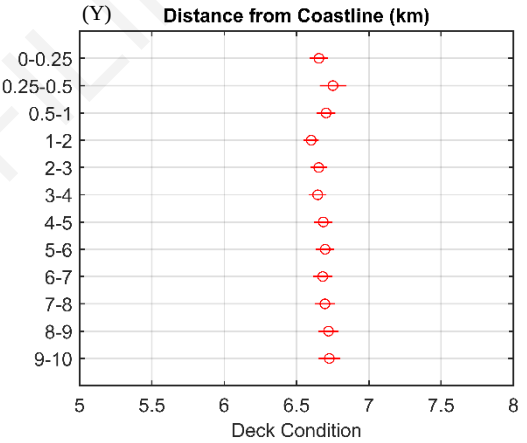

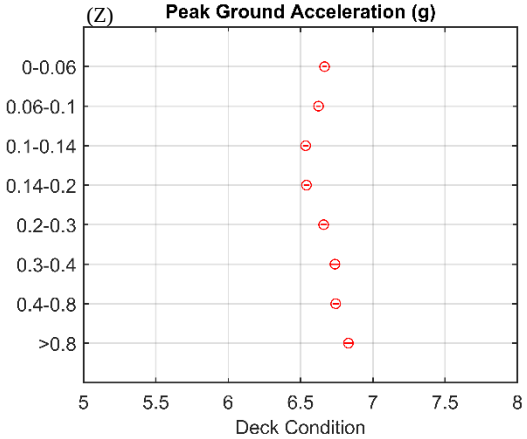

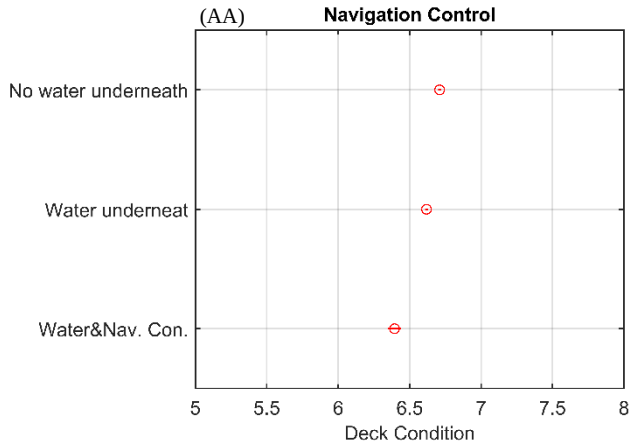

A-II.15 ANOVA Substructure condition

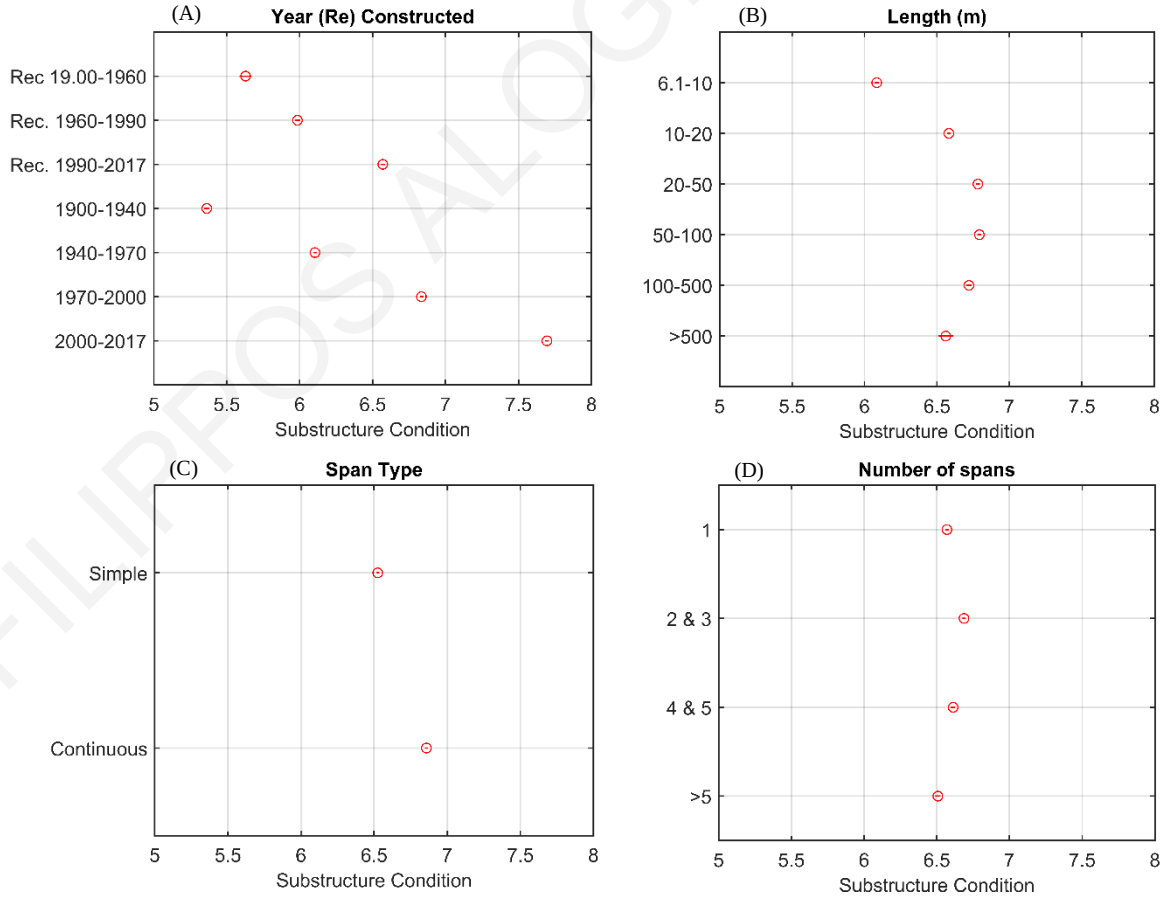

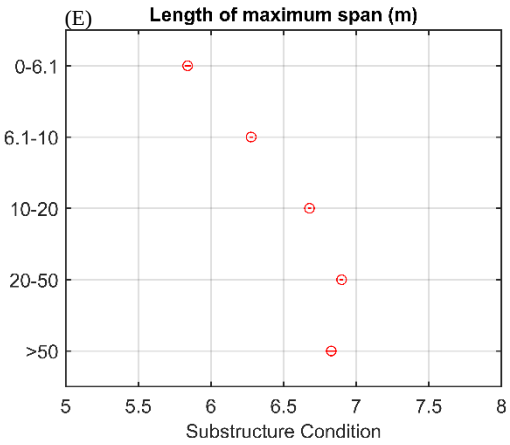

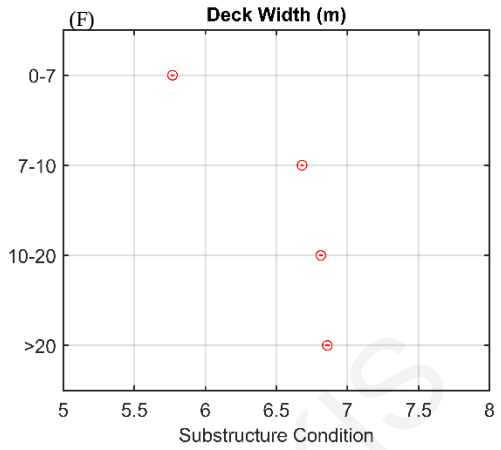

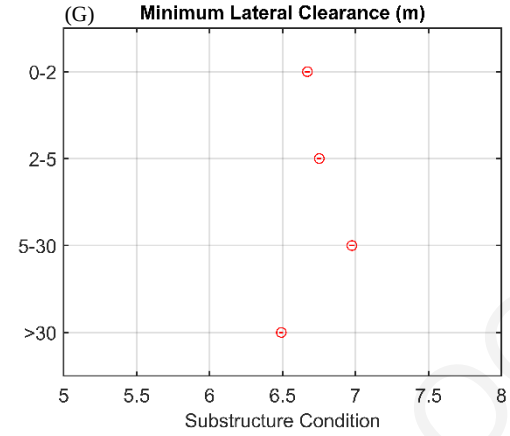

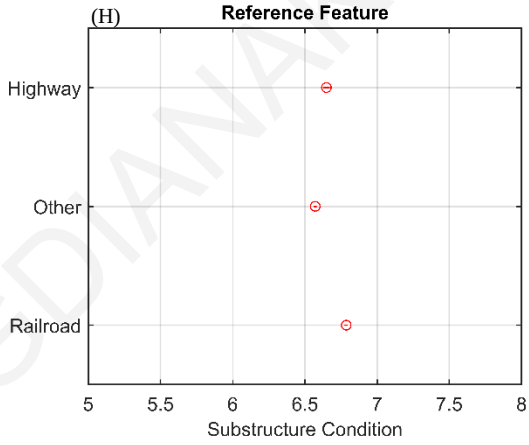

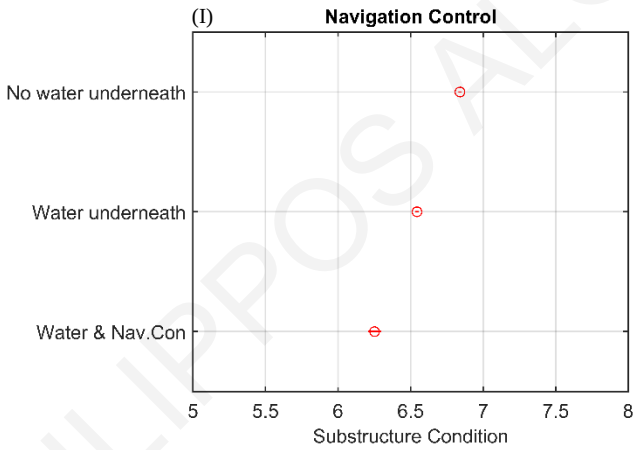

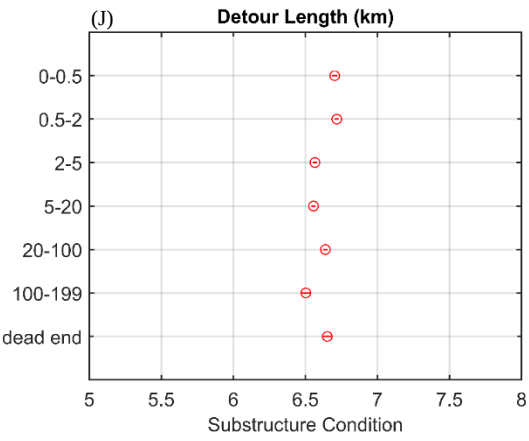

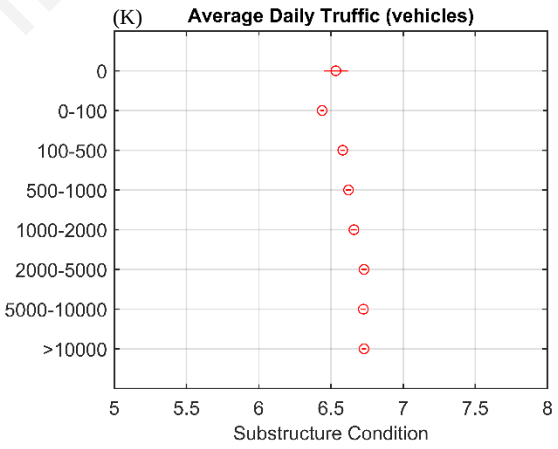

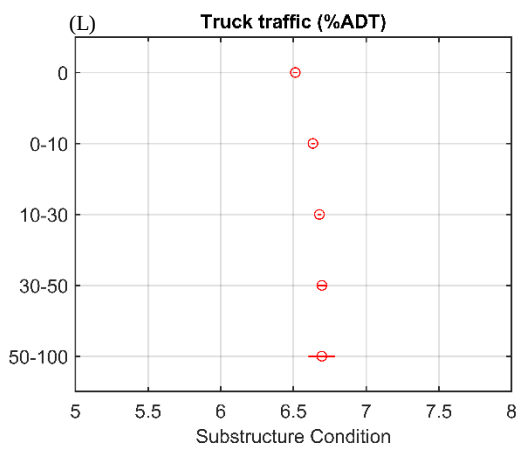

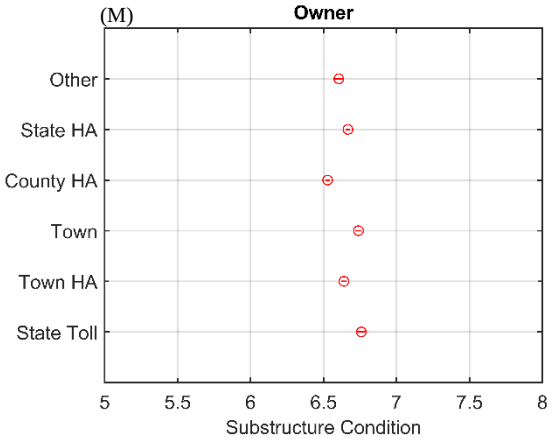

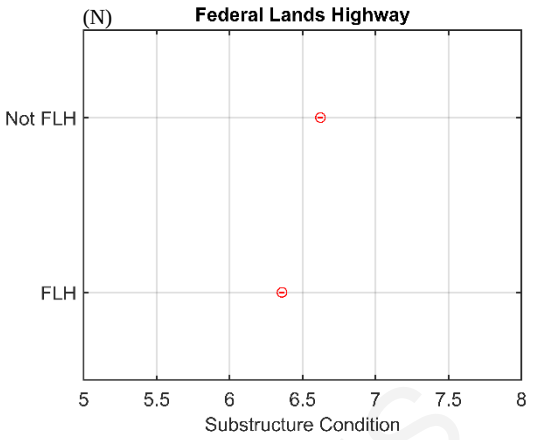

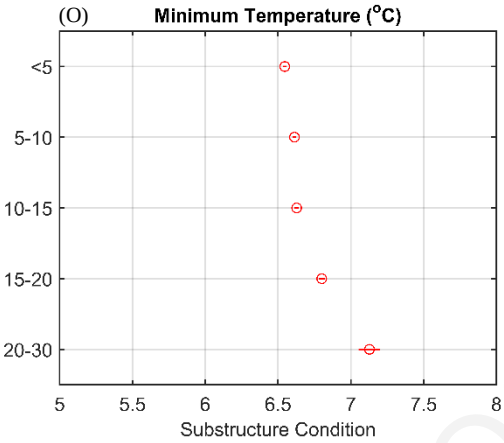

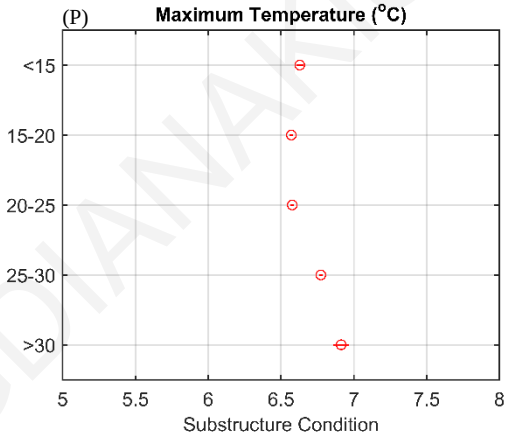

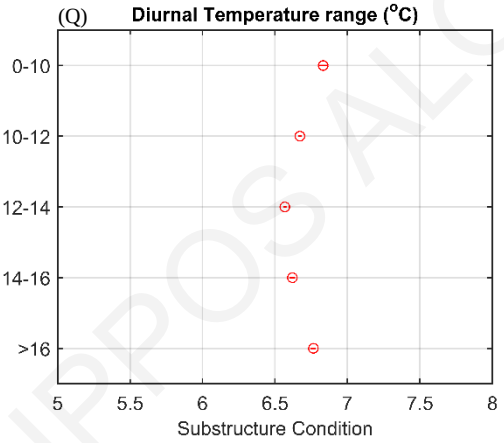

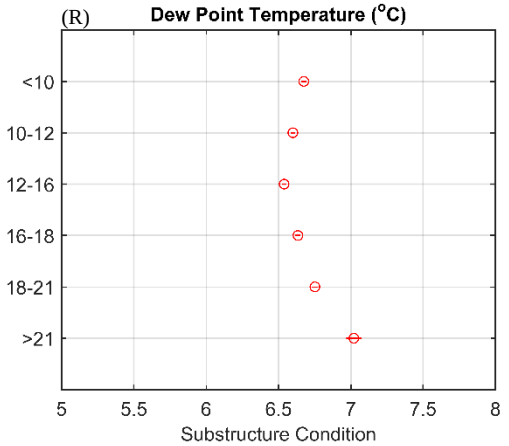

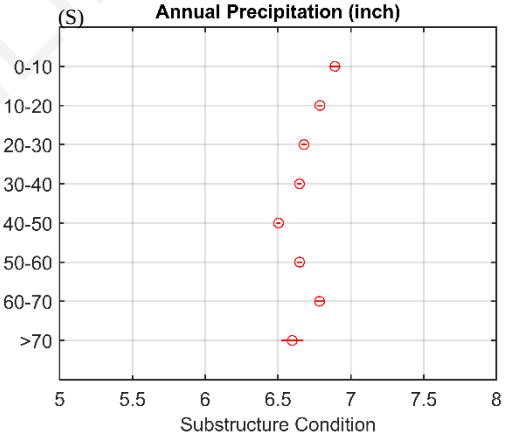

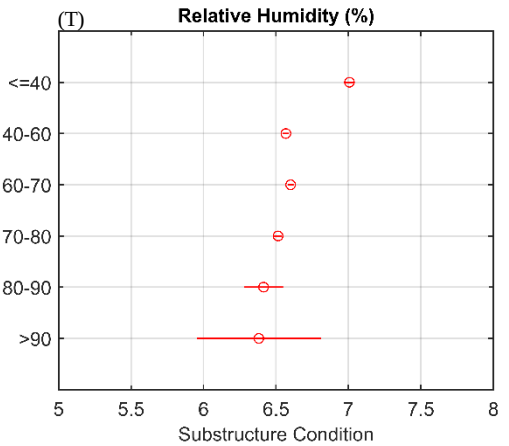

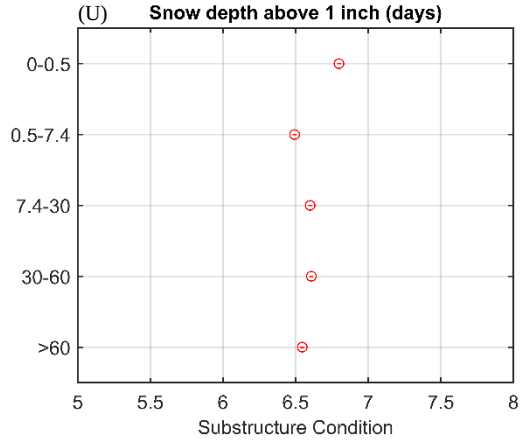

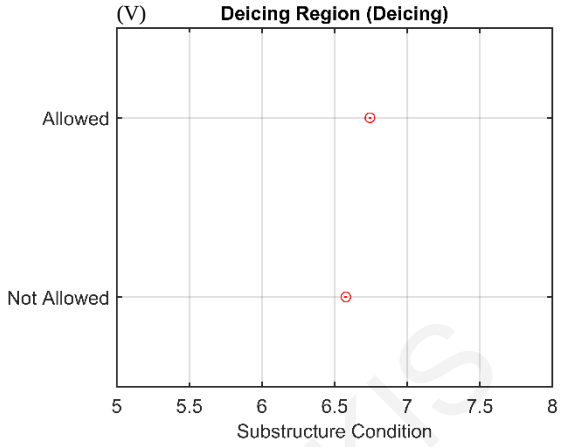

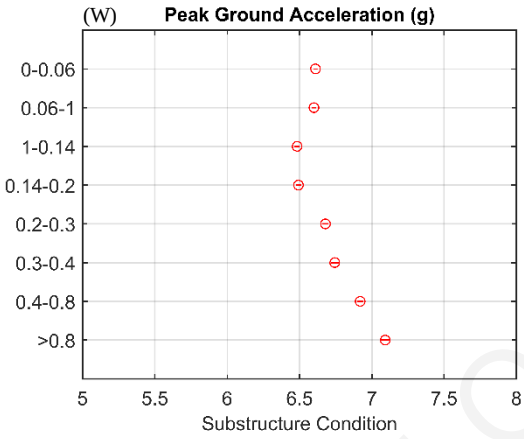

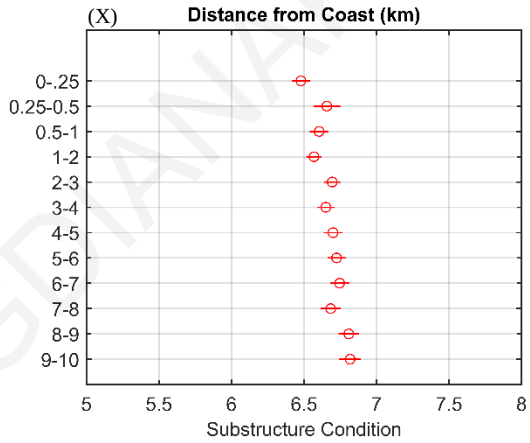

A-III. Appendix Chapter 5: Coastline effect on bridges

A-III.1. Hurricane prone areas of the coastline according to ASCE 7-10 (ASCE, 2010)

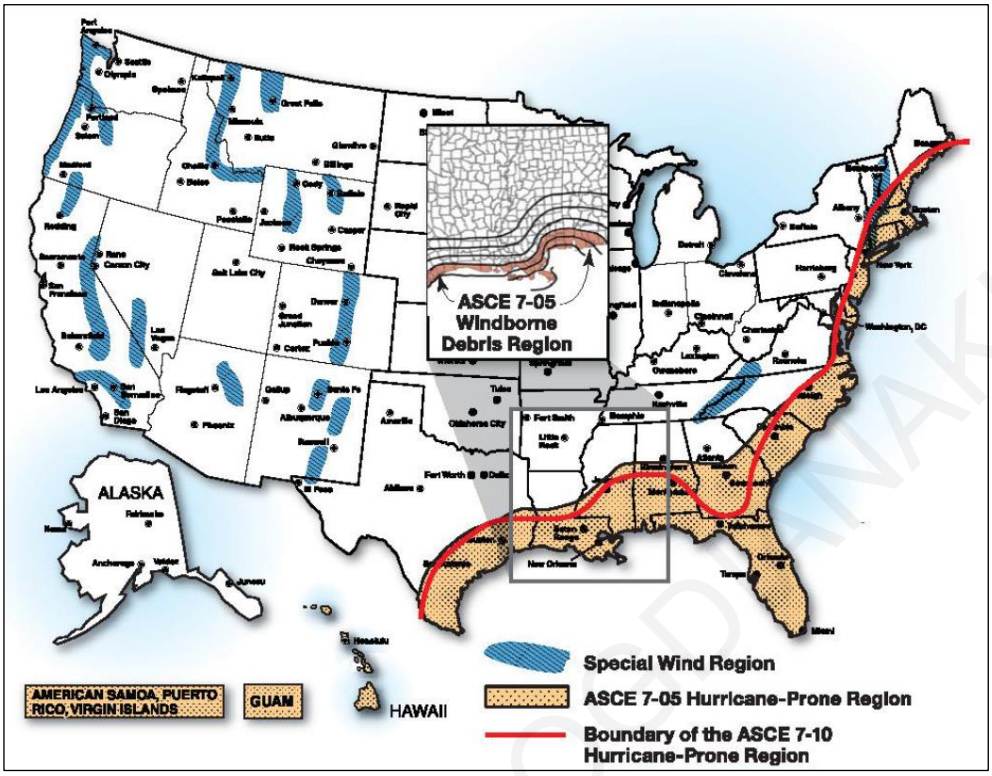

A-III. 2.Tsunami prone areas in the US (USGS, 2007).

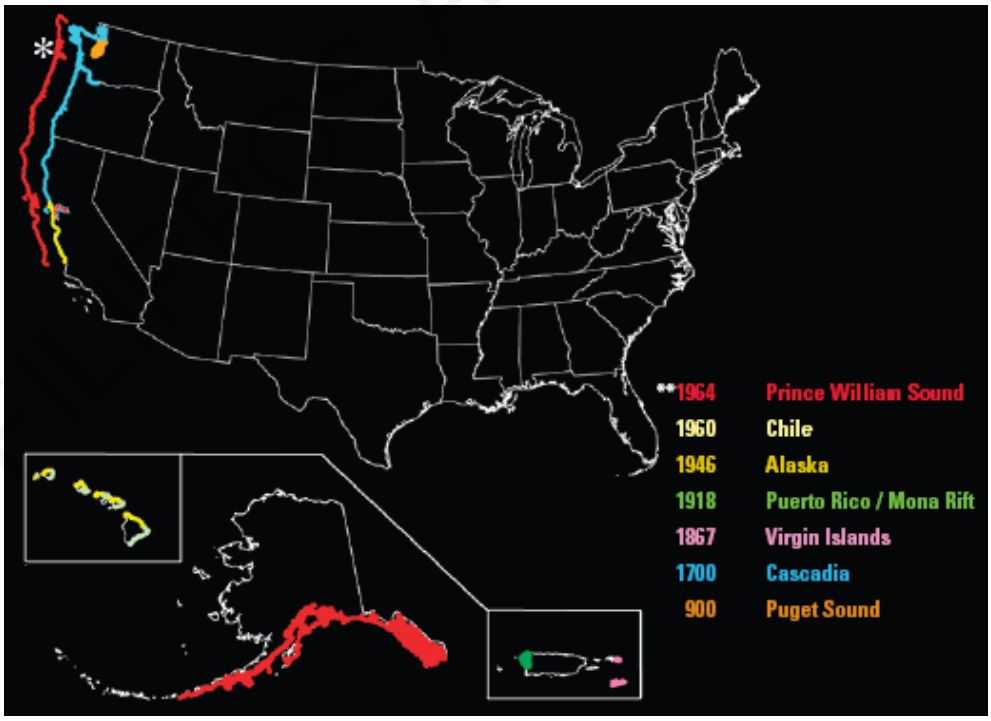

A-III.3. Ground elevation of bridges in the US by Kriging interpolation. Ordinary Kriging was used with the same parameters mentioned in Chapter 3 section 3.2.1. Furthermore, an exponential variogram was utilized exponential with parameters of: sill $4.86x10^4$, range 0.443 and nugget:0.

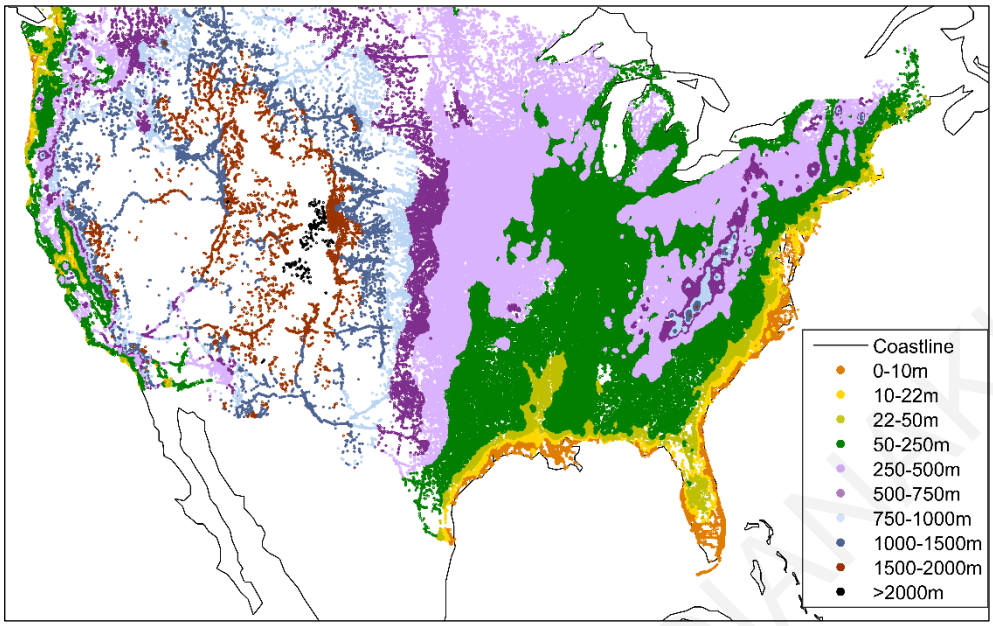

A-III.4.Descriptive statistics of continuous variables

	Min	Max	Mean	Median	St.d	Skew
Precipitation	9,85	112,18	47,11	48,49	14,29	-0,10
Elevation	-7,93	430,20	22,14	14,66	26,56	0,28
Pga	0,011	1,39	0,21	0,11	0,28	0,37
Not Reconstructed	1900	2016	1977,696	48,49373	20,81	92,70
Year Recostructed	1913	2016	1991,337	48,49373	15,49	125,42

A-III.5. Histograms for the variables of the coastline (vertical axis refers to number of bridges)

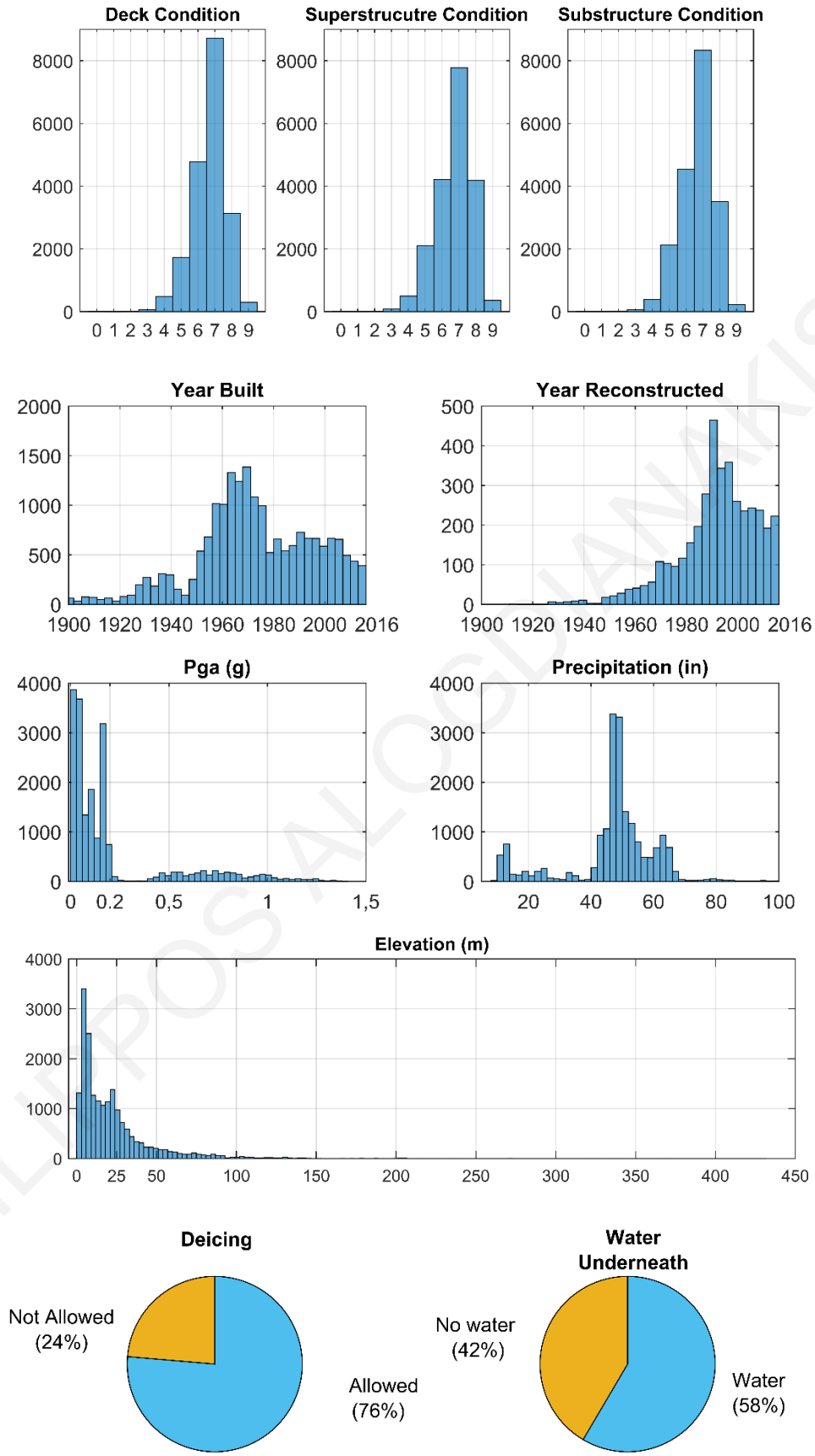

A-III.6. Interaction plots for structural condition of deck

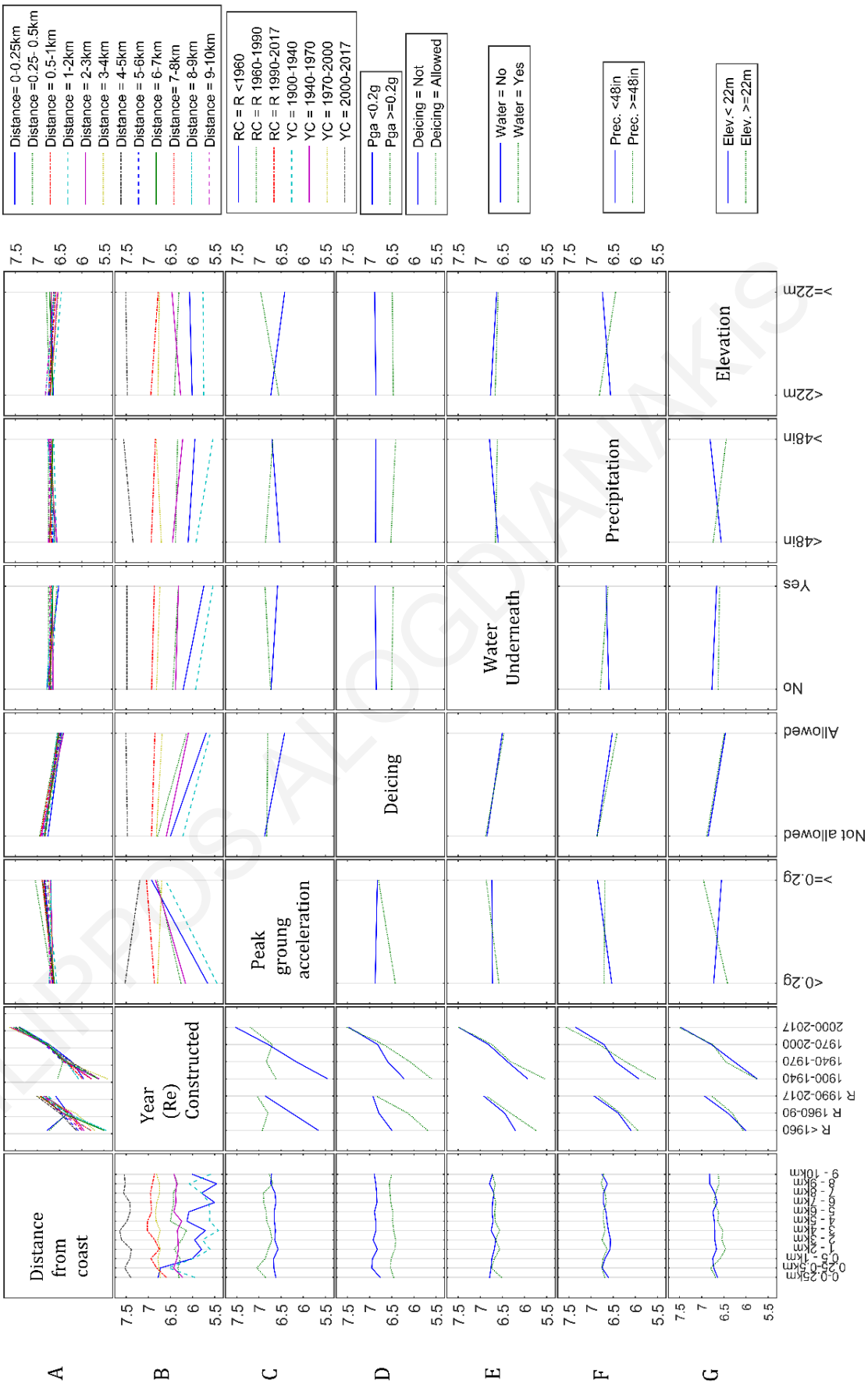

A-III.7. Interaction plots for structural condition of substructure

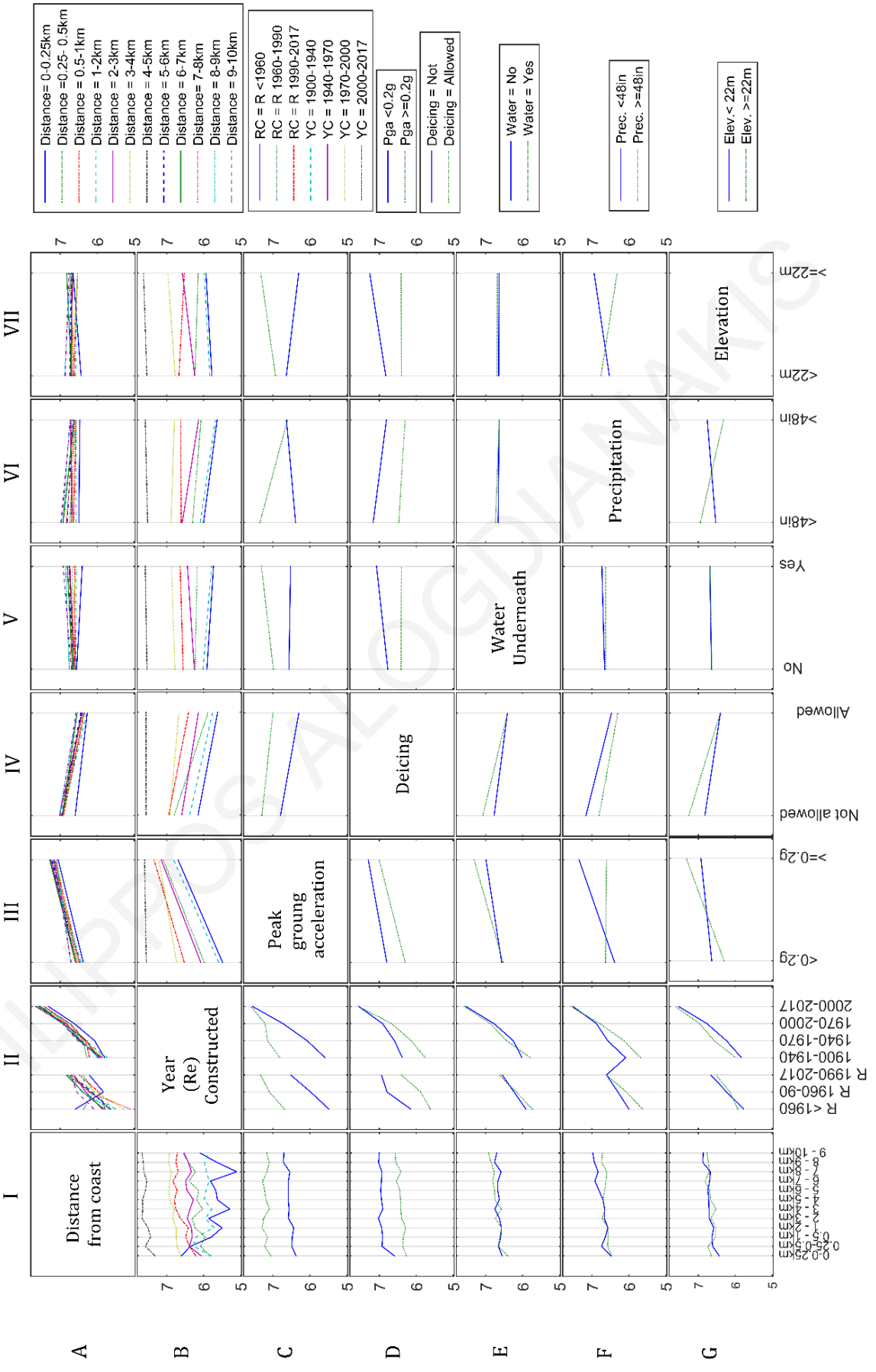

A-III.8. ANOVA for bridge elevations located within 250m inland from coastline

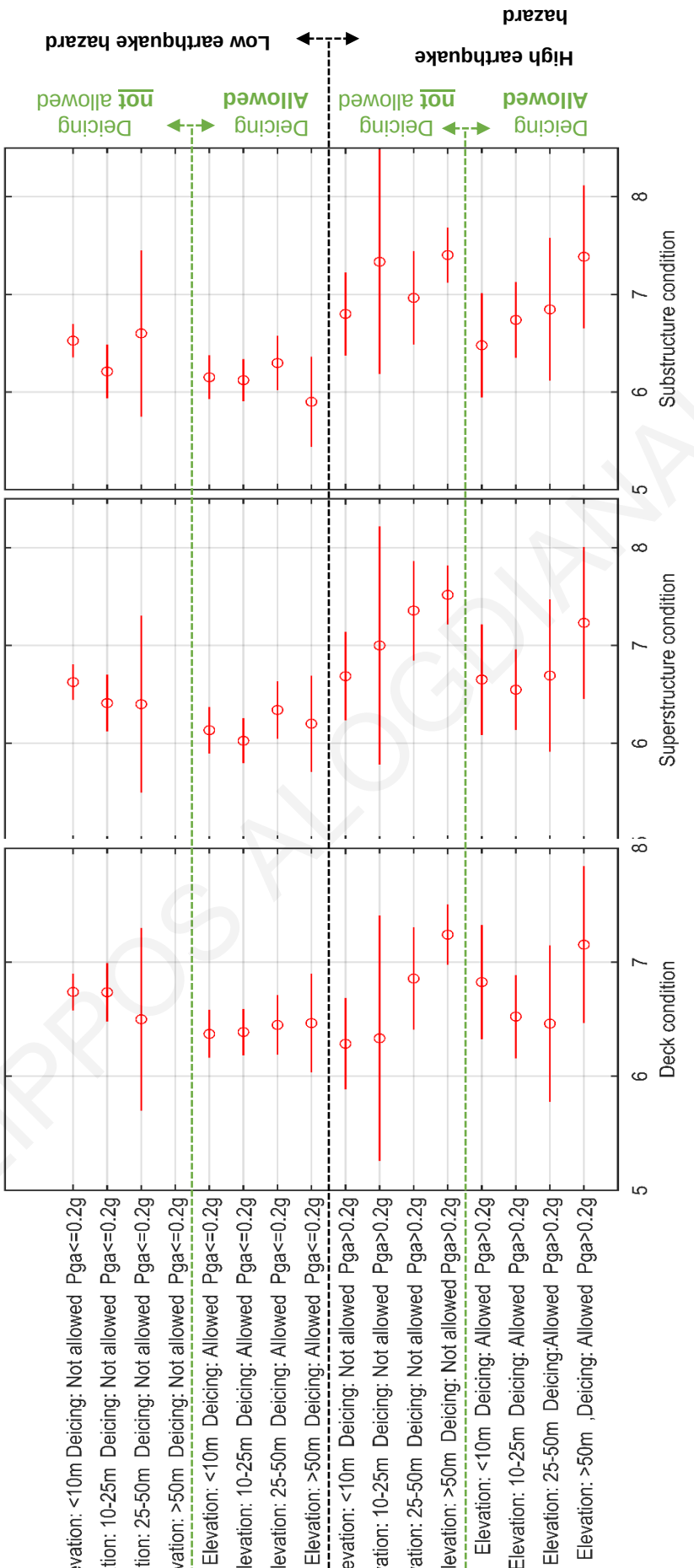

Results of ANOVA visualized by multiple comparisons. For the analysis 4 categories of elevation were organized (0-10m, 10-25m, 25-50m and above 50m). The analysis was carried out for the conditions of deck superstructure and substructure none of them had a significant difference based on the (α=0.05 level of significance)

A-IV. Appendix Chapter 6

A-IV.1 Deck condition interaction plot

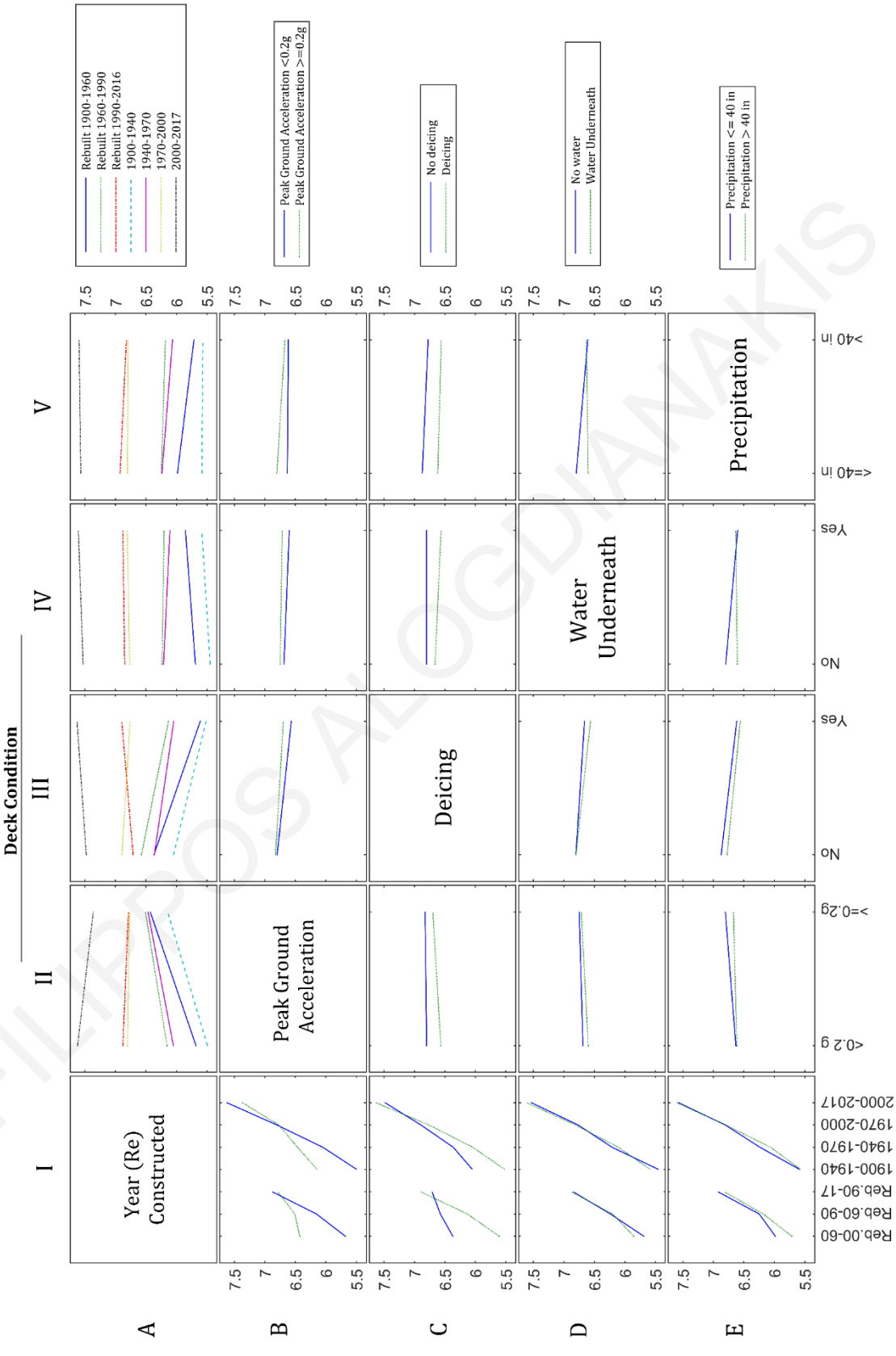

A-IV.2 Superstructure condition interaction plot

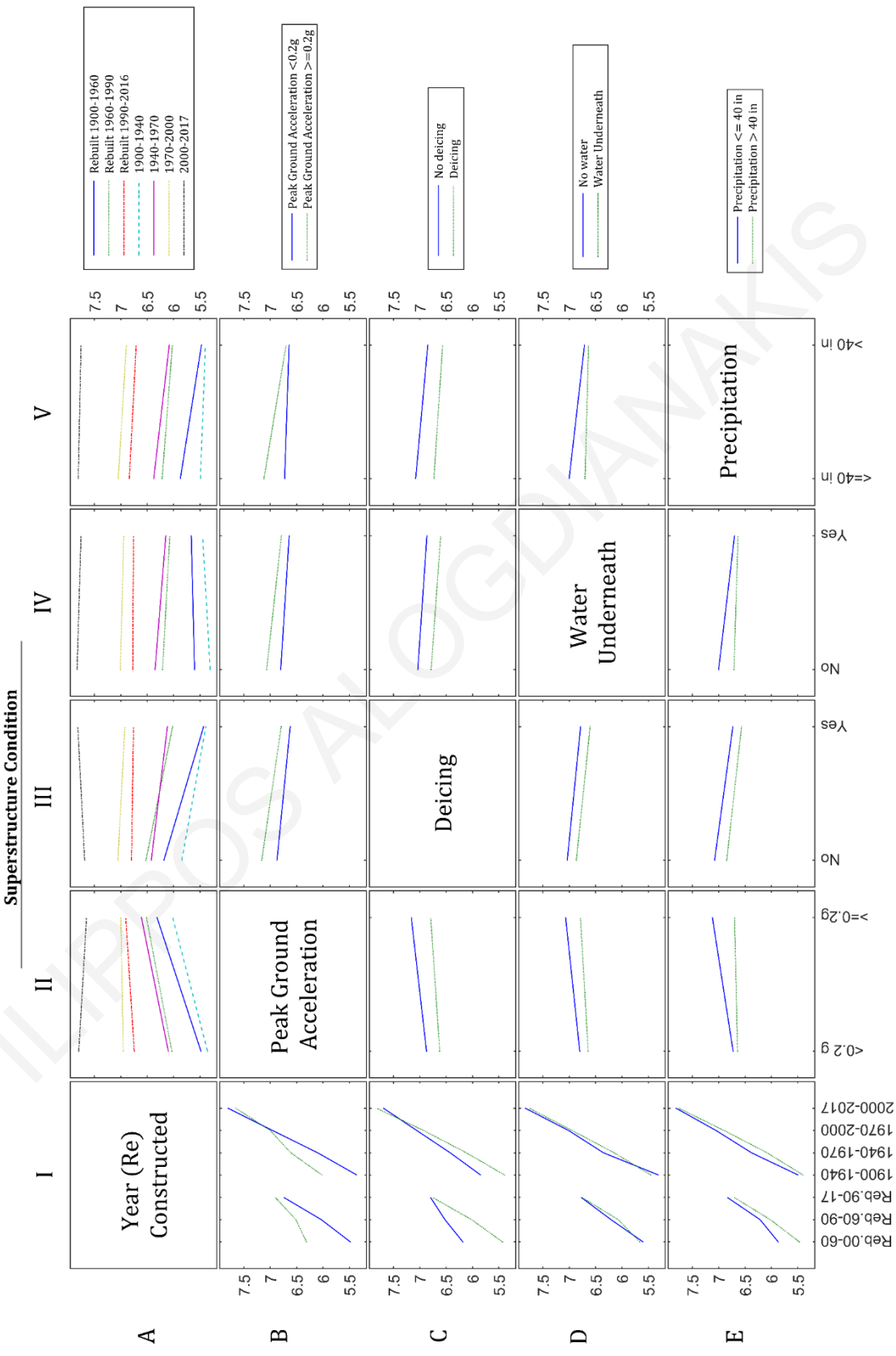

A-IV.3 Substructure condition interaction plot

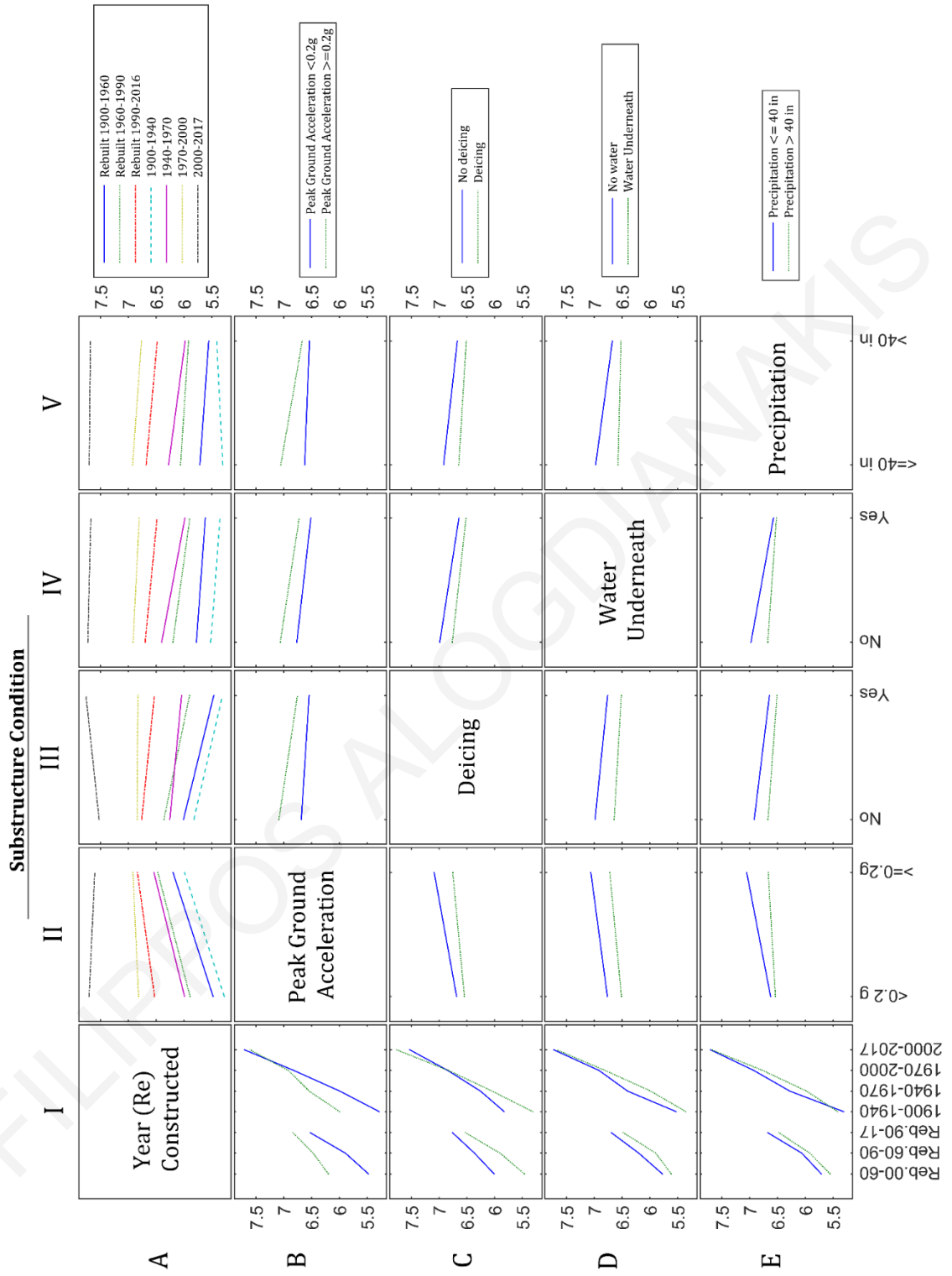

A-IV.4. Map distribution of superstructure materials

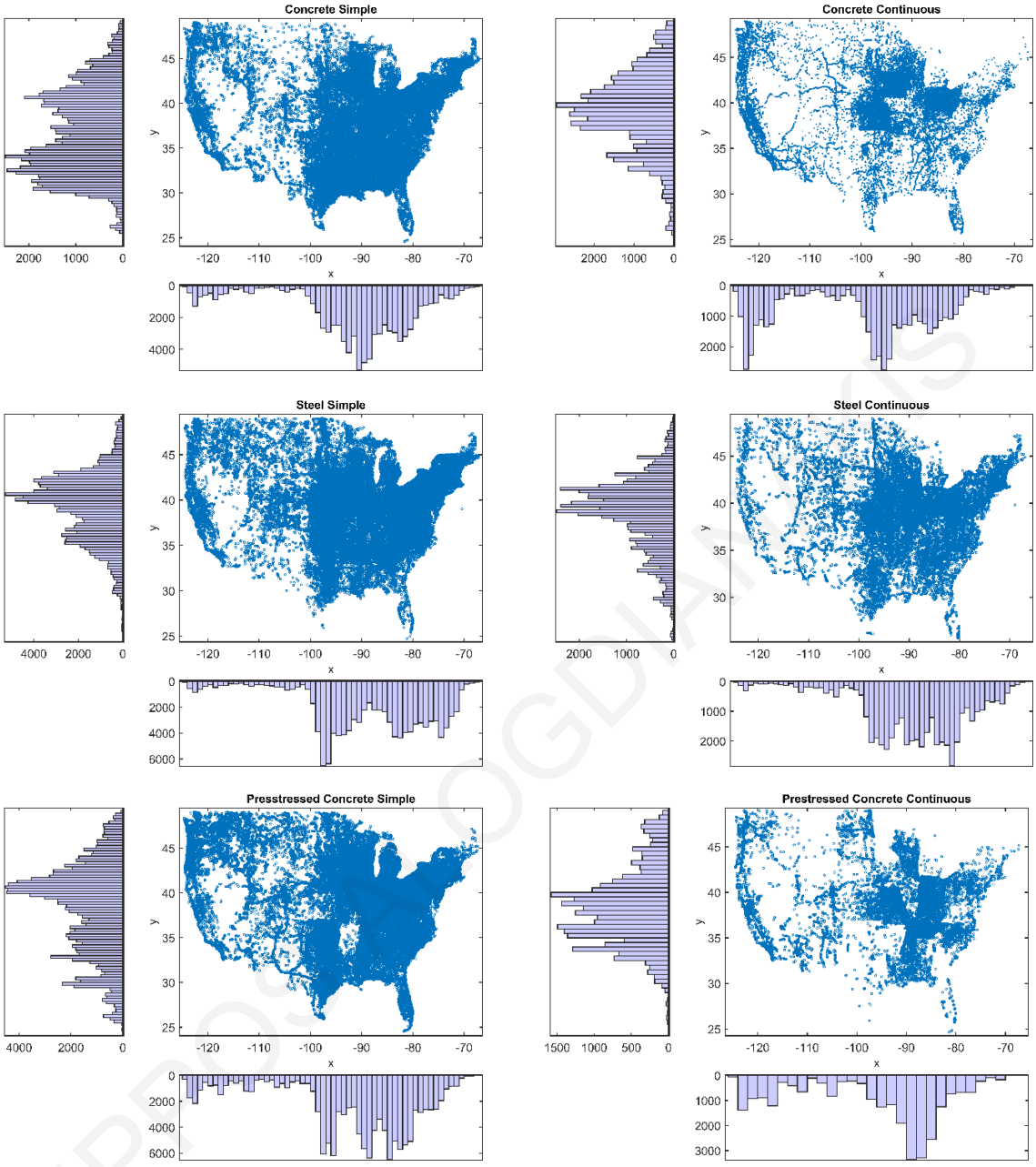

A-IV.5. Carbon dioxide emissions in the US from http://vulcan.project.asu.edu/

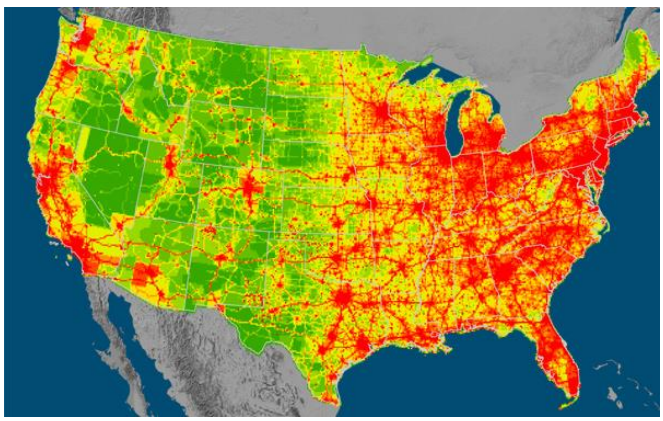

A-IV.6. Deck and Substructure age distributions for deicing water environment

Deicing no water

Descriptive statistics for 60 year sample

Material	Non rehabilitated					Rehabilitated (based on year built)					Rehabilitated based on year rehabilitated				
	size	mean	median	Std	Skew	size	mean	median	Std	Skew	size	mean	median	Std	Skew
Deck / Substructure- Simple spans	26352	30,6	33	17,9	-0,1	5625	50,3	51	7,1	-0,1	7469	20,50783	20	12,2	0,0
Deck / Substructure- Continuous spans	21225	31,5	35	16,9	-0,2	5732	49,6	51	7,2	-0,2	6656	18,21905	18	10,5	0,0

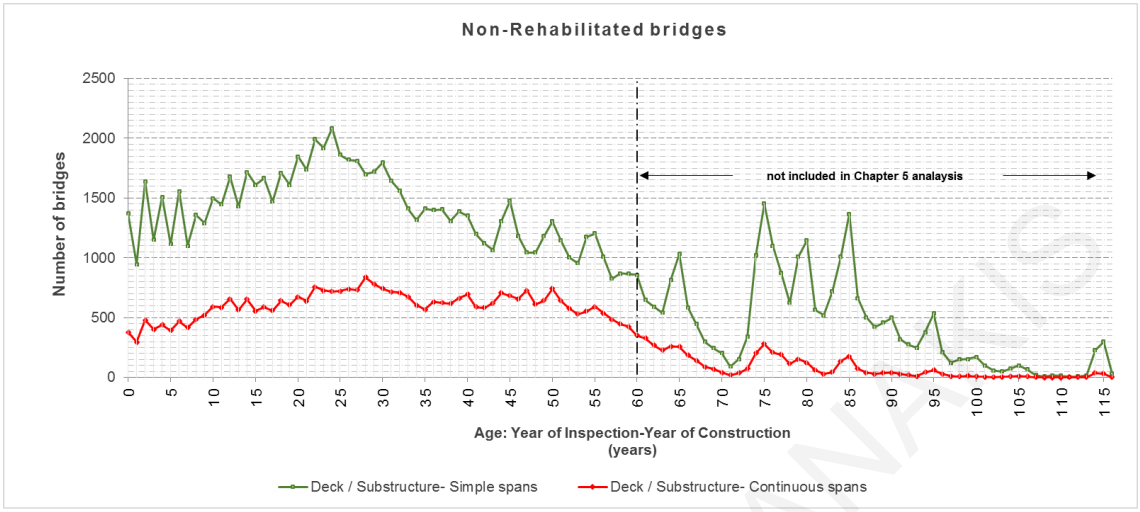

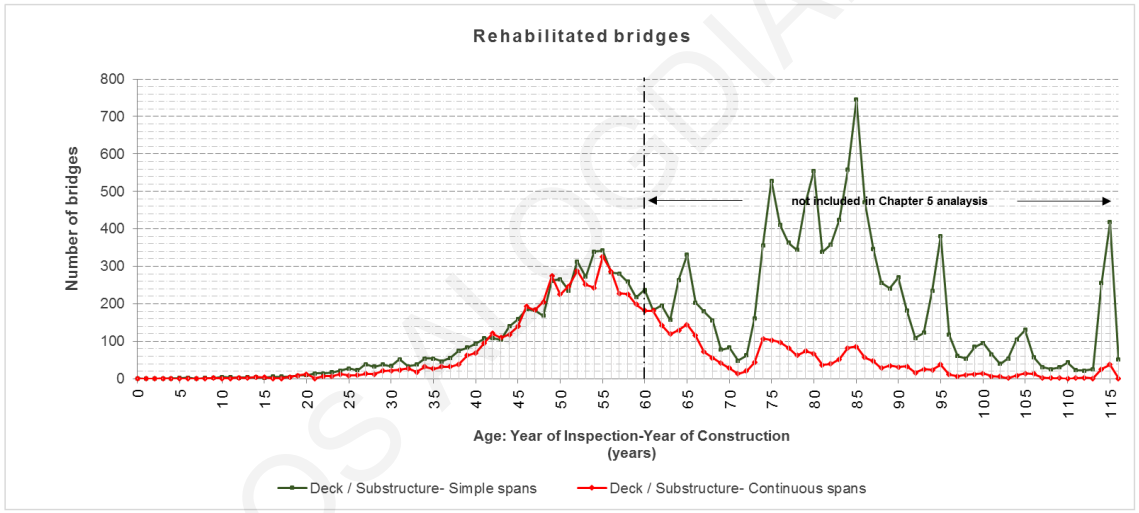

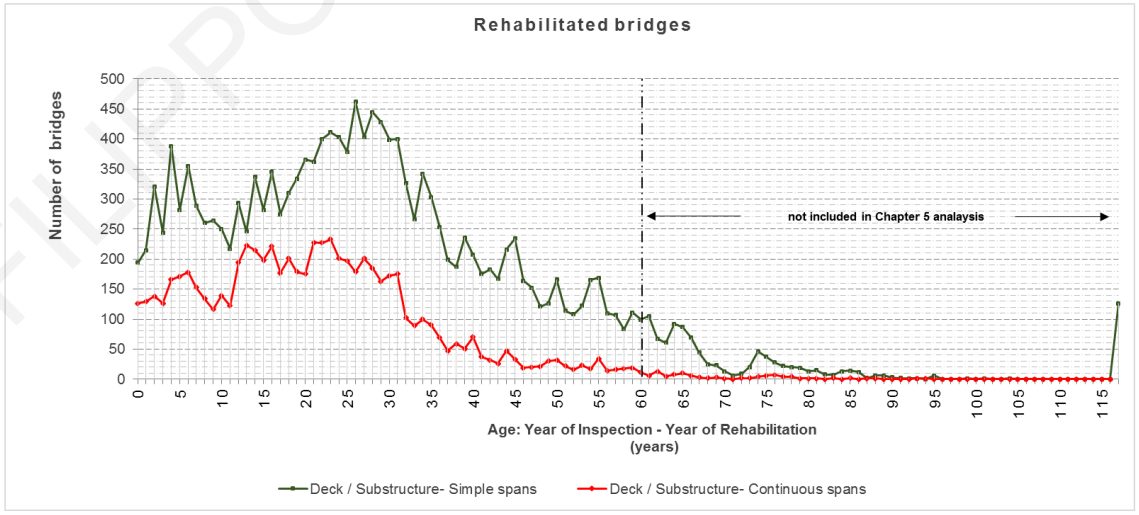

A-IV.7 Deck and Substructure age distributions for deicing no water environment

Deicing no water

Descriptive statistics for 60 year sample

Material	Non rehabilitated					Rehabilitated (based on year built)					Rehabilitated based on year rehabilitated				
	size	mean	median	Std	Skew	size	mean	median	Std	Skew	size	mean	median	Std	Skew
Deck / Substructure- Simple spans	26352	30,6	33	17,9	-0,1	5625	50,3	51	7,1	-0,1	7469	20,50783	20	12,2	0,0
Deck / Substructure- Continuous spans	21225	31,5	35	16,9	-0,2	5732	49,6	51	7,2	-0,2	6656	18,21905	18	10,5	0,0

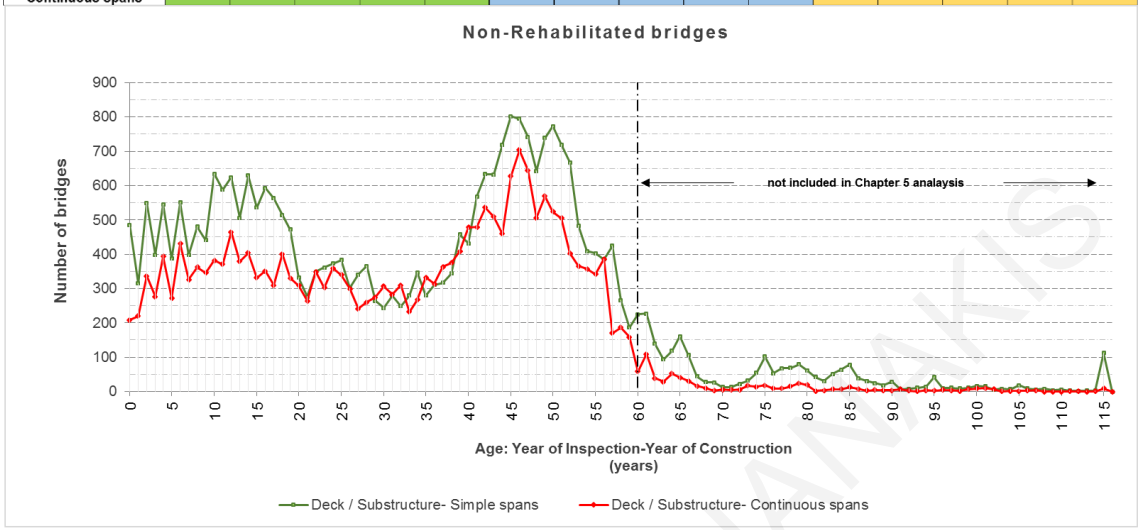

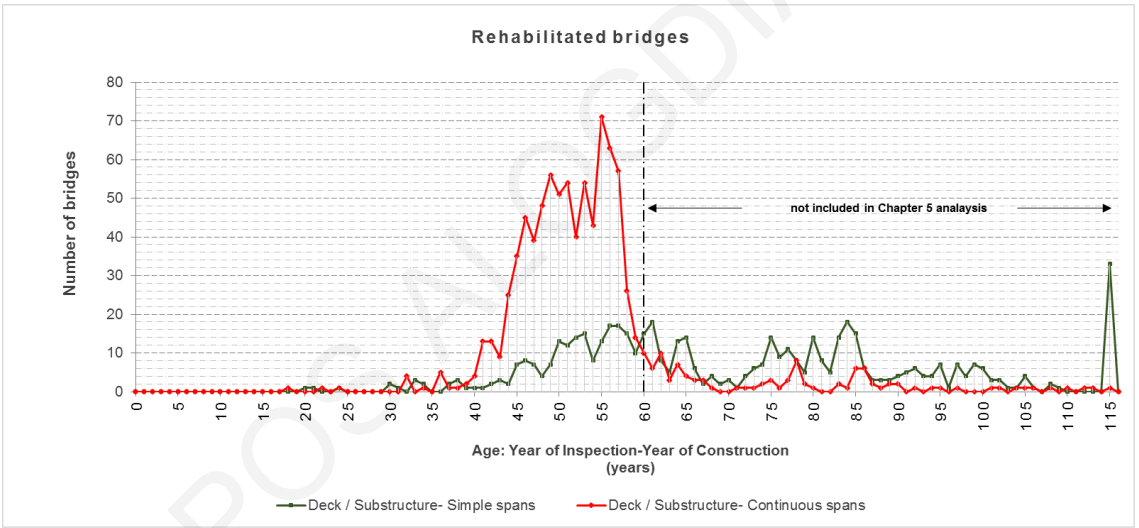

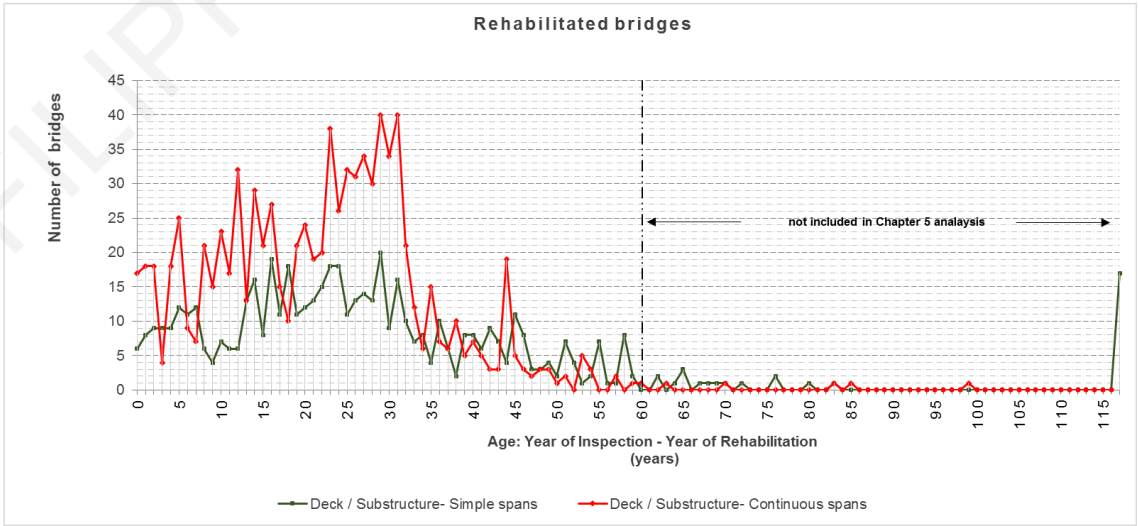

A-IV.8. Deck and Substructure age distributions for no deicing water environment

No Deicing Water Descriptive statistics for 60 year sample															
Material	Non rehabilitated					Rehabilitated (based on year built)					Rehabilitated based on year rehabilitated				
	size	mean	median	Std	Skew	size	mean	median	Std	Skew	size	mean	median	Std	Skew
Deck / Substructure-Simple spans	43688	29,5	29	17,2	0,0	2749	46,4	49	10,5	-0,3	4859	28,81828	26	16,8	0,2
Deck / Substructure-Continuous spans	5566	28,4	26	17,2	0,1	502	46,5	50	11,9	-0,3	1060	28,98491	27	15,5	0,1

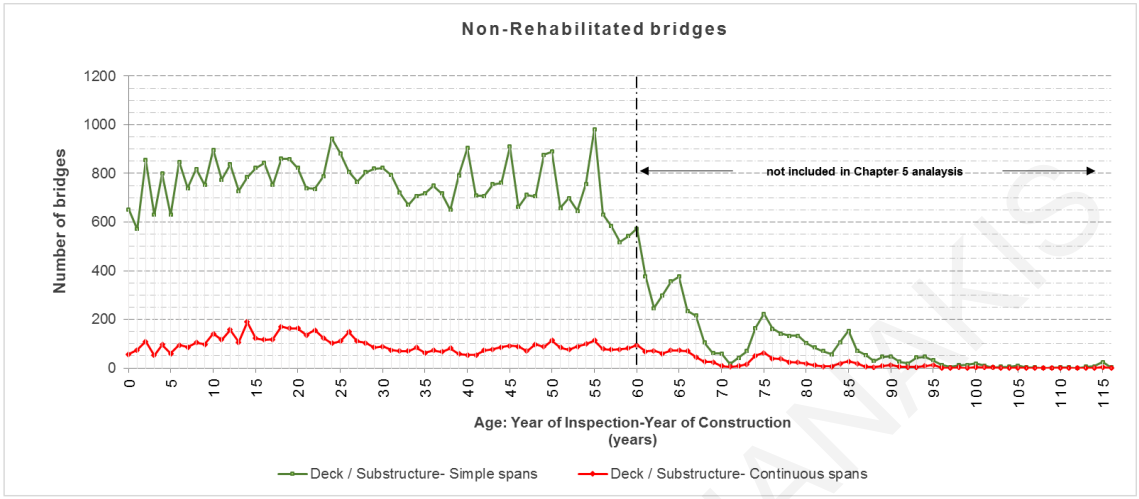

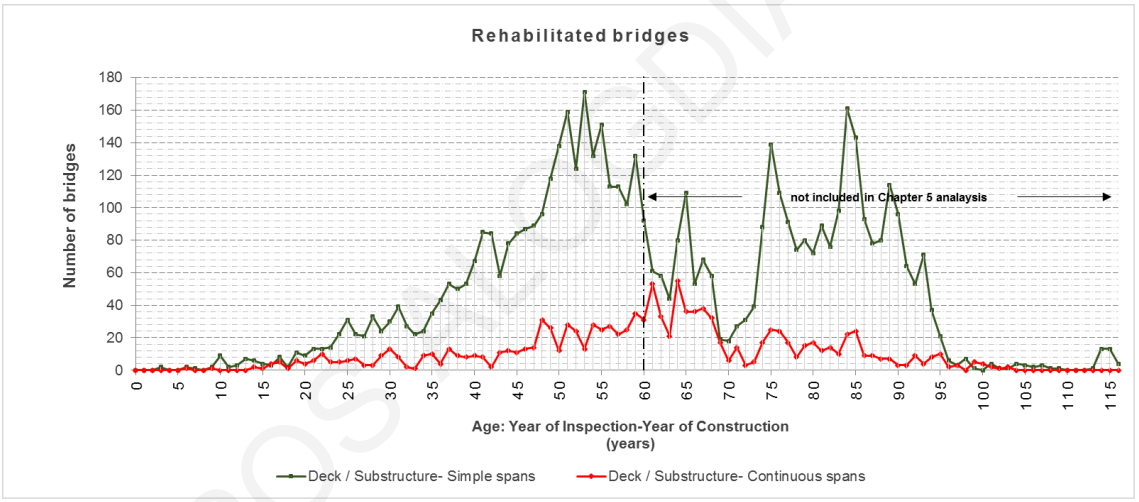

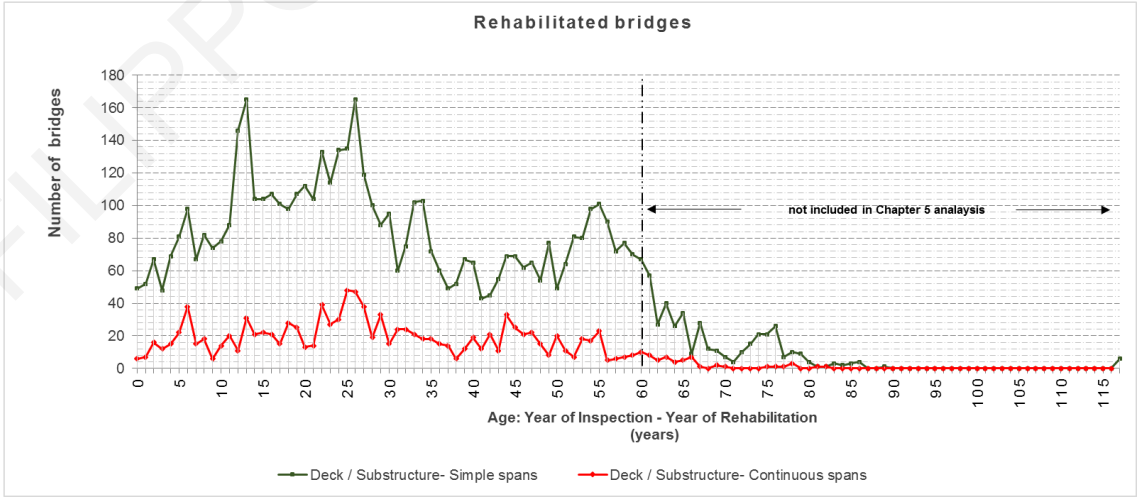

A-IV.9. Deck and Substructure age distributions for no deicing no water environment

No deicing no water

Descriptive statistics for 60 year sample

Material	Non rehabilitated					Rehabilitated (based on year built)					Rehabilitated based on year rehabilitated				
	size	mean	median	Std	Skew	size	mean	median	Std	Skew	size	mean	median	Std	Skew
Deck / Substructure- Simple spans	12423	28,5	28	17,0	0,0	1655	43,8	47	10,5	-0,3	1810	18,49282	18	12,3	0,0
Deck / Substructure- Continuous spans	5923	32,1	35	16,7	-0,2	574	47,7	50	8,9	-0,3	629	21,98251	23	12,0	-0,1

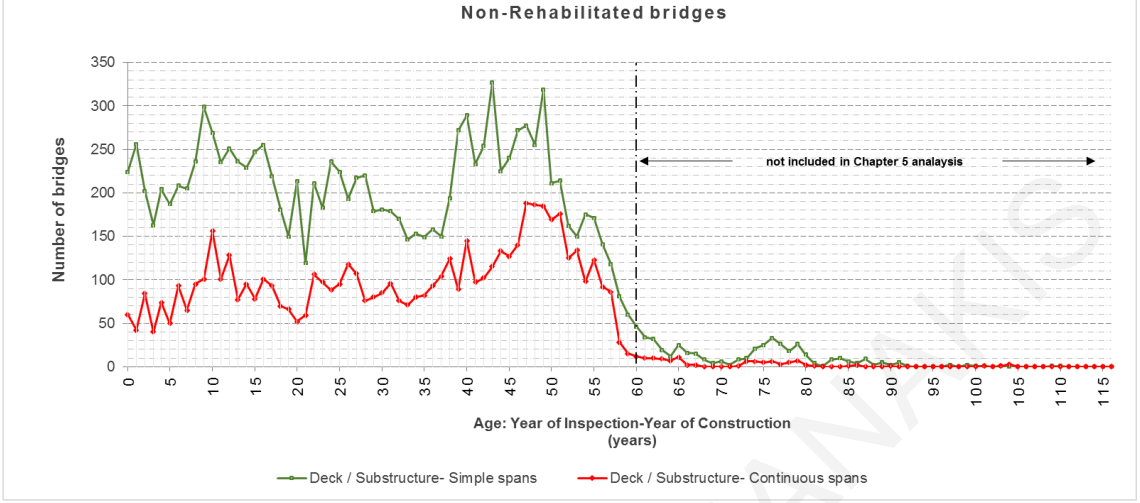

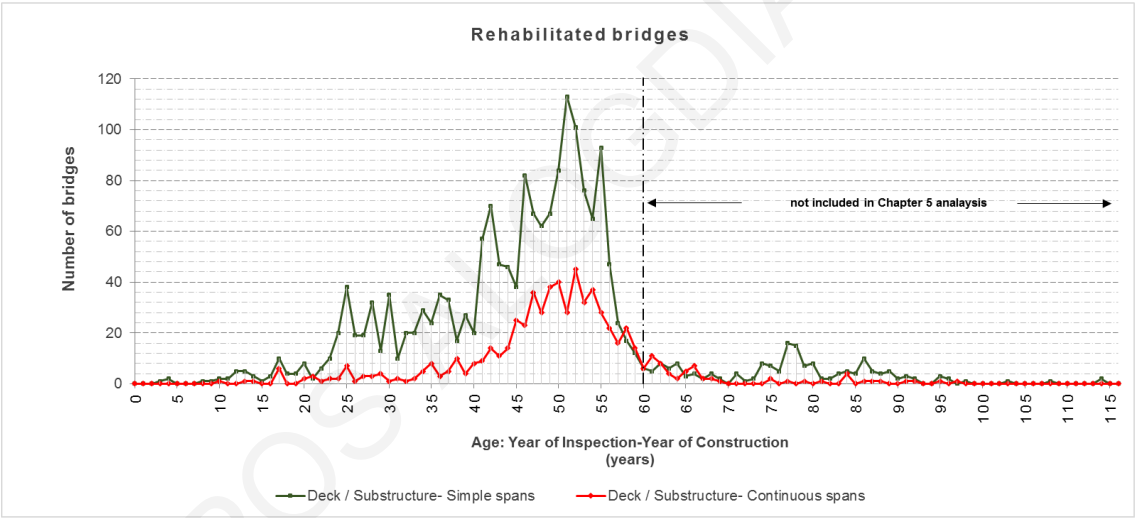

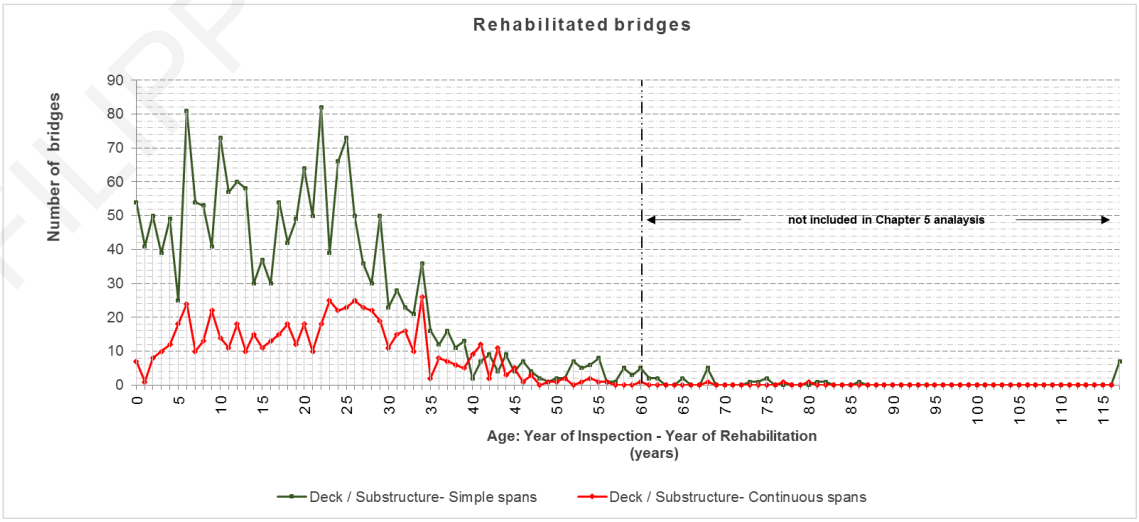

A-IV.10. Superstructure age distributions for deicing water environment

Deicing Water Descriptive statistics for 60 year sample															
Material	Non rehabilitated					Rehabilitated (based on year built)					Rehabilitated based on year rehabilitated				
	size	mean	median	Std	Skew	size	mean	median	Std	Skew	size	mean	median	Std	Skew
Concrete Simple	14730	34,4	35	17,5	0,0	774	50,0	53	8,8	-0,3	3803	30,3	30	16,9	0,0
Concrete Continuous	16902	33,0	33	16,4	0,0	1303	49,8	51	7,9	-0,2	2027	23,2	21	14,4	0,2
Steel Simple	23732	29,4	27	17,3	0,1	2138	49,9	52	9,2	-0,2	7463	25,1	25	15,2	0,0
Steel Continuous	11313	34,3	37	16,1	-0,2	2747	50,5	52	7,4	-0,2	4167	19,3	19	12,2	0,0
Prestressed Conc. Simple	46735	25,3	25	14,7	0,0	2464	46,9	49	9,5	-0,2	5124	20,8	21	13,3	0,0
Prestressed Conc. Continuous	8356	21,3	21	12,2	0,0	608	44,9	46	9,5	-0,1	839	17,3	17	10,5	0,0

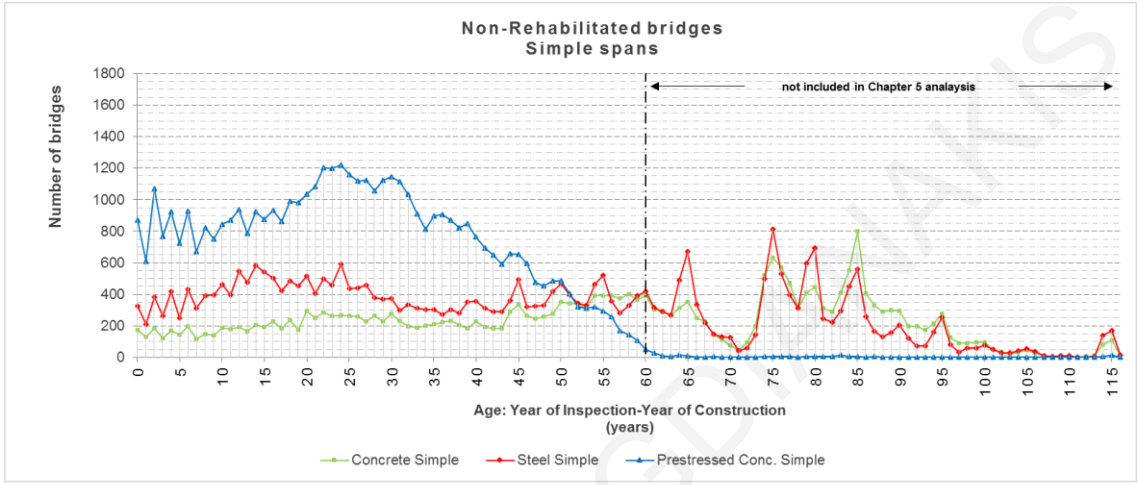

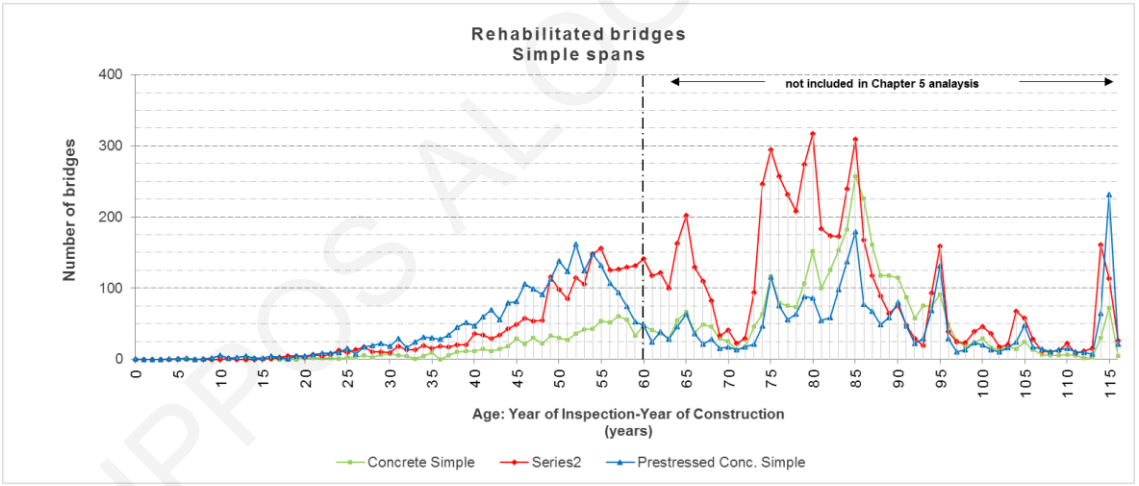

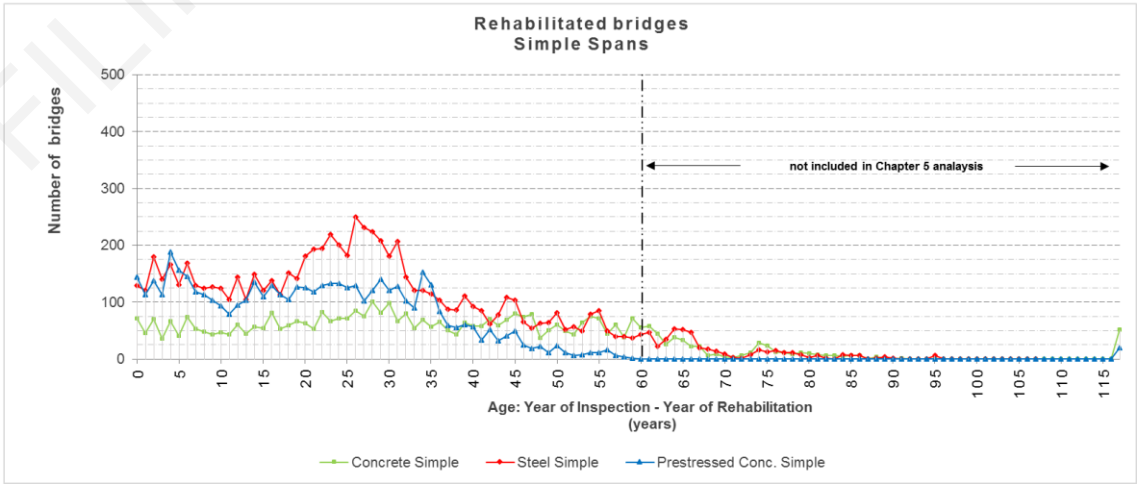

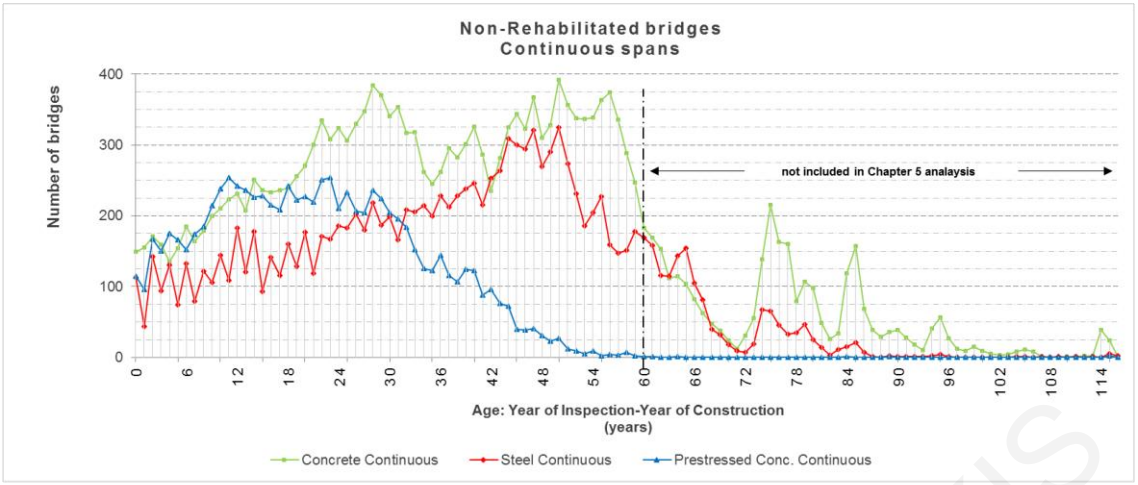

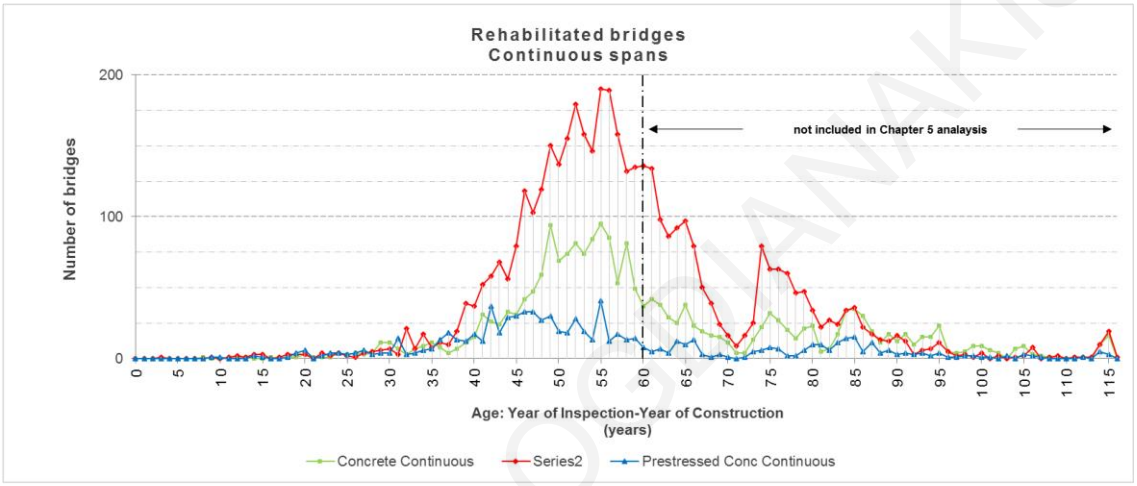

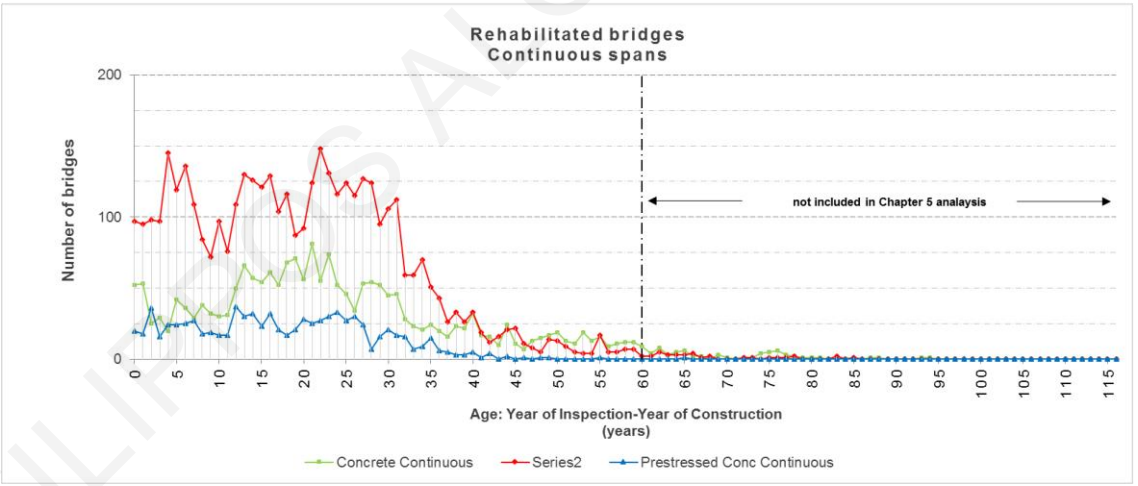

A-IV.11. Superstructure age distributions for deicing no water environment

Deicing no water

Descriptive statistics for 60 year sample

Material	Non rehabilitated					Rehabilitated (based on year built)					Rehabilitated based on year rehabilitated				
	size	mean	median	Std	Skew	size	mean	median	Std	Skew	size	mean	median	Std	Skew
Concrete Simple	3147	21,2	15	17,7	0,4	170	51,5	53	7,3	-0,2	429	24,0	23	14,0	0,1
Concrete Continuous	4570	38,6	45	17,0	-0,4	758	50,8	51	5,3	0,0	838	21,4	23	11,6	-0,1
Steel Simple	10517	38,3	43	15,7	-0,3	3630	51,5	52	6,5	-0,1	4819	21,1	21	12,1	0,0
Steel Continuous	12144	33,5	37	15,7	-0,2	4577	49,7	51	7,0	-0,2	5392	17,8	17	10,3	0,1
Prestressed Conc. Simple	12688	26,6	24	17,2	0,2	1825	48,0	50	7,7	-0,3	2221	18,6	18	11,6	0,1
Prestressed Conc. Continuous	4511	19,1	16	13,2	0,2	397	46,5	48	10,1	-0,2	426	17,1	16	9,6	0,1

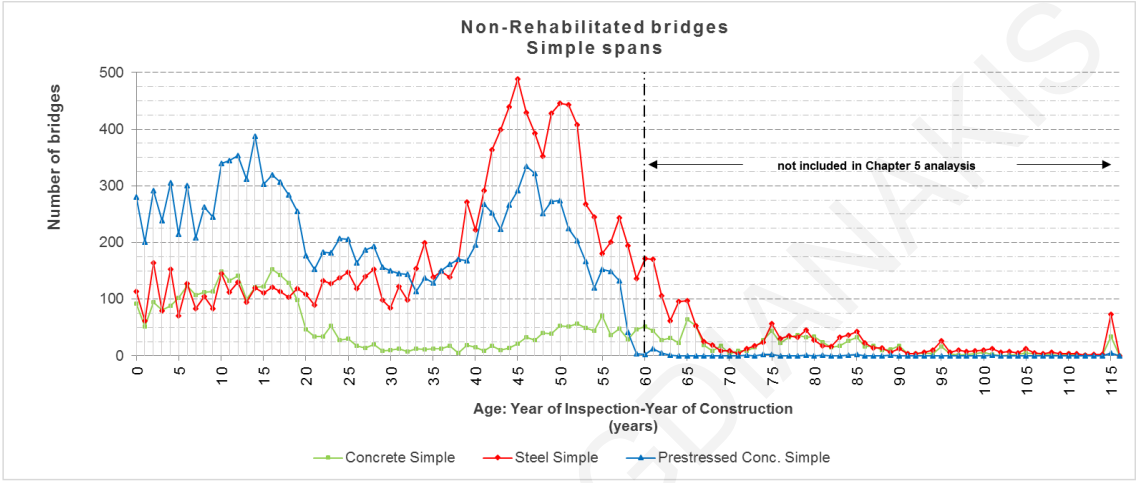

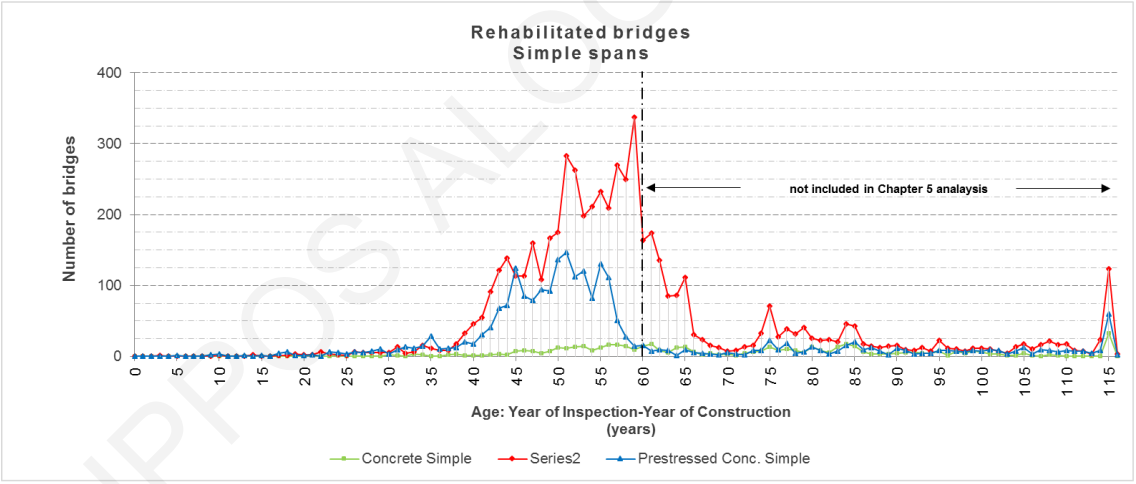

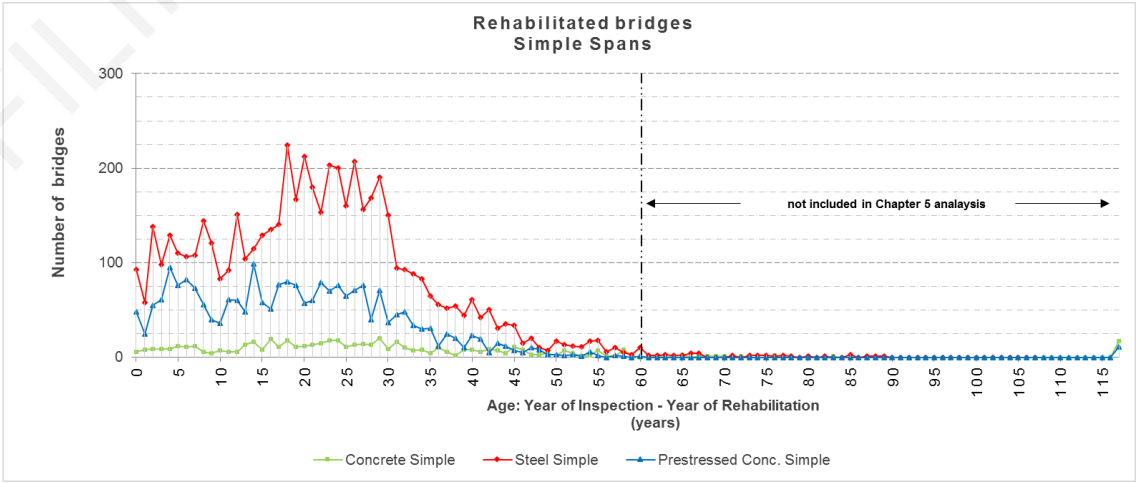

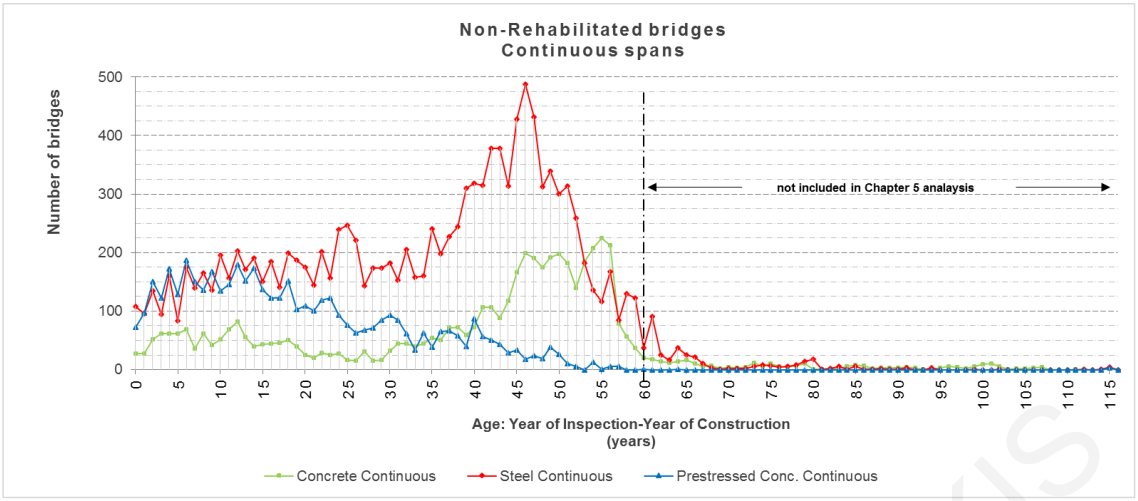

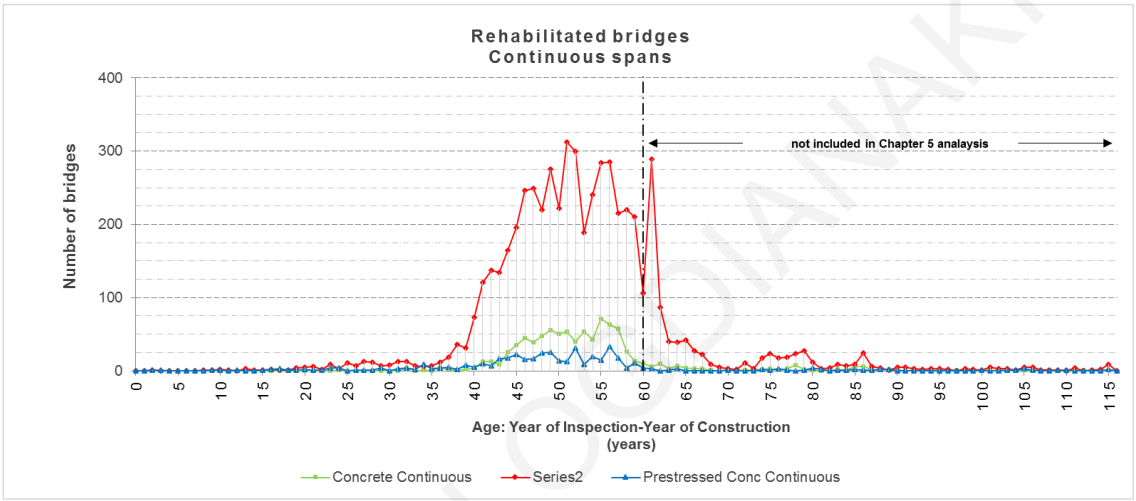

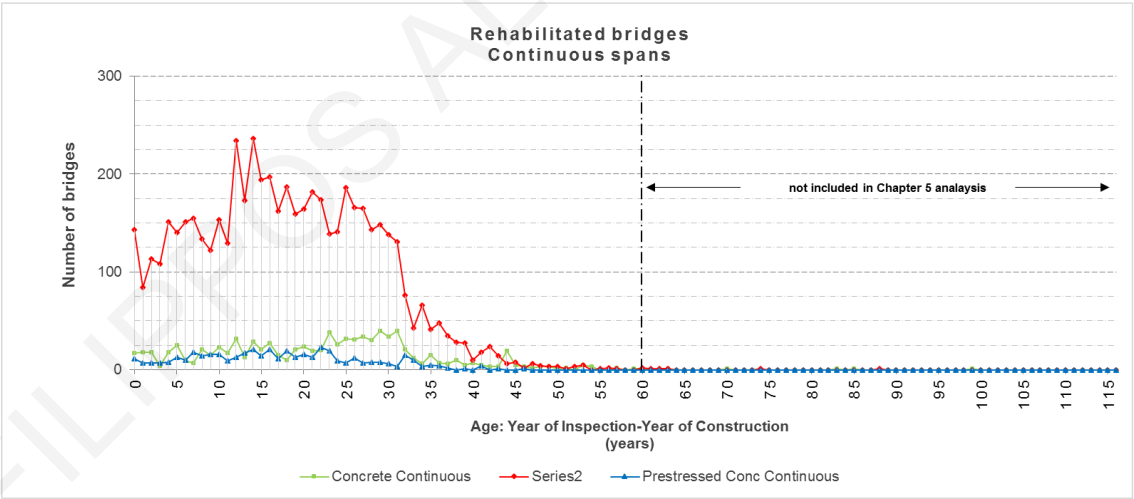

A-IV.12. Superstructure age distributions for no deicing water environment

No Deicing water

Descriptive statistics for 60 year sample

Material	Non rehabilitated					Rehabilitated (based on year built)					Rehabilitated based on year rehabilitated				
	size	mean	median	Std	Skew	size	mean	median	Std	Skew	size	mean	median	Std	Skew
Concrete Simple	21887	34,9	37	16,4	-0,1	1547	49,3	51	8,1	-0,2	3128	31,6	29	17,1	0,2
Concrete Continuous	2061	32,1	29	17,3	0,2	233	46,5	49	11,2	-0,2	574	32,1	31	15,4	0,1
Steel Simple	3334	33,4	36	19,2	-0,1	224	45,0	51	13,5	-0,4	642	32,7	32	16,0	0,0
Steel Continuous	1635	34,6	38	18,3	-0,2	251	47,5	52	12,3	-0,4	466	25,8	25	14,8	0,1
Prestressed Conc. Simple	18467	22,4	21	15,1	0,1	978	42,1	45	11,5	-0,3	1089	18,4	19	11,6	-0,1
Prestressed Conc. Continuous	1870	18,9	18	11,2	0,1	18	32,9	33,5	7,6	-0,1	20	12,9	10	9,4	0,3

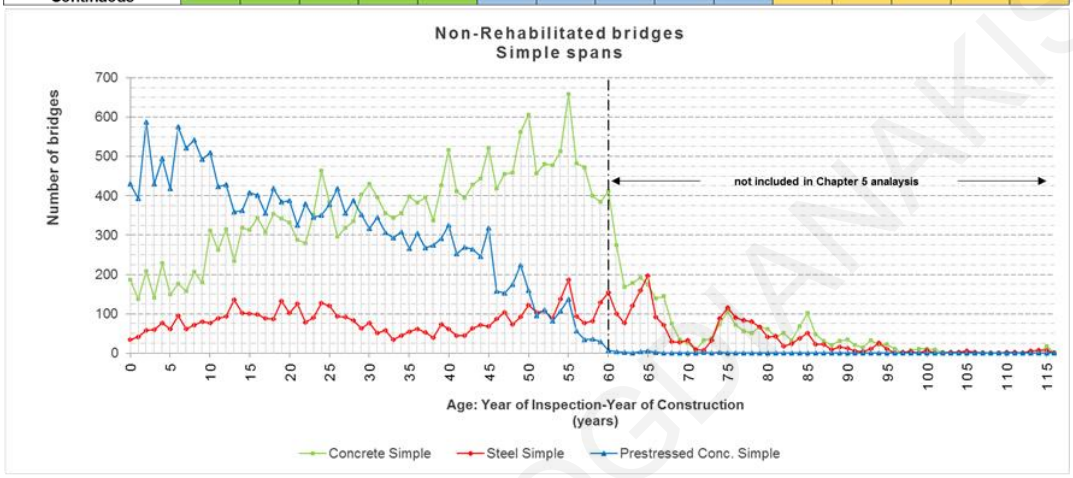

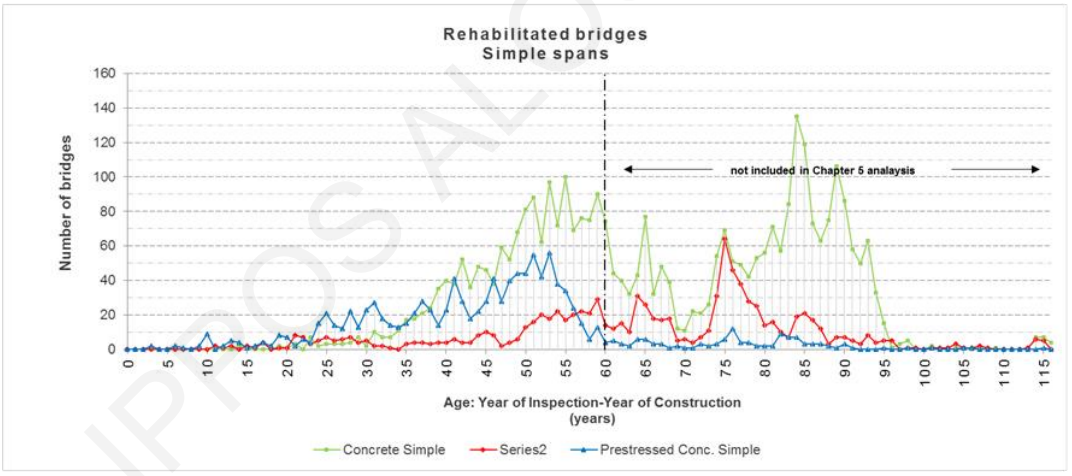

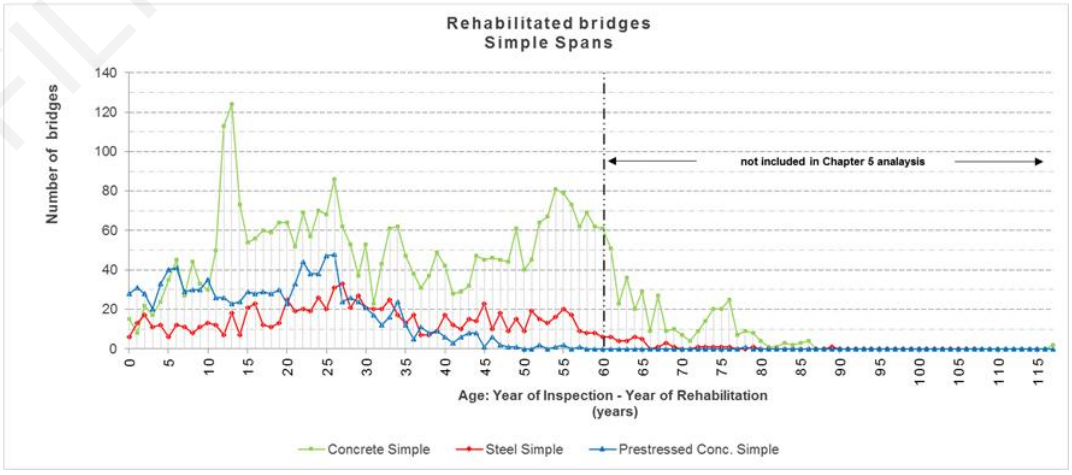

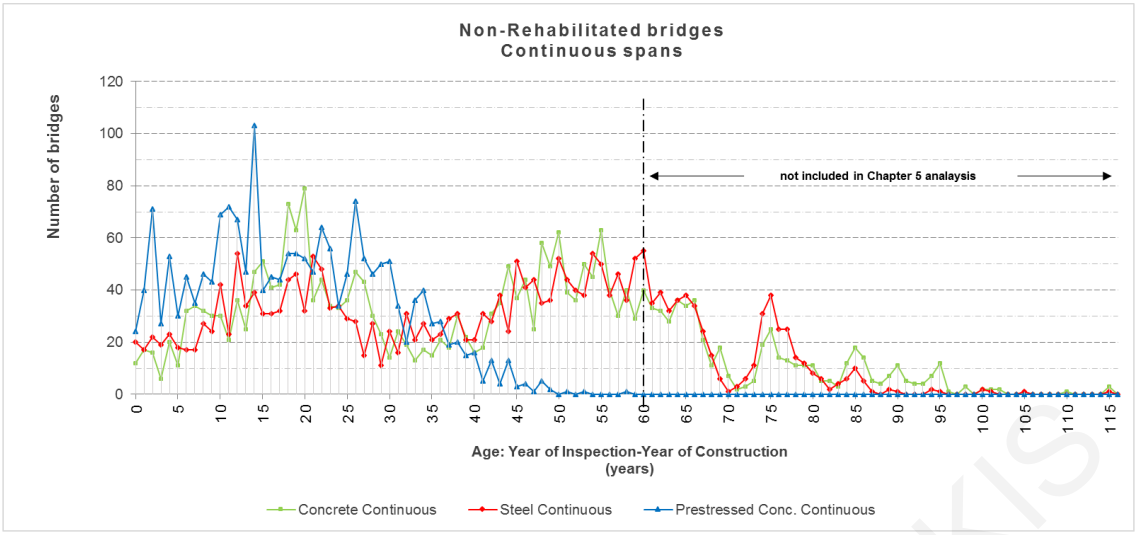

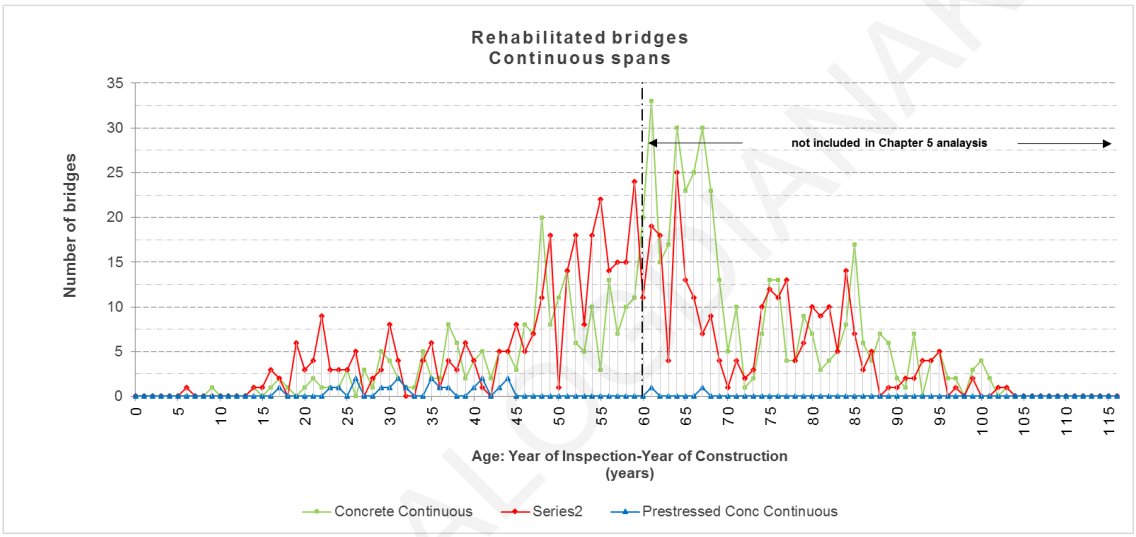

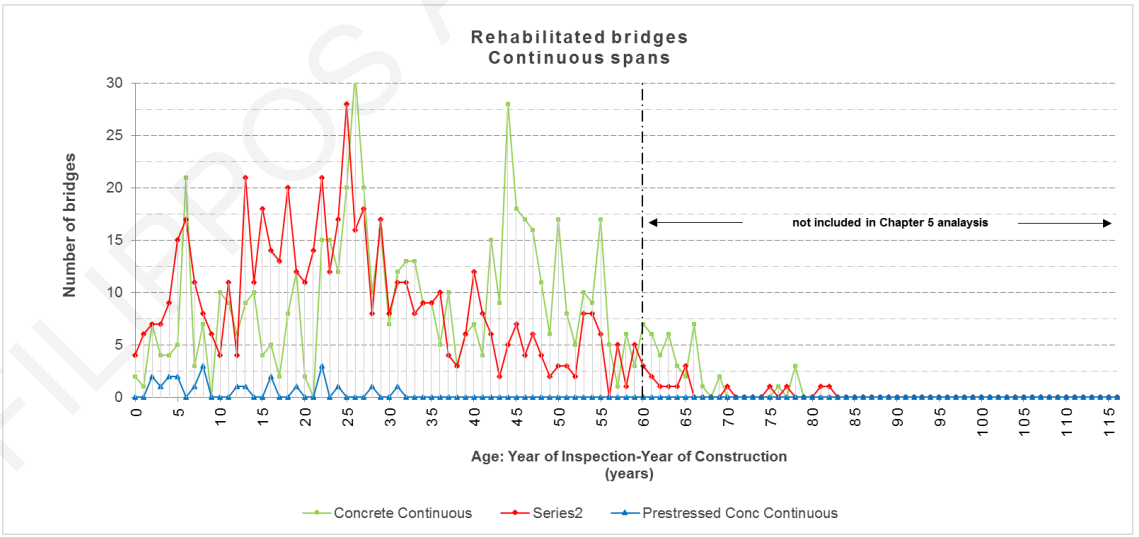

A-IV.13. Superstructure age distributions for no deicing no water environment

No Deicing no Water

Descriptive statistics for 60 year sample

Material	Non rehabilitated					Rehabilitated (based on year built)					Rehabilitated based on year rehabilitated				
	size	mean	median	Std	Skew	size	mean	median	Std	Skew	size	mean	median	Std	Skew
Concrete Simple	1198	31,7	30	19,5	0,1	64	48,7	51	9,3	-0,2	134	31,8	29	14,5	0,2
Concrete Continuous	1254	45,2	49	12,4	-0,3	111	50,6	50	4,8	0,1	125	24,1	23	12,6	0,1
Steel Simple	2316	37,2	41	15,4	-0,2	350	47,9	49	7,6	-0,1	427	23,8	24	13,0	0,0
Steel Continuous	3062	32,9	38	16,1	-0,3	400	49,0	50	7,3	-0,1	441	23,0	24	11,5	-0,1
Prestressed Conc. Simple	8909	25,9	25	16,2	0,1	1241	42,4	45	10,9	-0,2	1249	15,3	14	10,0	0,1
Prestressed Conc. Continuous	1607	20,3	20	11,6	0,0	63	34,1	35	11,7	-0,1	63	10,4	9	7,0	0,2

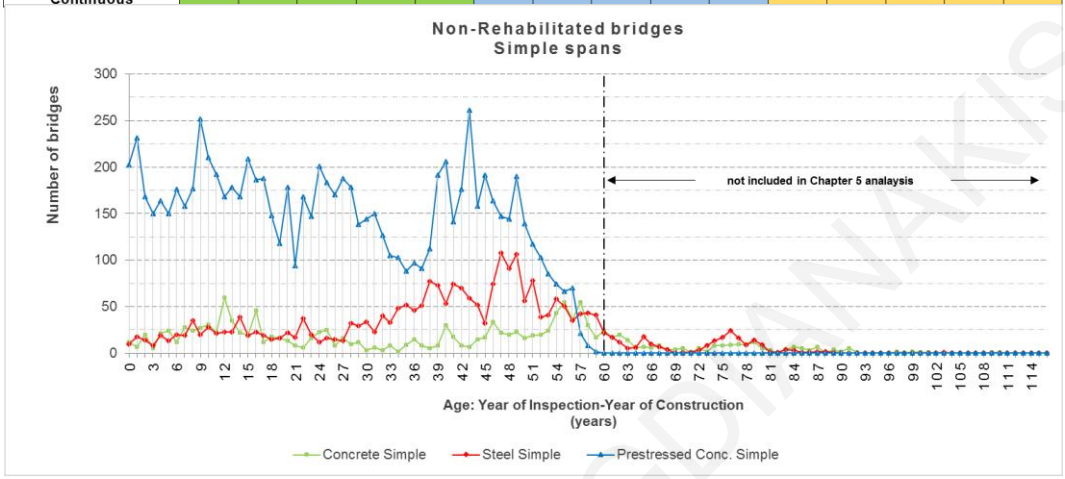

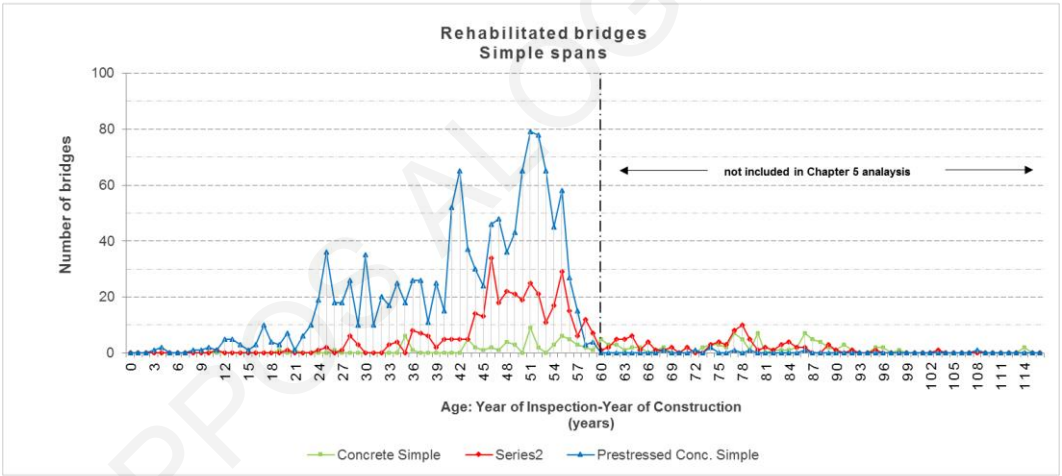

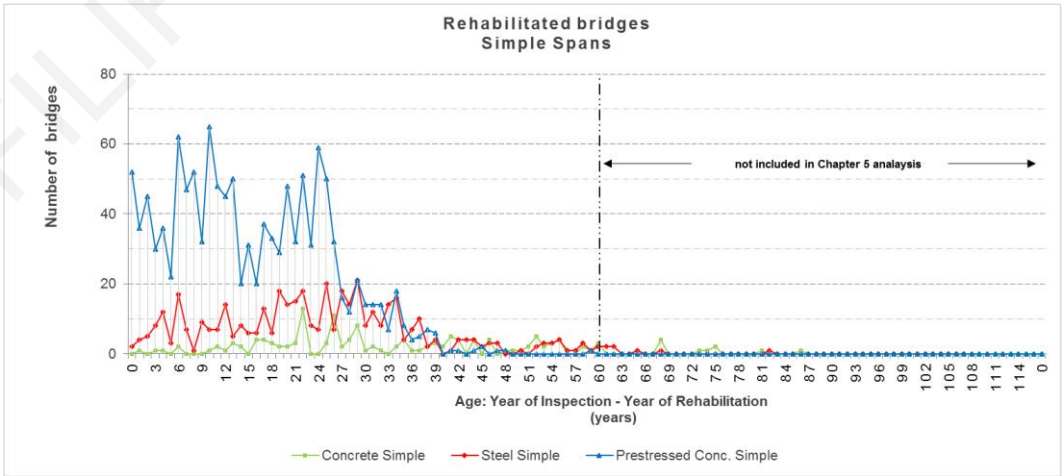

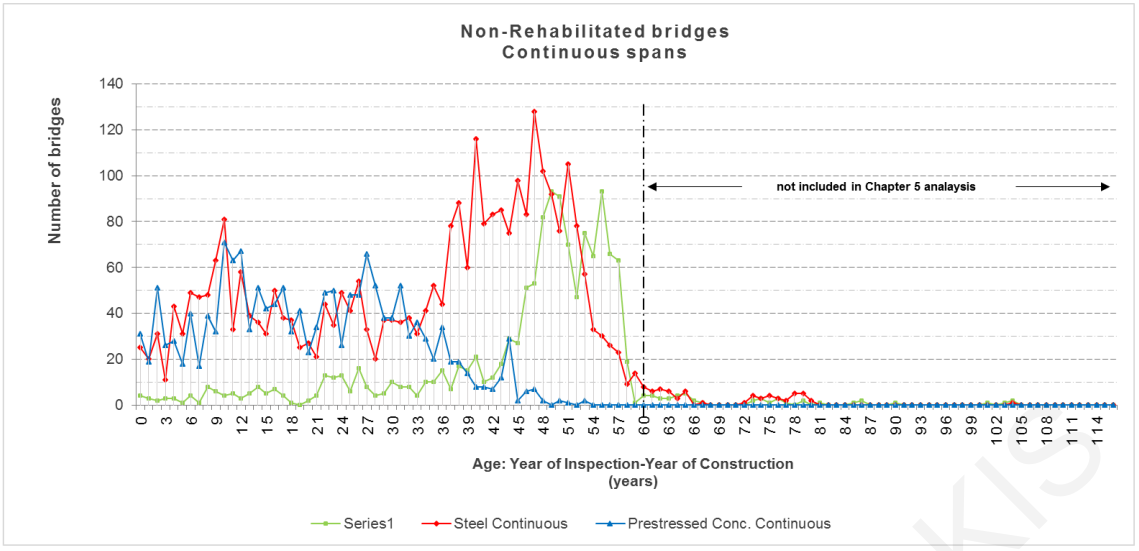

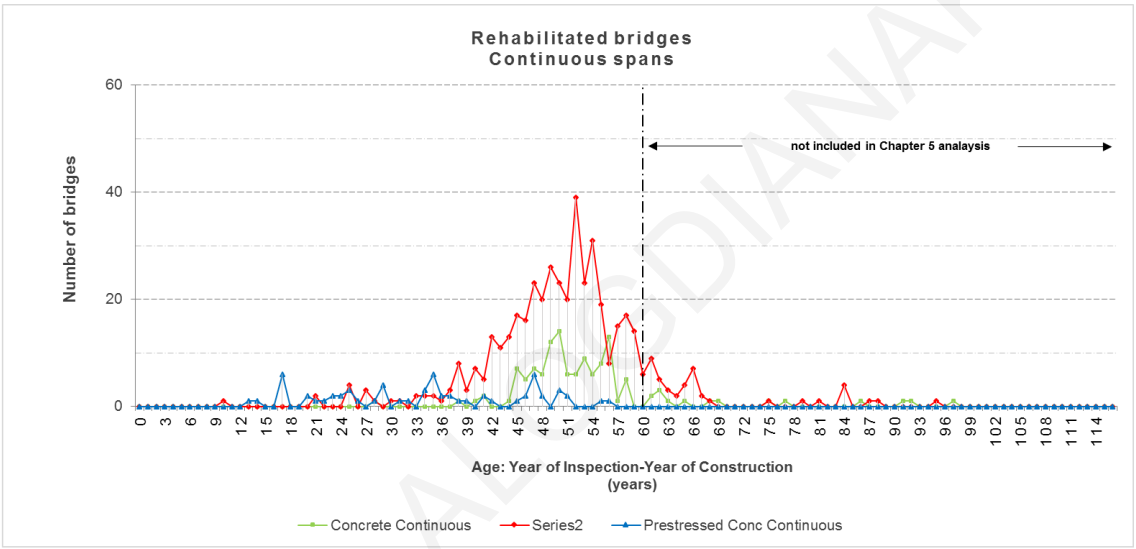

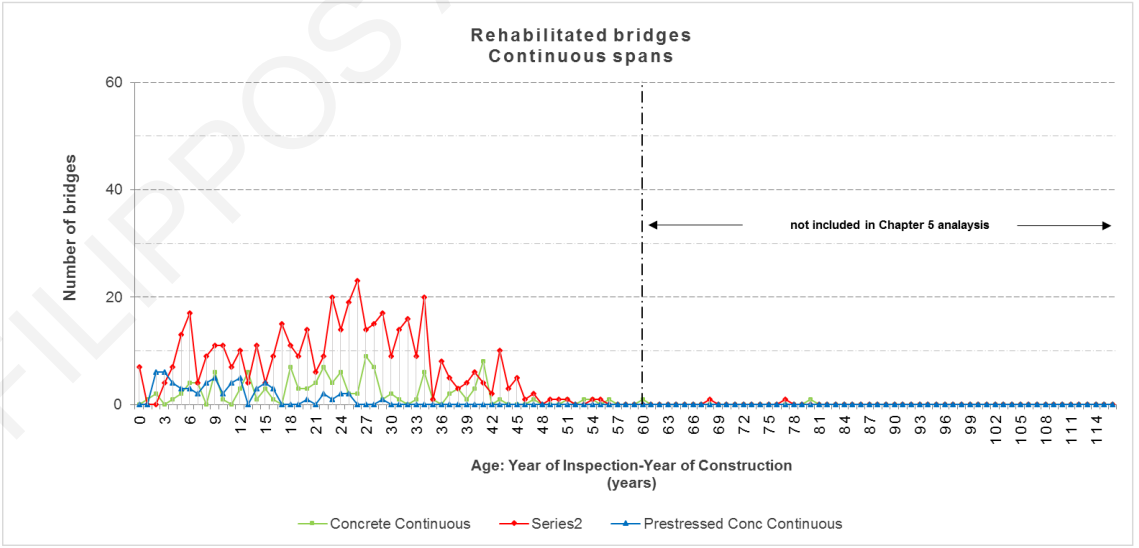

A-IV.14. Comparisons of individual environmental exposures for superstructure materials.